

**Research and Development of  
Imidazolidinone Organocatalysts**

**Leopold Samulis**

**A Thesis Submitted for the Degree of Doctor  
of Philosophy**

**at**

**Cardiff University**

**2011**

UMI Number: U567156

All rights reserved

INFORMATION TO ALL USERS

The quality of this reproduction is dependent upon the quality of the copy submitted.

In the unlikely event that the author did not send a complete manuscript and there are missing pages, these will be noted. Also, if material had to be removed, a note will indicate the deletion.



UMI U567156

Published by ProQuest LLC 2013. Copyright in the Dissertation held by the Author.  
Microform Edition © ProQuest LLC.

All rights reserved. This work is protected against  
unauthorized copying under Title 17, United States Code.



ProQuest LLC  
789 East Eisenhower Parkway  
P.O. Box 1346  
Ann Arbor, MI 48106-1346

## DECLARATION

This work has not previously been accepted in substance for any degree and is not concurrently submitted in candidature for any degree.

Signed U. S. (candidate) Date 23/5/11

## STATEMENT 1

This thesis is being submitted in partial fulfillment of the requirements for the degree of PhD

Signed U. S. (candidate) Date 23/5/11

## STATEMENT 2

This thesis is the result of my own independent work/investigation, except where otherwise stated.

Other sources are acknowledged by explicit references.

Signed U. S. (candidate) Date 23/5/11

## STATEMENT 3

I hereby give consent for my thesis, if accepted, to be available for photocopying and for inter-library loan, and for the title and summary to be made available to outside organisations.

Signed U. S. (candidate) Date 23/5/11

## Abstract

Iminium ion organocatalysis is a fast-growing area of contemporary organic chemistry in which primary or secondary amines may be used to accelerate a diverse array of stereoselective transformations in the presence of air and water. At the outset of this work, three primary limitations were identified with state-of-the-art technology:

- High catalyst loadings
- Low temperature requirement for conjugate additions
- Specificity for aldehyde substrates

Within this thesis chemical and theoretical methods to address these deficiencies were undertaken.

In Chapter 3, a direct comparison between the imidazolidinone and the diarylprolinol ether scaffold under optimised literature conditions revealed the imidazolidinone architecture to exhibit superior performance in the Diels-Alder cycloaddition between cinnamaldehyde and cyclopentadiene.

In Chapter 2, the introduction of an electron withdrawing group onto the imidazolidinone scaffold was investigated and its effect on performance on a benchmark Diels-Alder cycloaddition determined. The upper limits of electron-withdrawing group strength that may be tolerated in a functioning imidazolidinone organocatalyst were revealed.

In Chapter 4, twelve novel catalysts were prepared by incorporating electron-withdrawing groups into the imidazolidinone scaffold and their effects on both rate and enantioselectivity determined.

In Chapter 5, a one-step air- and water-tolerant method for the preparation of the MacMillan imidazolidinone catalysts was developed.

In Chapters 6 and 7, efforts to develop a predictive computational model for imidazolidinone catalyst activity is described based around the experimental results obtained previously in the thesis. The knowledge gained was then used to design structures with the potential to exhibit high turnovers and extremely high levels of stereoselectivity. Expansion of this model to encompass  $C_2$ -symmetric catalysts was further explored in Chapter 8.

Chapter 9 summarises the work in Chapters 2–8 and highlights avenues of inquiry along which this research may be continued.



## Acknowledgements

Thanks to:

Nick, for being an easy-going yet efficient supervisor and for demonstrating that elusive balance between work responsibilities and family life.

Jamie Platts, for supervising the computational aspects of this project.

Everyone in 1.119, especially:

Kevin Jones, my brother from the hood;

John Brazier, for his limitless chemical understanding;

Achim Porzelle, for his practical knowledge and German efficiency.

Everyone in 1.95, especially Adam Thetford.

All the technical staff, especially Rob Jenkins.

Benson Kariuki, for his X-ray crystallography services.

All the administrative staff.

Steve Morris, Alun Davies, and John Cavanagh for being cracking geezers and for helping me fix up my motorbike whenever I slid it down the road.

## Table of Contents

|          |  |           |
|----------|--|-----------|
| <b>1</b> | <b>Introduction to Iminium Ion Organocatalysis.....</b>                              | <b>2</b>  |
| 1.1      | Overview .....   | 2         |
| 1.2      | The Emergence of Organocatalysis .....   | 2         |
| 1.3      | Types of Organocatalysis .....   | 3         |
| 1.4      | Mechanistic Insight.....   | 7         |
| 1.5      | Mechanistic Investigations within the Group .....                                    | 9         |
| 1.6      | Catalyst Development within the Group .....  | 11        |
| 1.7      | Project Aims .....   | 13        |
| <b>2</b> | <b>Fluorinated Imidazolidinones .....</b>  | <b>15</b> |
| 2.1      | Introduction .....   | 15        |
| 2.2      | Piperazine-2,6-dione work .....  | 16        |
| 2.3      | Fluorinated Imidazolidinones.....  | 20        |
| 2.4      | Synthetic attempts towards 30 .....  | 21        |
| 2.5      | Trifluoroacetophenone .....  | 29        |
| 2.6      | Benchmark Reaction Attempted .....   | 40        |
| 2.7      | Trifluoroacetone based catalysts .....   | 40        |
| 2.8      | Benchmark Reaction Re-attempted .....  | 42        |
| 2.9      | Trichloromethyl EWG attempts.....  | 44        |
| 2.10     | Conclusions .....  | 46        |
| 2.11     | Further Work.....  | 47        |
| <b>3</b> | <b>Direct Comparison of Imidazolidinone and Diarylprolinol Ether Reactivity.....</b> | <b>49</b> |
| 3.1      | Attribution.....   | 49        |
| 3.2      | Introduction .....   | 49        |
| 3.3      | Catalyst Acquisition .....   | 49        |
| 3.4      | Experiment Design.....   | 50        |
| 3.5      | Experimental Results .....   | 52        |
| 3.6      | Analysis .....   | 53        |
| 3.7      | Conclusions .....  | 54        |
| <b>4</b> | <b>High-Performance Imidazolidinones .....</b>                                       | <b>56</b> |
| 4.1      | Introduction .....   | 56        |

|      |  |     |
|------|--|-----|
| 4.2  | EWG Imidazolidinone Synthesis .....            | 57  |
| 4.3  | Quantifying the Background Reaction .....      | 60  |
| 4.4  | Catalytic Performance.....                     | 61  |
| 4.5  | Performance Analysis .....                     | 62  |
| 4.6  | Methyl Analogue Synthesis .....                | 63  |
| 4.7  | Acetophenone Analogue Performance .....        | 66  |
| 4.8  | Acetophenone Analogue Analysis .....           | 67  |
| 4.9  | Non-EWG Imidazolidinone Synthesis .....        | 67  |
| 4.10 | Non-EWG Evaluation .....                       | 69  |
| 4.11 | Non-EWG Analysis .....                         | 70  |
| 4.12 | Changing the EWG - Synthesis .....             | 70  |
| 4.13 | Thermal Syntheses.....                         | 73  |
| 4.14 | Performance Evaluation.....                    | 77  |
| 4.15 | Performance Analysis .....                     | 78  |
| 4.16 | Catalyst Enantiopurity.....                    | 79  |
| 4.17 | Recrystallisation attempts .....               | 80  |
| 4.18 | Amino Amide Recrystallisation.....             | 81  |
| 4.19 | Minimising Epimerisation .....                 | 82  |
| 4.20 | Improved Enantiocontrol .....                  | 85  |
| 4.21 | Iminium Ion Selectivity .....                  | 86  |
| 4.22 | Solvent Screening .....                        | 87  |
| 4.23 | Reaction Dilution .....                        | 90  |
| 4.24 | Conclusions .....                              | 90  |
| 5    | Synthesis of Literature Imidazolidinones ..... | 93  |
| 5.1  | Introduction .....                             | 93  |
| 5.2  | Target Selection.....                          | 93  |
| 5.3  | Precursor Preparation.....                     | 95  |
| 5.4  | Initial Investigations.....                    | 98  |
| 5.5  | Racemate Synthesis .....                       | 100 |
| 5.6  | Synthesis Refinement .....                     | 101 |
| 5.7  | Solvent Screening .....                        | 104 |
| 5.8  | Acetone Equivalents .....                      | 106 |
| 5.9  | Temperature Screening .....                    | 107 |

|      |   |     |
|------|---|-----|
| 5.10 | Reaction Time Optimization.....                 | 108 |
| 5.11 | Final Conditions.....                           | 109 |
| 5.12 | UV active derivative synthesis.....             | 111 |
| 5.13 | Scale-up and Recycling.....                     | 112 |
| 5.14 | Conclusions .....                               | 113 |
| 6    | Computer Modelling.....                         | 115 |
| 6.1  | Introduction .....                              | 115 |
| 6.2  | Model Design.....                               | 115 |
| 6.3  | Acetophenone Catalysts Evaluated .....          | 122 |
| 6.4  | Conclusions .....                               | 123 |
| 7    | Computer-Aided Catalyst Design.....             | 126 |
| 7.1  | Introduction .....                              | 126 |
| 7.2  | Proton Affinity Calculation .....               | 126 |
| 7.3  | Substrate Shielding .....                       | 128 |
| 7.4  | E/Z Selectivity .....                           | 131 |
| 7.5  | The H-bond Effect.....                          | 133 |
| 7.6  | Fluorine H-bonders.....                         | 135 |
| 7.7  | 2-( $\beta$ -Acetamido)-Imidazolidinones.....   | 137 |
| 7.8  | Imidazolidinones with benzyl arm control.....   | 141 |
| 7.9  | Conclusions .....                               | 145 |
| 7.10 | Future Work .....                               | 146 |
| 8    | C <sub>2</sub> -Symmetric Catalysts .....       | 148 |
| 8.1  | Introduction .....                              | 148 |
| 8.2  | Piperazine-2,6-dione architecture.....          | 150 |
| 8.3  | C <sub>2</sub> -symmetric imidazolidinone ..... | 153 |
| 8.4  | Isoindolines .....                              | 155 |
| 8.5  | Conclusions .....                               | 157 |
| 9    | Conclusions and Future Work.....                | 160 |
| 9.1  | Overview .....                                  | 160 |
| 9.2  | Architectural Comparisons.....                  | 161 |
| 9.3  | EWG Investigation .....                         | 161 |
| 9.4  | Synthetic Development.....                      | 163 |
| 9.5  | Improved Stereocontrol.....                     | 164 |

|      |  |     |
|------|--|-----|
| 9.6  | Background Reaction .....                                | 166 |
| 9.7  | Future work.....   | 167 |
| 10   | Experimental .....                                       | 170 |
| 10.1 | General Procedures .....                                 | 170 |
| 10.2 | Benchmark Reaction Development.....                      | 170 |
| 10.3 | Final Benchmark Reaction.....                            | 172 |
| 10.4 | Standard Preparation A: 2-Aryl-imidazolidinones .....    | 174 |
| 10.5 | Standard Preparation B: MacMillan imidazolidinones ..... | 174 |
| 10.6 | Standard Preparation C: hydrochloride salts .....        | 175 |
| 10.7 | Compounds .....  | 175 |
| 11   | Appendix A .....   | 211 |
| 11.1 | X-ray data for 82.....                                   | 211 |
| 11.2 | X-ray data for 110·HCl.....                              | 217 |
| 11.3 | X-ray data for 119·HCl.....                              | 224 |
| 11.4 | X-ray data for 121·HCl.....                              | 230 |
| 11.5 | X-ray data for 158.....                                  | 235 |
| 12   | References.....  | 241 |

## Abbreviations

|                       |   |
|-----------------------|---|
| Ac                    | acetyl  |
| Ar                    | aromatic  |
| Bn                    | benzyl  |
| Boc                   | <i>tert</i> -butoxycarbonyl                         |
| Bu                    | butyl   |
| B3LYP                 | Becke, three-parameter, Lee-Yang-Parr               |
| cat.                  | catalytic   |
| column chromatography | flash column chromatography                         |
| d                     | days(s)   |
| d                     | doublet   |
| DCM                   | dichloromethane                                     |
| DEPT                  | distortionless enhancement by polarisation transfer |
| DFT                   | density functional theory                           |
| DMF                   | dimethylformamide                                   |
| DMSO                  | dimethyl sulfoxide                                  |
| DNPH                  | 2,4-dinitrophenylhydrazine                          |
| Et                    | ethyl   |
| ES                    | electrospray  |
| EWG                   | electron-withdrawing group                          |
| ee                    | enantiomeric excess                                 |
| eq.                   | equivalent(s)                                       |
| h                     | hour(s)   |
| HF                    | Hartree-Fock  |

|          |  |
|----------|--|
| HMBC     | heteronuclear multiple bond correlation experiment |
| HPLC     | high performance liquid chromatography             |
| HRMS     | high resolution mass spectrometry                  |
| HSQC     | heteronuclear single quantum coherence             |
| <i>i</i> | <i>iso</i>   |
| IR       | infra red  |
| LA       | Lewis acid   |
| M        | molar  |
| m        | multiplet  |
| min      | minute(s)  |
| MM       | molecular mechanics                                |
| mmol     | millimole(s)                                       |
| mol      | mole(s)  |
| Mpt.     | melting point                                      |
| MS       | mass spectrometry                                  |
| Ms       | methanesulfonyl                                    |
| <i>n</i> | <i>normal</i>                                      |
| n.d      | not determined                                     |
| NMR      | nuclear magnetic resonance                         |
| <i>p</i> | <i>para</i>  |
| Ph       | phenyl   |
| Pr       | propyl   |
| q        | quartet  |
| RDS      | rate determining step                              |
| rt       | room temperature                                   |

|             |                                    |
|-------------|------------------------------------|
| s           | singlet                            |
| T           | temperature                        |
| <i>t</i>    | <i>tertiary</i>                    |
| t           | triplet                            |
| <i>tert</i> | <i>tertiary</i>                    |
| TFA         | trifluoroacetic acid               |
| TFAA        | trifluoroacetic anhydride          |
| Tf          | trifluoromethanesulfonyl           |
| THF         | tetrahydrofuran                    |
| TLC         | thin layer chromatography          |
| PTSA        | <i>para</i> -toluene sulfonic acid |
| UV          | ultra violet                       |
| vol.        | volume(s)                          |
| vs.         | versus                             |
| Å           | Angstrom(s)                        |
| Δ           | heat                               |



---

## **Chapter 1: Introduction to Iminium Ion Organocatalysis**

---

# 1 Introduction to Iminium Ion Organocatalysis

## 1.1 Overview

Building on work previously performed within the group, a project was undertaken to design and develop high performance catalysts to address shortcomings within iminium ion organocatalysis.

## 1.2 The Emergence of Organocatalysis

In his review published in 1990 and titled "Organic Synthesis – Where now?", Seebach states that "new synthetic methods are most likely to be encountered in the fields of biological and organometallic chemistry".<sup>1</sup> In the two decades since this review was published, the use of organic molecules to catalyse organic reactions has gone from being an oft-overlooked curiosity to a rapidly growing and universally recognised field within organic chemistry, and also one in which Seebach himself is now a major player.

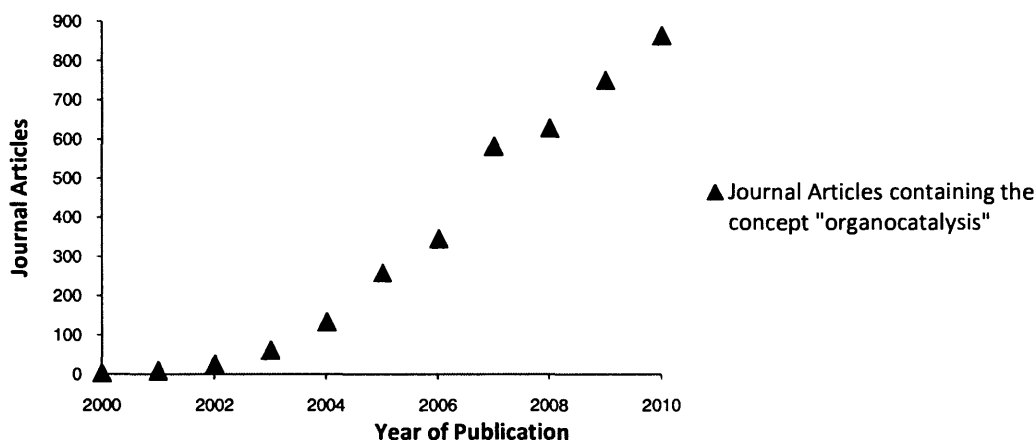


Figure 1.1

One of the milestones that led to this explosion of interest occurred when, in 2000, MacMillan coined the term "organocatalysis" in his first publication in the field of iminium catalysis.<sup>2</sup> Since then, the number of publications on the topic has increased every year, showing both the increasing number of discoveries being made within the field, as well as the growing acceptance of the term "organocatalysis" as a suitable anchor around which to unify the many diverse lines of research (Figure 1.1).<sup>3</sup>

Two of the factors driving the incredible interest in this field of organic synthesis have been the increasing interest in asymmetric synthesis and also in the drive towards greener chemical processes.

With a global revenue stream expected to top \$1 trillion USD by 2014 and an interest in target compounds of ever increasing stereocomplexity, the pharmaceuticals industry has been a strong driving force in the development of asymmetric chemical processes.<sup>4</sup> The agrochemicals, electronics, food, flavours and fragrances industries also drive the development of asymmetric synthetic processes.<sup>5</sup>

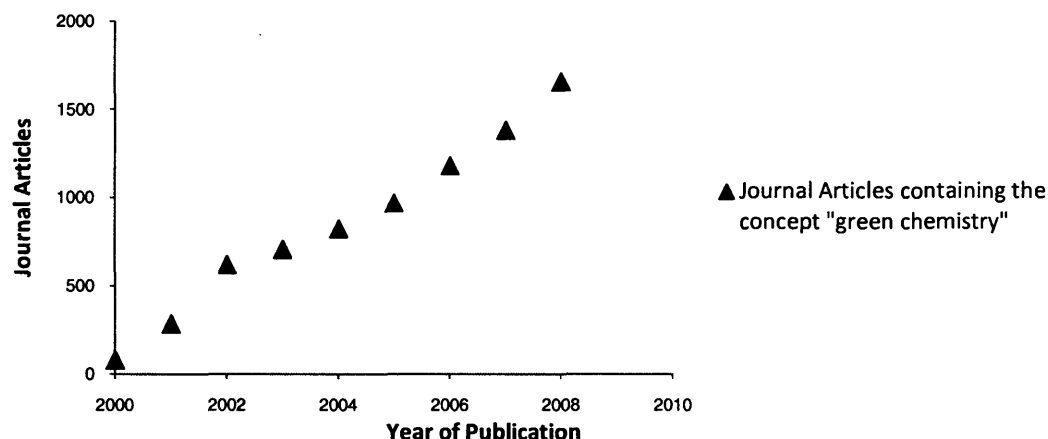


Figure 1.2

The other major factor that simultaneously drives interest in organocatalysis and also guarantees its future relevance is the drive towards “greener” chemical processes. From the latter half of the 20<sup>th</sup> century onwards, there has been an ever-growing awareness of the inseparability of our own biological substrates from the biosphere at large. The resultant backlash towards environmentally destructive technology has given rise to an ever increasing amount of legislation designed to encumber polluting processes and drive commercial interests towards the development and use of environmentally benign chemical processes. This is reflected in the ever increasing number of publications on the topic of “green chemistry” and the launch of a journal by the RSC dedicated solely to the field (Figure 1.2).<sup>6,7</sup>

As purely organic molecules that are required only in catalytic amounts, and with chirality that may frequently be derived from natural amino acids, organocatalysts are perfectly positioned to benefit from the drive towards asymmetric synthesis and green chemistry.

### 1.3 Types of Organocatalysis

MacMillan describes 5 modes of activation by organocatalysts in his 2008 review.<sup>8</sup> In decreasing order of new reactions discovered, he lists iminium catalysis (50), hydrogen-bonding catalysis (30), enamine catalysis (25), SOMO catalysis (4), and counterion catalysis (2).

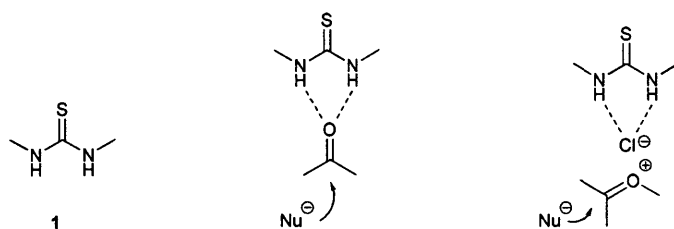
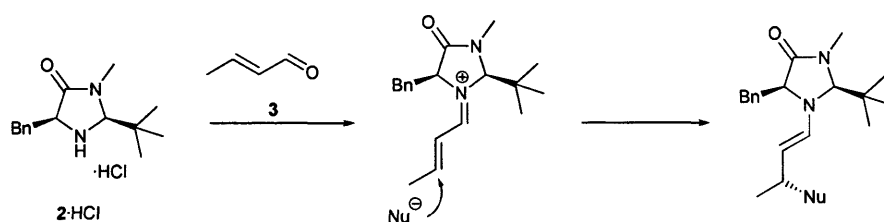
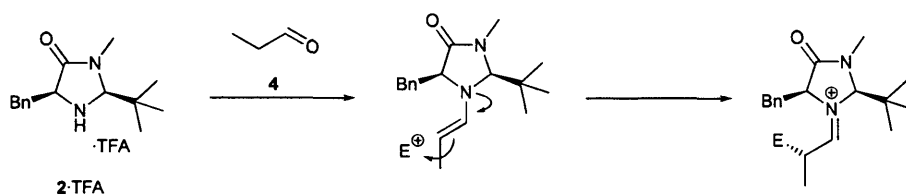


Figure 1.3

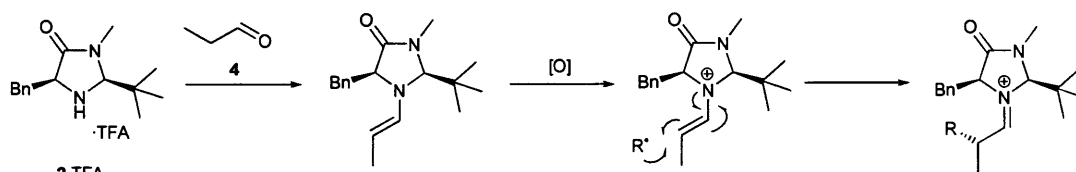
These activation modes may be grouped into two distinct classes, according to catalyst functionality. Hydrogen bond donors such as **1** may be used to effect both hydrogen-bonding catalysis as well as counterion catalysis (Figure 1.3).<sup>9</sup>



Scheme 1.4

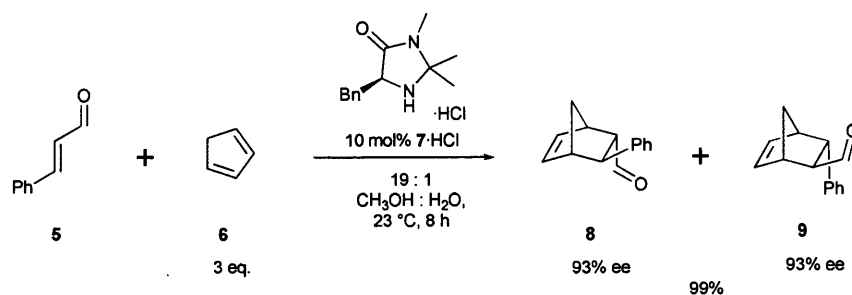


Scheme 1.5



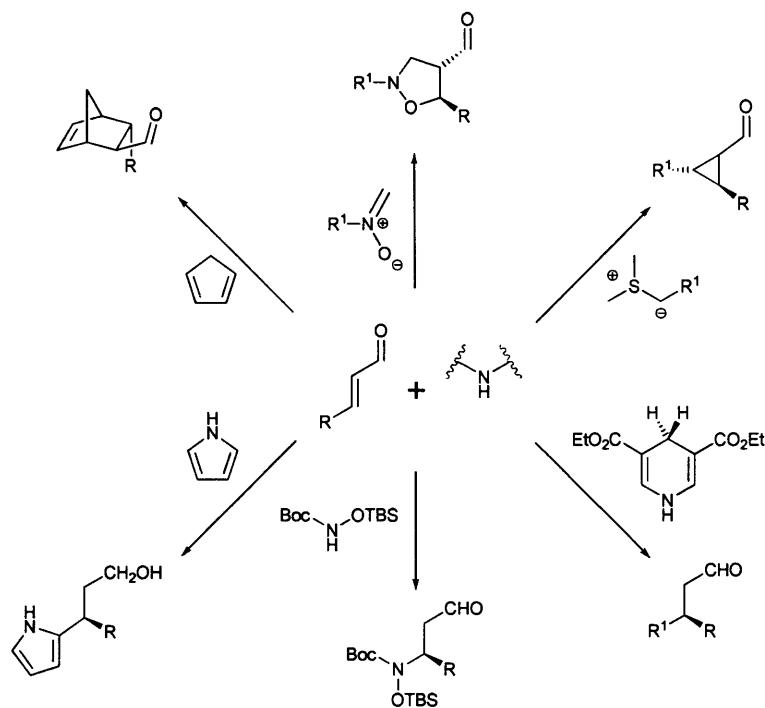
Scheme 1.6

Likewise, amines such as **2** may be used to effect iminium catalysis (Scheme 1.4), enamine catalysis (Scheme 1.5), or SOMO catalysis (Scheme 1.6), depending on the reaction conditions used.



Scheme 1.7

The seminal paper in the field of iminium ion organocatalysis was published in 2000 by MacMillan and showed how the use of 7·HCl at 10 mol% could catalyse the Diels-Alder reaction of 5 and 6 in 19:1 methanol:water at 23 °C to achieve 99% conversion in 8 hours, with 93% ee for both the *endo*- and *exo*-diastereomers, 8 and 9 (Figure 1.7).<sup>2</sup>



Scheme 1.8

This activation mode was further explored by the MacMillan group in subsequent papers detailing 3+2 cycloadditions, cyclopropanations, conjugate additions with open and closed transition states, aminations and hydride reductions (Scheme 1.8).<sup>10-16</sup>

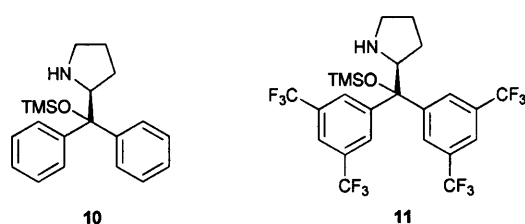


Figure 1.9

While the work done by MacMillan in the field of organocatalysis has almost exclusively used catalysts based on the imidazolidinone architecture (e.g **2** and **7**), other architectures have also shown catalytic ability. In particular, diarylprolinol ether catalysts such as **10** and **11** have been used to accelerate a wide variety of transformations with high degrees of asymmetry (Figure 1.9).<sup>17</sup>

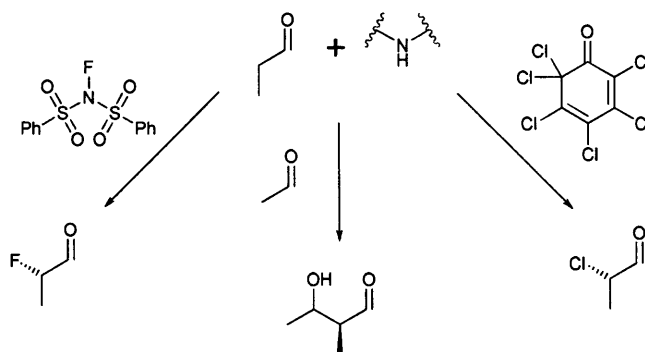
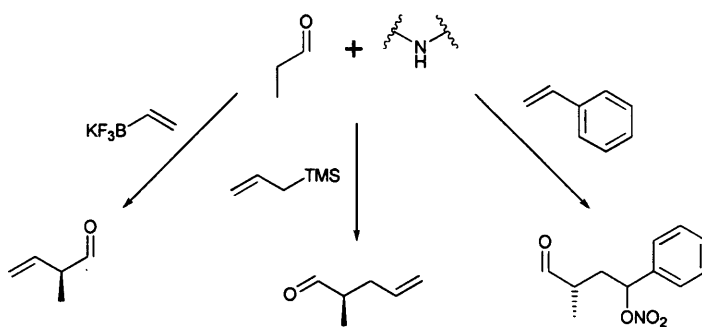


Figure 1.10: Enamine processes catalysed by the imidazolidinone architecture

While not directly relevant to this project, the developments within enamine catalysis illustrate the versatility of imidazolidinone organocatalysts and show areas in which insights gained through research into iminium organocatalysis may also be utilised. The MacMillan group has also shown the use of the enamine activation mode for effecting  $\alpha$ -chlorination and  $\alpha$ -fluorination of aldehydes,  $\alpha$ -fluorination of ketones and aldol reactions (Scheme 1.10).<sup>18–21</sup>

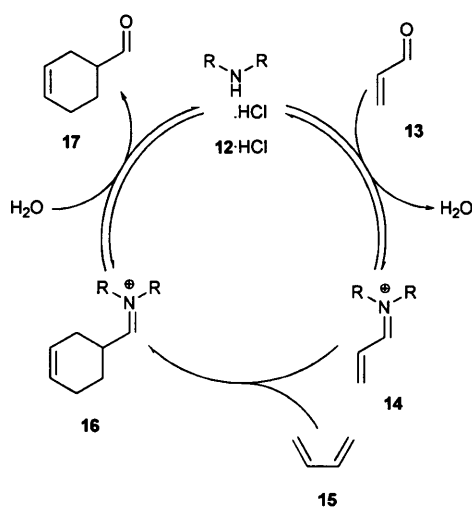


Scheme 1.11

The more recently discovered SOMO catalysis has been used by MacMillan to induce allylation, vinylation, carbo-oxidation, epoxidation, and arylation (Scheme 1.11).<sup>22–26</sup>

#### 1.4 Mechanistic Insight

Before the development of iminium ion organocatalysis within his group, MacMillan postulated that the LUMO-lowering ability and kinetic lability of Lewis acid catalysts “might also be available with a carbogenic system that exists as a rapid equilibrium between an electron-deficient and electron-rich state”.<sup>2</sup>



Scheme 1.12

This postulate led to the idea of iminium ion organocatalysis, in which an alkylammonium salt (**12**·HCl) may reversibly condense with an aldehyde (**13**) or ketone to yield an iminium ion (**14**) (Scheme 1.12). **14** would then be expected to have a lower LUMO energy than **13** and readily react with a diene (**15**), or other suitable reagent, to give a product iminium ion (**16**). **16** could then hydrolyse to provide the product (**17**) and regenerate **12**·HCl.

The concept of iminium organocatalysis was embodied in MacMillan's seminal publication.<sup>2</sup> In it, he described the use of iminium organocatalysis to allow the Diels-Alder reaction of **5** and **6** to proceed to completion within a few hours at room temperature (Scheme 1.7). Additionally, by employing a chiral catalyst, MacMillan was able to observe substantial stereoselectivity, attaining product ees of 84 – 93%.

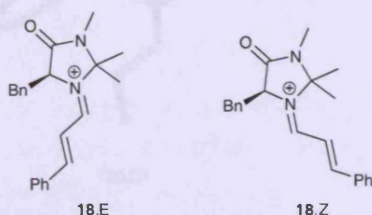


Figure 1.13

In explaining the mechanism by which the reaction proceeds, MacMillan implied that the Diels-Alder reaction proceeds only through the intermediary of iminium ions and that no other active species were present. MacMillan also asserted that **18.E** forms exclusively, as steric interactions between the geminal dimethyl groups and the proton  $\alpha$ - to the iminium carbon render **18.Z** highly unfavourable (Figure 1.13).

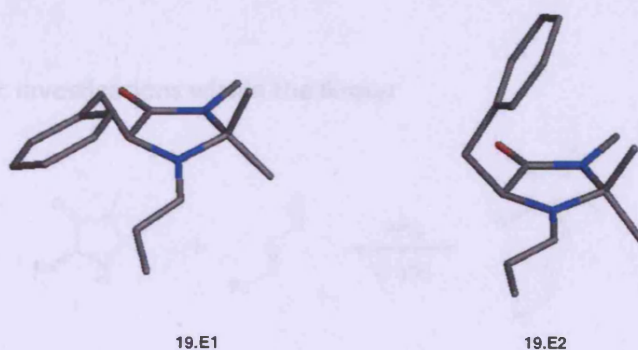


Figure 1.14

To explain the mechanism by which the benzyl arm extending from the chiral centre of **7** imparts stereoinformation into the product, MacMillan used computer-aided computational analysis to study the preferred conformations of **19.E**. Using a relatively crude Molecular Mechanics function, he found that **19.E1** was the preferred conformation and that approach of **6** from the top face of the substrate was effectively blocked, leading to only one product enantiomer (Figure 1.14). More recently, work by Houk and also work within our group has shown that, largely due to a favoured  $\pi$ -hydrogen interaction, **19.E2** is in fact the preferred conformation.<sup>27,28</sup> **19.E2** effectively blocks only the carbon  $\alpha$ - to the iminium ion, but still provides sufficient shielding to allow good enantiocontrol in closed transition state reactions, such as the Diels-Alder reaction and conjugate addition of pyrroles.<sup>2,12</sup> This finding



explains the inability of **7** to effect good stereocontrol in open transition state reactions, in which the  $\beta$ -carbon alone is targeted, such as conjugate addition of indoles.<sup>13</sup>

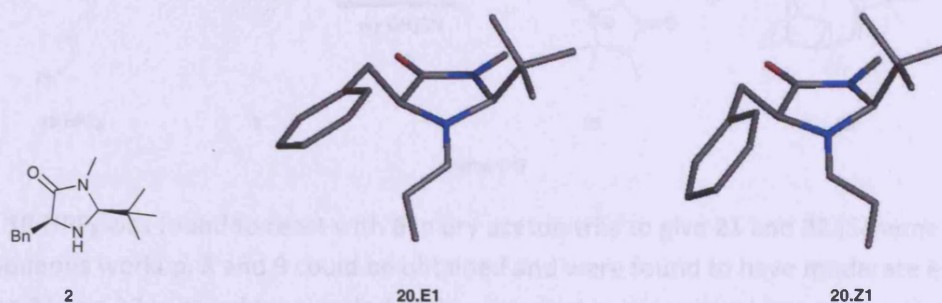
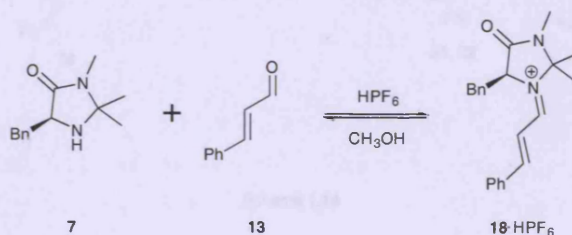


Figure 1.15

For open transition state reactions, the MacMillan group first found success with **2** (Figure 1.15). Modelled iminium ions of **2** were found to preferentially reside in **20.E1**, as the conformation analogous to **19.E2** was disfavoured due to steric interactions between the benzyl arm and *tert*-butyl group.<sup>29</sup> Unfortunately, **2** has only been shown to achieve good stereocontrol at low temperatures. This was suspected to be due to a lack of iminium geometry control.

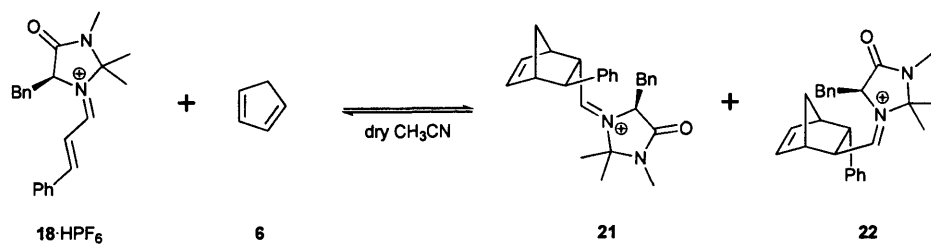
### 1.5 Mechanistic Investigations within the Group



Scheme 1.16

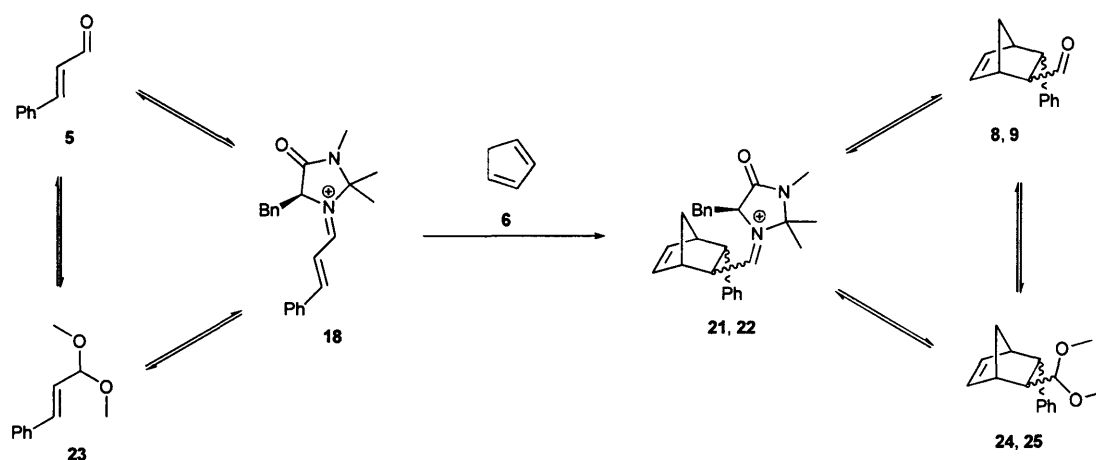
The mechanisms of iminium catalysis have been extensively studied within our group. A breakthrough occurred when **18**·HPF<sub>6</sub> was obtained as a stable compound that could be dried *in vacuo* (Scheme 1.16).<sup>30</sup>

In contradicting MacMillan's position that cycloaddition was the key to the Diels-Alder reaction, research within our group has shown that the RDS is the formation of the iminium ion, and that the cycloaddition is extremely rapid. The presence of water thus retards the rate of the bimolecular iminium formation step by increasing the concentration of a species that is known to react with **2** far more rapidly than **13**.<sup>31</sup>



Scheme 1.17

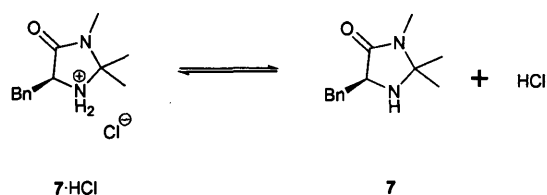
**18-HPF<sub>6</sub>** was found to react with **6** in dry acetonitrile to give **21** and **22** (Scheme 1.17). Upon aqueous workup, **8** and **9** could be obtained and were found to have moderate ee's.<sup>31</sup> Allowing **21** and **22** to stand for a period of days resulted in the gradual loss of enantiopurity. This result indicated that the Diels-Alder reaction is reversible in dry acetonitrile and that the forward reaction is under kinetic control. In both wet acetonitrile and in wet methanol, the Diels-Alder reaction appears irreversible, indicating that hydrolysis/methanolysis of **21** and **22** is more rapid than the retro Diels-Alder reaction.



Scheme 1.18

Further complexity arose when research performed within our group elucidated the multitude of species present under reaction conditions (Scheme 1.18).<sup>31</sup> It was shown that all aldehydes existed in equilibrium with their dimethylacetals and that the presence of water drives the equilibrium towards the aldehyde.

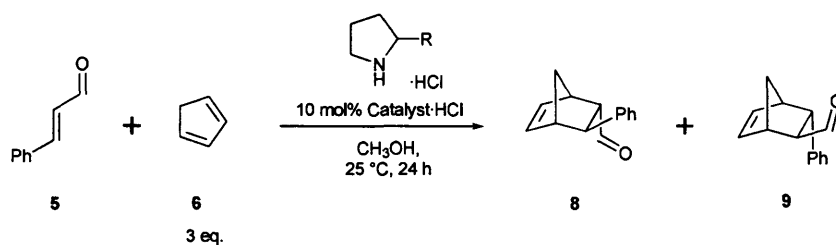
In contradicting MacMillan's postulate that cycloaddition was the RDS in the benchmark reaction, research within our group has shown that the RDS is **18** formation and that the cycloaddition is extremely rapid. The presence of water thus increases the rate of the bimolecular iminium formation step by increasing the concentration of **6**, which has been shown to react with **7** far more rapidly than **23**.<sup>31</sup>



Scheme 1.19

The finding that the RDS is iminium ion formation indicates that the concentration of **7**, which exists in rapid equilibrium with **7**·HCl, is also critical to attaining high turnover (Scheme 1.19).

## 1.6 Catalyst Development within the Group



|                | <b>26</b> | <b>27</b>          | <b>28</b>       |
|----------------|-----------|--------------------|-----------------|
| R =            | H         | CO <sub>2</sub> Et | CF <sub>3</sub> |
| Conversion (%) | <5        | 62                 | 93              |

Scheme 1.20

While conducting a structure activity relationship study, the ability of EWGs to enhance catalyst efficacy was observed. The performance difference between **26**, **27**, and **28** in the benchmark Diels-Alder reaction between **5** and **6** serves to highlight this effect (Scheme 1.20).<sup>30</sup> **26**, lacking any EWG's, was seen to be a very poor catalyst, attaining less than 5% conversion after 24 hours. **27** featured the ethyl ester EWG and was seen to effect 62% conversion in the same time period, while **28** which featured the much stronger trifluoromethyl EWG allowed the reaction to proceed nearly to completion in the same time period.

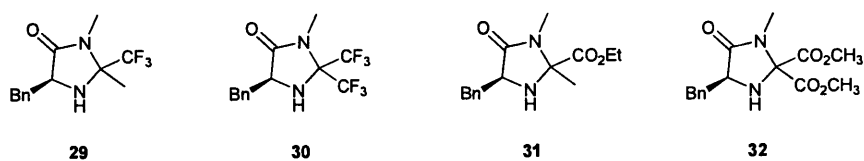
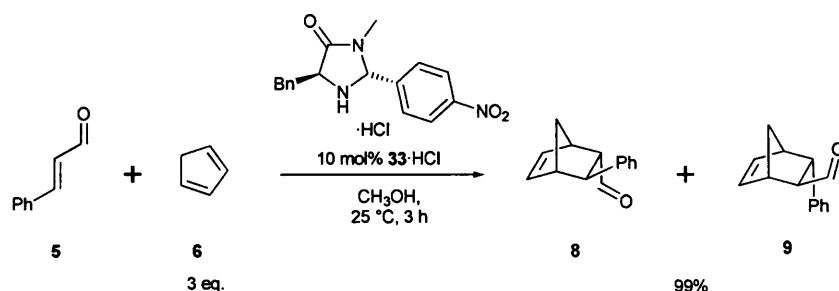


Figure 1.21

Seeking to reproduce this rate enhancement in the already high-performing imidazolidinone architecture, **29–32** were envisioned (Figure 1.21). Unfortunately, the attempted syntheses of these compounds all failed and the catalytic activity of **29–32** remained unknown.<sup>30</sup>



Scheme 1.22

After failing to reach other target structures, **33** was prepared. In the benchmark Diels-Alder reaction, it was found able to reach 99% conversion of **5** to **8** and **9** in 3 hours when used at 10 mol% in methanol at 25 °C (Scheme 1.22).<sup>30</sup> At the same loading, MacMillan's seminal catalyst **7** required 8 hours to attain the same conversion at 23 °C.<sup>2</sup>

This finding established that the premise of rate enhancement through addition of an EWG was applicable to the imidazolidinone architecture and highlighted a path towards lower organocatalyst loadings.

## 1.7 Project Aims

As the most widely published subfield of organocatalysis, iminium catalysis appeared a fruitful area in which to work. Additionally, there had been a long-running thread of research into iminium organocatalysis within the group and many of the initial hurdles to gain entry into the field had been overcome. This project aimed to build upon this research and to address the primary shortcomings with iminium catalysis, which were seen to be:

- High catalyst loadings
- Low temperature requirements for conjugate additions
- Specificity for aldehyde substrates

As such, research was embarked upon with the goal of increasing catalyst turnover, removing low temperature requirements from conjugate addition reactions, and investigating the possibility of adapting catalysts for use with enone substrates.

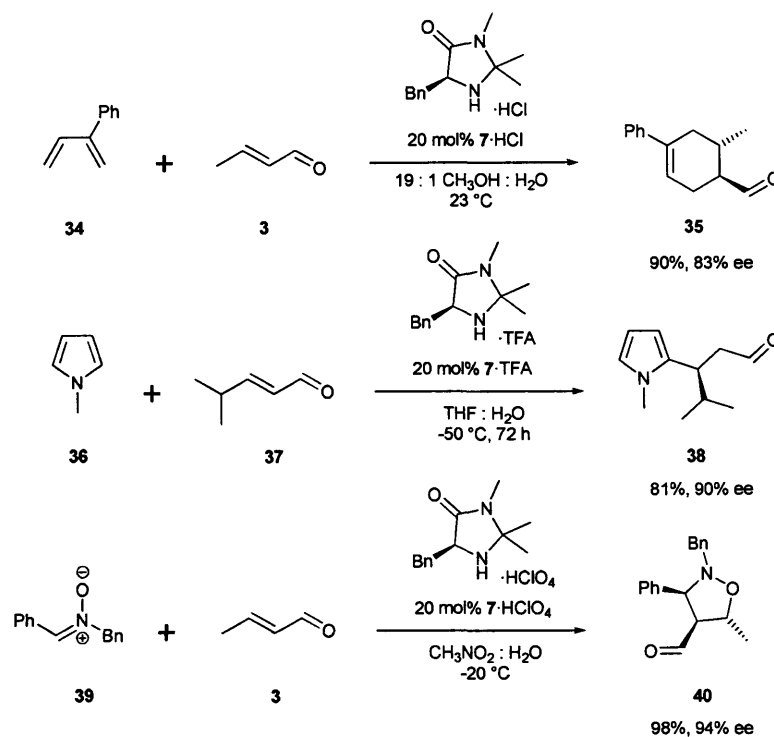
---

## **Chapter 2: Fluorinated Imidazolidinones**

---

## 2 Fluorinated Imidazolidinones

### 2.1 Introduction



Scheme 2.1

In his seminal paper on organocatalysis, MacMillan reported the use of up to 20 mol% of **7**·HCl to accelerate the Diels-Alder reaction (Scheme 2.1).<sup>2</sup> MacMillan has also reported the use of up to 20 mol% **7** in conjunction with TFA for catalysing the conjugate additions of pyrroles into enals and the use of up to 20 mol% of **7**·HClO<sub>4</sub> for catalysing 1,3-dipolar cycloadditions.<sup>12,10</sup> These high loadings are prohibitive to scale-up, as expense would be incurred during catalyst synthesis and waste disposal. Informal discussions with industrial process chemists raised the requirement for high loadings as the main barrier to using organocatalysis on a large scale.<sup>32</sup>

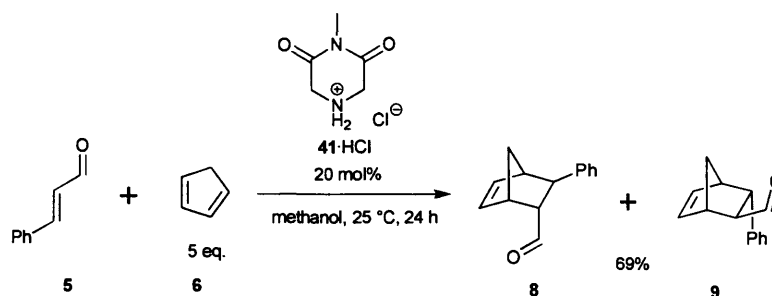
Previous work within our group had shown that cyclic amines have rate advantages over comparable acyclic amines and also that an electron-withdrawing group beta to the active nitrogen could improve the turnover of a secondary amine catalyst, as seen in the series of catalysts **26**, **27**, and **28** (Scheme 1.20).<sup>30</sup>

At the time this work was performed, the RDS in the benchmark Diels-Alder reaction was thought to be the cycloaddition itself, as had been shown to be the case when using

**28**·HCl in the benchmark reaction.<sup>33</sup> As such, it was postulated that EWGs raised reaction rates by lowering the LUMO energy of the iminium ion. Recent work within the group has shown that the RDS in the benchmark Diels-Alder reaction with **7**·HCl, when conducted in a methanol:water mixture, is iminium ion formation and that the cycloaddition is relatively rapid.<sup>31</sup> Later research used <sup>1</sup>H NMR to monitor the complex equilibria occurring under reaction conditions and showed the importance of considering all the species in Scheme 1.18.<sup>31</sup> EWGs are now believed to increase rate by increasing the acidity of catalyst salts and giving rise to higher concentrations of free amine under reaction conditions.

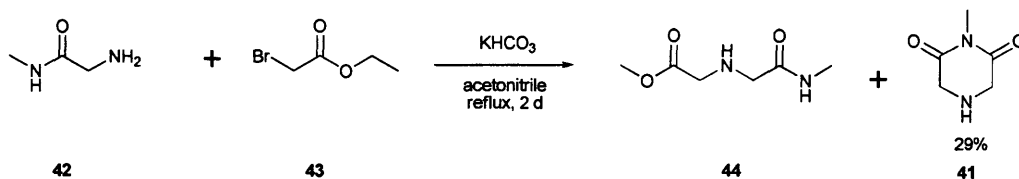
The goal of the work performed within this chapter was to increase catalyst performance and allow for lower catalyst loadings by synthesising and evaluating EWG-containing secondary amine catalysts.

## 2.2 Piperazine-2,6-dione work



Scheme 2.2

One of the key catalysts discovered during previous investigations within the group, **41**, was found able to achieve 69% conversion in the benchmark reaction at 20 mol% loading and 25 °C for 24 hours, using 5 equivalents of **6** (Scheme 2.2).<sup>30</sup> This architecture was also thought to hold promise as the foundation around which a C<sub>2</sub>-symmetric catalyst capable of catalyzing the reactions of ketones as well as aldehydes could be constructed. Further investigation was therefore undertaken with the aim of replacing the methyl group at N-1 position with an EWG to yield a more efficient catalyst.

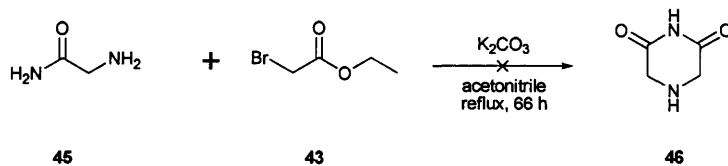


Scheme 2.3

The synthetic route taken previously to reach **41** was the reaction of **42** and **43** in the presence of potassium hydrogen carbonate in refluxing acetonitrile (Scheme 2.3). An initial

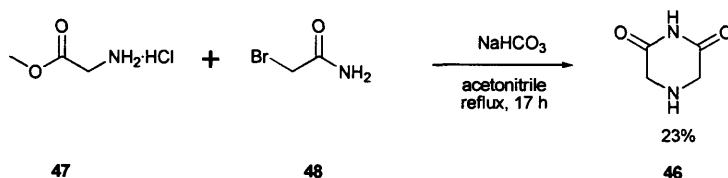


$S_N2$  attack of the amine nitrogen upon the  $\alpha$ -bromoester **43** was thought to yield the acyclic intermediate **44**, which could then undergo a 6-*exo-trig* cyclisation, favoured under Baldwin's rules, to yield **41** (29%).<sup>34</sup>



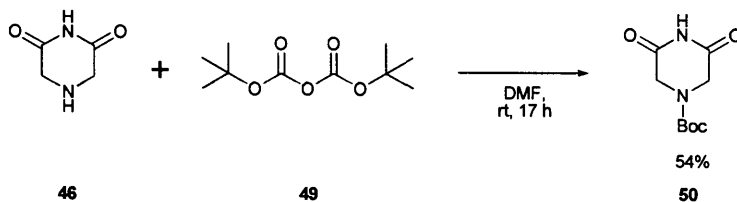
Scheme 2.4

An analogous approach towards **46** using **45** instead of **42** failed to provide the desired product upon workup, and the reaction was assumed to have failed (Scheme 2.4).



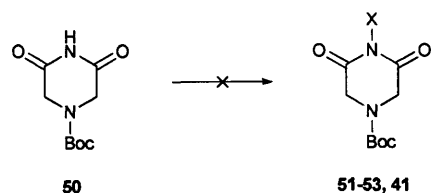
Scheme 2.5

An alternative approach allowed **46** to be obtained from **47** and **48** in 23% yield (Scheme 2.5).



Scheme 2.6

**50** was formed from **46** and **49** in 54% yield (Scheme 2.6). Due to the low solubility of **46**, the reaction had to be performed in DMF.



| Reagents                    | Solvent | Conditions  | X                  | Target    |
|-----------------------------|---------|-------------|--------------------|-----------|
| Pyridine, Tf <sub>2</sub> O | DCM     | -50 °C - rt | Tf                 | <b>51</b> |
| NaH, Ac <sub>2</sub> O      | DMF     | rt, 18 h    | Ac                 | <b>52</b> |
| NaH, TFAA                   | DMF     | rt, 16 h    | CF <sub>3</sub> CO | <b>53</b> |
| NaH, CH <sub>3</sub> I      | DMF     | rt, 21 h    | CH <sub>3</sub>    | <b>41</b> |

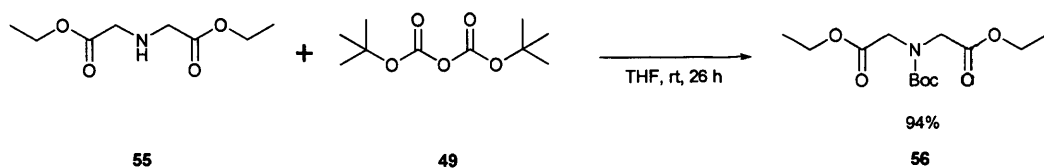
Scheme 2.7

A solution of **50** was treated with triflic anhydride at -50 °C and then warmed to room temperature (Scheme 2.7). No product could be isolated and only unidentified side products could be seen. This was explained when a publication was found describing the reactive nature of the complex formed between valerolactam and triflic anhydride.<sup>35</sup>

**50** was then treated with sodium hydride, followed by acetic anhydride. Analysis of the crude reaction mixture by <sup>1</sup>H NMR showed the continued presence of the peak corresponding to the imidic proton, indicating the reaction had failed to give the desired product.

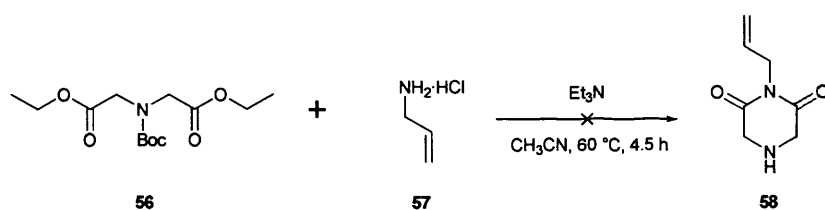
The reaction was then repeated using the more reactive TFAA. Once again, <sup>1</sup>H NMR showed the presence of an unsubstituted imide.

As the methodology of deprotonation using sodium hydride followed by addition of an electrophile was in doubt, a test reaction was performed whereby **50** was stirred in DMF with methyl iodide and sodium hydride. <sup>1</sup>H NMR showed the presence of multiple products with signatures indicating that methylation was occurring on the carbon atoms α- to the imide. This result was surprising as the relatively acidic imide functionality, estimated to have a pK<sub>a</sub> of around 15, was expected to be readily deprotonated by sodium hydride and the resultant anion expected to react with methyl iodide through its nitrogen atom.<sup>36</sup>



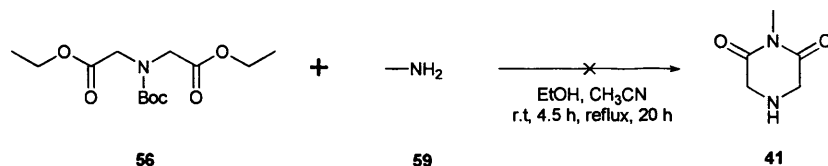
Scheme 2.8

The reaction of **55** and **49** in THF proceeded to completion (Scheme 2.8). A slight excess of **55** was used and the residual amount was removed by twice washing an ethereal solution of the crude mixture with citric acid (1 M). Evaporation of the ethereal solution provided **56** in 94% yield.



Scheme 2.9

An attempt at inducing a reaction between allylamine, generated in-situ from **57**, and triethylamine failed and starting materials were recovered (Scheme 2.9).



Scheme 2.10

Using **59** also failed to induce any reaction as only **56** was recovered from the reaction mixture (Scheme 2.10). No traces of product or acyclic intermediate were noted. At this stage, a lack of results prompted the abandonment of research into the piperazine-2,6-dione architecture so as to focus efforts on the more promising imidazolidinone architecture.

### 2.3 Fluorinated Imidazolidinones

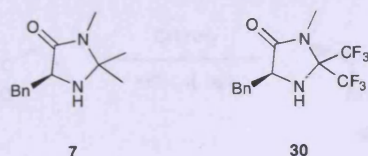


Figure 2.11

A longstanding goal within the group had been the synthesis of **30** (Figure 2.11). Computer modelling had shown that the iminium ion formed upon its condensation with acrolein would have a significantly lower energy LUMO ( $-5.99$  eV) than that formed with benchmark catalyst **7** ( $-5.71$  eV).<sup>30</sup> It was assumed at the time that this would result in a very high performance catalyst.

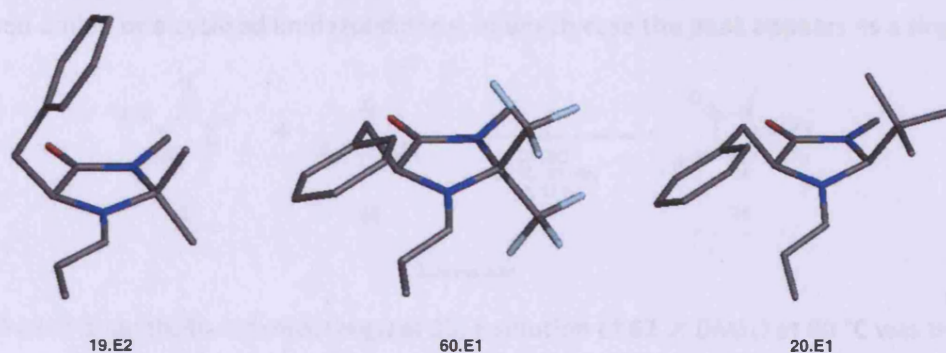
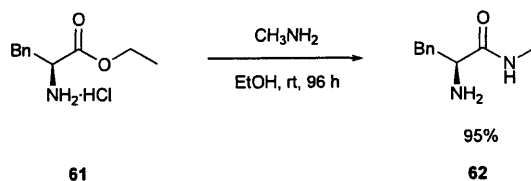


Figure 2.12

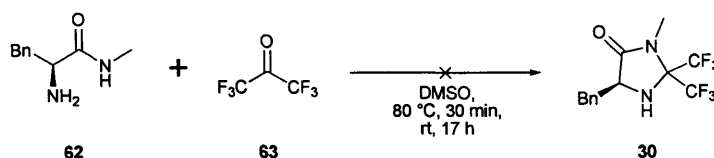
Additionally, **30** was thought to hold potential for use in a wider range of reactions. When compared to **19.E2**, The  $\pi$ -hydrogen bond that favours this conformation is replaced with a repulsive  $\pi$ -fluorine interaction, rendering **60.E1** the preferred conformation (see Chapter 7.3). This conformation offers comparable substrate shielding to **20.E1**, the preferred conformation of **20.E**, and may impart stereocontrol into reactions going *via* open transition states (Figure 2.12).

## 2.4 Synthetic attempts towards 30



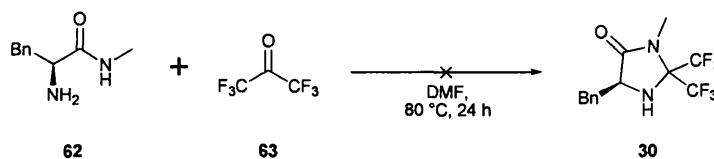
Scheme 2.13

**61** was stirred in 33% (w/w) ethanolic methylamine for 5 days at room temperature, and **62** obtained in 95% yield after aqueous workup (Scheme 2.13). The  $^1\text{H}$  NMR spectra of **62** showed a doublet ( $J = 4.99$  Hz) at 2.82 ppm, corresponding to the *N*-methyl group. The splitting arose from coupling to the amidic proton and has been established within the group as a reliable diagnostic tool to determine whether the amidic methyl group is part of an uncyclised amide or a cyclised imidazolidinone, in which case the peak appears as a singlet.



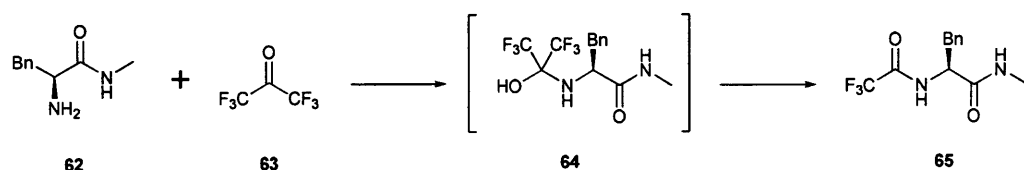
Scheme 2.14

As a first synthetic attempt towards **30**, a solution of **62** in DMSO at 80 °C was treated with gaseous **63**, generated by the action of concentrated sulfuric acid on the liquid sesquihydrate (Scheme 2.14). After stirring for 17 h at room temperature, an aqueous workup was performed.  $^1\text{H}$  NMR of the organic fraction showed a complex mixture of products.



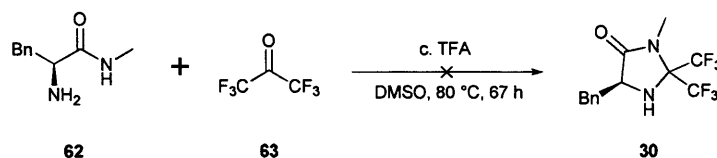
Scheme 2.15

A second attempt was then made by substituting DMF for DMSO and repeating the procedure in the first experiment, stirring for 24 hours at 80 °C instead of room temperature (Scheme 2.15). A complex mixture of products was returned, and column chromatography failed to isolate any fractions with  $^1\text{H}$  NMR signatures matching those expected of **30**.



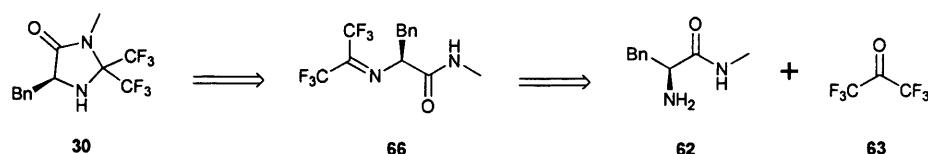
Scheme 2.16

To allay fears that the presence of water may be hindering the reaction, dry DMF was used and the second attempt was repeated, stirring for 4 hours instead of 24 hours (Scheme 2.16). Once again, the reaction did not proceed cleanly and resulted in a complex mixture of products. A crystalline product was isolated by precipitation from the crude mixture and was found to be insoluble in almost all organic solvents. Accordingly, the product was purified by successive washings with chloroform. A doublet of integration 3 and coupling constant 4.87 Hz at 2.62 ppm matched closely the N-methyl doublet of **62** and indicated this material to be uncyclised. Consideration of DEPT, HSQC and HMBC spectra alluded to **65** as a possible structure. This was confirmed when **65** was independently synthesized from **62** and TFAA. At this stage, it appeared that **64** was forming but, rather than dehydrating to give an imine, was undergoing a fluoroform elimination to give **65**.



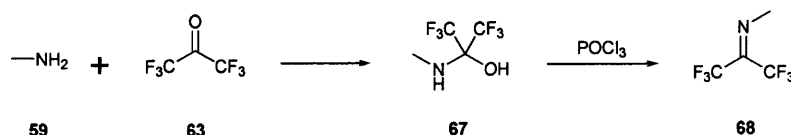
Scheme 2.17

To disfavour this elimination and encourage dehydration, the reaction was repeated in DMSO and in the presence of catalytic TFA (Scheme 2.17). Once again, the spectrum of the crude mixture was ambiguous while column chromatography yielded a complex mixture of products, none of which bore the signature of an imidazolidinone.



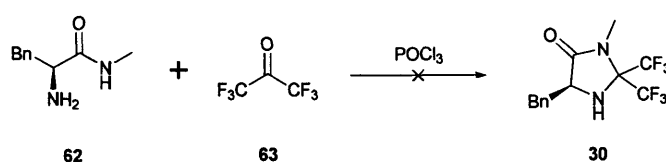
Scheme 2.18

Fluoroform elimination was a quite unexpected side reaction that presented a barrier to further progression with this synthetic methodology. Rather than trying for a one-step synthesis of **30**, it was decided that isolation of **66** followed by a separate cyclisation step might be a more profitable approach (Scheme 2.18). A search of the literature for the preparation of  $\alpha$ -polyfluorinated imines showed that almost all methods employed a dehydrating agent. This indicated that the intermediate aminols did not readily dehydrate.



Scheme 2.19

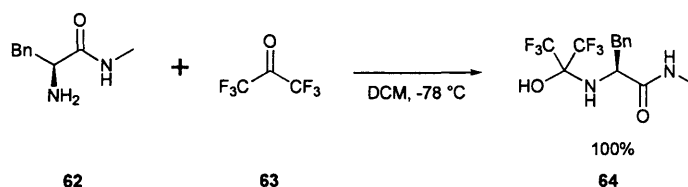
One notable technique for aminol dehydration was the method of Middleton and Krespan.<sup>37</sup> In a representative synthesis, **59** and **63** were allowed to combine at low temperature to yield **67**. POCl<sub>3</sub> was then added, and **68** was isolated by distillation (Scheme 2.19).



Scheme 2.20

Using this methodology, **62** was dissolved in anhydrous pyridine, cooled to  $-20\text{ }^\circ\text{C}$  and treated with **63** and then with phosphorus oxychloride. The reaction mixture was stirred at  $-20\text{ }^\circ\text{C}$  for 1 hour and then refluxed for 2 hours (Scheme 2.20). Extensive column chromatography of the crude reaction mixture failed to isolate any fractions resembling **30**.

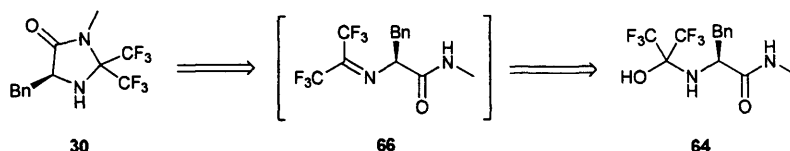
This experiment was reattempted using 1:1 pyridine:acetonitrile as a solvent, allowing the temperature to be lowered to  $-78\text{ }^\circ\text{C}$  before the phosphorus oxychloride was added. Extensive column chromatography was performed on the crude reaction mixture, but failed to isolate the desired product or shed light on why such a diverse array of side products was being formed.



Scheme 2.21

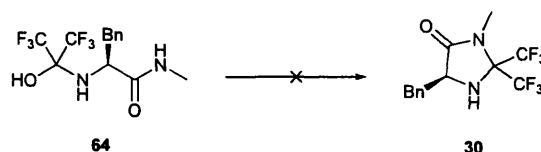
Results so far had been discouraging. While there was indisputable evidence that **62** and **63** were interacting, the only product that had been isolated in any significant yield was **65**. The wide array of side products observed indicated conditions were too forcing. In order to ascertain whether **62** and **63** may form a stable complex under mild conditions, a solution of **62** in anhydrous DCM was cooled to  $-78\text{ }^\circ\text{C}$  and treated with an excess of **63**. Upon warming to room temperature and evaporation of the solvent and excess **63**, pure **64** was obtained in quantitative yield (Scheme 2.21). **64** proved to be a stable compound with a

structure that could be confirmed by full characterization. Further study showed **64** to undergo slow elimination of **63** at room temperature, gradually reverting to **62** over the course of a few weeks. The presence of water or protic solvents was found to speed up this process dramatically, whereas minimal degradation was observed after storage in the absence of air and moisture at low temperature for around a year.



Scheme 2.22

Having formed one of the desired bonds and overcome the problems of dealing with a gas by fixating the trifluoromethyl groups in a stable aminol, attention was focused around converting this intermediate into the desired product **30**. As the trifluoromethyl groups appeared to impart a strong preference for  $sp^3$  hybridisation upon their attached carbon atom, it was envisaged that if imine **66** could be formed in the absence of strong nucleophiles, spontaneous cyclisation should yield **30**, potentially a stable product (Scheme 2.22).



| Reagent                            | Solvent           | Conditions               |
|------------------------------------|-------------------|--------------------------|
| H <sub>2</sub> SO <sub>4</sub>     | -                 | rt, 4h                   |
| CSA                                | CDCl <sub>3</sub> | rt, 16 h                 |
| TFA                                | CDCl <sub>3</sub> | rt, 16h                  |
| BBr <sub>3</sub>                   | CDCl <sub>3</sub> | rt, 5 min                |
| BF <sub>3</sub> ·Et <sub>2</sub> O | CHCl <sub>3</sub> | rt, 5 min                |
| MgSO <sub>4</sub>                  | CDCl <sub>3</sub> | rt, 97 h                 |
| P <sub>4</sub> O <sub>10</sub>     | CDCl <sub>3</sub> | rt, 98 h                 |
| FeCl <sub>3</sub>                  | THF               | rt, 16 h, N <sub>2</sub> |

Scheme 2.23

**64** was stirred in concentrated sulfuric acid for 4 hours, then basified and extracted with ether (Scheme 2.23). Upon evaporation, a mixture of **62** and **64** was returned.

A solution of **64** in deuterated chloroform was treated with catalytic CSA. This also induced elimination of **63** and reversion to **62**.



A solution of **64** in deuterated chloroform was treated with catalytic TFA. Leaving the tube to stand overnight at room temperature induced partial conversion to an unidentified product.  $^1\text{H}$  NMR showed a doublet ( $J = 4.7$  Hz) at 2.50 ppm, indicating the material was uncyclised.

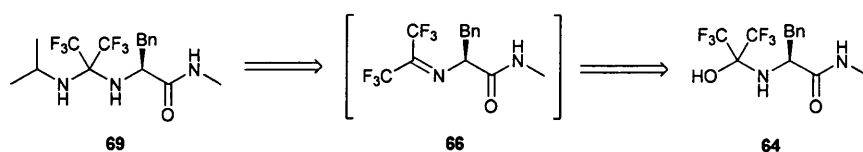
A solution of **64** in deuterated chloroform was treated with catalytic boron tribromide. An immediate reaction occurred and precipitate was formed. Due to the presence of precipitate,  $^1\text{H}$  NMR yielded a poor quality spectrum. It did indicate, however, that a mixture of products had been formed and that treatment of **64** with boron tribromide was unlikely to provide any single product in good yield.

A solution of **64** in deuterated chloroform was treated with catalytic boron trifluoride etherate. A precipitate formed immediately and the reaction was discarded. The reaction was repeated in regular chloroform, using stoichiometric boron trifluoride etherate. The precipitate was filtered, dried, and dissolved in DMSO- $d_6$  for  $^1\text{H}$  NMR. The spectrum appeared to show a complexing of **64** with the boron trifluoride, but did not show any chemical conversion.

A solution of **64** in deuterated chloroform was stirred over magnesium sulphate for 97 hours, then filtered and analysed by  $^1\text{H}$  NMR. This showed that the reaction mixture consisted mainly of **64** with small amounts of **62**.

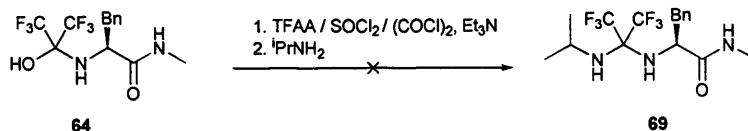
A solution of **64** in deuterated chloroform was stirred over phosphorus pentoxide for 98 hours before being filtered through Celite®. Decomposition or polymerisation appeared to have occurred, as the Celite® retained a quantity of insoluble organic matter, while the deuterated chloroform appeared to contain no solutes.

**64** and 0.3 equivalents iron(III) chloride were stirred in dry THF under nitrogen. Filtration through silica to remove iron complexes and residues returned a small amount of an unidentified compound. The reaction was repeated with stoichiometric iron(III) chloride, and the only product that could be isolated was **65**.



Scheme 2.24

As dehydration of the aminol followed by *in-situ* cyclisation appeared to have failed, attempts were made to test for the presence of an intermediate by capturing it with an amine (Scheme 2.24). Isopropylamine was chosen for its availability in the lab and low boiling point, allowing any excess reagent to be readily evaporated.

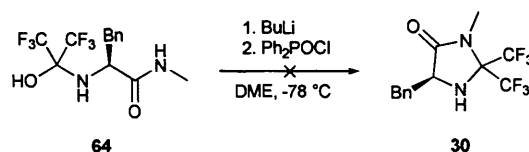


Scheme 2.25

A solution of **64** in deuterated chloroform was treated with TFAA and triethylamine then stirred for 90 hours at room temperature, before excess isopropylamine was added (Scheme 2.25). The solvent and residual isopropylamine were removed by evaporation and the residue was found to contain **62** and **64**, but no trace of **69**.

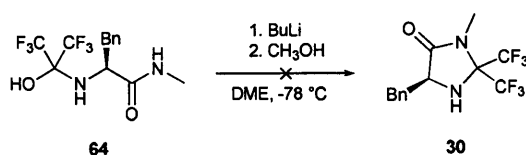
The previous reaction was repeated using thionyl chloride instead of TFAA. Septuplets at 4.73 and 4.53 ppm suggested that the isopropyl moiety had been incorporated, but only in trace quantities.

The experiment was then repeated using oxalyl chloride as the dehydrating agent and gave rise to a mixture of products. Column chromatography was performed, yielding a significant quantity of a bright yellow solid. The structure of this product was not deduced.



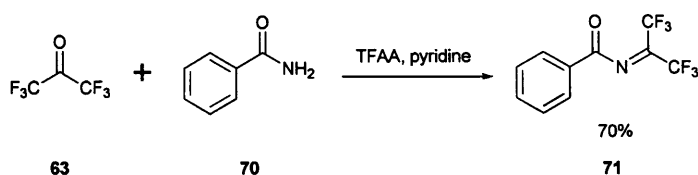
Scheme 2.26

Earlier attempts at dehydrating **64** using phosphorus oxychloride had failed. It was proposed that failure could be due to the phosphorus undergoing attack from the amide functionality of the aminol, as occurs in the Vilsmeier-Haack reaction. As the hydroxyl group of the aminol functionality was acidic, it was conceived that the use of base to remove this proton could lead to its reaction with a dehydrating agent. A solution of **64** in DME at  $-78\text{ }^{\circ}\text{C}$  was treated with butyllithium, followed by diphenyl chlorophosphate (Scheme 2.26). Upon workup, a mixture of products was obtained, including one chloroform-insoluble white solid. A structure for this compound was not elucidated, but  $^1\text{H}$  NMR showed it to be uncyclised while  $^{13}\text{C}$  NMR showed it to be free of trifluoromethyl groups.



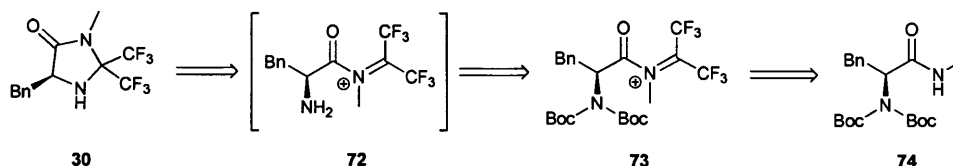
Scheme 2.27

Methanol was substituted for diphenyl chlorophosphate and the reaction repeated (Scheme 2.27). This resulted in a crude reaction mixture consisting mostly of **62**, showing that loss of **63** had occurred.



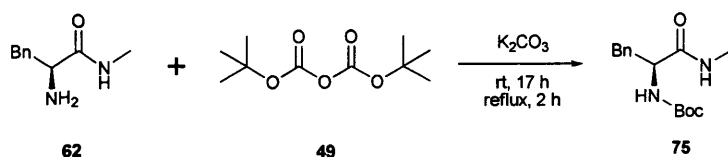
Scheme 2.28

As a testimony to the extreme reactivity of **63**, a search of the literature had revealed its ability to condense with amides to yield N-carbonylimines.<sup>38,39</sup> In the example of Burger *et al*, **63** condensed with **70** in the presence of TFAA and pyridine to furnish **71** (Scheme 2.28). Compounds of this nature appear to be stable, as evidenced by the commercial availability of **71**.



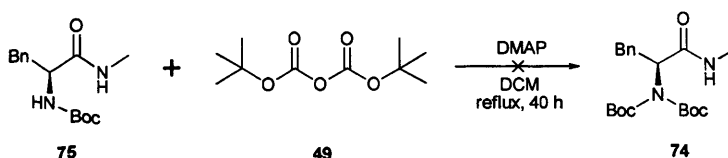
Scheme 2.29

It was envisaged that if the amine functionality of **62** could be protected as compound **74**, condensation with **63** could yield iminium ion **73**. Removal of the Boc groups under acidic conditions would then yield intermediate **72**, which would spontaneously cyclise to the desired compound **30** (Scheme 2.29). As carbamates are more nucleophilic than amides, it was deemed necessary to add two Boc groups such that **74** would condense only with the amide.



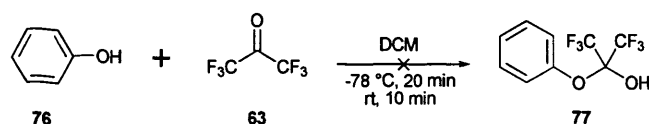
Scheme 2.30

A first attempt at preparing **74** involved stirring **62** in the presence of 2 equivalents of **49** over potassium carbonate in THF for 19 hours at room temperature and 2 hours at reflux (Scheme 2.30). Upon workup, the crude reaction mixture was seen only to contain **49** and **75**, with no trace of **74**.



Scheme 2.31

Refluxing **75** in DCM with DMAP and **49** for 40 hours failed to yield **74**; **75** was returned unchanged (Scheme 2.31). Due to the complexity of the route envisaged towards **30** via **72** and the difficulty in obtaining the initial **74**, these synthetic adventures were curtailed.

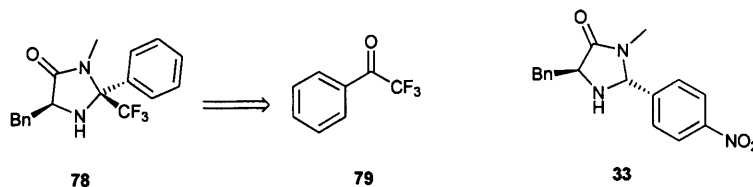


Scheme 2.32

As an investigation to see whether a stable complex between a less powerful nucleophile and **63** could be isolated, a solution of **76** in DCM at  $-78\text{ }^{\circ}\text{C}$  was treated with an excess of **63**. Fixation appeared not to occur, as when the solution was warmed slowly to room temperature and the DCM and excess **63** evaporated, only **76** was returned (Scheme 2.32).

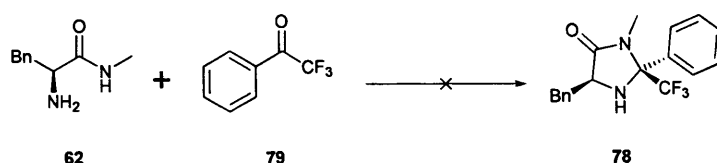
At this point, a lot of synthetic effort had been expended and minimal progress towards **30** had been made. It appeared novel synthetic approaches would be required to access such a highly fluorinated compound and the development of such approaches was beyond the scope of this project. As such, efforts towards **30** were discontinued.

## 2.5 Trifluoroacetophenone



Scheme 2.33

Attempts to incorporate **63** into an imidazolidinone had failed. Accordingly, the less fluorinated structure **78** was targeted. **78** was seen as having similarity to **33**, a catalyst previously developed within the group, as well as theoretically being synthetically accessible from **79**, a relatively cheap and easily handled ketone (Scheme 2.33).



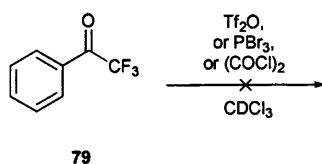
| Catalyst | Solvent           | Conditions         |
|----------|-------------------|--------------------|
| PTSA     | DMF               | MW, 120 °C, 60 min |
| PTSA     | DMF               | 120 °C, 68 h       |
| AcOH     | CHCl <sub>3</sub> | reflux, 42 h       |

Scheme 2.34

An attempt analogous to the synthesis of **33** was made whereby **62**, **79** and catalytic PTSA in DMF were subjected to microwave irradiation at 120 °C for 1 hour (Scheme 2.34). This resulted in a distribution of uncyclised products, but no imidazolidinone was detected by <sup>1</sup>H NMR analysis.

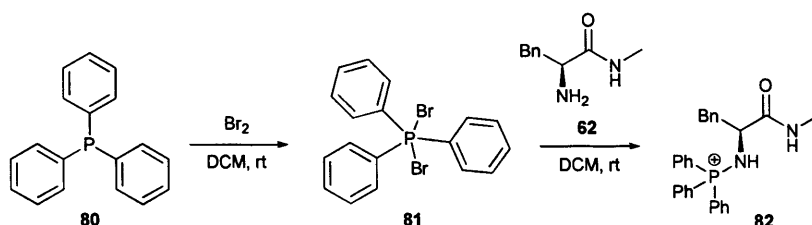
Under thermal conditions, stirring **62** and **79** in DMF at 120 °C with catalytic PTSA for 68 hours resulted in extensive side product formation and no trace of the desired product.

**62** and **79** were then refluxed in chloroform in the presence of acetic acid for 42 hours. Upon analysis by <sup>1</sup>H NMR, the crude was found to contain mainly starting materials, with traces of an unidentified uncyclised product.



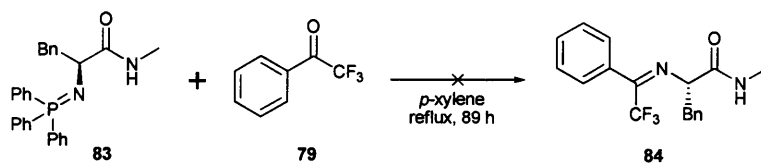
Scheme 2.35

Curious about the apparent unreactivity of **79**, a brief assay was performed to see whether it would react with powerful electrophiles. Solutions of **79** in deuterated chloroform were treated with 1 equivalent of either triflic anhydride, phosphorus(III) bromide, or oxalyl chloride (Scheme 2.35). In each case, no reaction was observed after standing overnight at room temperature.



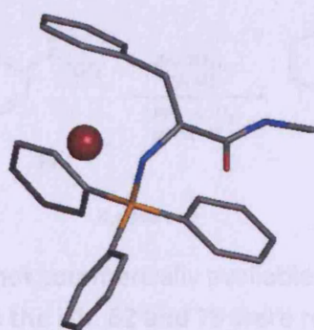
Scheme 2.36

The aza-Wittig reaction can be used to obtain imines from phosphorimines and ketones. The reaction is believed to go *via* a 4-membered intermediate, extruding triphenylphosphine oxide in a manner analogous to the Wittig reaction. Publications were found describing its use in forming fluoroalkylated imines and it was deemed worthy of investigation.<sup>40,41</sup> A solution of **81** was prepared *in-situ* by the reaction of **80** with elemental bromine. Upon the addition of **62**, **82** was formed in qualitative yield (Scheme 2.36). To attempt deprotonation, **82** was then stirred overnight in DCM with potassium carbonate and a material believed to be the phosphorimine **83** isolated.



Scheme 2.37

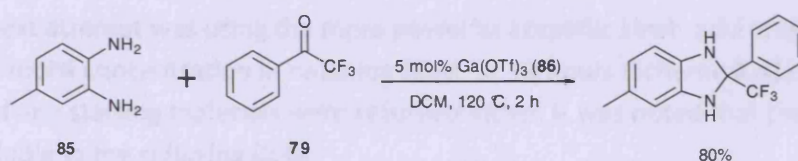
The suspected phosphorimine was then refluxed with **79** for 89 hours in *p*-xylene, but failed to produce **84** (Scheme 2.37).



82

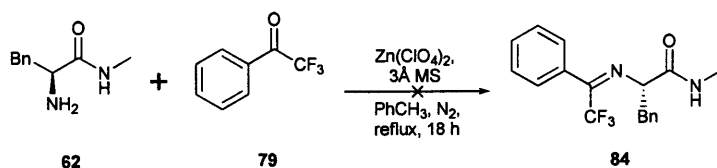
Figure 2.38

After the first isolation of suspected iminophosphorane **83**, crystals were grown by slow evaporation of a DCM solution of the material and submitted for X-ray crystallographic structure determination. Results were returned some time later and showed that rather than the crystalline material being a phosphimine, it was in fact **82**, an aminophosphonium bromide (Figure 2.38). This result explained the failing of the aza-Wittig attempt and showed that the deprotonation of **83** would require more basic conditions to yield **82**.



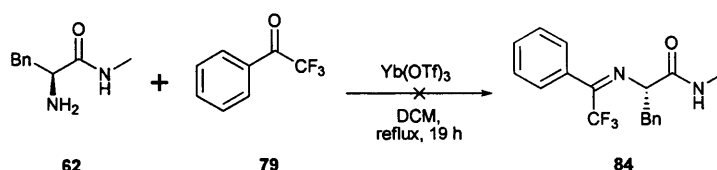
Scheme 2.39

At this time, and before further attempts at deprotonating the iminophosphonium bromide could be made, a paper was found detailing the use of gallium(III) triflate **86** as a catalyst in the formation of benzimidazolines, benzothiazolines, benzoxazolines, and dihydrobenzoxazinones.<sup>42</sup> In the most relevant procedure, **85**, 1.5 equivalents of **79** and 5 mol% gallium triflate **86** were heated in DCM in a sealed tube at 120 °C for 2 hours (Scheme 2.39). After workup, the desired product was obtained in 80% yield. While work within the group had traditionally used protic acids for the synthesis of imidazolidinones, the use of Lewis acids held promise for more facile syntheses. The synthetic challenge of attaining **78** presented an ideal opportunity to investigate the use of Lewis acids in the formation of imidazolidinones.



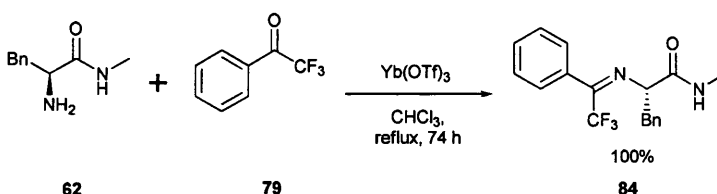
Scheme 2.40

Gallium(III) triflate **86** was not commercially available and initial attempts were made with Lewis acids already present in the lab. **62** and **79** were refluxed in toluene for 18 hours in the presence of 5 mol% zinc perchlorate, a mild Lewis acid (Scheme 2.40). The reaction failed to produce the desired product, and the crude was found to consist solely of starting materials.



Scheme 2.41

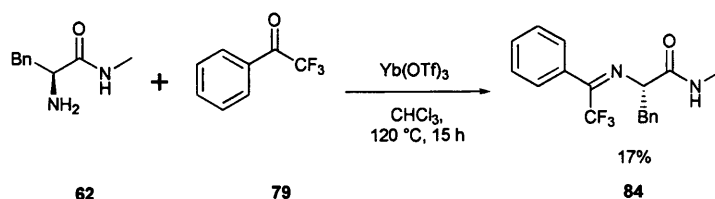
The next attempt was using the more powerful azaphilic Lewis acid ytterbium(III) triflate at 7.5 mol% concentration in refluxing DCM for 19 hours (Scheme 2.41). No reaction was observed and starting materials were returned intact. It was noted that the catalyst seemed insoluble in the refluxing DCM.



Scheme 2.42

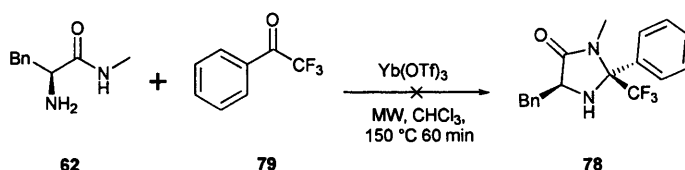
Another attempt in refluxing chloroform using 9 mol% catalyst achieved quantitative conversion to imine **84** but failed to produce any imidazolidinone (Scheme 2.42). While this result was very encouraging, further attempts to discover a one-step condensation and cyclisation reaction seemed warranted.





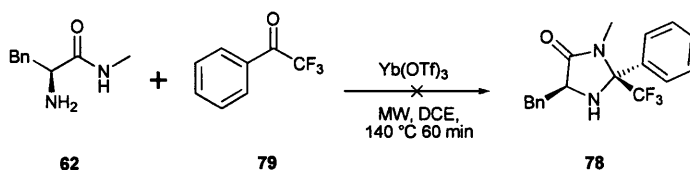
Scheme 2.43

Increasing the temperature to  $120^\circ\text{C}$  by heating **62**, **79**, and ytterbium(III) triflate at  $120^\circ\text{C}$  in a sealed vessel did not induce cyclisation and also yielded lower quantities of imine (Scheme 2.43).



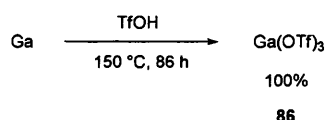
Scheme 2.44

The reaction was then repeated under microwave irradiation at  $150^\circ\text{C}$  for 60 minutes, resulting in widespread decomposition (Scheme 2.44).



Scheme 2.45

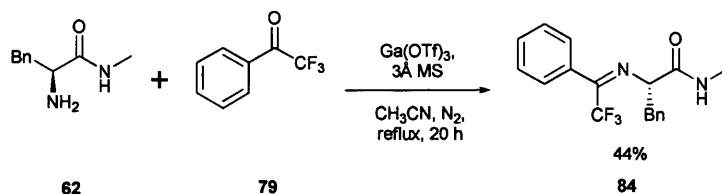
Lowering the temperature to  $140^\circ\text{C}$  and changing the solvent to DCE to reduce pressure in the reaction vessel did not alleviate the decomposition, and the reaction again failed to produce **78** (Scheme 2.45).



Scheme 2.46

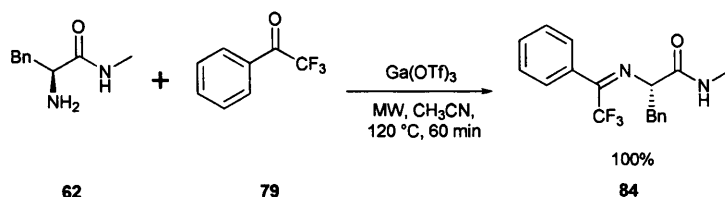
Given the ability of ytterbium(III) triflate to cleanly catalyse the formation of **84**, the investigation into Lewis acids appeared to be bearing fruit. It was deemed worthwhile to synthesise gallium(III) triflate **86** so as to investigate its catalytic efficacy. Accordingly, the synthesis was performed by heating gallium metal in excess triflic acid at  $150^\circ\text{C}$  for 4 days (Scheme 2.46).<sup>43</sup> The progress of the reaction could be observed as lustrous beads of gallium metal rose atop pillars of the light grey triflate. When the majority of gallium had converted to the triflate, the reaction was cooled to room temperature, then poured into water.

Residual gallium metal was removed by filtration and the filtrate was evaporated and the residue dried *in vacuo* at 240 °C to yield gallium(III) triflate **86** in 66% yield. None of the usual forms of characterization were possible due to the nature of the compound. A neutral pH reading indicated the absence of triflic acid and the compound, a freeflowing gray powder, was assumed to be pure.



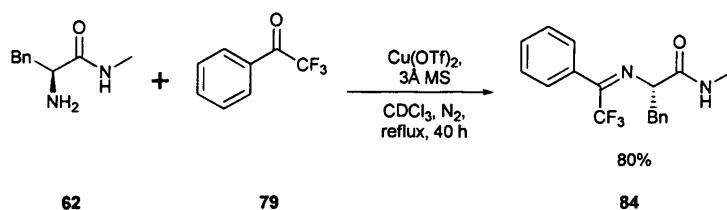
Scheme 2.47

As gallium(III) triflate **86** appeared completely insoluble in chloroform, acetonitrile was used as a reaction solvent. **62** and **79** were refluxed over 3Å molecular sieves in the presence of 5 mol% of the catalyst (Scheme 2.47). This facilitated 44% conversion to **84** but did not induce cyclisation to **78**.



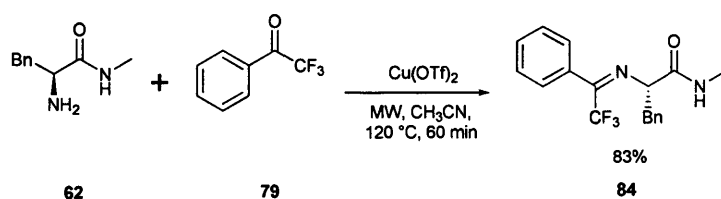
Scheme 2.48

**62** and **79** were then subjected to microwave irradiation in the presence of 15 mol% of gallium(III) triflate **86** at 120 °C for 60 minutes, which induced clean conversion to **84** as a single isomer but again failed to produce any imidazolidinone (Scheme 2.48). Subjectively, in the reactions between **62** and **79**, gallium(III) triflate (**86**) appeared comparable to ytterbium(III) triflate, if a little less potent.



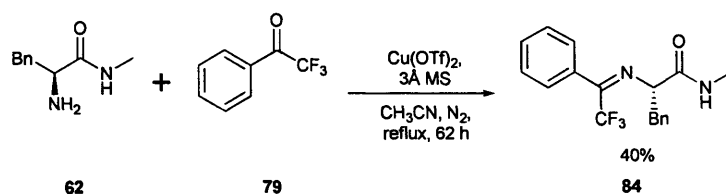
Scheme 2.49

As a final attempt towards a one-step synthesis of **78**, copper(II) triflate was used to catalyse the reaction between **62** and **79**. An attempt under thermal conditions using 8 mol% catalyst under dry conditions induced conversion to **84**, but at a lower rate than ytterbium(III) triflate (Scheme 2.49).



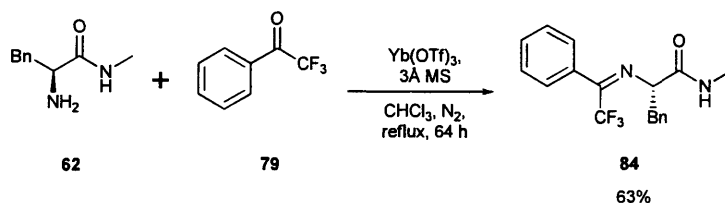
Scheme 2.50

It was suspected that water formed during the condensation of **62** and **79** was moderating the reactivity of the copper catalyst and surmised that by increasing the catalyst loading, the relative effect may be reduced. To investigate this, microwave irradiation of a dry acetonitrile solution of **62** and **79** at  $120^\circ\text{C}$  for 60 minutes in the presence of 29 mol% catalyst was performed (Scheme 2.50). This resulted in 83% conversion to **84** with no detectable cyclisation.



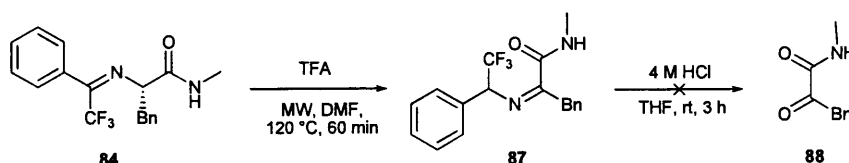
Scheme 2.51

Applying the methodology developed so far, **62** and **79** were refluxed in acetonitrile for 62 hours under nitrogen, over molecular sieves and in the presence of 37 mol% copper(II) triflate. After aqueous workup, column chromatography was used to provide 0.97 g of **84** in 40% isolated yield (Scheme 2.51).



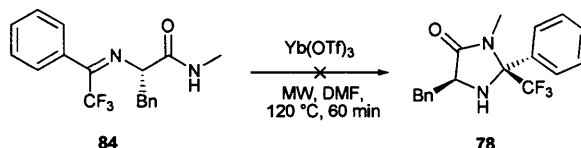
Scheme 2.52

The comparable reaction using 5 mol% ytterbium(III) triflate in refluxing chloroform furnished 1.27 g of **84** in 63% yield (Scheme 2.52). **84** was found to be a stable, air-insensitive, compound and was fully characterised. Having obtained **84**, methodology for its cyclisation to imidazolidinone **78** was developed.



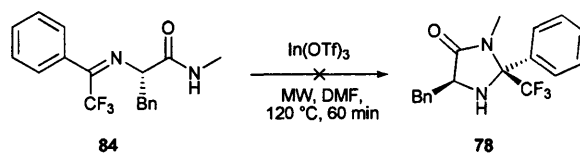
Scheme 2.53

For the sake of simplicity, a protic acid, TFA was tried first. **84** and 36 mol% TFA in DMF were subjected to microwave irradiation at 120 °C for 60 minutes (Scheme 2.53). The  $^1\text{H}$  NMR spectra of the crude showed partial conversion to a single compound that was isolated by column chromatography. Full characterisation was not performed, but the  $^1\text{H}$  NMR spectra acquired indicated the structure to be that of **87**, which may have arisen *via* a 1,3-hydride shift. A doublet of 5.13 Hz and integration 3 at 2.87 ppm indicated the material to be uncyclised, while the benzylic protons originating from the amino amide portion of the molecule appeared as two doublets of coupling 14.42 Hz, indicating the absence of the  $\alpha$ -carbonyl proton with which they normally appeared as an ABX system. The  $\alpha$ -carbonyl proton, normally present at 4.18 ppm and coupled to the benzylic system, had been replaced by a quartet at 5.01 ppm with a coupling constant of 7.23 Hz, a potential value for a  $^3J_{\text{FH}}$  coupling constant.<sup>44</sup> An attempt was made to convert **87** to known compound **88** by stirring in 1:1 4 M hydrochloric acid:THF, but no organic material was recovered upon evaporation and extraction with diethyl ether.



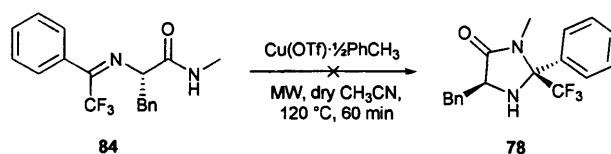
Scheme 2.54

A solution of **84** and ytterbium(III) triflate (13 mol%) in DMF was subjected to microwave irradiation at 120 °C for 60 minutes (Scheme 2.54). Although previous attempts to generate **78** directly from **62** and **79** using ytterbium(III) triflate under microwave irradiation had resulted in decomposition, it was hoped that in the absence of the starting materials and in the absence of the water arising from their condensation, there may exist potential for **84** to cyclise to **78**. This potential was not borne out, as the crude reaction mixture contained mainly **84**, with no traces of **78** appearing.



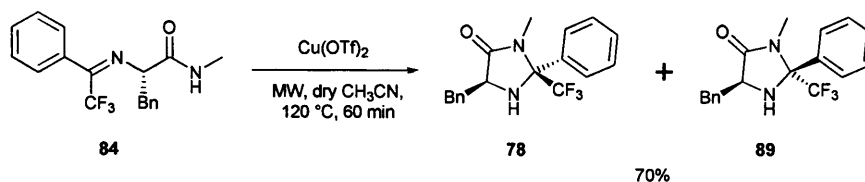
Scheme 2.55

A solution of **84** and indium(III) triflate (31 mol%) in DMF were subjected to microwave irradiation at 120 °C for 60 minutes (Scheme 2.55). The result was similar to the previous experiment and the crude was almost entirely starting material, with traces of **79**.



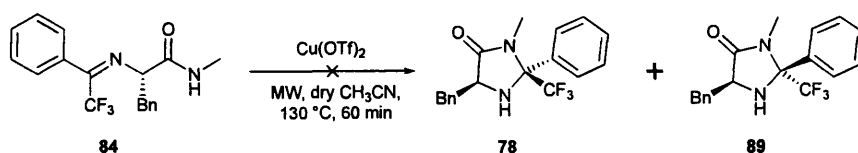
Scheme 2.56

A solution of **84** and copper(I) triflate toluene complex (23 mol%) in dry acetonitrile were subjected to microwave irradiation at 120 °C for 60 minutes (Scheme 2.56). No reaction occurred, and the starting material was returned.



Scheme 2.57

A solution of **84** and copper(II) triflate complex (28 mol%) in dry acetonitrile were subjected to microwave irradiation at 120 °C for 60 minutes (Scheme 2.57). This resulted in clean conversion of **84** into equal amounts of **78** and **89** (70% combined yield).



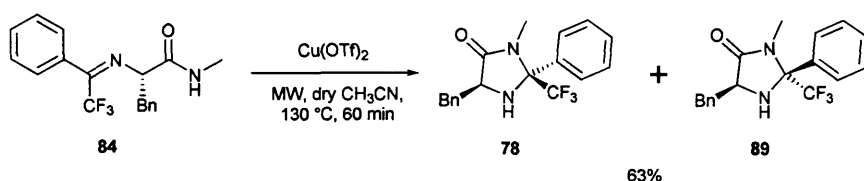
| Cu(OTf) <sub>2</sub> (mol%) | Solvent                | Conditions         |
|-----------------------------|------------------------|--------------------|
| 14                          | CH <sub>3</sub> CN     | MW, 130 °C, 60 min |
| 37                          | CH <sub>3</sub> CN     | MW, 120 °C, 60 min |
| 9                           | dry CH <sub>3</sub> CN | MW, 130 °C, 60 min |

Scheme 2.58

An attempt to lower the catalyst loading by using 14 mol% copper(II) triflate and 130 °C reaction temperature failed and **84** was returned unchanged (Scheme 2.58). It was suspected that improperly dried acetonitrile was deactivating the catalyst.

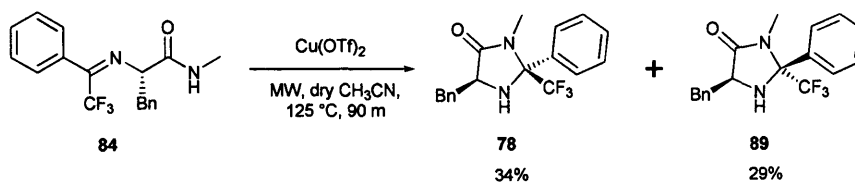
Irradiating **84** in bench acetonitrile in the presence of 37 mol% copper(II) triflate at 120 °C for 60 minutes also failed to induce any cyclisation and **84** was returned. It was observed at this point that if the reagents and reaction solvent were dried, the reaction mixture would initially be a pale turquoise colour, while the presence of water would result in a deep blue colouration. It was therefore surmised that the attempt to reduce the catalyst loading failed due to the presence of water in the reaction mixture.

Noting that the copper(II) triflate in the bottle had a pale blue tinge, it was dried by heating at 100 °C *in vacuo* for 30 minutes, during which time the colouration disappeared. **84** was also dried by heating at 60 °C *in vacuo* for 1 hour then dissolved in freshly distilled acetonitrile. 9 mol% freshly dried catalyst was added and the pale blue solution irradiated at 130 °C for 60 minutes. Unfortunately, despite the attempts to keep the reaction anhydrous, only traces of product were detected and the bulk of the material remained as **84**.



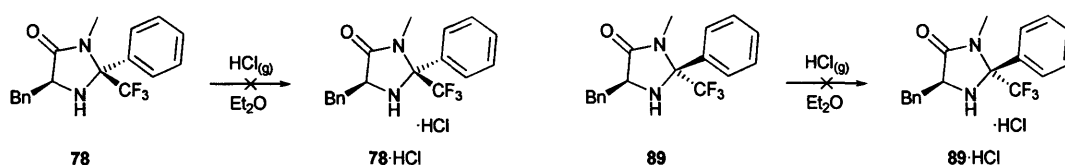
Scheme 2.59

Repeating the previous reaction using 65 mol% pre-dried catalyst in dry acetonitrile resulted in complete conversion of **84** to **78** and **89** (Scheme 2.59). Whereas running the reaction at 120 °C had resulted in a 1:1 ratio of the diastereomers, this reaction provided **78** and **89** in a 2:1 ratio (63% combined yield).



Scheme 2.60

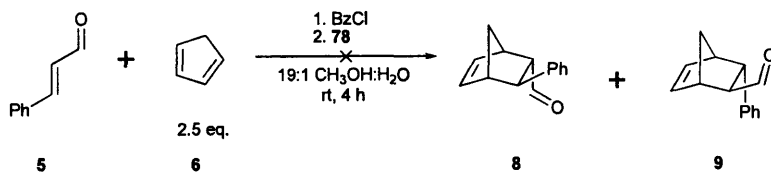
Having determined the conditions required for the cyclisation of **84** to occur, the reaction was scaled up. 0.95 g of **78** and 50 mol% copper(II) triflate in 15 mL dry acetonitrile were irradiated at 125 °C for 90 minutes (Scheme 2.60). An aqueous workup was performed to remove the catalyst, and column chromatography provided clean **78** and **89**, in 34% and 29% yield, respectively.



Scheme 2.61

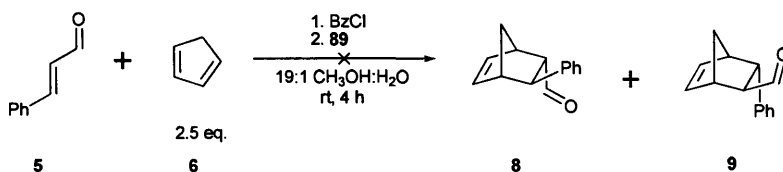
An unexpected barrier to further progress was stumbled upon when attempting to form hydrochloride salts of **78** and **89**. In accordance with the standard procedure for forming catalyst hydrochloride salts, ethereal solutions of **78** and **89** were treated with anhydrous hydrogen chloride gas generated from the reaction of concentrated sulfuric acid upon ammonium chloride (Scheme 2.61). In the usual case, upon treatment with hydrogen chloride gas, the formerly clear ethereal solution was seen to turn cloudy for a few seconds, before regaining transparency as a precipitate appears. Precipitate formation is usually complete after 10 minutes and the product may be obtained in a pure form by filtering and washing with ether. When this procedure was attempted with **78** and **89**, however, no reaction of the ethereal solution with the hydrogen chloride gas was noted, even when the gas was bubbled through for 1 hour. Evaporation of the now-fuming ethereal solutions returned **78** and **89** as free amines. While unexpected at the time, literature descriptions of similarly fluorinated amines indicate that low basicity and an unwillingness to form salts is not unprecedented.<sup>45,46</sup>

## 2.6 Benchmark Reaction Attempted



Scheme 2.62

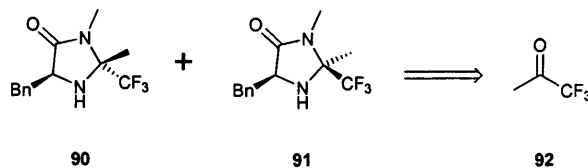
Discovery of a synthetic route to **78** and **89** had proved most troublesome and required substantially more effort than expected. As such, it was deemed necessary to properly test for catalytic activity, rather than assuming their inability to form hydrochloride salts would render them catalytically inactive. In a modification to the standard procedure for performing Diels-Alder reactions, benzoyl chloride was preadded to methanol, generating 1 equivalent of hydrogen chloride *in situ*, after which water and **78** was added, followed by **5** and **6** (Scheme 2.62). After stirring the homogenous solution for 4 hours, no conversion to **8** or **9** was observed.



Scheme 2.63

The reaction was repeated with **89**, which also resulted in no conversion after 4 hours (Scheme 2.63). These results, combined with the lack of basicity observed with **78** and **89**, led to the conclusion that **78** and **89** were not catalytically active in the Diels-Alder reaction of **5** and **6**. Further investigations were not performed.

## 2.7 Trifluoroacetone based catalysts

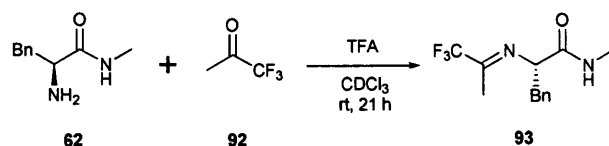


Scheme 2.64

Loath to discard hard won experience in the incorporation of fluoroalkyl groups into the imidazolidinone architecture, a final attempt at a functional trifluoromethylated catalyst

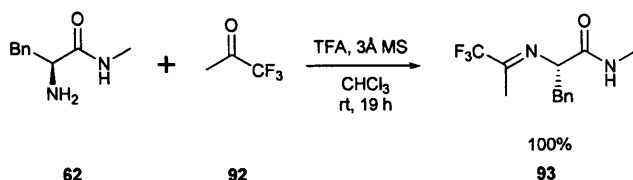


was made. **90** and **91**, lacking the phenyl EWG of **78** and **89**, were seen to have the potential to be basic and nucleophilic enough to be viable catalysts (Scheme 2.64) (calculated basicities: Chapter 7.2).



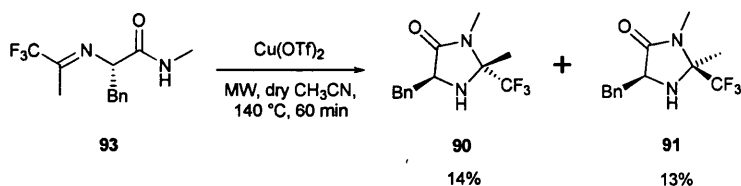
Scheme 2.65

**92** proved difficult to handle, due to its low viscosity and low boiling point (22 °C). In order to assess the ease with which **62** and **92** may condense to form **93**, conveniently fixating the trifluoromethyl moiety, **62**, 4 equivalents of **92** and a drop of TFA were dissolved in deuterated chloroform and reaction progress monitored by <sup>1</sup>H NMR (Scheme 2.65). Total conversion of **62** to **93** was observed after the NMR tube was allowed to stand overnight at room temperature.



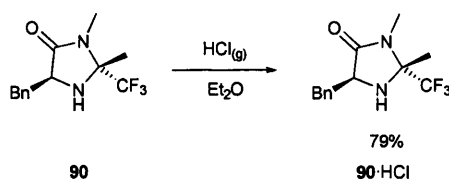
Scheme 2.66

**62** and 2 equivalents of **92** were stirred with 1 drop of TFA in chloroform for 19 hours. Upon evaporation of the solvent and excess **92**, 8.1 g of **93** was obtained in qualitative yield (Scheme 2.66).



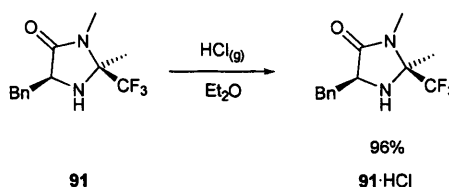
Scheme 2.67

Using the same procedure as was developed for the cyclisation of **84**, **93** and 22 mol% copper(II) triflate in dry acetonitrile were irradiated at 140 °C for 60 minutes. After aqueous workup and column chromatography, **90** and **91** were obtained in 14% and 13% yield, respectively (Scheme 2.67).



Scheme 2.68

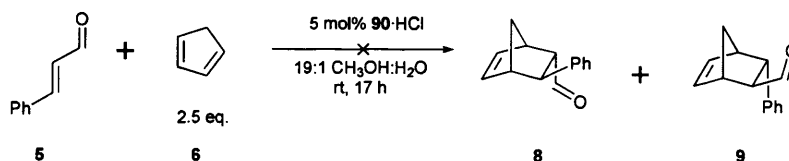
In line with the normal procedure for forming hydrochloride salts, an ethereal solution of **90** was treated with hydrogen chloride gas (Scheme 2.68). Initially, no interaction was noted and the hydrogen chloride gas was observed to bubble freely through the solution. After around 40 minutes, an abrupt change was noted as precipitate began to form and gas absorption began. A further 5 – 10 minutes later, hydrogen chloride was once again seen to be passing freely through the solution and the insoluble product was isolated by filtration, yielding **90·HCl** (79%). The procedure was repeated using fresh **90** and once again, a prolonged period of apparent inactivity occurred before precipitate was seen to form.



Scheme 2.69

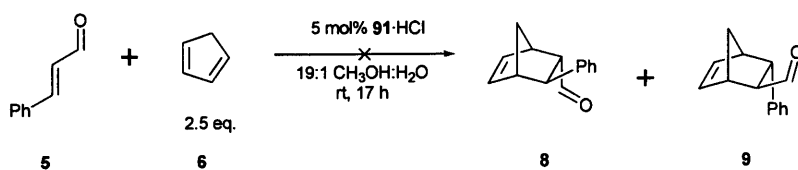
An ethereal solution of **91** exhibited the same behaviour when treated with hydrogen chloride gas, yielding **91·HCl** in 96% yield (Scheme 2.69).

## 2.8 Benchmark Reaction Re-attempted



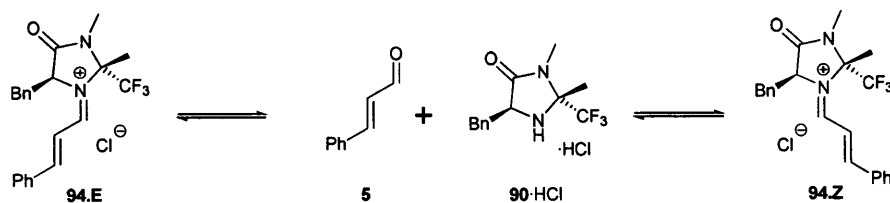
Scheme 2.70

**90·HCl** was evaluated in the benchmark reaction, but failed to catalyse any product formation even after the reaction had been run for 17 hours at room temperature (Scheme 2.70).



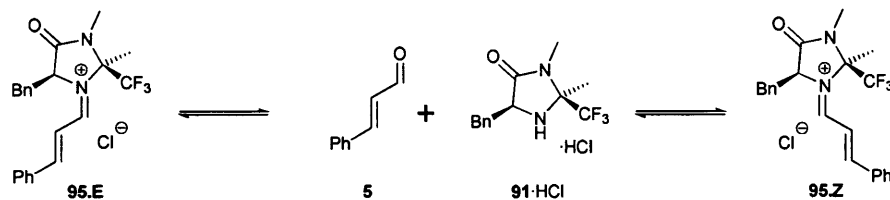
Scheme 2.71

**91·HCl** was evaluated in the same manner and found to be without activity (Scheme 2.71).



Scheme 2.72

A 0.1 M solution of **90·HCl** in 19:1 deuterated methanol:deuterated water was treated with 5 equivalents of **5** and the results observed by  $^1\text{H}$  NMR (Scheme 2.72). No traces of **94.E** or **94.Z** were observed even after more than 48 hours standing at room temperature.



Scheme 2.73

The experiment was repeated with **91·HCl** and showed no sign of iminium ions after standing for over 48 hours at room temperature (Scheme 2.73). These experiments indicated that the reason for the lack of catalytic activity observed with **90** and **91** is rooted in their unwillingness to form iminium ions with **5** under the conditions examined. It appeared that while the elimination of the phenyl group of **78** and **89** had allowed hydrochloride salt formation to occur, the trifluoromethyl EWG was still too strong to allow **90** and **91** to exhibit iminium ion formation and catalytic activity.

## 2.9 Trichloromethyl EWG attempts

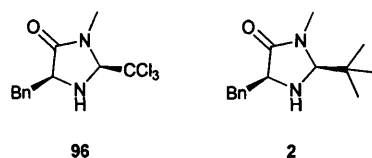
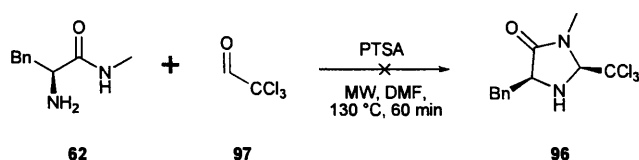


Figure 2.74

As the trifluoromethyl group had proved too strong an EWG to be incorporated at the 2-position of an imidazolidinone catalyst, the trichloromethyl group was considered. The longer carbon-chlorine bond length and greater van der Waals radius of the chlorine atoms renders the trichloromethyl group a closer steric match to a *tert*-butyl group than a methyl group. Accordingly, **96** presented a sensible target structure that could be considered as an analogue of **2** and may thus have potential for use in open transition state reactions (Figure 2.74).



| Reagents                  | Solvent | Conditions               |
|---------------------------|---------|--------------------------|
| PTSA                      | DMF     | MW, 130 °C, 60 min       |
| FeCl <sub>3</sub> , 3Å MS | dry THF | rt, 41 h, N <sub>2</sub> |
| FeCl <sub>3</sub>         | dry THF | rt, 22 h, N <sub>2</sub> |

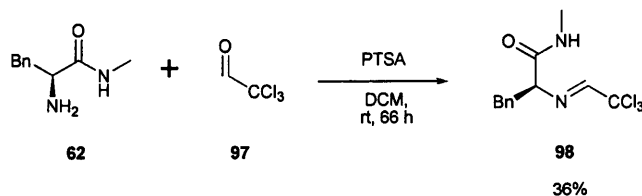
Scheme 2.75

A one-step synthesis of **96** was attempted when **62**, **97** and 17 mol% PTSA were subjected to microwave irradiation in DMF at 130 °C for 60 minutes (Scheme 2.75). The resultant dark oil was found to contain a large number of unidentified compounds and the reaction was deemed to have failed.

In a preparation analogous to that published for **2**, **62**, **97** and 23 mol% iron(III) chloride were stirred over 3Å molecular sieves in dry THF at room temperature.<sup>12</sup> Multiple products were observed in the crude mixture, including traces of a possible imine.

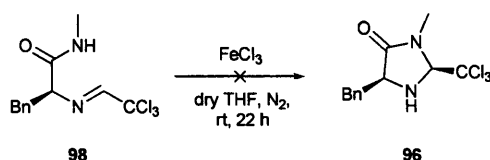
As the formation of brown iron(III) oxide indicated that the reaction was generating water, it was hoped that by using a larger amount of catalyst, the water of condensation may be absorbed without deactivating all of the iron(III) chloride. Molecular sieves were omitted as they appeared unable to sequester water before it reacted with the iron(III) chloride. **62**, 1.7 equivalents of **97** and 93 mol% iron(III) chloride were stirred in dry THF for 22 hours.

Once again, a mixture of products was observed, including a potential imine. As a one-step synthesis appeared out of reach, a two-step solution was sought.



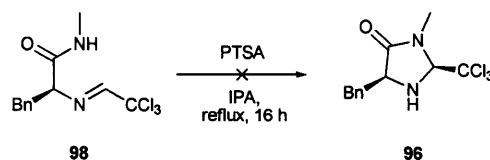
Scheme 2.76

**62** and **97** were stirred in DCM with 9 mol% PTSA at room temperature for 66 hours (Scheme 2.76). A aqueous workup was performed to remove the PTSA and the crude was subjected to column chromatography, providing **98** in 36% yield.



Scheme 2.77

**98** and iron(III) chloride were stirred in dry THF under nitrogen at room temperature for 22 hours. The crude was taken up in diethyl ether and washed with water and brine. Upon evaporation, no residue was obtained, indicating the products were lost in the aqueous layers (Scheme 2.77).



Scheme 2.78

**98** and 14 mol% PTSA were refluxed in IPA for 16 hours (Scheme 2.78). After aqueous workup, the resultant mixture was seen to contain a mixture of products, none of which appeared to be **96**. **98** appeared to have a marked propensity for decomposing rather than cyclising. No further efforts towards **96** were performed.

## 2.10 Conclusions

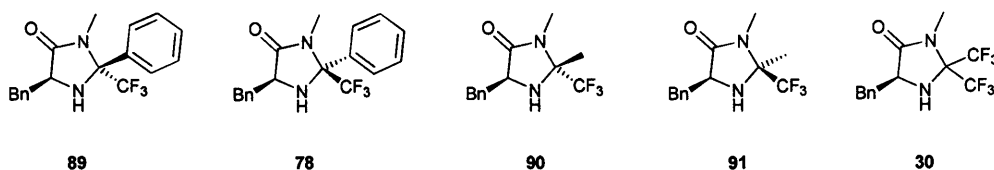
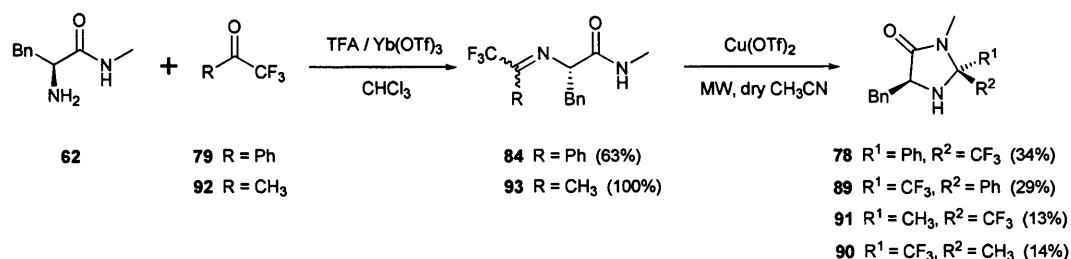


Figure 2.79

Before the research in this chapter was conducted, an upper limit to the strength of EWGs capable of being incorporated into a functioning imidazolidinone catalyst had not been envisaged, and it was imagined that performance might scale linearly with EWG strength. This has now been proven false and the fatal effect of the trifluoromethyl group upon an imidazolidinone's catalytic ability has been established by the synthesis and evaluation of **89**, **78**, **90**, and **91** (Figure 2.79). **30**, which was previously seen as a desirable target, is still believed to be synthetically accessible yet now believed to be catalytically inactive.



Scheme 2.80

A novel synthetic route capable of furnishing previously unreported imidazolidinones in good yields has been developed (Scheme 2.80). Ytterbium(III) triflate was found to catalyse the condensation of **62** and **79** in refluxing chloroform providing **84** in up to 63% yield. TFA was found to catalyse the condensation of **62** and **92** in chloroform at room temperature, giving quantitative conversion to **93**. Both **84** and **93** were found to cyclise in the presence of copper(II) triflate under microwave irradiation to provide **78**, **89**, **91**, and **90**, in 34%, 29%, 13% and 14% isolated yield, respectively. A search of the literature revealed that, to date, this work represents the first general purpose route to 2-fluoroalkylated imidazolidinones. The experience and knowledge gained in imidazolidinone synthesis should allow for access to a wider range of target structures and permit greater freedom in catalyst design.

## 2.11 Further Work

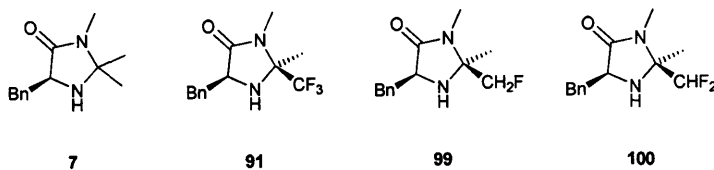
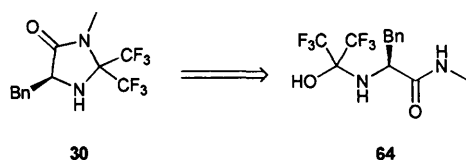


Figure 2.81

**7** is a functioning, albeit slow, catalyst. It has now been established that **91**, possessing a trifluoromethyl EWG is bereft of catalytic activity in the presence of hydrogen chloride as a co-acid (Figure 2.81). An obvious line of research would therefore be to synthesise **99** and **100**, adapting existing synthetic procedures as necessary.



Scheme 2.82

While unlikely to possess catalytic activity, **30** is expected to be a stable compound and might be attainable *via* dehydrating of **64** (Scheme 2.82). This would present the first general synthesis of such a heavily fluorinated imidazolidinone and could allow the formation of differentially substituted 2,2-bis(trifluoromethyl)imidazolidinones, which, being deactivated mimics of imidazolidinone rings, may have potential in pharmaceutical design.

---

## **Chapter 3: Direct Comparison of Imidazolidinone and Diarylprolinol Ether Reactivity**

---



### 3 Direct Comparison of Imidazolidinone and Diarylprolinol Ether Reactivity

#### 3.1 Attribution

The experimental work within this chapter was performed largely by Ronan Pommereuil, an Erasmus project student working under my supervision.

#### 3.2 Introduction

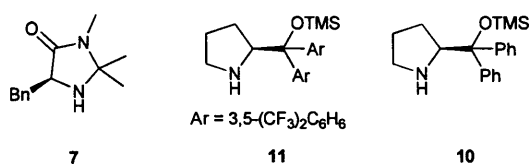
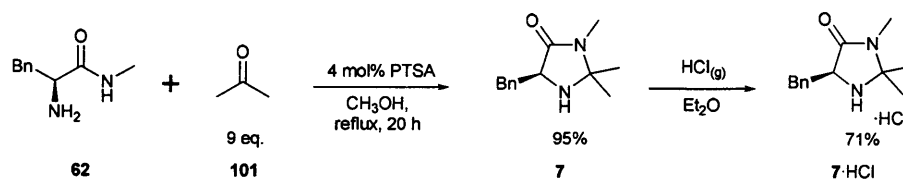


Figure 3.1

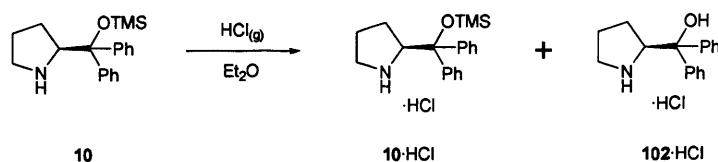
For catalysing the Diels-Alder reaction, **7** is the preferred imidazolidinone and **11** is the preferred diarylprolinol ether catalyst (Figure 3.1).<sup>47,48</sup> The goal of the work documented within this chapter was to perform a fair comparison of **7** and **11** and determine which architecture holds the most promise for accelerating Diels-Alder reactions. **10** has seen use in catalysing asymmetric Michael reactions and was included for the sake of comparison.<sup>49</sup>

#### 3.3 Catalyst Acquisition



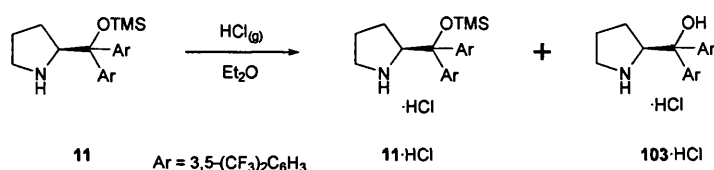
Scheme 3.2

**62** was refluxed in methanol with an excess of acetone and catalytic PTSA for 16 hours to provide **7** in 95% yield (Scheme 3.2). Treatment of an ethereal solution of **7** with hydrogen chloride gas yielded **7·HCl** (71%).



Scheme 3.3

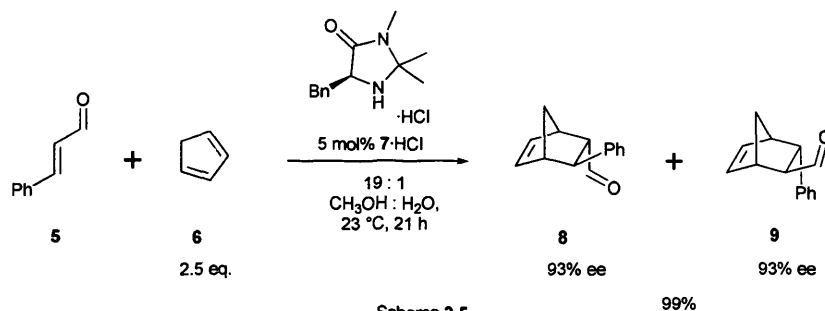
Catalyst **10** was obtained commercially. Upon treatment of an ethereal solution of **10** with hydrogen chloride gas, a mixture of **10·HCl** and **102·HCl** was obtained (Scheme 3.3).



Scheme 3.4

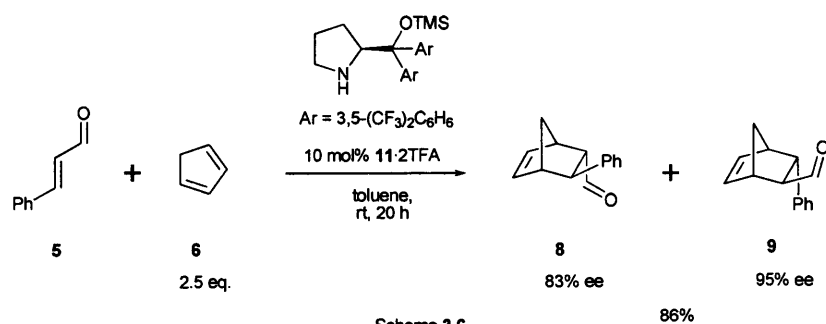
Catalyst **11** was also obtained commercially. Upon treatment of an ethereal solution of **11** with hydrogen chloride gas, partial deprotection of the silyl ether occurred and a mixture of **11·HCl** and **103·HCl** was returned (Scheme 3.4).

### 3.4 Experiment Design



Scheme 3.5

In his seminal paper on the organocatalysed Diels-Alder reaction, MacMillan showed **7·HCl** to be his catalyst of choice.<sup>2</sup> **7·HCl** was shown to catalyse the reaction between **5** and **6** at  $23^\circ\text{C}$  in 19:1 methanol:water to yield **8** (93% ee) and **9** (93% ee) in 99% combined yield in 8 hours (Scheme 3.5).



Scheme 3.6

As published by Hayashi in 2007, 10 mol% **11** and 20 mol% TFA catalysed the reaction between **5** and **6** in toluene at room temperature in 20 hours to yield **8** (83% ee) and **9** (95% ee) in 86% combined isolated yield (Scheme 3.6).<sup>47</sup>

The differing conditions used by MacMillan and Hayashi prompted the design of a comparison that would be fair to both architectures. The most comprehensive comparison would be the use of **7**·HCl, **10**·HCl and **11**·HCl in both 19:1 methanol:water and in toluene, as well as the use of **7**, **10** and **11** in conjunction with 2 equivalents of TFA in 19:1 methanol:water and in toluene. Unfortunately, the failure of **10** and **11** to form hydrochloride salts without partial loss of the TMS protecting group meant that only **7** could be used as its hydrochloride salt.

### 3.5 Experimental Results

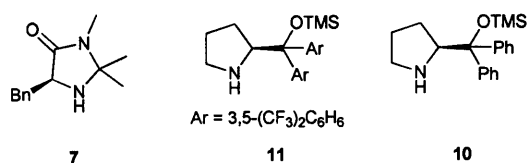
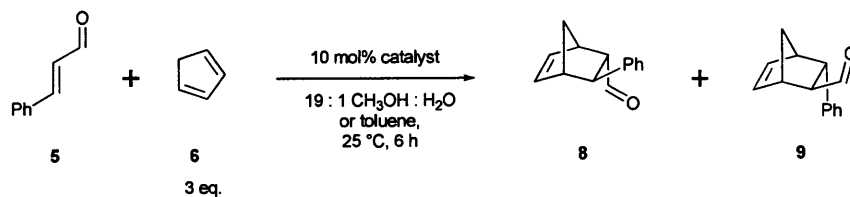


Figure 3.7



Scheme 3.8

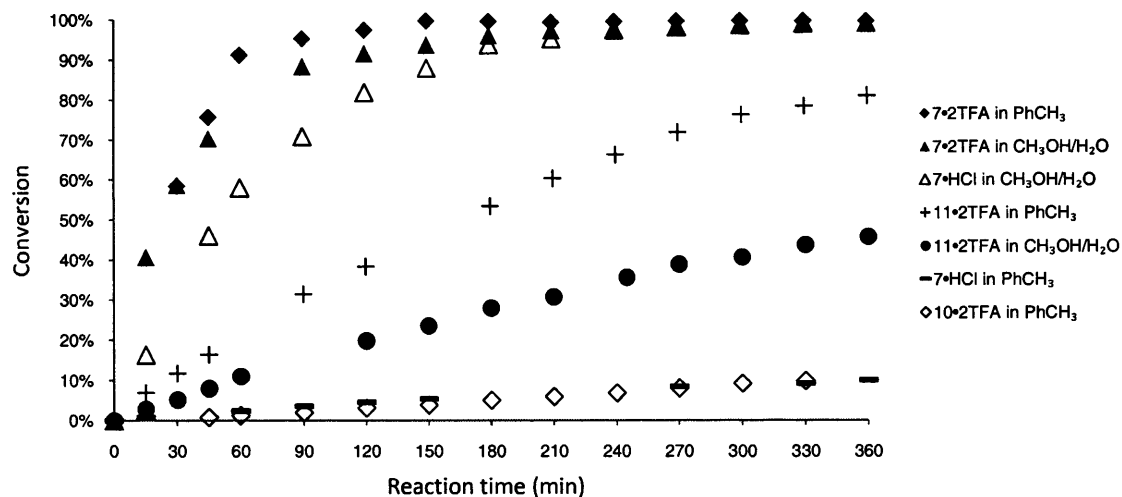


Figure 3.9

| Catalyst | Solvent                                  | 9 ee | 8 ee |
|----------|--|------|------|
| 7·2TFA   | 19:1 CH <sub>3</sub> OH:H <sub>2</sub> O | 93   | 96   |
| 7·HCl    | 19:1 CH <sub>3</sub> OH:H <sub>2</sub> O | 93   | 93   |
| 11·2TFA  | 19:1 CH <sub>3</sub> OH:H <sub>2</sub> O | 90   | 95   |
| 11·2TFA  | PhCH <sub>3</sub>                        | 91   | 89   |
| 7·2TFA   | PhCH <sub>3</sub>                        | 86   | 89   |

Figure 3.10

All reactions were run at 25 °C for 6 hours, at 0.5 M **5** concentration, with 2.5 equivalents of **6** and 10 mol% catalyst or catalyst hydrochloride loading (Scheme 3.8). Where needed, TFA was used at 20 mol% loading. For the reactions performed in 19:1 methanol:water, aliquots were taken at periodic intervals and worked up as per the

benchmark Diels-Alder procedure (see Chapter 10.2 for full details). For reactions performed in toluene, the hydrolysis step was omitted and aliquots were subjected directly to a basic workup then the diethyl ether evaporated and relative aldehyde concentrations determined by  $^1\text{H}$  NMR.

### 3.6 Analysis

The low performance of **10**·2TFA in toluene ( $\diamond$ ) was surprising, especially when compared to the much higher performance of **11**·2TFA in the same solvent system (+). It appeared that the four trifluoromethyl EWGs had a very pronounced effect on the performance of the diarylprolinol architecture. Due to the low performance shown by **10** in this system, no attempts were made to measure product ee's. **10**'s performance in the 19:1 methanol:water system was not investigated.

**11**·2TFA showed higher performance and also greater enantiocontrol when used in toluene (+) than when used in 19:1 methanol:water ( $\bullet$ ). Its turnover in toluene was far higher than that achieved by **10**·2TFA ( $\diamond$ ) yet still lower than that achieved by **7**·2TFA in toluene ( $\blacklozenge$ ) and 19:1 methanol:water ( $\blacktriangle$ ) and **7**·HCl in 19:1 methanol:water ( $\Delta$ ).

The poor performance of **7**·HCl in toluene ( $-$ ) was expected, as it showed very little solubility in this medium. Accordingly, no attempt to determine product ee's was undertaken. In 19:1 methanol:water, **7**·HCl was readily soluble and demonstrated good turnover and good enantiocontrol ( $\Delta$ ).

**7**·2TFA in 19:1 methanol:water ( $\blacktriangle$ ) showed higher turnover than **7**·HCl in the same solvent ( $\Delta$ ), and also exhibited greater enantiocontrol.

**7**·2TFA in toluene ( $\blacklozenge$ ) showed the highest turnover of all systems tested, but also exhibited lower levels of enantiocontrol than any of the other systems for which ee's were measured.

### 3.7 Conclusions

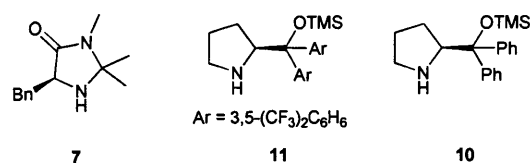


Figure 3.11

The results indicated that **7** consistently attained higher turnover and greater enantiocontrol than **11**, the favoured prolinol-based catalyst (Figure 3.11). This reinforced the choice of the imidazolidinone architecture as the main target of investigations carried out in this project.

Most interestingly, the conditions published by MacMillan for use of **7** were found to be suboptimal for the Diels-Alder reaction used in our investigations. **7**·2TFA in 19:1 methanol:water was seen to exhibit higher turnover and greater enantiocontrol than **7**·HCl in the same solvent system. As no rationale for the effects of co-acid and solvent system has been devised, it is quite possible that a brute force screening of reaction parameters could find a still more optimal system for the use of **7** in the reaction between **5** and **6**.

---

## **Chapter 4: High-Performance Imidazolidinones**

---

## 4 High-Performance Imidazolidinones

### 4.1 Introduction

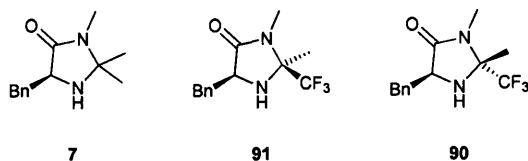


Figure 4.1

The primary goal of this project was to develop a catalyst for iminium-ion catalysed reactions that was both fast and selective. Benchmark catalyst **7** displayed high levels of enantiocontrol and it was thought that by adding EWGs, a turnover increase could be attained (Figure 4.1). In Chapter 2.7, the synthesis of **91** and **90** was described. **91**·HCl and **90**·HCl were prepared but were found to be inactive in the benchmark Diels-Alder reaction. It was believed that the trifluoromethyl EWG rendered **91** and **90** insufficiently nucleophilic to form iminium ions.

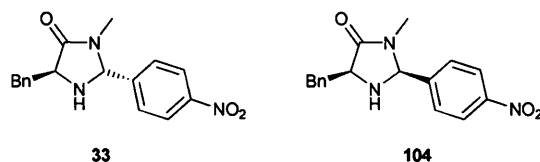
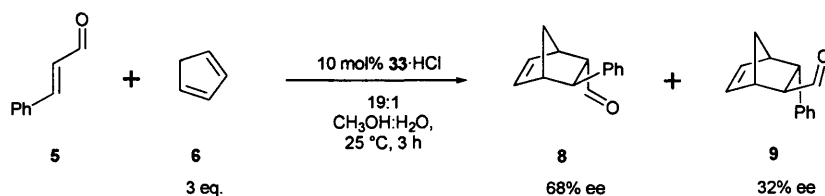


Figure 4.2

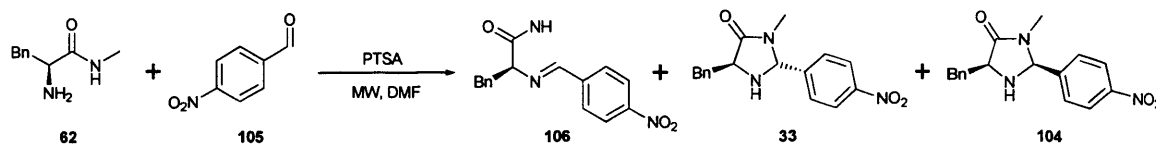


Scheme 4.3

Previous work within the group had found **33** to be a powerful catalyst (Figure 4.2). 10 mol% of **33**·HCl was found to catalyse the reaction between **5** and 3 equivalents of **6** in 19:1 methanol:water at 25 °C, achieving 78% conversion to **8** (68% ee) and **9** (34% ee) in 3 hours (Scheme 4.3).<sup>30</sup> Although this catalyst exhibited poor stereocontrol, the rate of conversion was significantly higher than that of **7**. Synthesis and re-evaluation of **33** and its diastereomer **104** appeared a suitable starting point for the work within this chapter.



## 4.2 EWG Imidazolidinone Synthesis

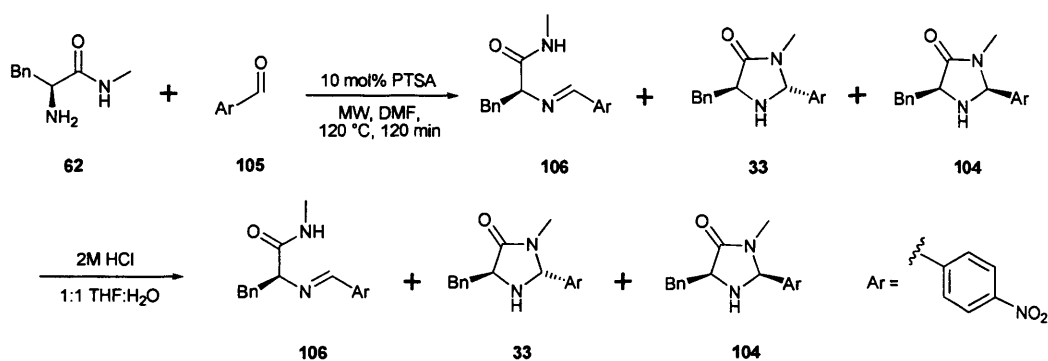


Scheme 4.4

Using the method discovered previously within the group, **62**, **105** and 12 mol% PTSA in DMF were subjected to microwave irradiation at 120 °C for 30 minutes (Scheme 4.4). After a basic aqueous workup to remove PTSA and DMF,  $^1\text{H}$  NMR showed the crude to contain mainly **106**. **33** and **104** were present in small amounts, but isolation was not attempted.

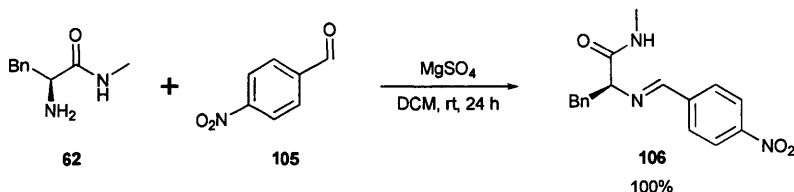
**62**, **105** and 12 mol% PTSA in DMF were subjected to microwave irradiation at 120 °C for 60 minutes.  $^1\text{H}$  NMR of the crude showed that the extended reaction time had increased conversion to **33** and **104** but the continued presence of **106** rendered purification by column chromatography troublesome.

**62**, **105** and 13 mol% PTSA in DMF were subjected to microwave irradiation at 150 °C for 60 minutes.  $^1\text{H}$  NMR of the crude showed increased presence of **33** and **104** when compared to previous experiments. Column chromatography was attempted using 95:4:1 DCM:CH<sub>3</sub>OH:Et<sub>3</sub>N but streaking was observed and neither **33** nor **104** could be obtained pure using this eluent system.



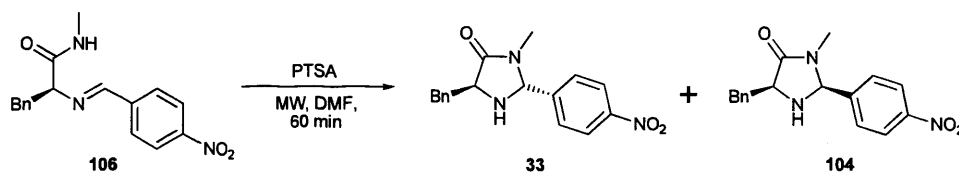
Scheme 4.5

The reaction was repeated when **62**, **105** and 10 mol% PTSA in DMF were irradiated at 120 °C for 120 minutes (Scheme 4.5). The crude showed relatively clean conversion to **33** and **104** with **106** present in small amounts. In an attempt to hydrolyse **106**, the crude was stirred in 1:1 THF:hydrochloric acid (4 M) for an hour. Unfortunately, **106** remained intact.



Scheme 4.6

Before further attempts towards a one-step synthesis of **33** were undertaken, it was discovered that stirring **62** and **105** over magnesium sulphate in DCM for 24 hours resulted in complete conversion to **106** (Scheme 4.6).



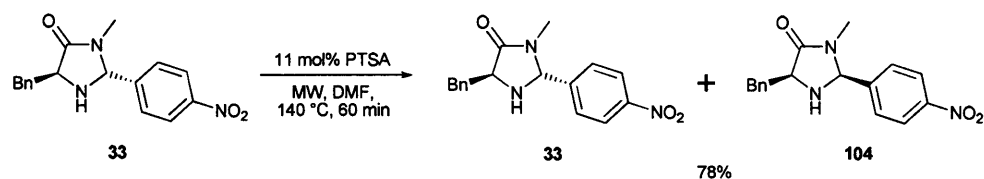
| PTSA (mol%) | Temperature | <b>33</b> (%) | <b>104</b> (%) |
|-------------|-------------|---------------|----------------|
| 12          | 140         | 50            | 18             |
| 11          | 150         | 41            | 24             |
| 11          | 130         | 41            | 35             |

Scheme 4.7

**106** and 12 mol% PTSA in DMF were irradiated at 140 °C for 60 minutes (Scheme 4.7).  $^1\text{H}$  NMR of the crude showed the presence of **33** and **104** as well as traces of side products. After column chromatography, **33** (50%) and **104** (18%) were obtained.

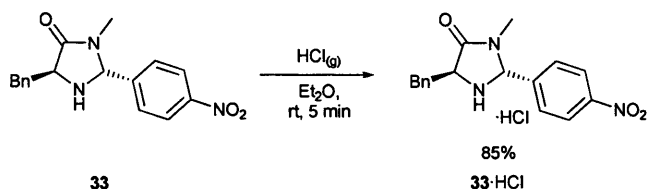
To investigate the effect of raising the temperature, **106** and 11 mol% PTSA in DMF were irradiated at 150 °C for 60 minutes.  $^1\text{H}$  NMR of the crude showed the presence of **33** and **104** as well as small amounts of side products. After column chromatography, **33** (41%) and **104** (24%) were obtained.

It was suspected that the reaction would proceed more cleanly at a lower temperature. 4.5 g of **106** and 11 mol% PTSA in DMF were irradiated at 130 °C for 60 minutes.  $^1\text{H}$  NMR of the crude showed very clean conversion to **33** and **104**. Column chromatography yielded **33** (41%) and **104** (35%) in quantities sufficient for evaluation.



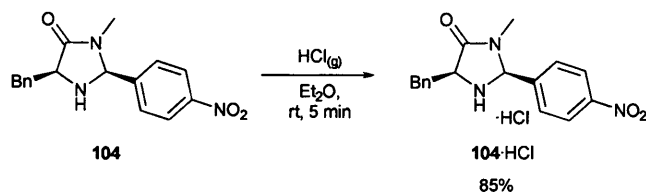
Scheme 4.8

To determine whether the whole reaction was reversible and hence under thermodynamic control, **33** was subjected to microwave irradiation at 140 °C for 60 minutes in DMF in the presence of 11 mol% PTSA (Scheme 4.8). The  $^1\text{H}$  NMR spectra of the crude showed the presence of **33** and **104** in a 1.2:1 ratio and showed that under these conditions, the cyclisation step was reversible.



Scheme 4.9

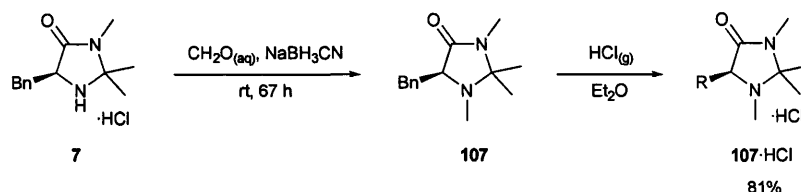
Having produced sufficient quantities of **33** and **104**, the next step was to form the hydrochloride salts. A rapidly stirred etheric solution of **33** was treated with hydrogen chloride gas for 5 minutes before the precipitate was washed with excess diethyl ether and dried *in vacuo* to yield **33·HCl** (85%) as a yellow solid (Scheme 4.9).



Scheme 4.10

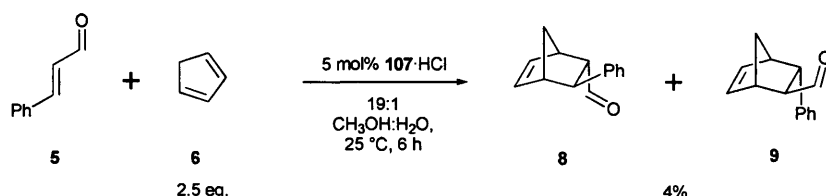
An etheric solution of **104** was treated with hydrogen chloride gas for 5 minutes and the product isolated in the same manner as used for **33·HCl**. **104·HCl** was obtained as a white solid (85%) (Scheme 4.10).

### 4.3 Quantifying the Background Reaction



Scheme 4.11

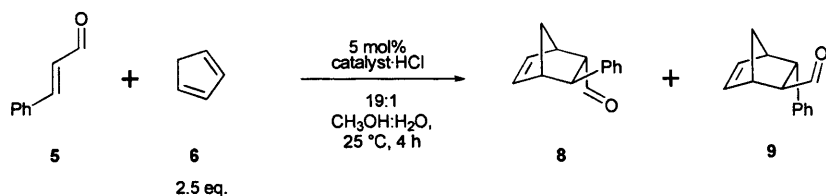
While it was assumed that Diels-Alder reactions catalysed by imidazolidinone hydrochlorides proceed exclusively *via* iminium ions, this had never been conclusively shown and no efforts had been undertaken to quantify the background reaction. To remedy this omission, synthetic efforts were made towards **107**, a structural analogue of **7** incapable of forming iminium ions yet still capable of effecting acid catalysis and forming aminols. **7**·HCl was stirred with sodium cyanoborohydride in 37% aqueous formaldehyde for 67 hours at room temperature. After basic workup and extraction with diethyl ether, **107** was obtained. **107** was found to rapidly turn pink when exposed to the air, necessitating immediate conversion to the more stable **107**·HCl (81% overall) *via* the usual method (Scheme 4.11).



Scheme 4.12

5 mol% of **107**·HCl was used in the benchmark Diels-Alder reaction between **5** and **6** in 19:1 methanol:water at 25 °C. After 6 hours, an aliquot was taken and the standard procedure used to determine that the combined conversion to **7** and **8** was 4% (Scheme 4.12).

#### 4.4 Catalytic Performance



Scheme 4.13

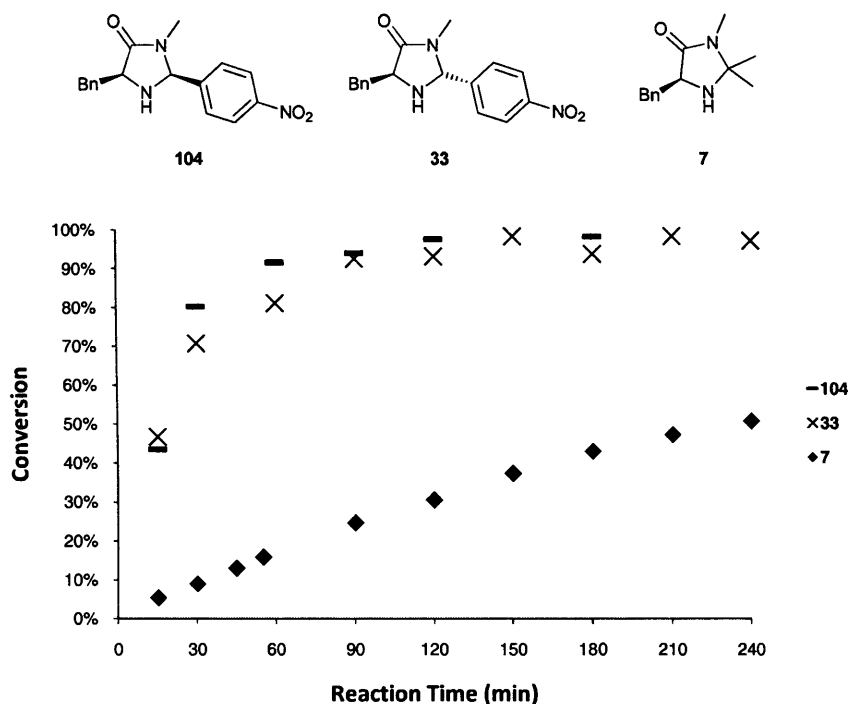


Figure 4.14

| Catalyst | 8 ee | 9 ee |
|----------|------|------|
| 104      | 12   | 30   |
| 33       | 75   | 34   |
| 7        | 93   | 93   |

Figure 4.15

5 and 2.5 equivalents of 6 in 19:1 methanol:water were stirred with 5 mol% of 7·HCl, 33·HCl, or 104·HCl for 6 hours at 25 °C (Scheme 4.13). Periodic aliquots were taken, worked up according to the benchmark procedure, and conversion determined by  $^1\text{H}$  NMR (Figure 4.14). After the 4 hours had elapsed, 8 and 9 were isolated as per the benchmark procedure. 8 and 9 were converted to their 2,4-DNPH adducts, which were subjected to HPLC to determine their enantiopurities (Figure 4.15).

#### 4.5 Performance Analysis

The results showed that both **33** and **104** achieved higher conversions than benchmark catalyst **7**. The reactions catalysed by **33**·HCl and **104**·HCl attained completion in approximately 2 hours, whereas **7**·HCl effected only 50% conversion after 4 hours. Additionally, while experimental errors were not quantified, it may be tentatively asserted that **104** is a more efficient catalyst than **33** under the conditions examined.

In terms of enantiocontrol, **7** clearly outperformed **33** and **104**. The scale of the difference indicated that **33** and **104** must have glaring design flaws.

Interestingly, the background reaction, as quantified using **107**·HCl, may be expected to play a larger role in lowering the ee's of **7** than **33** and **104**, due to the lower reactivity in iminium ion catalysed reaction pathways. This suggested that for an imidazolidinone to attain higher levels of enantiocontrol than **7** in the benchmark reaction, high turnover would be essential.

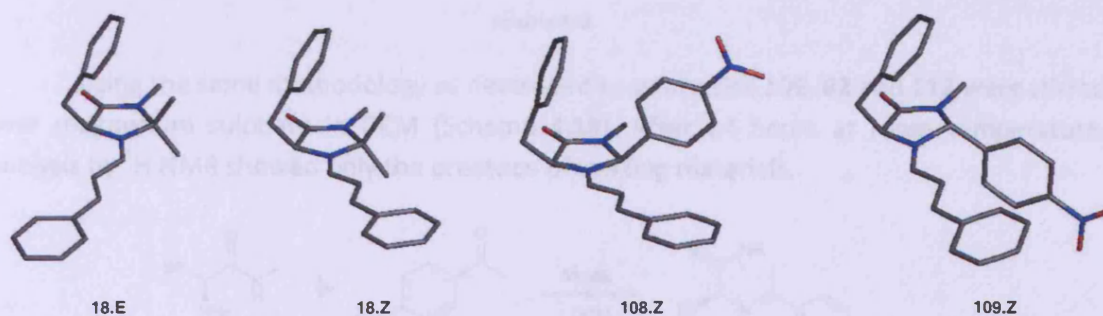
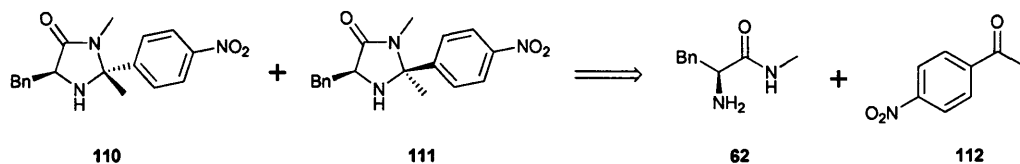


Figure 4.16

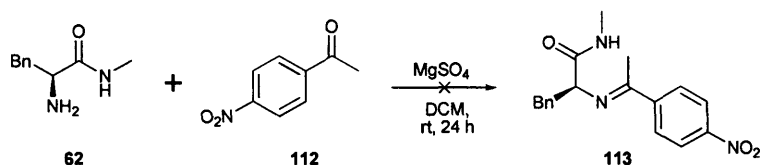
As first proposed in MacMillan's seminal paper, exclusive formation of **18.E** is considered to be a critical part of **7**'s stereocontrol (Figure 4.16).<sup>2</sup> Formation of **18.Z** was thought to be disfavoured by steric hindrance between the proton  $\alpha$ - to the iminium carbon and the geminal dimethyl groups of the imidazolidinone ring. Lacking the same degree of steric differentiation between the 2- and 5-positions, **33** and **104** may be expected to more readily form **108.Z** and **109.Z**, respectively. Upon reaction with **6**, **108.Z** would be expected to generate undesired enantiomers and lower the overall product ee. **109.Z** can be viewed as a pseudo  $C_2$ -symmetric iminium ion and this may explain the higher selectivity observed. The precise reasons for the lower selectivity than **7** were not apparent at this stage.

## 4.6 Methyl Analogue Synthesis



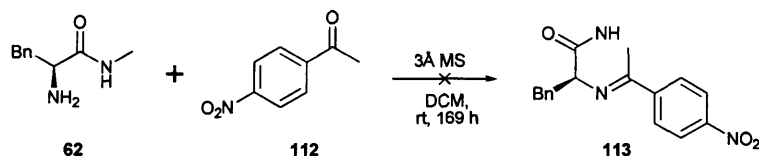
Scheme 4.17

If the rationale for the poor stereocontrol exhibited by **33** and **104** was accurate, the obvious solution to enhancing the enantiocontrol of these catalysts would be to increase steric bulk around the 2-position. This line of thinking gave rise to target structures **110** and **111**, analogues of **33** and **104** that should be obtainable *via* an analogous synthesis employing **112** (Scheme 4.17).



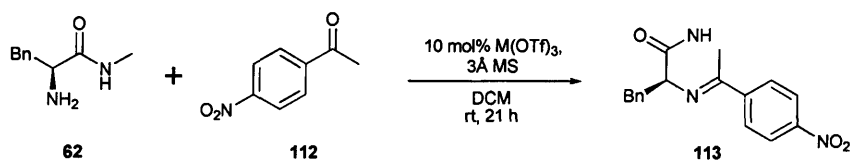
Scheme 4.18

Using the same methodology as developed to synthesise **106**, **62** and **112** were stirred over magnesium sulphate in DCM (Scheme 4.18). After 24 hours at room temperature, analysis by  $^1\text{H}$  NMR showed only the presence of starting materials.



Scheme 4.19

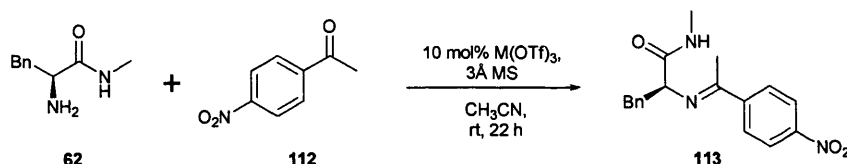
The use of 3Å molecular sieves in DCM had also been observed to catalyse formation of **106**. **62** and **112** were stirred over 3Å molecular sieves in DCM for 169 hours at room temperature (Scheme 4.19).  $^1\text{H}$  NMR showed only the presence of starting materials.



Scheme 4.20

In Chapter 2.5, the utility of Lewis acids in catalysing imine formation was discovered. It was thought that Lewis acids may also assist in formation of **113**. To this end, four reactions were performed using the Lewis acids gallium(III) triflate **86**, ytterbium(III) triflate, indium(III)

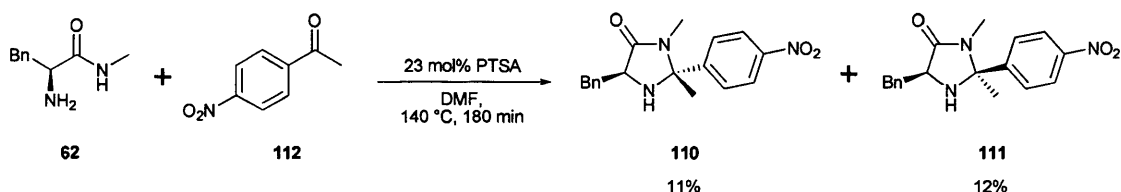
triflate and yttrium(III) triflate. In each case, **62**, **112** and 10 mol% metal(III) triflate were stirred over 3Å molecular sieves in DCM for 21 hours, after which an aqueous workup was performed and reaction progress observed by  $^1\text{H}$  NMR. In all cases, it was found that only traces of **113** had been formed (Scheme 4.20).



| M  | Conversion |
|----|------------|
| Ga | 16%        |
| Yb | 13%        |
| In | 10%        |
| Y  | 5%         |

Scheme 4.21

Noting the low solubility of the metal complexes in DCM, **62**, **112** and 10 mol% metal(III) triflate were stirred over 3Å molecular sieves in acetonitrile for 22 hours (Scheme 4.21). Aqueous workups were performed and conversion determined by  $^1\text{H}$  NMR. The results indicated that gallium(III) triflate **86** was the most suitable catalyst for **113** formation but that its conversion under these conditions was not high enough to render isolation of **113** an attractive option.



Scheme 4.22

As formation of **113** appeared difficult, a one-step synthesis of **110** and **111** was attempted. **62**, **112** and 23 mol% PTSA in DMF were subjected to microwave irradiation at 140 °C for 180 minutes (Scheme 4.22). After column chromatography, **110** (11%) and **111** (12%) were isolated and converted to **110**·HCl and **111**·HCl by the usual method.



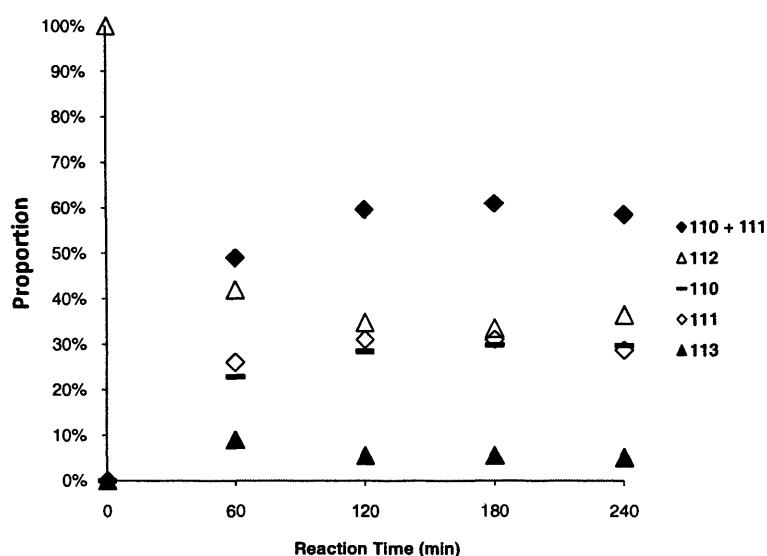
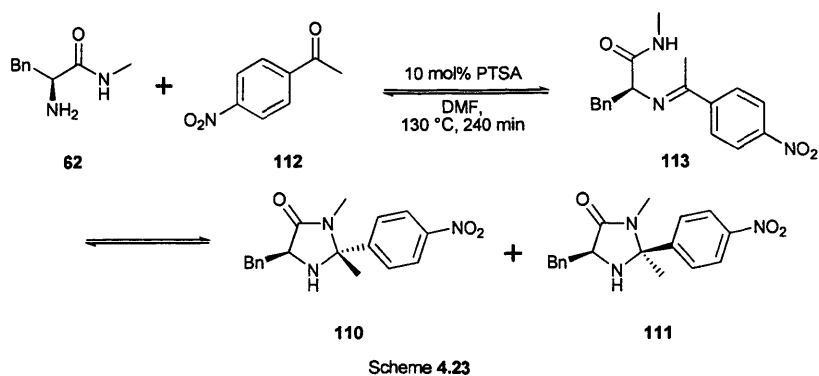
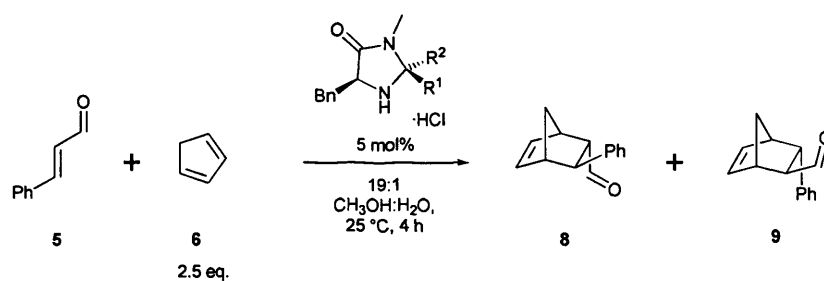


Figure 4.24

To gain further insight into this transformation, **62**, **112** and 10 mol% PTSA in DMF were subjected to microwave irradiation at 130 °C for 240 minutes (Scheme 4.23). Aliquots were taken every 60 minutes, extracted with diethyl ether and washed with water to remove the ytterbium(III) triflate. <sup>1</sup>H NMR was then used to assay the relative proportion of each of the four analytes **110–113** (Figure 4.24). **62** was not observed, due to it being lost in the aqueous factions.

Results showed that the reaction appeared to be under thermodynamic control, reaching equilibrium after approximately 2 hours. As large amounts of **112** were present at equilibrium, it was surmised that the equilibrium could be driven towards the right by employing a desiccant such as molecular sieves. Unfortunately, molecular sieves were found to be incompatible with the microwave reactors used in this project and no investigation of alternative desiccants was performed.

## 4.7 Acetophenone Analogue Performance



Scheme 4.25

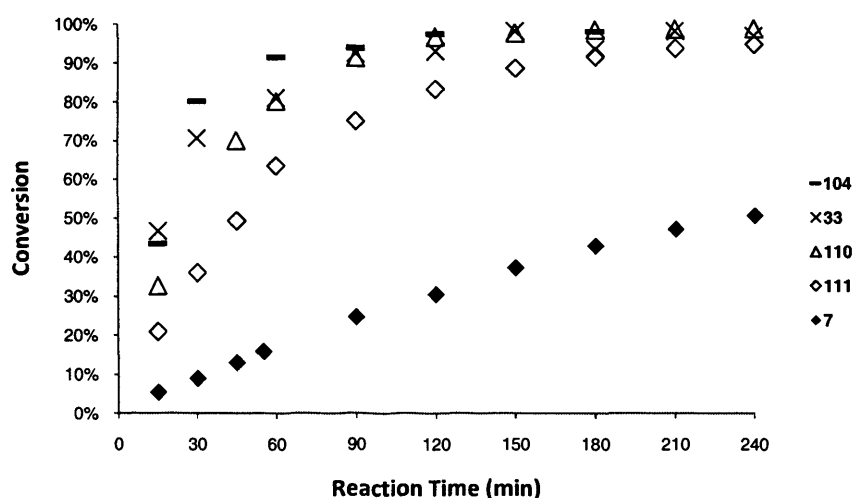


Figure 4.26

|                | 104   | 33  | 111   | 110   | 7               |
|----------------|---|---|---|---|-----------------|
| R <sup>1</sup> | <i>p</i> -NO <sub>2</sub> C <sub>6</sub> H <sub>4</sub> | H   | <i>p</i> -NO <sub>2</sub> C <sub>6</sub> H <sub>4</sub> | CH <sub>3</sub>   | CH <sub>3</sub> |
| R <sup>2</sup> | H   | <i>p</i> -NO <sub>2</sub> C <sub>6</sub> H <sub>4</sub> | CH <sub>3</sub>   | <i>p</i> -NO <sub>2</sub> C <sub>6</sub> H <sub>4</sub> | CH <sub>3</sub> |
| 8 ee           | 12  | 75  | 94  | 92  | 93              |
| 9 ee           | 30  | 34  | 78  | 87  | 93              |

Figure 4.27

5 and 2.5 equivalents of 6 in 19:1 methanol:water were stirred with 5 mol% of the catalyst hydrochloride for 4 hours at 25 °C (Scheme 4.25). Periodic aliquots were taken, worked up as per the benchmark procedure, and conversion determined by <sup>1</sup>H NMR (Figure 4.26). After the 4 hours had elapsed, 8 and 9 were isolated as per the benchmark procedure and converted to their 2,4-DNPH adducts for ee determination by HPLC (Figure 4.27).

#### 4.8 Acetophenone Analogue Analysis

Previously, it was proposed that **33** and **104** exhibited poor enantiocontrol due to their lack of selectivity in forming iminium ions and that increasing steric bulk around the 2-position would lead to improved stereocontrol. This hypothesis appeared to be validated, as **110** and **111** were seen to exhibit far greater enantiocontrol than **33** and **104**.

Pleasingly, while **110** and **111** showed lower performance than **33** and **104**, they still retained a large performance advantage over **7**.

Particularly noteworthy was **110**'s concurrent exhibition of high performance and good enantiocontrol, a previously unseen combination. It was evident that if the enantiocontrol could be improved, **110** would show comprehensively better catalytic performance than **7** in the benchmark Diels-Alder reaction, completing one of the stated goals of this project.

#### 4.9 Non-EWG Imidazolidinone Synthesis

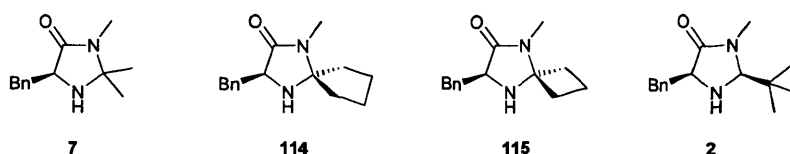
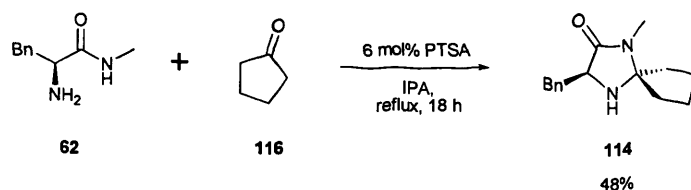


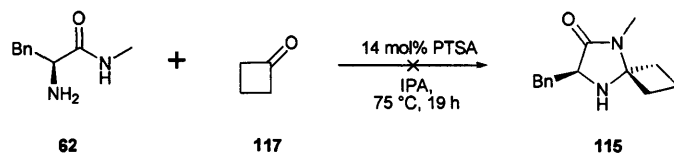
Figure 4.28

During the course of this work, only one non-EWG catalyst, **7**, had been evaluated (Figure 4.28). It was decided that **114** and **115** should be synthesised and evaluated, to ascertain the effect of small structural changes on the turnover and stereoselectivity of the Diels-Alder reaction. **2** has been reported by MacMillan for use in conjugate additions and the performance of this catalyst in the benchmark Diels-Alder reaction was also deemed worthy of investigation.



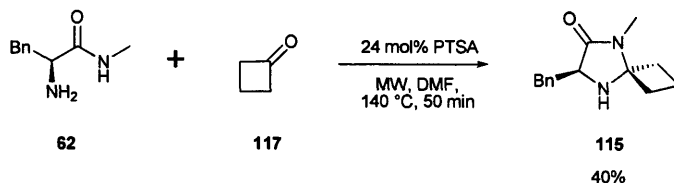
Scheme 4.29

**62**, **116** and 6 mol% PTSA were refluxed in IPA for 18 hours and column chromatography used to provide **114** (48%) (Scheme 4.29). The usual procedure for forming hydrochloride salts yielded **114**·HCl (41% overall).



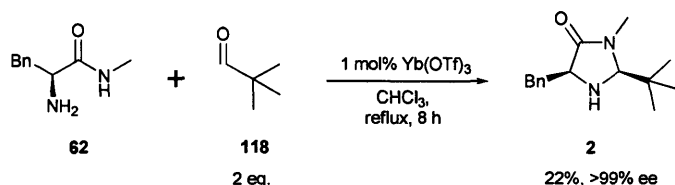
Scheme 4.30

**62**, **117** and 14 mol% PTSA were stirred in IPA at 75 °C for 18 hours (Scheme 4.30). The recovered material consisted largely of **62**, with **117** presumed to have evaporated. This indicated that more energy would be required to form **115**.



Scheme 4.31

**62**, **117** and 24 mol% PTSA in DMF were subjected to microwave irradiation at 140 °C for 50 minutes (Scheme 4.31). Aqueous workup and column chromatography yielded **115** (40%). The standard method for forming hydrochloride salts yielded **115**·HCl (76%, 30% overall).



Scheme 4.32

Using conditions developed in Chapter 5.11, **62** and **118** were refluxed with 1 mol% ytterbium(III) triflate in chloroform for 8 hours (Scheme 4.32). Column chromatography yielded **2** (22%, >99% ee), which was converted to **2**·HCl by the usual method.

#### 4.10 Non-EWG Evaluation

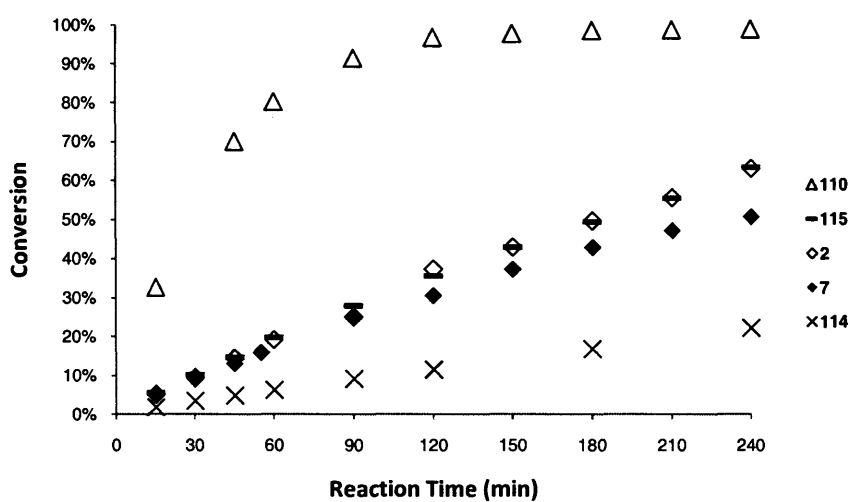
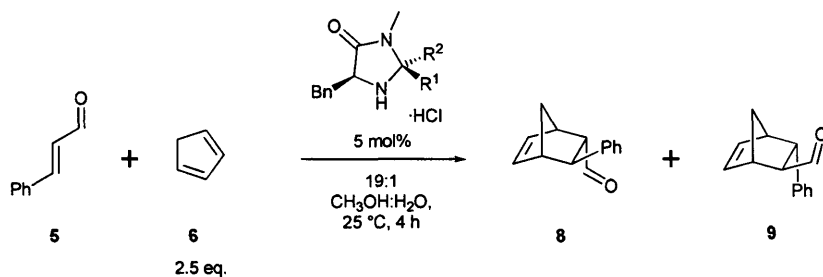


Figure 4.34

| Catalyst       | 110   | 2               | 115                             | 7               | 114                             |
|----------------|---|-----------------|---------------------------------|-----------------|---------------------------------|
| R <sup>1</sup> | CH <sub>3</sub>   | <sup>t</sup> Bu | (CH <sub>2</sub> ) <sub>3</sub> | CH <sub>3</sub> | (CH <sub>2</sub> ) <sub>4</sub> |
| R <sup>2</sup> | <i>p</i> -NO <sub>2</sub> C <sub>6</sub> H <sub>4</sub> | H               |                                 | CH <sub>3</sub> |                                 |
| <i>endo</i> ee | 92  | 5               | 91                              | 93              | 91                              |
| <i>exo</i> ee  | 87  | 55              | 87                              | 93              | 86                              |

Figure 4.35

5 and 2.5 equivalents of 6 in 19:1 methanol:water were stirred with 5 mol% of the catalyst hydrochloride for 6 hours at 25 °C (Scheme 4.33). Periodic aliquots were taken, worked up as per the benchmark procedure, and conversion determined by <sup>1</sup>H NMR (Figure 4.34). After the 4 hours had elapsed, 8 and 9 were isolated as per the benchmark procedure and converted to their 2,4-DNPH adducts for ee determination by HPLC (Figure 4.35).

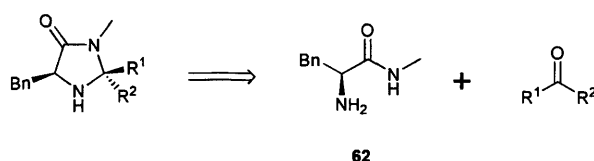
#### 4.11 Non-EWG Analysis

**114** and **115** exhibited good stereocontrol, attaining ee's very close to those of **7** but with *exo* ee's substantially less than that of **7**. **2** exhibited very poor stereocontrol. While the reasons for its poor stereocontrol are not understood, the large discrepancy between *endo* and *exo* ee's indicates that if E/Z selectivity is lacking, it is only part of the problem.

**2**, **7** and **115** showed similar levels of turnover. **114** showed very low turnover, less than half that of **7**. This result was very surprising, considering the structural similarity of **114** to **7** and **115** and its almost identical enantiocontrol to **115**.

These results showed an apparent performance ceiling for catalysts lacking EWGs. They also showed that subtle changes to a catalyst's structure can have dramatic and unforeseen effects on its performance.

#### 4.12 Changing the EWG - Synthesis



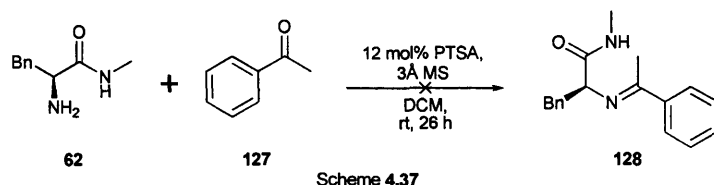
|                | <b>110</b>  | <b>119</b>   | <b>121</b>                    | <b>123</b>                                | <b>125</b>                                  |
|----------------|---|--|-------------------------------|---|---|
| R <sup>1</sup> | CH <sub>3</sub>   | CH <sub>3</sub>  | CH <sub>3</sub>               | CH <sub>3</sub>                           | CH <sub>3</sub>                             |
| R <sup>2</sup> | <i>p</i> -NO <sub>2</sub> C <sub>6</sub> H <sub>4</sub> | <i>p</i> -CH <sub>3</sub> OC <sub>6</sub> H <sub>4</sub> | C <sub>6</sub> H <sub>5</sub> | <i>p</i> -ClC <sub>6</sub> H <sub>4</sub> | <i>p</i> -(NC)C <sub>6</sub> H <sub>4</sub> |

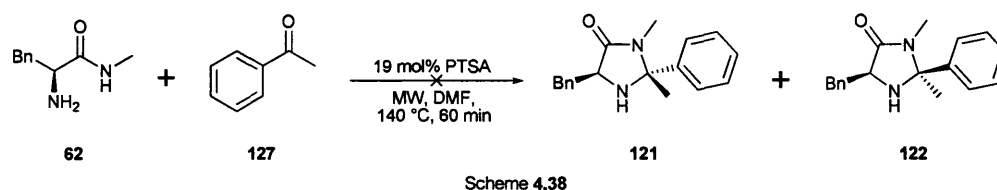
|                | <b>111</b>  | <b>120</b>   | <b>122</b>                    | <b>124</b>                                | <b>126</b>                                  |
|----------------|---|--|-------------------------------|---|---|
| R <sup>1</sup> | <i>p</i> -NO <sub>2</sub> C <sub>6</sub> H <sub>4</sub> | <i>p</i> -CH <sub>3</sub> OC <sub>6</sub> H <sub>4</sub> | C <sub>6</sub> H <sub>5</sub> | <i>p</i> -ClC <sub>6</sub> H <sub>4</sub> | <i>p</i> -(NC)C <sub>6</sub> H <sub>4</sub> |
| R <sup>2</sup> | CH <sub>3</sub>   | CH <sub>3</sub>  | CH <sub>3</sub>               | CH <sub>3</sub>                           | CH <sub>3</sub>                             |

Scheme 4.36

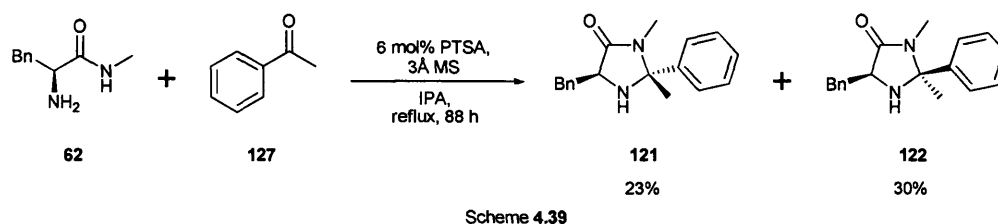
At this stage of the project, a catalyst **110** had been discovered that exhibited high performance in the benchmark reaction as well as good levels of stereocontrol. Lacking a clear understanding of how to produce more selective catalysts that retained the high performance of **110**, it was decided to synthesise a range of analogues based on differentially *para*-substituted acetophenones (Scheme 4.36). This would allow for a more detailed investigation of the effect of EWGs on catalyst turnover and perhaps also the discovery of a high performance catalyst with higher levels of enantiocontrol than benchmark catalyst **7**.



**62**, **127** and 12 mol% PTSA were stirred in DCM over 3Å molecular sieves for 26 hours at room temperature (Scheme 4.37). This reaction produced only traces of **128** and it was decided that **119–126** should be obtained by direct reaction of **62** and the relevant acetophenone.



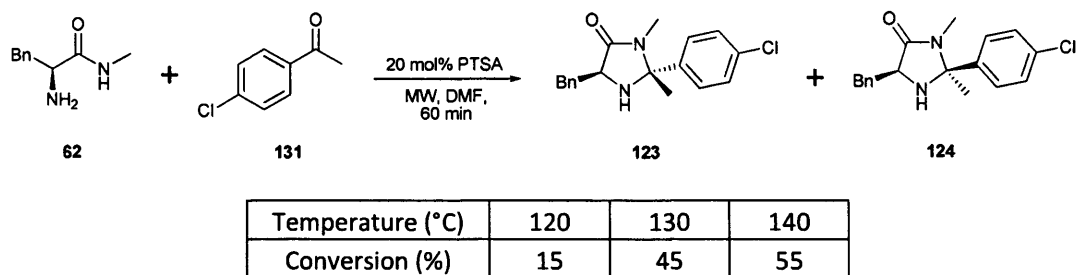
**62**, **127** and 19 mol% PTSA in DMF were irradiated at 140 °C for 60 minutes (Scheme 4.38). <sup>1</sup>H NMR showed a large number of unassignable peaks, indicating decomposition to have occurred.



Thermal conditions were then investigated. IPA appeared an obvious choice of solvent, due to its high boiling point, hydrogen bonding ability and reluctance to form acetals with ketones. In a successful synthesis, **62**, **127** and 6 mol% PTSA were refluxed in IPA over 3Å molecular sieves for 88 hours (Scheme 4.39). Basic workup and column chromatography yielded **121** (23%) and **122** (30%). Submitting **121** and **122** to the standard procedure for forming hydrochloride salts yielded **121**·HCl (89%) and **122**·HCl (82%).







Scheme 4.43

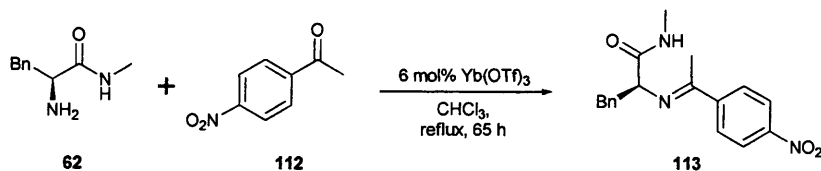
Three reactions were performed whereupon **62**, **131** and 20 mol% PTSA in DMF were subjected to microwave irradiation for 60 minutes, with reaction temperatures of 120 °C, 130 °C and 140 °C (Scheme 4.43). Total conversion of **131** to **123** and **124** was assayed by  $^1\text{H}$  NMR of the crude after aqueous workup to remove the catalytic acid and DMF. **62** was known to be partially water soluble and would be lost during aqueous workup. When the reaction was performed at 130 °C and 140 °C, **123** and **124** were present in a 1:1.0 ratio.

#### 4.13 Thermal Syntheses

At this point, before further work could be carried out, both the microwave reactors used so far in this project became unavailable and alternative facilities could not be sourced. The synthesis of **119–126** was a pressing concern and further investigation of thermal conditions was necessitated.

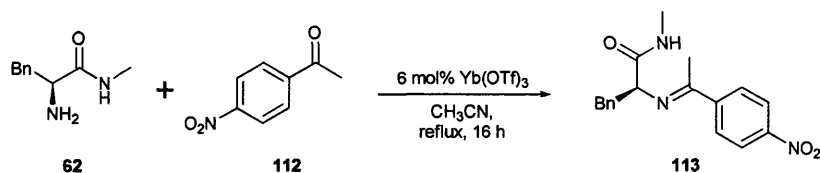
Whereas **121** and **122** would form readily in refluxing IPA (Scheme 4.45), the other imidazolidinones appeared to require more forcing conditions. **110** and **111** appeared to be the hardest to form and their synthesis was used as a worst case scenario in developing a universal thermal synthesis that may also be used to prepare **119–126**.

Efforts were centered around the potent and commercially available Lewis acid, ytterbium(III) triflate, as it appeared to more effective than PTSA for imidazolidinone formation.



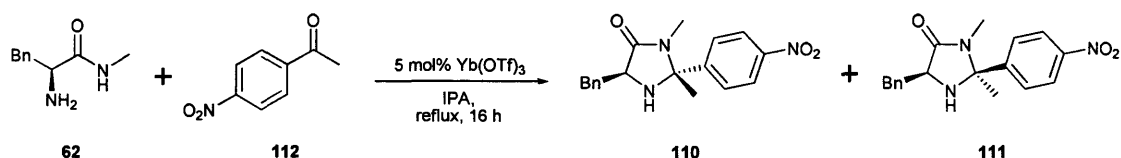
Scheme 4.44

**62**, **112** and 6 mol% ytterbium(III) triflate were refluxed in chloroform for 65 hours (Scheme 4.44). After aqueous workup to remove the catalyst,  $^1\text{H}$  NMR showed partial conversion of **112** to **113** but not **110** or **111**.



Scheme 4.45

**62**, **112** and 6 mol% ytterbium(III) triflate were refluxed in acetonitrile for 16 hours (Scheme 4.45). <sup>1</sup>H NMR showed partial conversion of **112** to **113** but not **110** or **111**.



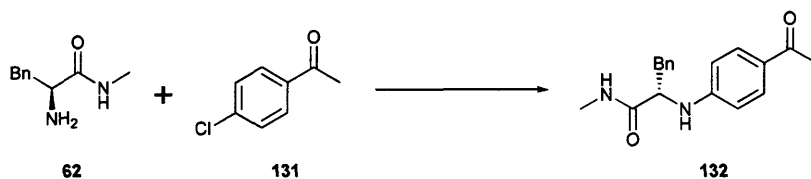
| Yb(OTf) <sub>3</sub> (mol%) | Solvent           | Conditions                           | <b>110</b> (%) | <b>111</b> (%) |
|-----------------------------|-------------------|--------------------------------------|----------------|----------------|
| 5                           | IPA               | reflux, 16 h                         | -              | -              |
| 12                          | PhCH <sub>3</sub> | reflux, 22 h, N <sub>2</sub> , 3Å MS | 28             | 26             |
| 8                           | PhCH <sub>3</sub> | reflux, 40 h, N <sub>2</sub> , 3Å MS | 35             | 35             |

Scheme 4.46

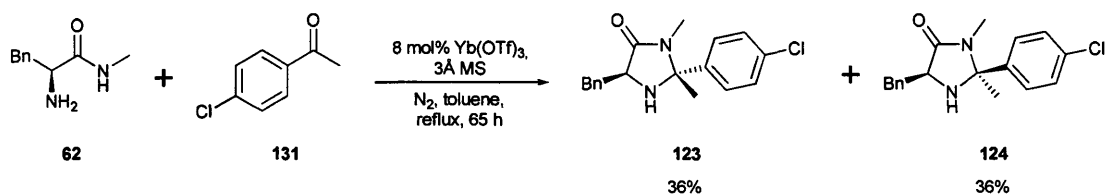
**62**, **112** and 5 mol% ytterbium(III) triflate were refluxed in IPA for 16 hours (Scheme 4.46). <sup>1</sup>H NMR showed **110** and **111**, but in quantities too low to be useful.

**62**, **112** and 12 mol% ytterbium(III) triflate were refluxed in toluene for 22 hours over 3Å molecular sieves and under nitrogen. <sup>1</sup>H NMR of the crude showed good conversion. Column chromatography then provided **110** (28%) and **111** (26%).

The reaction was scaled up as **62** (2.5 g) and **112** (2.2 g) were refluxed with 8 mol% ytterbium(III) triflate over 3Å molecular sieves and under nitrogen in toluene for 40 hours. Column chromatography provided **110** (36%) and **111** (35%).

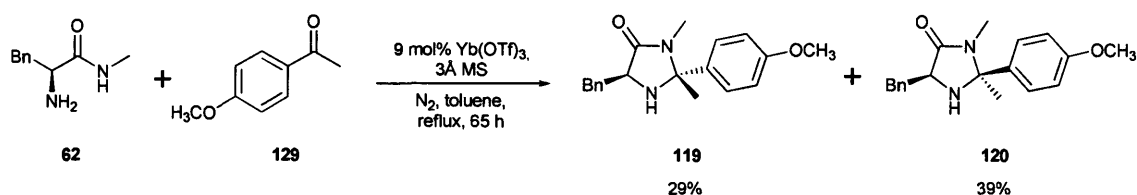


Scheme 4.47



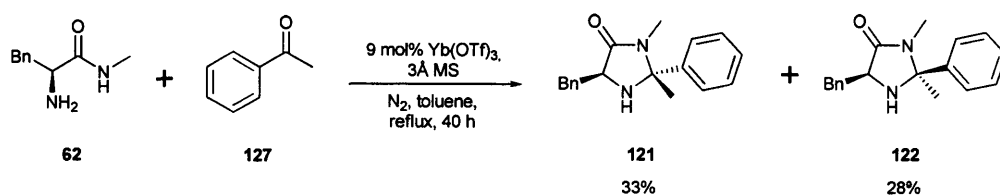
Scheme 4.48

It was anticipated that **123** and **124** may present difficulties, due the potential for **62** and **131** to undergo a  $S_NAr$  reaction, yielding **132** (Scheme 4.47). **62**, **131** and 8 mol% ytterbium(III) triflate were refluxed in toluene for 65 hours over 3Å molecular sieves and under nitrogen (Scheme 4.48). Column chromatography then provided **123** (36%) and **124** (36%).



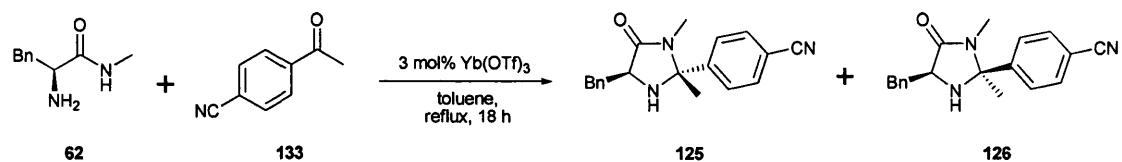
Scheme 4.49

**62**, **129** and 8 mol% ytterbium(III) triflate were refluxed in toluene for 65 hours over 3Å molecular sieves and under nitrogen (Scheme 4.49). Column chromatography then provided **119** (29%) and **120** (39%).



Scheme 4.50

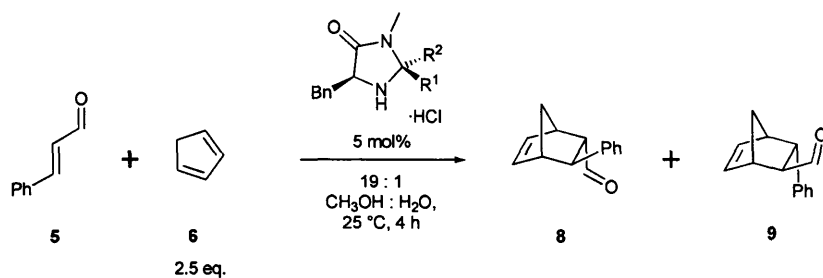
**62**, **127** and 8 mol% ytterbium(III) triflate were refluxed in toluene for 40 hours over 3Å molecular sieves and under nitrogen (Scheme 4.50). Column chromatography then provided **121** (33%) and **122** (28%).



Scheme 4.51

**62**, **133** and 3 mol% ytterbium(III) triflate were refluxed in toluene for 18 hours (Scheme 4.51). Column chromatography provided **125** and **126**, which were converted to **125**·HCl (21% overall) and **126**·HCl (19% overall) by the usual method.

#### 4.14 Performance Evaluation



Scheme 4.52

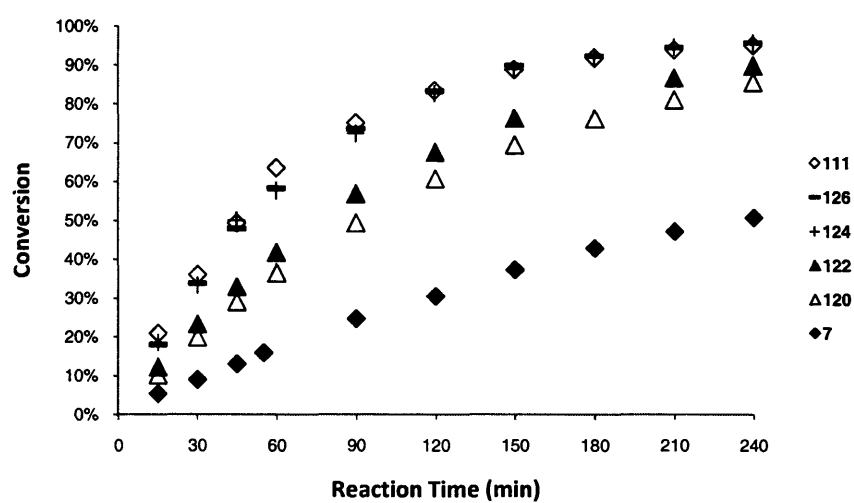


Figure 4.53

|                | 111   | 126   | 124                                       | 122                           | 120  | 7               |
|----------------|---|---|---|-------------------------------|--|-----------------|
| R <sup>1</sup> | <i>p</i> -NO <sub>2</sub> C <sub>6</sub> H <sub>4</sub> | <i>p</i> -(CN)C <sub>6</sub> H <sub>4</sub> | <i>p</i> -ClC <sub>6</sub> H <sub>4</sub> | C <sub>6</sub> H <sub>5</sub> | <i>p</i> -CH <sub>3</sub> OC <sub>6</sub> H <sub>4</sub> | CH <sub>3</sub> |
| R <sup>2</sup> | CH <sub>3</sub>   | CH <sub>3</sub>                             | CH <sub>3</sub>                           | CH <sub>3</sub>               | CH <sub>3</sub>  | CH <sub>3</sub> |
| 8 ee           | 94  | 52  | 59  | 65                            | 68   | 93              |
| 9 ee           | 78  | 42  | 50  | 61                            | 53   | 93              |
| 8:9            | 1:1.53  | 1:1.57                                      | 1:1.67                                    | 1:1.84                        | 1.78:1   | 1:1.32          |

Figure 4.54

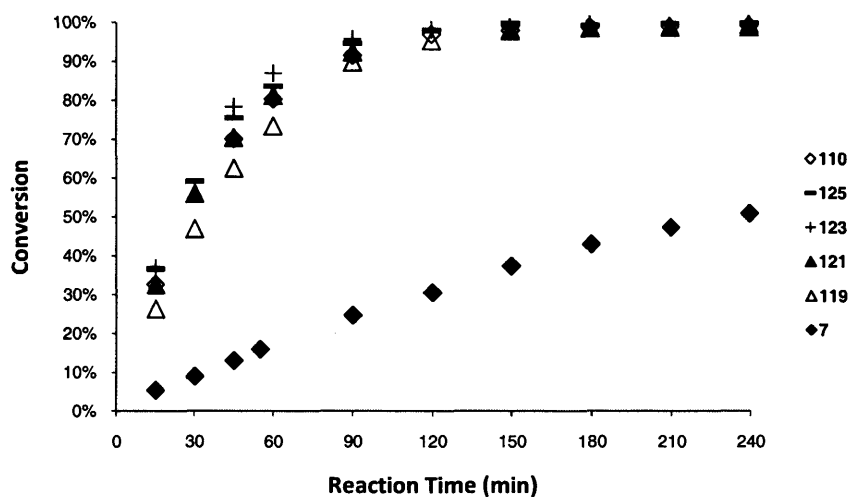


Figure 4.55

|                | 110   | 125   | 123                                       | 121                           | 119  | 7               |
|----------------|---|---|---|-------------------------------|--|-----------------|
| R <sup>1</sup> | CH <sub>3</sub>   | CH <sub>3</sub>                             | CH <sub>3</sub>                           | CH <sub>3</sub>               | CH <sub>3</sub>  | CH <sub>3</sub> |
| R <sup>2</sup> | <i>p</i> -NO <sub>2</sub> C <sub>6</sub> H <sub>4</sub> | <i>p</i> -(CN)C <sub>6</sub> H <sub>4</sub> | <i>p</i> -ClC <sub>6</sub> H <sub>4</sub> | C <sub>6</sub> H <sub>5</sub> | <i>p</i> -CH <sub>3</sub> OC <sub>6</sub> H <sub>4</sub> | CH <sub>3</sub> |
| 8 ee           | 92  | 83  | 90  | 96                            | 95   | 93              |
| 9 ee           | 87  | 73  | 78  | 82                            | 84   | 93              |
| 8:9            | 1:1.05  | 1.08:1                                      | 1:1.18                                    | 1.24:1                        | 1:1.20   | 1:1.32          |

Figure 4.56

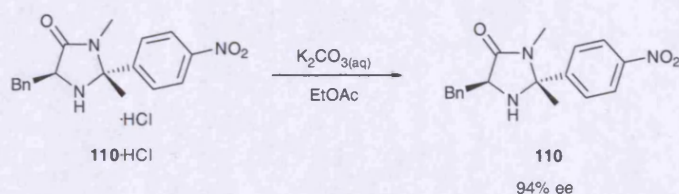
5 and 2.5 equivalents of **6** in 19:1 methanol:water were stirred with 5 mol% of the catalyst hydrochloride salts for 6 hours at 25 °C (Scheme 4.52). Periodic aliquots were taken, worked up as per the benchmark procedure, and conversion and **8:9** determined by <sup>1</sup>H NMR. After the 4 hours had elapsed, **8** and **9** were isolated as per the benchmark procedure and converted to their 2,4-DNPH adducts for ee determination by HPLC.

#### 4.15 Performance Analysis

The turnover order amongst the (2*S*,5*S*) catalysts was **111** ≈ **126** ≈ **124** > **122** > **120**, showing a correlation between stronger EWGs and higher performance within this data set (Figure 4.53).

Turnover amongst the (2*R*,5*S*) catalysts was harder to judge, as all reactions had almost attained completion after 2 hours (Figure 4.55). The performance order was **123** ≈ **125** > **110** ≈ **121** > **119**, suggesting that in this case EWGs were beneficial up to a point, beyond which performance again decreased.

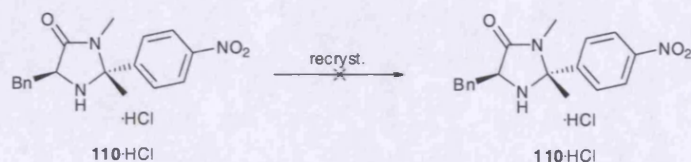




Scheme 4.58

A sample of the **110·HCl** used in the benchmark reaction was converted to **110** by shaking with ethyl acetate and 4M potassium carbonate (Scheme 4.58). This was subjected to HPLC and its ee found to be 94%. This showed that enantiocontrol in the benchmark reaction had the potential to improve markedly if optically pure **110·HCl** could be obtained.

#### 4.17 Recrystallisation attempts



Scheme 4.59

Recrystallisation of **110·HCl** appeared an obvious way to improve its enantiopurity. **110·HCl** was found to be highly soluble in methanol, acetonitrile and DCM, yet insoluble in hexanes, ethyl acetate, diethyl ether, toluene and water. Slow cooling and slow evaporation at room temperature both failed to produce a crystalline product (Scheme 4.59). In every case, **110·HCl** was obtained as an amorphous residue and was found to have an ee identical to that of the starting **110·HCl**.

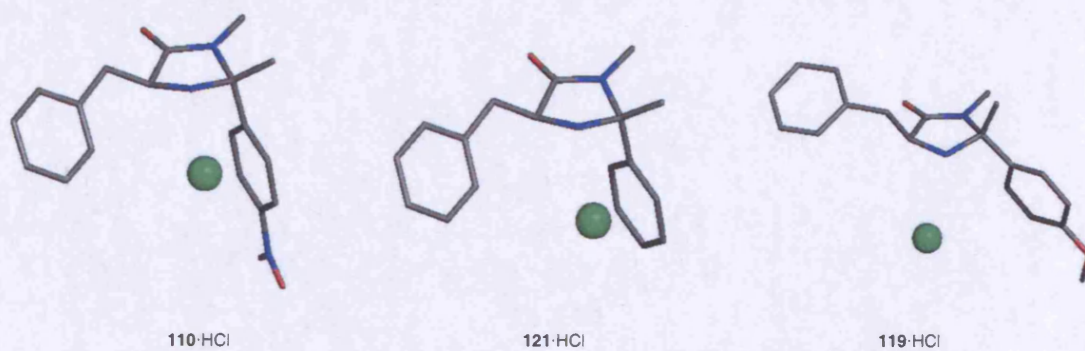


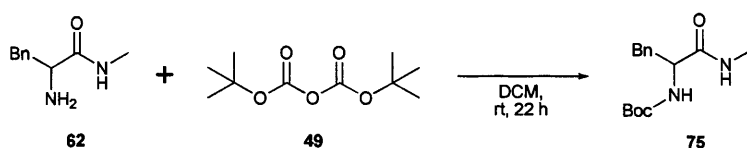
Figure 4.60

After the work in this chapter had been completed, crystals of **110·HCl** were seen to have formed in one of the vials set up as part of recrystallisation attempts. After careful washing of the crystals, X-ray crystallography was used to confirm the structure and



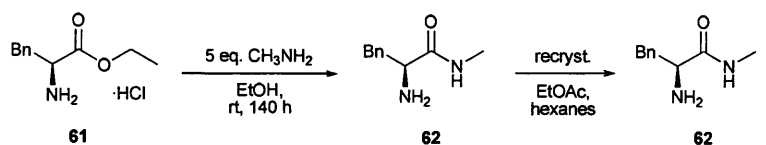
stereochemistry of **110**·HCl (Figure 4.60).  $^1\text{H}$  NMR showed the crystals to be chemically identical to a fresh sample of **110**·HCl. X-ray crystallography was also used to confirm the structures of **121**·HCl and **119**·HCl, both of which were found to crystallise readily upon evaporation of DCM:hexanes solutions.

#### 4.18 Amino Amide Recrystallisation



Scheme 4.61

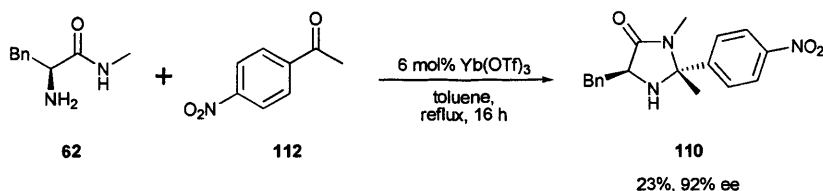
Having failed to directly boost the enantiopurity of **110**·HCl, investigations were turned towards reducing epimerisation during its synthesis. Accordingly, the first step was deemed to be the investigation of the optical purity of **62**. Separation of **62** on the HPLC could not be achieved. As such, racemic **62** and **49** were stirred in DCM for 22 hours and an aliquot of the solution containing racemic **75** subjected to HPLC (Scheme 4.61). It was found to separate on the Chiralcel OJ column using a 39:1 hexanes:IPA mobile phase at a flow rate of  $1.5\text{ mL min}^{-1}$  ( $t = 7.1\text{ min}$ ,  $11.8\text{ min}$ ). Subjecting previously synthesised batches of **62** to this protocol showed them to have ee's of 98–99%.



Scheme 4.62

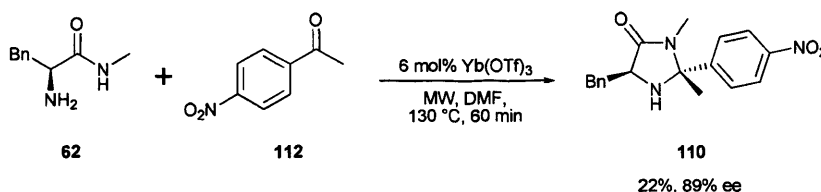
It was found that **62** could be recrystallised from ethyl acetate:hexanes. In a representative synthesis, **61** was stirred in 5 equivalents of 33% ethanolic methylamine for 140 hours at room temperature (Scheme 4.62). Evaporation and basic workup yielded **62** which was recrystallised from ethyl acetate:hexanes to provide optically pure **62** (52%).

#### 4.19 Minimising Epimerisation



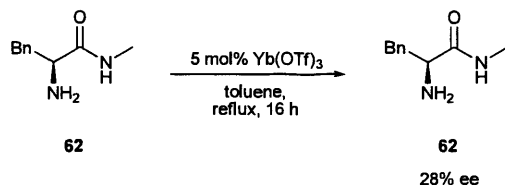
Scheme 4.63

As attempts to recrystallise **110**·HCl had failed, work was undertaken towards minimising epimerisation during synthesis of **110**. **62**, **112**, and 6 mol% ytterbium(III) triflate were refluxed in toluene for 16 hours (Scheme 4.63). Column chromatography provided **110** (23%, 92% ee).



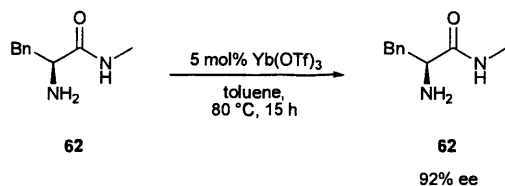
Scheme 4.64

**62**, **112**, and 6 mol% ytterbium(III) triflate in DMF were irradiated at 130 °C for 60 minutes (Scheme 4.64). Column chromatography provided **110** (22%, 89% ee).



Scheme 4.65

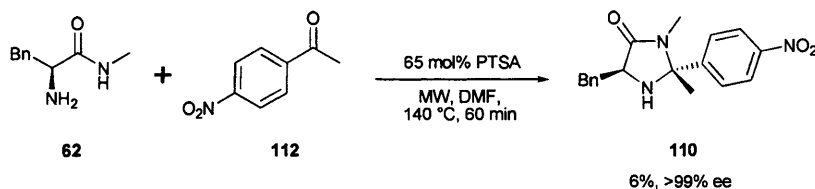
Curious as to the stage of the reaction at which epimerisation was taking place, optically pure **62** was refluxed with 5 mol% ytterbium(III) triflate in toluene for 16 hours (Scheme 4.65). After aqueous workup to remove the catalyst, the returned **62** was found to have an ee of 28%.



Scheme 4.66

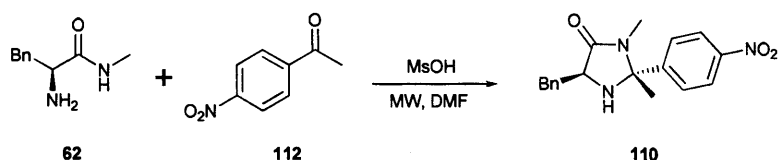
Optically pure **62** was stirred with 5 mol% ytterbium(III) triflate in toluene at 80 °C for 15 hours (Scheme 4.66). After aqueous workup to remove the catalyst, the returned **62** was found to have an ee of 92%. This showed that while lowering the temperature may help, the

use of ytterbium(III) triflate in imidazolidinone syntheses may always be expected to induce some degree of epimerisation.



Scheme 4.67

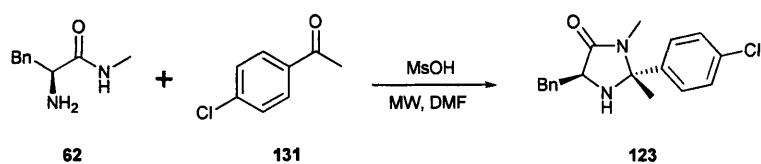
To determine whether the use of PTSA may result in less epimerisation, **62**, **112**, and 65 mol% PTSA in DMF was irradiated at 140 °C for 60 minutes (Scheme 4.67). Column chromatography provided **110** (6%, >99% ee).



| MsOH<br>mol % | Temp<br>°C | Time<br>min | <b>110</b> yield<br>% | <b>110</b> ee<br>% |
|---------------|------------|-------------|-----------------------|--------------------|
| 100           | 130        | 60          | 10                    | 96                 |
| 94            | 140        | 60          | 10                    | 88                 |
| 22            | 140        | 60          | 13                    | >99                |
| 22            | 150        | 25          | 19                    | >99                |
| 22            | 160        | 10          | 11                    | >99                |
| 36            | 160        | 10          | -                     | >99                |
| 22            | 150        | 60          | 11                    | >99                |

Scheme 4.68

Switching to the more easily measured methanesulfonic acid, the effect of catalyst loading, time, and temperature upon the reaction of **62** and **112** in DMF under microwave irradiation was studied (Scheme 4.68). It was found that at moderate catalyst loadings, the reaction may proceed with very little epimerisation. The final set of conditions in Scheme 4.76 was used to synthesise 0.72 g of **110** in 11% isolated yield, which was converted to 0.64 g **110**·HCl (9% overall), a sufficient quantity for further investigations.

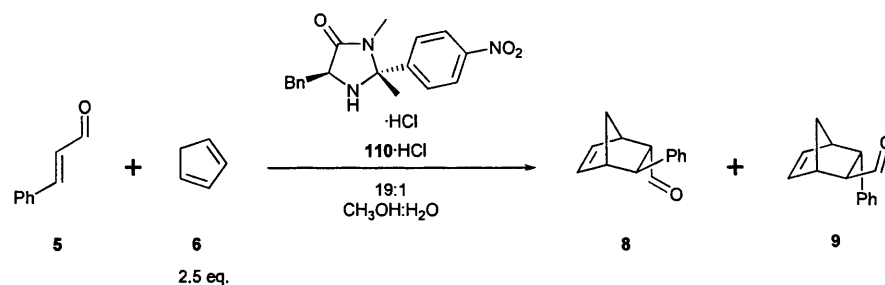


| MsOH<br>mol % | Temp<br>°C | Time<br>min | <b>123</b> yield<br>% | <b>123</b> ee<br>% |
|---------------|------------|-------------|-----------------------|--------------------|
| 22            | 150        | 60          | 18                    | 95                 |
| 22            | 160        | 25          | -                     | 97                 |
| 22            | 170        | 10          | 15                    | 98                 |
| 22            | 170        | 20          | 14                    | 97                 |
| 21            | 180        | 10          | 15                    | 97                 |
| 22            | 180        | 5           | 14                    | 96                 |

Scheme 4.69

The effect of catalyst loading, time, and temperature upon the reaction of **62** and **131** in DMF under microwave irradiation was studied (Scheme 4.69). Under the conditions tested, it was not possible to obtain **123** with >99% ee. These results indicated that epimerisation may be strongly substrate-dependant and that differing levels of enantiocontrol in the benchmark Diels-Alder reaction amongst differentially-substituted 2-arylimidazolidinones may be in part due to differences in catalyst enantiopurity.

#### 4.20 Improved Enantiocontrol

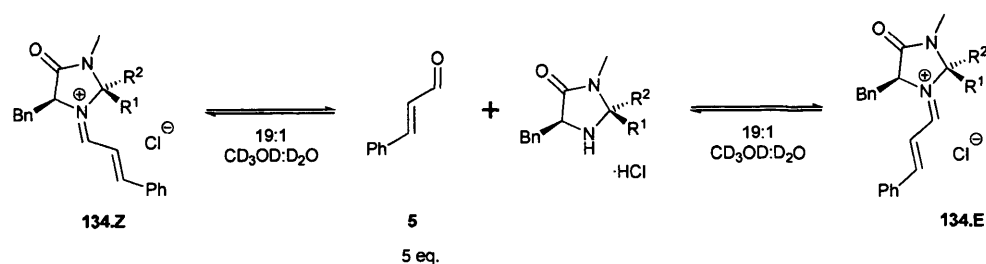


| Loading<br>mol % | Temp<br>°C | Time<br>hours | <b>8</b> ee<br>% | <b>9</b> ee<br>% |
|------------------|------------|---------------|------------------|------------------|
| 5                | 25         | 2             | 97               | 87               |
| 5                | 20         | 2             | 97               | 88               |
| 1                | room       | 16            | 95               | 88               |

Scheme 4.70

Using **110**·HCl of >99% ee, the benchmark reaction was re-run according to the conditions in Scheme 4.70. When the reaction was run for 2 hours at 25 °C using 5 mol% **110**·HCl, **8** ee was substantially improved over the previous result of 92%. **9** ee was identical to the previous result of 87%. Lowering the reaction temperature by 5 °C did little to improve results, only raising **9** ee by 1%. Using 1 mol% **110**·HCl and letting the reaction run overnight at room temperature resulted in a lower **8** ee but did not affect **9** ee.

## 4.21 Iminium Ion Selectivity



|            | R <sup>1</sup>   | R <sup>2</sup>   | [134.E] / [134.Z] |
|------------|--|--|-------------------|
| <b>7</b>   | CH <sub>3</sub>  | CH <sub>3</sub>  | 46.6              |
| <b>110</b> | CH <sub>3</sub>  | <i>p</i> -NO <sub>2</sub> C <sub>6</sub> H <sub>4</sub>  | 7.5               |
| <b>125</b> | CH <sub>3</sub>  | <i>p</i> -(NC)C <sub>6</sub> H <sub>4</sub>              | 6.9               |
| <b>121</b> | CH <sub>3</sub>  | C <sub>6</sub> H <sub>5</sub>                            | 6.1               |
| <b>123</b> | CH <sub>3</sub>  | <i>p</i> -ClC <sub>6</sub> H <sub>4</sub>                | 5.1               |
| <b>119</b> | CH <sub>3</sub>  | <i>p</i> -CH <sub>3</sub> OC <sub>6</sub> H <sub>4</sub> | 5.0               |
| <b>111</b> | <i>p</i> -NO <sub>2</sub> C <sub>6</sub> H <sub>4</sub>  | CH <sub>3</sub>  | 4.4               |
| <b>126</b> | <i>p</i> -(NC)C <sub>6</sub> H <sub>4</sub>              | CH <sub>3</sub>  | 3.8               |
| <b>124</b> | <i>p</i> -ClC <sub>6</sub> H <sub>4</sub>                | CH <sub>3</sub>  | 3.6               |
| <b>122</b> | C <sub>6</sub> H <sub>5</sub>                            | CH <sub>3</sub>  | 2.5               |
| <b>33</b>  | H  | <i>p</i> -NO <sub>2</sub> C <sub>6</sub> H <sub>4</sub>  | 2.4               |
| <b>120</b> | <i>p</i> -CH <sub>3</sub> OC <sub>6</sub> H <sub>4</sub> | CH <sub>3</sub>  | 2.4               |

Scheme 4.71

Up until this point, it had been assumed that for imidazolidinone catalysts disubstituted at the 2-position, **134.E** formed exclusively and that the reaction occurring through **134.Z** was negligible.

An experiment was devised to assay the thermodynamic ratio **134.E:134.Z** present under benchmark reaction conditions in the absence of a diene. Solutions of the catalyst hydrochloride salt (0.1 M) and cinnamaldehyde (5 equivalents, 0.5 M) in 19:1 deuterated methanol:deuterium oxide were allowed to stand at room temperature until equilibrium was reached, at which point the ratio **134.E:134.Z** was determined by <sup>1</sup>H NMR (Scheme 4.71).

As expected, **33** had a low **134.E:134.Z** ratio, explaining the low stereocontrol shown in the benchmark reaction and validating the rationale that drove investigation of the acetophenone-based catalysts.

Despite the good enantiocontrol demonstrated by some of the 2,2-disubstituted catalysts in the benchmark reaction, none of these catalysts had **134.E:134.Z** ratios approaching that of benchmark catalyst **7**.

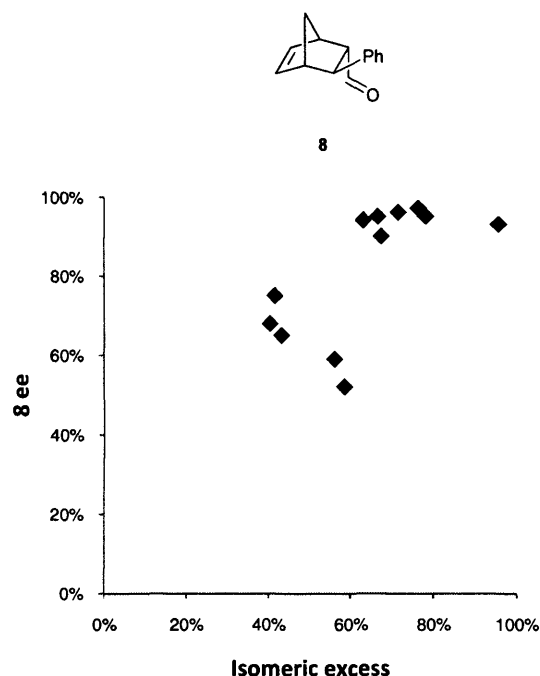


Figure 4.72

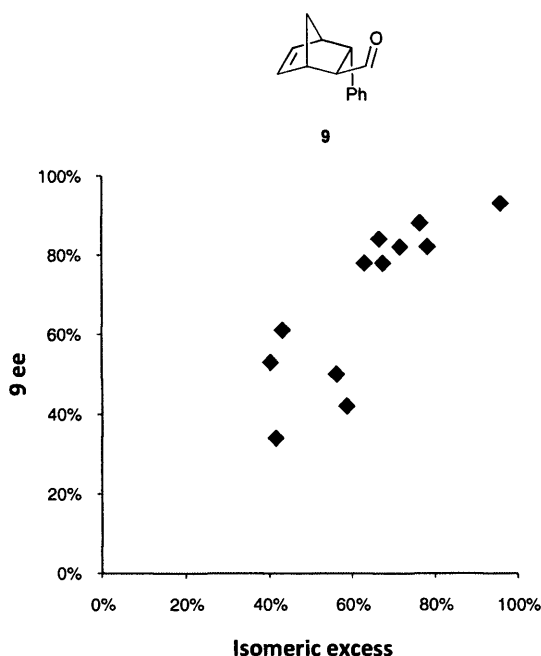
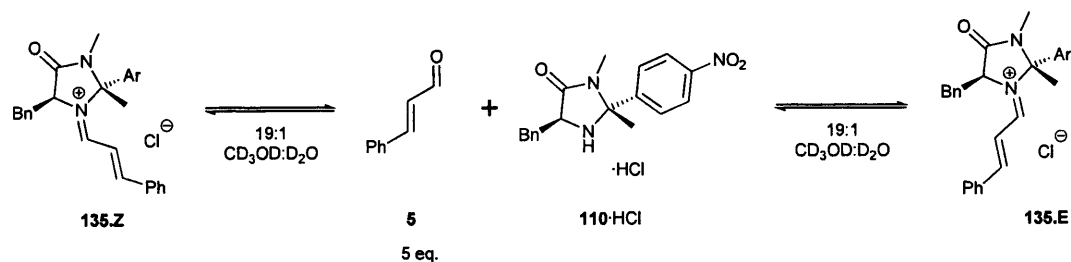


Figure 4.73

Using the same formula as to calculate an ee from the ratio of two enantiomers, an “isomeric excess” was calculated from the **8:9** ratio of each catalyst. When experimentally-attained **8** and **9** ee’s were plotted against the catalysts’ isomeric excesses, a strong trend emerged (Figure 4.72, Figure 4.73). These correlations vindicated the choice of thermodynamic iminium ion distribution as a catalyst characterization tool.

## 4.22 Solvent Screening

In efforts to improve the enantiocontrol of flagship catalyst **110** in the benchmark Diels-Alder reaction, catalyst enantiopurity had been improved and the effect of temperature upon the reaction had been investigated. The discovery that the thermodynamic **8:9** ratio may be rapidly determined with some degree of accuracy suggested that solvent systems could be screened to determine whether a more suitable solvent system for the use of **110**·HCl in the Diels-Alder reaction may exist.



| Expt. | Solvent Mixture  | [135.E] / [135.Z] | [110·HCl] / [135.E] |
|-------|--|-------------------|---------------------|
| A     | 89:11 CD <sub>3</sub> CN:D <sub>2</sub> O  | 8.2               | 9.1                 |
| B     | 19:1 CD <sub>3</sub> OD:D <sub>2</sub> O   | 7.5               | 2.2                 |
| C     | 9:1 CD <sub>3</sub> OD:D <sub>2</sub> O  | 7.1               | 2.7                 |
| D     | 19:6 (CD <sub>3</sub> ) <sub>2</sub> CDOD:D <sub>2</sub> O   | 6.7               | 8.1                 |
| E     | 93:7 (CD <sub>3</sub> ) <sub>2</sub> CO:D <sub>2</sub> O   | 6.3               | 24.9                |
| F     | 19:1 (CD <sub>3</sub> ) <sub>2</sub> SO:D <sub>2</sub> O   | 6.0               | 25.0                |
| G     | 67:19:9:5 CDCl <sub>3</sub> :CD <sub>3</sub> OD:(CD <sub>3</sub> ) <sub>2</sub> CDOD:D <sub>2</sub> O                | 5.8               | 10.7                |
| H     | 67:17:12:6 CD <sub>3</sub> NO <sub>2</sub> :(CD <sub>3</sub> ) <sub>2</sub> CDOD:D <sub>2</sub> O:CD <sub>3</sub> OD | 4.4               | 10.2                |

Scheme 4.74

**110·HCl** and 5 equivalents of **5** were dissolved in a solvent system and left to stand at room temperature until equilibrium was reached, at which point the relative concentrations of **135.E** and **135.Z** were determined by <sup>1</sup>H NMR (Scheme 4.74). Due to solubility issues in most solvent systems, aliquots of more polar solvents had to be added until a homogenous monophasic system was attained, at which point the mixture was allowed to reach equilibrium and the **135.E:135.Z** ratio determined. The effect of dilution upon the **135.E:135.Z** ratio is unknown.

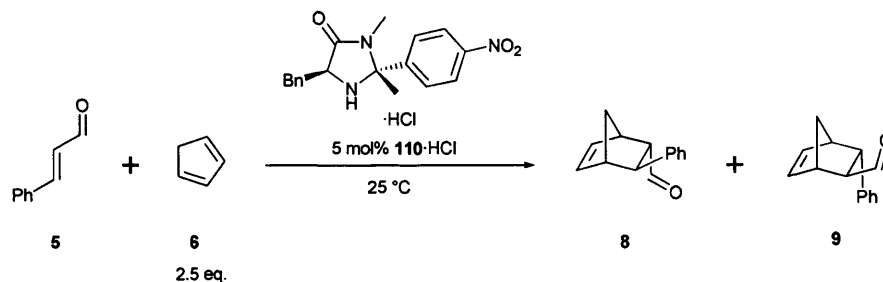
A regular feature of all spectra was the gradual conversion of the doublets corresponding to the aldehyde and iminium protons into singlets of approximately the same chemical shift. This process occurred over the period of a few days and indicated slow deuteration was occurring at the α-position of **5**, **135.E** or **135.Z**, possibly *via* the β-hydroxyenamine or β-alkoxyenamine.

The deuterated acetonitrile:deuterium oxide solvent system had the highest **135.E:135.Z** ratio, showing greater **135.E** selectivity than both deuterated methanol:deuterium oxide systems.

It was of note that **135.E:135.Z** ratios varied markedly across solvent systems. This indicated that the deuterated methanol:deuterium oxide solvent systems were proficient in



stabilising **135.E**, whereas the deuterated acetone:deuterium oxide and deuterated DMSO:deuterium oxide solvent systems were not.



Scheme 4.75

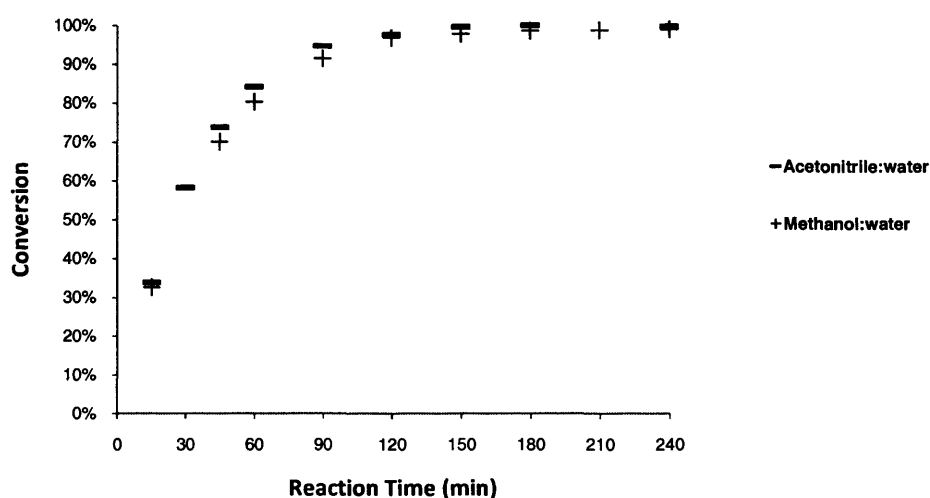


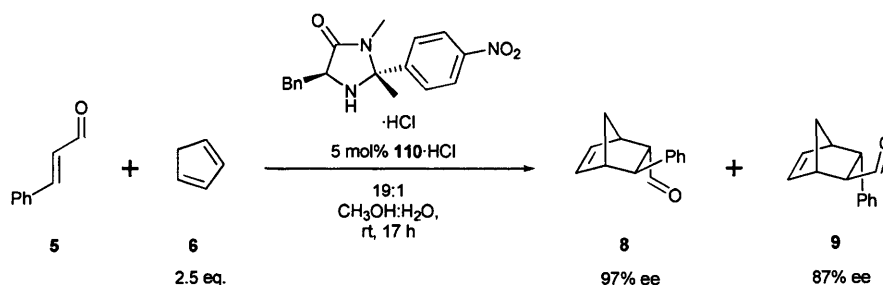
Figure 4.76

| Solvent                                  | 8 ee | 9 ee |
|--|------|------|
| 9:1 CH <sub>3</sub> CN:H <sub>2</sub> O  | 95   | 82   |
| 19:1 CH <sub>3</sub> OH:H <sub>2</sub> O | 97   | 87   |

Figure 4.77

The benchmark Diels-Alder reaction was then performed using 5 mol% **110**·HCl at 25 °C in a 9:1 acetonitrile:water system (Scheme 4.75). It was found that although the 9:1 acetonitrile:water system allowed for a slightly higher reaction rate than the 19:1 methanol:water system, it exhibited poorer enantiocontrol (Figure 4.76, Figure 4.77).

#### 4.23 Reaction Dilution



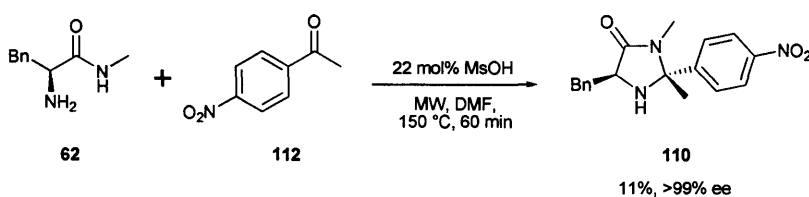
Scheme 4.78

A final attempt at attaining improved enantiocontrol from the flagship catalyst **110**·HCl was made when the benchmark reaction was diluted by a factor of 5, being performed at 0.1 M with respect to **5**, rather than the usual 0.5 M (Scheme 4.78). It was envisaged that by diluting the reaction mixture, the effect of the **5**, **6**, **8** and **9** upon the bulk solvent properties would be reduced, perhaps allowing for better iminium ion selectivity and greater enantiocontrol.

This proved not to be the case, as the ee's obtained from this reaction exactly matched the ee's obtained from the reaction performed at higher concentration.

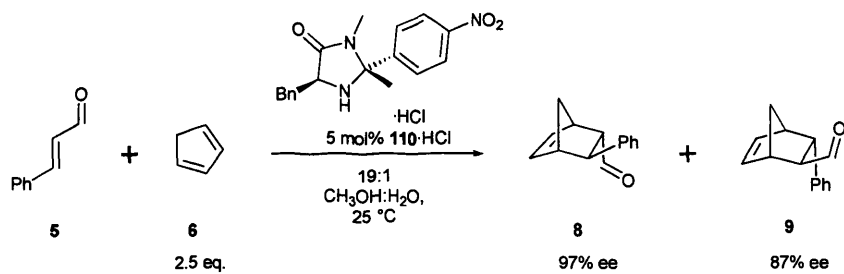
#### 4.24 Conclusions

During the course of the research documented within this chapter, 11 new 2-aryl imidazolidinone catalysts were synthesised and evaluated. All of these catalysts demonstrated higher turnovers than the benchmark catalyst **7**.



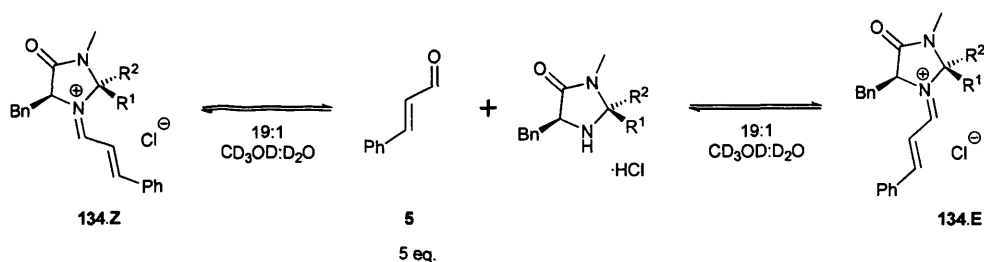
Scheme 4.79

The use of protic acids and Lewis acids in the formation of imidazolidinones under thermal and microwave conditions was further investigated. This knowledge was utilised to synthesise **110** in >99% ee (Scheme 4.79).



Scheme 4.80

**110** exhibited promise for use in asymmetric synthesis but could not be coerced into demonstrating comprehensively better enantiocontrol than benchmark catalyst **7** in the Diels-Alder reaction between **5** and **6** (Scheme 4.80). **110** may nonetheless have the potential to achieve higher levels of enantiocontrol when used with different substrates and is noteworthy among imidazolidinone catalysts for being able to attain high turnover as well as good enantioselectivity.



Scheme 4.81

The use of <sup>1</sup>H NMR to observe the distribution of catalyst hydrochloride and iminium ions in deuterated solvent systems was found to be a useful tool by which to characterise catalysts (Scheme 4.81). This technique strongly suggested that the imperfect enantiocontrol of the catalysts developed within this chapter could be attributed to a lack of geometric selectivity when forming iminium ions.

Finally, two design premises were firmly established. Future imidazolidinone catalysts must:

- Possess an EWG to enhance turnover
- Exhibit very high levels of iminium ion selectivity

---

## **Chapter 5: Synthesis of Literature Imidazolidinones**

---

## 5 Synthesis of Literature Imidazolidinones

### 5.1 Introduction

Although the overarching goal of this project was the development of novel high performance, selective catalysts for iminium ion catalysed reactions, the majority of project time had, at this point, been spent discovering and developing methodology for the synthesis of imidazolidinones.

Although many imidazolidinone catalysts have been described and their use widely reported, the literature was lacking in information regarding their preparation. Procedures were found to be absent from the primary literature, technically challenging, or of dubious efficacy (*vide infra*).

Adapting synthetic methodology already developed within this project to produce a range of prominent imidazolidinone catalysts was seen to be a much needed contribution to the field.

### 5.2 Target Selection

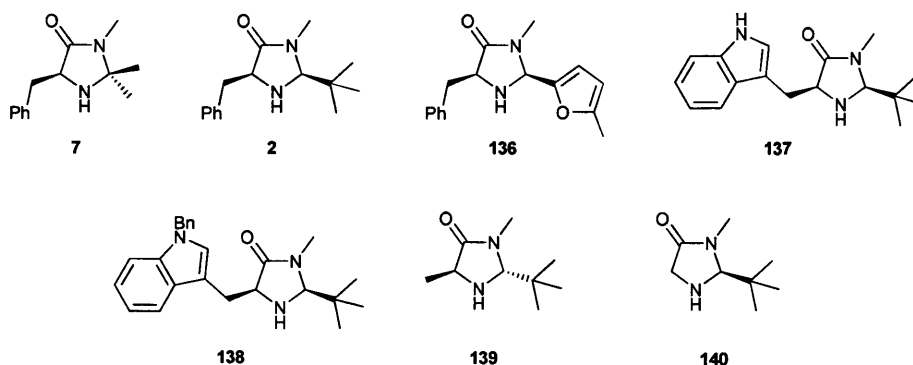
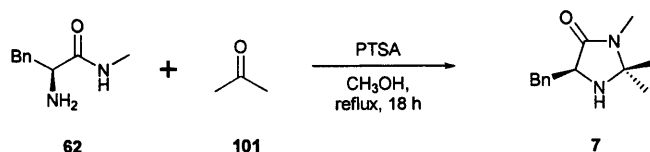
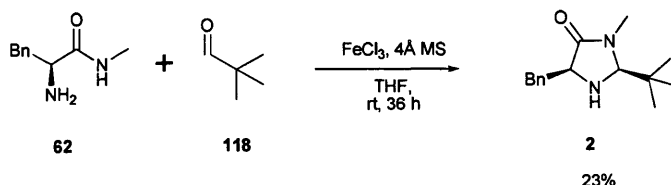


Figure 5.1

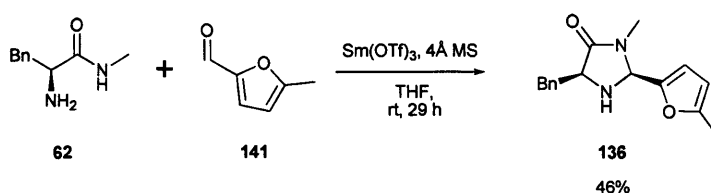
Seven target imidazolidinones **7**, **2**, **136–140** were identified, each of which were first described by MacMillan and co-workers (Figure 5.1). **7** is used for cycloaddition and closed transition state conjugate addition reactions of  $\alpha,\beta$ -unsaturated aldehydes as well as a number of enamine-catalysed processes.<sup>2,12,50</sup> **2** is effective at catalysing conjugate addition, enamine and SOMO reactions and has seen use in iminium/enamine cascade reactions.<sup>13,51–62</sup> **136** can facilitate iminium ion catalysed reactions of selected  $\alpha,\beta$ -unsaturated ketones.<sup>63</sup> **137** and **138** provide similar reactivity profiles to **2** but can provide higher enantiocontrol in some reactions.<sup>64–66</sup> **139** and **140** have recently been shown to be suitable for asymmetric catalysis of SOMO reactions.<sup>24,25,67</sup>



Scheme 5.2



Scheme 5.3

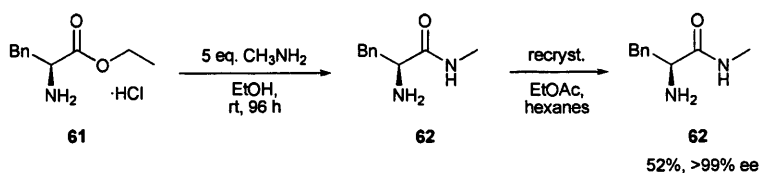


Scheme 5.4

Literature methods for the preparation of **7**, **2**, **136** are shown in Scheme 5.4. Catalyst **7** is made by refluxing **62** in 1:4 acetone:methanol in the presence of PTSA. Catalyst **2** is described as being obtained from an iron(III) chloride-catalysed reaction between **62** and **118**, although work within our group had showed that modification of this procedure by pre-forming the imine by stirring **62** and **118** over magnesium sulphate was required for the cyclisation to be effective. When this step was omitted, formation of a brown precipitate, presumed to be iron(III) oxide, was visible and the reaction failed. It was therefore assumed that water from the initial condensation was deactivating the iron(III) chloride catalyst. The literature procedure for **136** appeared troublesome, requiring freshly distilled **141**, and a glove box in which to work with the air-sensitive samarium(III) triflate. Before this work was performed, an exhaustive search of the primary literature failed to uncover procedures for the preparation of **137–140**. Since the completion of this work, a preparation of **139** was published by the MacMillan group.<sup>68</sup>

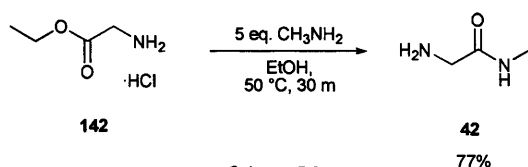
The goal of the work described within this chapter was therefore to develop methodology that was robust, reliable, easy to perform, and capable of providing **7**, **2**, and **136–140** in good yield and high enantiopurity.

### 5.3 Precursor Preparation



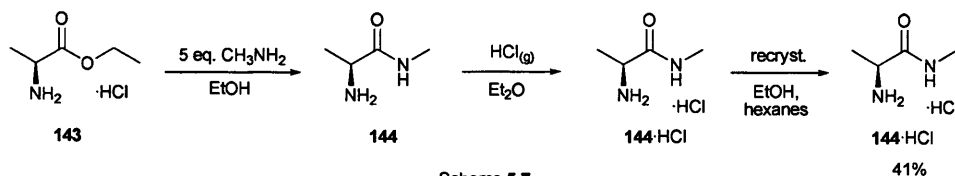
Scheme 5.5

The logical first step towards discovering a universal synthesis for the seven target compounds **7**, **2**, and **136–140** was to synthesise the amino amide precursors. A route to optically pure **62** had already been discovered, and this was employed for the work in this chapter, providing optically pure **62** in 52% overall yield (Scheme 5.5).



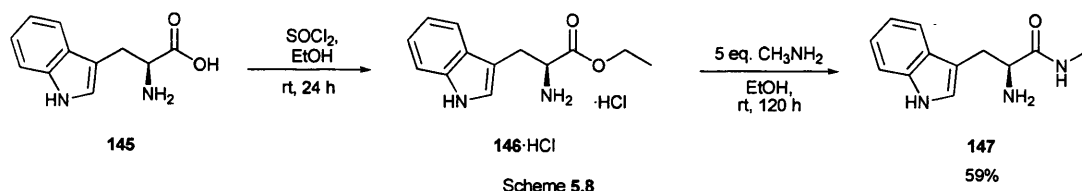
Scheme 5.6

A literature procedure describing the synthesis of **42** was found to work without modification.<sup>69</sup> Accordingly, **142** was stirred in ethanolic methylamine at 50 °C for 30 minutes and a basic workup was performed to yield pure **42** (77%) (Scheme 5.6).



Scheme 5.7

In a method analogous to the route used for **62**, **143** was stirred in ethanolic methylamine for 3 days and an aqueous workup performed. An ethereal solution of **144** was treated with gaseous hydrogen chloride and the precipitate recrystallised from ethanol and hexanes to yield needle-like crystals of **144·HCl**, assumed to be optically pure, in 41% overall yield (Scheme 5.7). The formation of a hydrochloride salt was a necessary step, as **144** existed as an oil at room temperature.

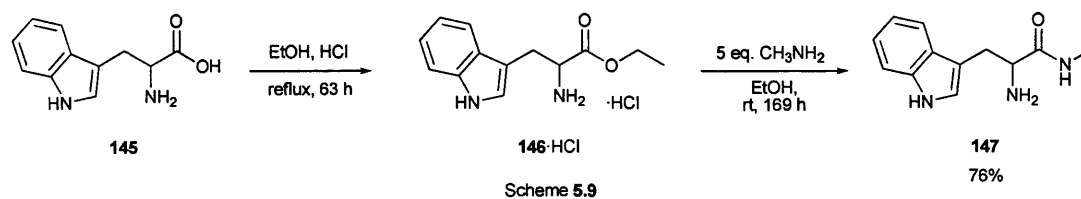


Scheme 5.8

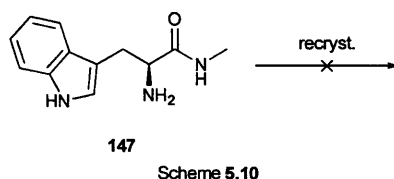
Thionyl chloride was added dropwise to a stirred solution of ethanol. When the reaction was complete and hydrogen chloride had been generated, **145** was added and the



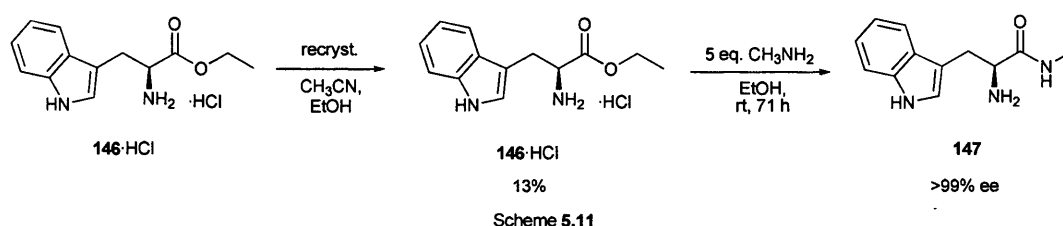
mixture stirred for 24 hours at room temperature. The solvent was evaporated and the residue washed with ethyl acetate and petroleum ether to provide **146**·HCl. This was then stirred in an excess of ethanolic methylamine for 120 hours at room temperature and the solvent removed to provide **147** in 59% overall yield (Scheme 5.8).



Using the methodology devised for **147**, racemic **145** was refluxed in ethanolic hydrogen chloride for 63 hours and after workup, the resultant racemic **146**·HCl stirred in ethanolic methylamine for 169 hours at room temperature to give racemic **147** in 76% overall yield (Scheme 5.9). Screening of HPLC conditions found that the enantiomers would separate on a Chiralcel OD-R column using a 7:3 acetonitrile:water solvent system. Previously synthesised batches of **147** were then subjected to analysis using this protocol and found to have ee's of 95–98%.



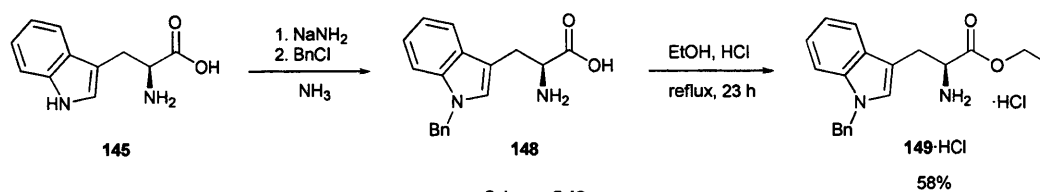
An attempt was made to crystallise **147** from toluene, which resulted only in a sludge being returned (Scheme 5.10). The dioxane:water solvent system was tried and showed ability to dissolve **147** at reflux, but did not reprecipitate the desired product when the temperature was lowered. Recrystallisation from THF:water yielded a crystalline product, but only with very low recovery of material.



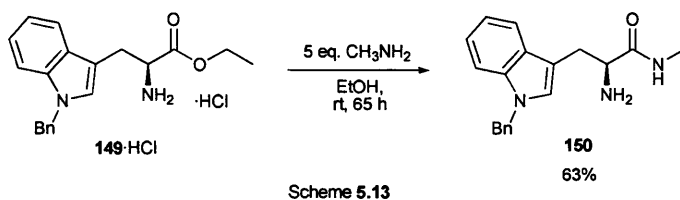
Visually, **146**·HCl appeared to have more crystallisation potential than **147** and efforts were refocused on boosting its optical purity. A solvent screen showed **146**·HCl to dissolve well in acetonitrile, less well in water, ethanol, and IPA, and to be virtually insoluble in toluene and ethyl acetate. An acetonitrile:ethanol system proved to be best amongst those tested and provided recrystallised **146**·HCl in 13% yield. This was then free-based and stirred



with ethanolic methylamine for 71 h, providing **147** of >99% ee (Scheme 5.11). While the overall yield of **147** was decidedly low, the quantities obtained proved sufficient for the work performed within this chapter and no attempt to optimise this process was made.

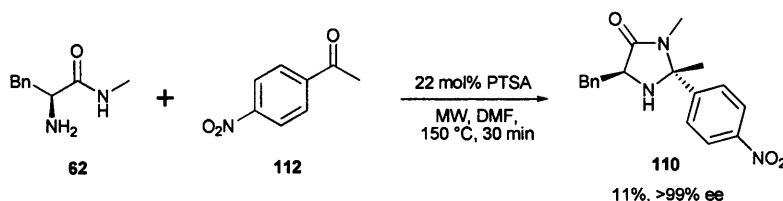


Neither **148** nor **149**·HCl could be sourced commercially, necessitating the synthesis of **148** from **145**. As published by Magnus *et al.*, **148** may be prepared by doubly deprotonating **145** and reacting the resultant dianion with benzyl chloride.<sup>70</sup> Accordingly, a solution of sodamide was prepared by dissolving metallic sodium in refluxing ammonia containing catalytic iron(III) nitrate nonahydrate. **145** was then added and the mixture was stirred to effect deprotonation of both the amino acid moiety and the proton at the 1-position of the indole ring. The solution was then treated with a slight excess of freshly distilled benzyl chloride and the reaction allowed to boil dry overnight. The residue was quenched with water, filtered to remove iron residues, and treated with glacial acetic acid to induce precipitation of **148**. **148** was then refluxed overnight in ethanolic hydrogen chloride to yield **149**·HCl in 58% overall yield (Scheme 5.12).



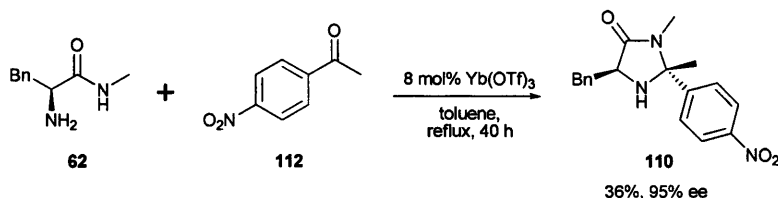
In a modification to the usual route for converting ethyl ester hydrochlorides to amino amides, an aqueous freebasing was performed prior to stirring the material in ethanolic methylamine. This eliminated the need to expose the more water-soluble product to an aqueous workup. **150** was thus obtained in 63% yield from **149**·HCl (Scheme 5.13). Racemic **149**·HCl was then used to synthesise racemic **150**. This material was found to separate on the Chiralcel OJ column using a 9:1 hexanes:IPA mobile phase at 1.5 mL min<sup>-1</sup> (*t* = 27.9 min, 39.5 min) and showed that the **150** synthesised from optically pure **149**·HCl had an ee of >99%.

## 5.4 Initial Investigations



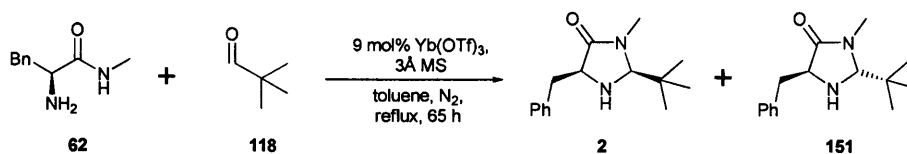
Scheme 5.14

In the previous chapter, a synthetic method for production of the acetophenone-based imidazolidinones using methanesulfonic acid under microwave irradiation had been developed and found to involve very little epimerisation (Scheme 5.14). Unfortunately, the requirement for a microwave reactor would place limitations upon the utility of this work and reduce the feasibility of scale-up. A logical starting point for development of a suitable synthesis therefore seemed to be the use of ytterbium(III) triflate under thermal conditions.



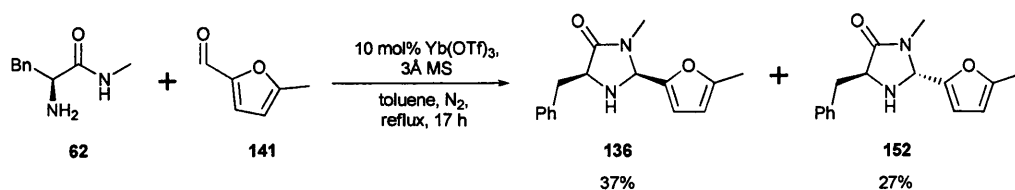
Scheme 5.15

The use of ytterbium(III) triflate in refluxing toluene had shown the ability to facilitate imidazolidinone formation (Scheme 5.15). This system appeared to be a good starting point for the synthesis of **7**, **2**, and **136–140**. Having previously observed the thermodynamic nature of the reaction under microwave conditions and deduced how removal of water may be expected to boost yields, reactions were performed under nitrogen and over 3Å molecular sieves.



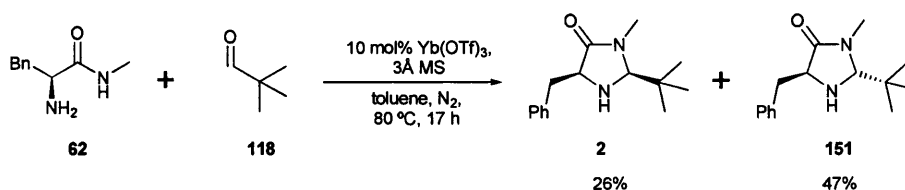
Scheme 5.16

It was anticipated that the sterically hindered aldehyde **118** could present difficulties. **118** was refluxed with **62** in the presence of 9 mol% ytterbium(III) triflate for 65 hours (Scheme 5.16). After an aqueous workup to remove the paramagnetic catalyst, <sup>1</sup>H NMR showed the reaction to have been a success. **2** and **151** were observed in a 1:1.3 ratio.



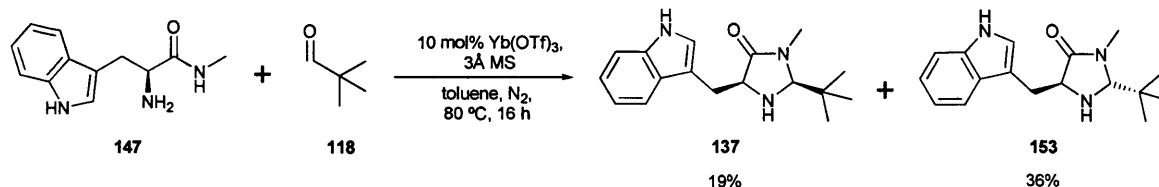
Scheme 5.17

The electron-rich aromatic aldehyde **141** was also found to react readily with **62** when refluxed together in the presence of 10 mol% ytterbium(III) triflate for 17 hours. Column chromatography was performed and the desired product **136** (37%) was isolated, along with unwanted diastereomer **152** (27%) (Scheme 5.17).



Scheme 5.18

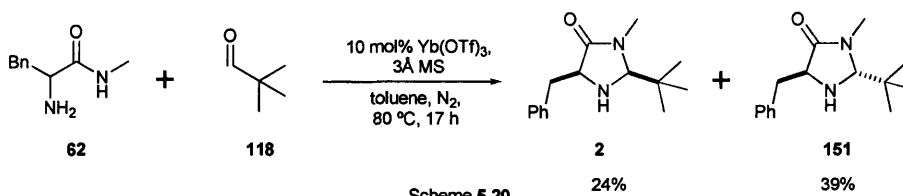
Having discovered during the synthesis of acetophenone-based imidazolidinones that refluxing in toluene can be expected to induce significant epimerisation, milder conditions were examined. **62** and **118** were stirred at 80 °C in toluene in the presence of 10 mol% ytterbium(III) triflate. After aqueous workup and column chromatography, **2** (26%) and **151** (47%) were obtained (Scheme 5.18).



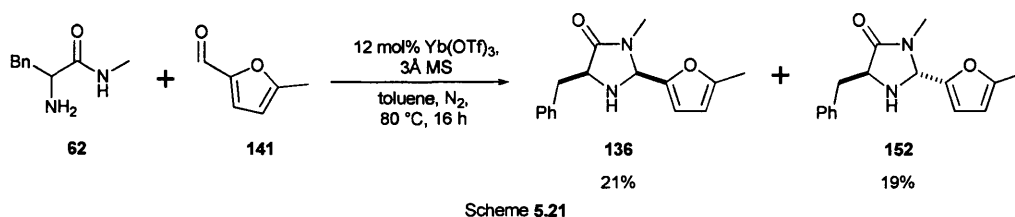
Scheme 5.19

**147** was thought to be potentially problematic as it exhibited low solubility in toluene. **147**, **118**, and 10 mol% ytterbium triflate were stirred in toluene at 80 °C for 16 hours. Column chromatography yielded **137** (19%) **153** (36%) (Scheme 5.19).

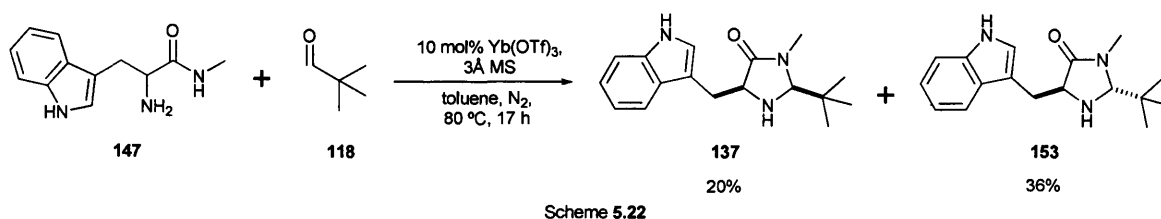
## 5.5 Racemate Synthesis



Having established that **2**, **136** and **137** may be synthesised under conditions less likely to cause racemisation (Scheme 5.20), a protocol for establishing the enantiopurity of the target imidazolidinones was desired. Racemic **62** and **118** were stirred at 80 °C in the presence of 10 mol% ytterbium(III) triflate in toluene for 17 hours (Scheme 5.20). Subjecting the crude mixture to column chromatography yielded racemic **2** (24%) and **151** (39%). It was found that **2** would separate on a Chiralcel OJ column using 19:1 hexanes:IPA at a flow rate of 1.5 mL min<sup>-1</sup> (*t* = 7.2 min, 10.5 min) and that **151** would separate on the same column using a 99:1 hexanes:IPA mobile phase at a flow rate of 1.5 mL min<sup>-1</sup> (*t* = 18.2 min, 22.3 min). A variable wavelength UV detector was used and set to 220 nm, close to the peak absorption of both **2** and **151**.

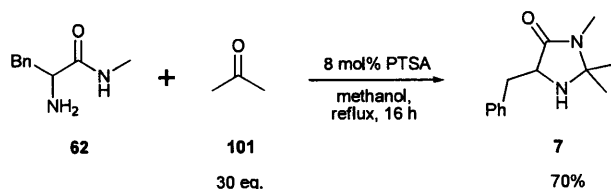


Stirring racemic **62** with **141** and 12mol% ytterbium(III) triflate in toluene at 80 °C for 16 hours yielded, after chromatography, racemic **136** (21%) and **152** (19%) (Scheme 5.21). It was found that **136** would cleanly separate on a Chiralcel OJ column using 9:1 hexanes:IPA at a flow rate of 1.5 mL min<sup>-1</sup> (*t* = 10.2 min, 27.3 min) while **152** would partially separate on the same column using a 99:1 hexanes:IPA mobile phase at a flow rate of 1.5 mL min<sup>-1</sup> (*t* = 67.3 min, 72.8 min).



Racemic **147** and **118** were stirred at 80 °C in the presence of 10 mol% ytterbium(III) triflate in toluene for 17 hours (Scheme 5.22). Subjecting the crude mixture to column chromatography yielded racemic **137** (20%) and **153** (36%). It was found that **137** would

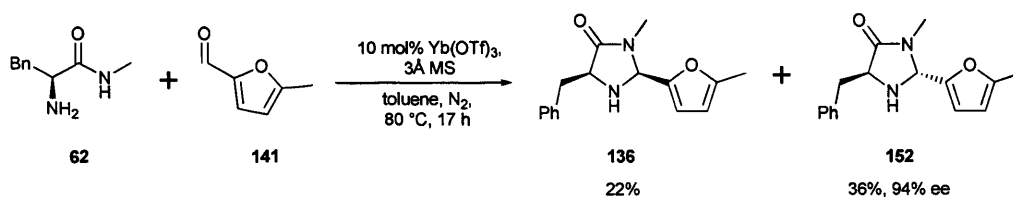
separate on a Chiralcel OD column using 37:3 hexanes:IPA at a flow rate of  $1.5 \text{ mL min}^{-1}$  ( $t = 22.9 \text{ min}, 29.7 \text{ min}$ ). Conditions for the separation of **153** were not discovered.



Scheme 5.23

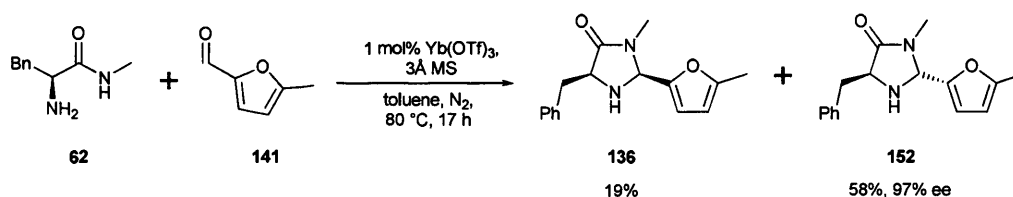
Using the literature preparation of **7**, racemic **62** was refluxed in 2:1 methanol:acetone for 16 hours and **7** was obtained after aqueous workup in 70% yield (Scheme 5.23). **7** was found to separate on a Chiralcel OJ column using a 97:3 hexanes:IPA mobile phase at a flow rate of  $1.5 \text{ mL min}^{-1}$  ( $t = 16.9 \text{ min}, 18.5 \text{ min}$ ).

## 5.6 Synthesis Refinement



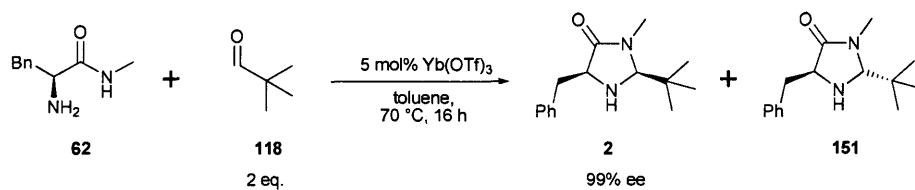
Scheme 5.24

**62** and **141** were stirred in toluene at 80 °C in the presence of 10 mol% ytterbium(III) triflate for 17 hours. After column chromatography, pure **136** (22%, ee not determined) and **152** (36%, 94% ee) were obtained (Scheme 5.24).



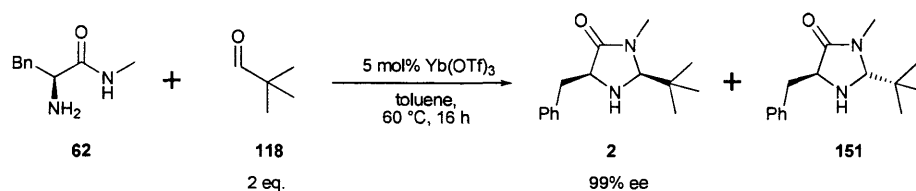
Scheme 5.25

To investigate whether lowering the catalyst loading could reduce epimerisation, **62**, **141**, and 1 mol% ytterbium(III) triflate were stirred in toluene at 80 °C (Scheme 5.25). Column chromatography yielded **136** (19%, ee not determined) and **152** (58%, 97% ee).



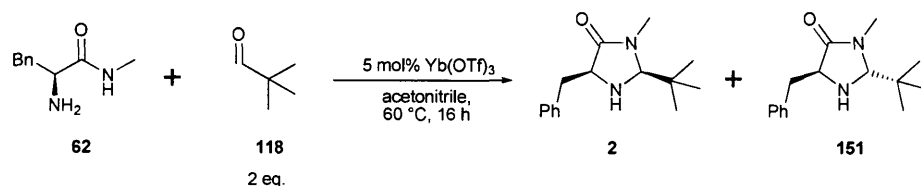
Scheme 5.26

At this stage, the use of a nitrogen atmosphere and molecular sieves were discontinued, in order to be able to claim air insensitivity and broaden the appeal of the methodology. The effect of lower temperature was also investigated when **62** and **118** were stirred together with 5 mol% ytterbium(III) triflate at 70 °C in toluene (Scheme 5.26). **2** was isolated after column chromatography and found to have an ee of 99%.



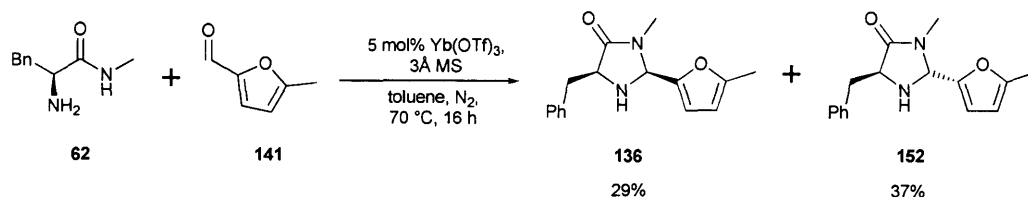
Scheme 5.27

Lowering the temperature still further, **62** and **118** were stirred together with 5 mol% ytterbium(III) triflate at 60 °C in toluene (Scheme 5.27). **2** was isolated after column chromatography and again found to have an ee of 99%.



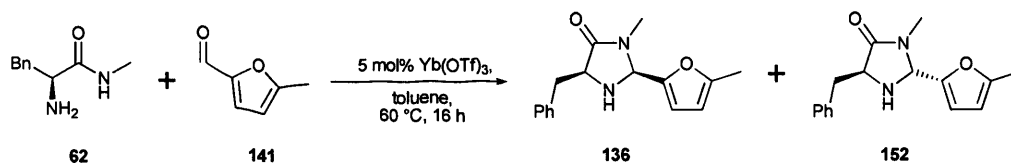
Scheme 5.28

As the catalyst appeared to be almost insoluble in toluene at 60 °C, **62**, **118**, and 5 mol% ytterbium(III) triflate were stirred together in acetonitrile at 60 °C for 16 hours (Scheme 5.28).  $^1\text{H}$  NMR showed the crude reaction mixture to contain **2**, **151** and multiple side products and this choice of solvent was not investigated further.



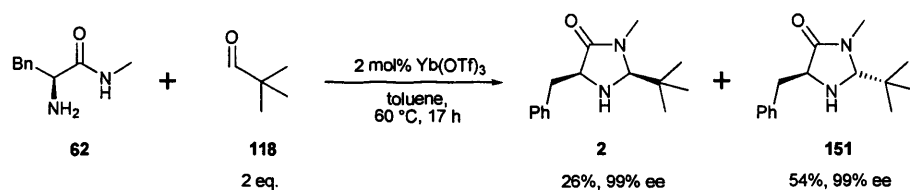
Scheme 5.29

To see whether reduced temperature would still facilitate formation of **62**, **141** and 5 mol% ytterbium(III) triflate were stirred in toluene with 5 mol% ytterbium(III) triflate at 70 °C for 16 hours (Scheme 5.29). Column chromatography provided **136** (29%) and **152** (37%).



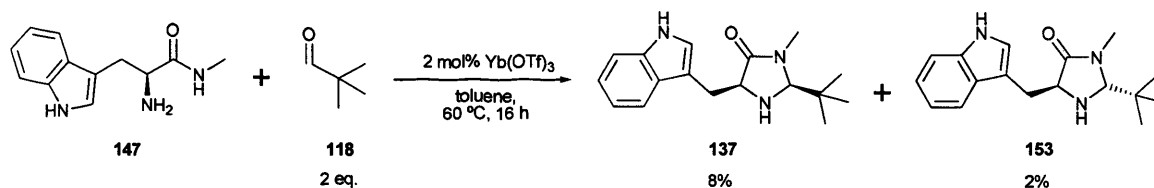
Scheme 5.30

**62** and **141** were then stirred with 5 mol% ytterbium(III) triflate at 60 °C in toluene (Scheme 5.30). Column chromatography was not performed as <sup>1</sup>H NMR of the reaction mixture showed a similar level of conversion to that attained in Scheme 5.29.



Scheme 5.31

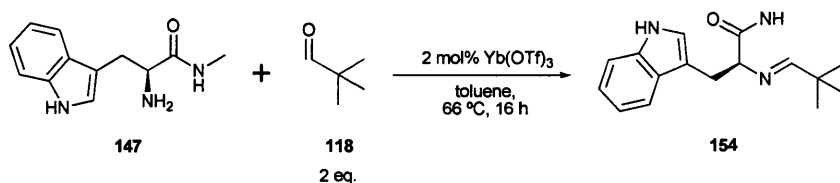
To investigate a lower catalyst loading at the reduced temperature, **62** and **118** were stirred with 2 mol% ytterbium(III) triflate at 60 °C in toluene for 16 hours (Scheme 5.31). After column chromatography, **2** (26%, 99% ee) and **151** (54%, 99% ee) were isolated.



Scheme 5.32

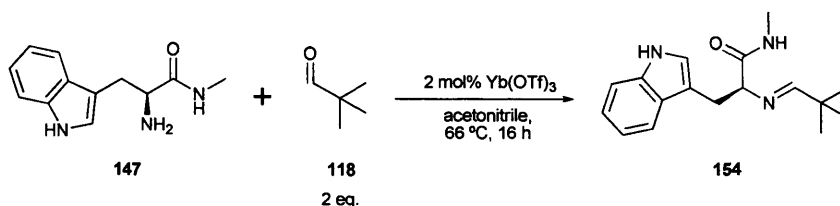
**147** and **118** were stirred with 2 mol% ytterbium(III) triflate at 60 °C in toluene for 16 hours (Scheme 5.32). Isolated yields of **137** and **153** were extremely low (8% and 2%, respectively) and the problem was assumed to be the low solubility of **147** in the reaction medium.

## 5.7 Solvent Screening



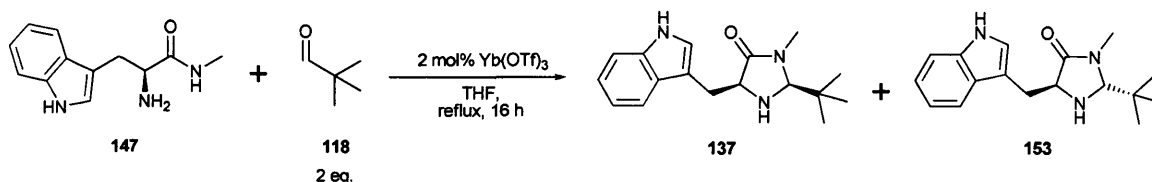
Scheme 5.33

Re-attempting the reaction between **147** and **118** at a slightly higher temperature, the starting materials were stirred with 2 mol% ytterbium(III) triflate in toluene for 16 hours at 66 °C (Scheme 5.33). After aqueous workup, <sup>1</sup>H NMR showed the crude to consist largely of **154** with smaller amounts of **137** and **153**. This indicated that the issue with this reaction was not the low solubility of **147** but was in fact the inability of **154** to cyclise under these conditions. As such, it appeared impossible to induce formation of **137** in good yields and good enantiopurity by varying only the catalyst loading and temperature of this system.



Scheme 5.34

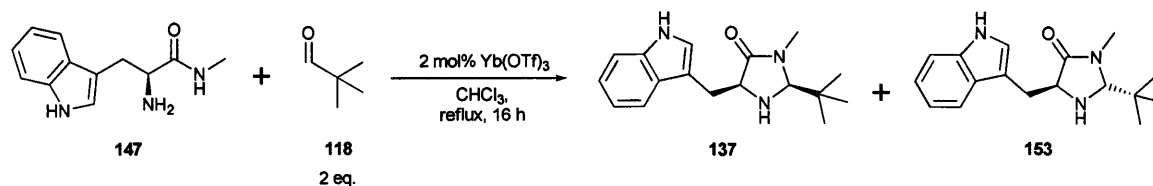
Using the reaction of **147** and **118** as a test case, alternative solvents were investigated and the results qualitatively assayed by <sup>1</sup>H NMR of the crude reaction mixture. **147** and **118** were stirred with 2 mol% ytterbium(III) triflate at 66 °C in acetonitrile for 16 hours (Scheme 5.34). The crude was seen to be similar to that of Scheme 5.33 and to consist largely of **154**, with some traces of **137** and **153**.



Scheme 5.35

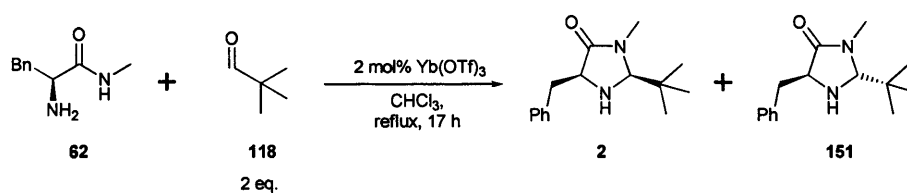
**147** and **118** were stirred with 2 mol% ytterbium(III) triflate in refluxing THF for 16 hours (Scheme 5.35). The crude was seen to be a mixture of **137** and **153** in a ratio of 1:1.9.





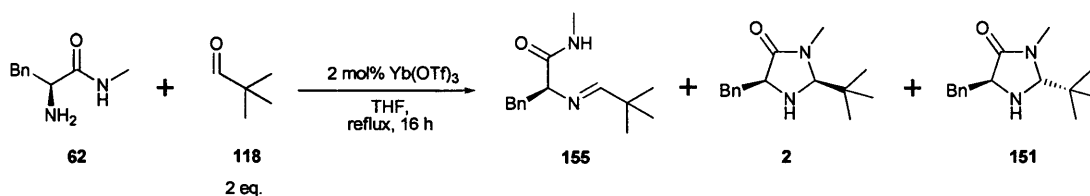
Scheme 5.36

**147** and **118** were stirred with 2 mol% ytterbium(III) triflate in refluxing chloroform for 16 hours (Scheme 5.36). The crude was seen to be a mixture of **137** and **153** in a ratio of 1:1.3. This result showed chloroform to be the best candidate for synthesis of **137**.



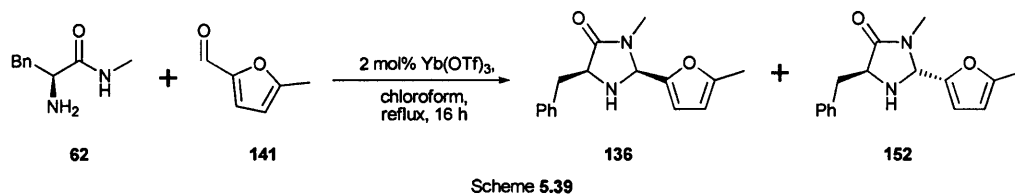
Scheme 5.37

Acetonitrile and toluene appeared unsuitable for synthesis of **137**, while THF and chloroform appeared to facilitate clean formation. The logical next step was to determine whether chloroform or THF would be most suitable for synthesis of the other target imidazolidinones. **62** and **118** were stirred with 2 mol% ytterbium(III) triflate in refluxing chloroform for 16 hours (Scheme 5.37). The crude mixture consisted of **2** and **151** in a 1:1.4 ratio.

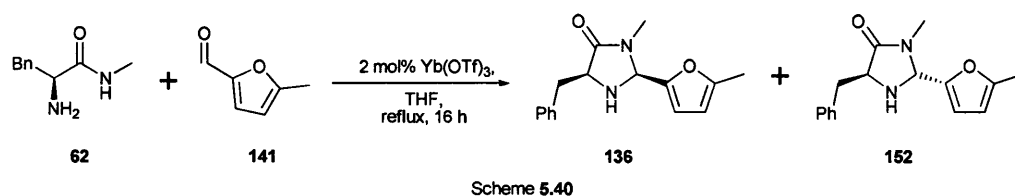


Scheme 5.38

**62** and **118** were stirred with 2 mol% ytterbium(III) triflate in refluxing THF for 16 hours (Scheme 5.38). The crude mixture consisted of **155**, **2** and **151** in a 1:1.0:2.3 ratio. This result established chloroform as the solvent of choice for the thermal ytterbium(III) triflate-catalysed synthesis of **137**.

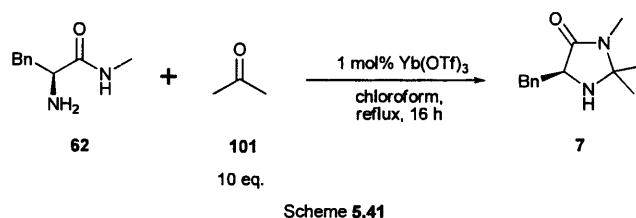


**62** and **141** were stirred with 2 mol% ytterbium(III) triflate in refluxing chloroform for 16 hours (Scheme 5.39). The crude mixture consisted of **136** and **152** in a 1:1.0 ratio, together with traces of the intermediate imine.

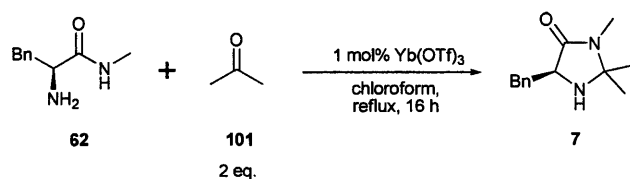


**62** and **141** were stirred with 2 mol% ytterbium(III) triflate in refluxing chloroform for 16 hours (Scheme 5.40). The crude mixture consisted of **136** and **152** in a 1:1.3 ratio and traces of the intermediate imine. This established chloroform as the preferred media for the thermal ytterbium(III) triflate-catalysed synthesis of **136** and suggested it as the solvent around which this synthetic methodology should be standardised.

## 5.8 Acetone Equivalents



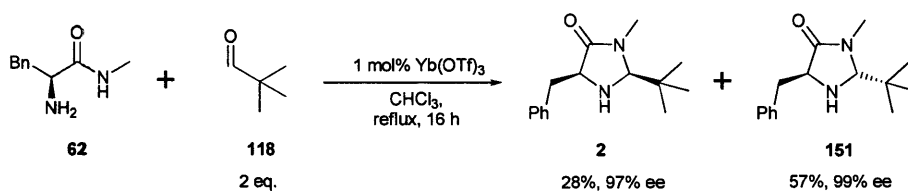
The literature synthesis of **62** uses a 4:1 methanol:acetone mixture as a reaction solvent, equivalent to a vast excess of **101**. In order to determine whether a vast excess was required for the synthetic methodology developed in this chapter, two experiments were performed. Additionally, it was thought that lowering the catalyst loading to 1 mol% would not significantly hinder target compound formation but would enhance the aesthetic appeal of the methodology. **62** and 10 equivalents of **101** were stirred with 1 mol% ytterbium(III) triflate in refluxing chloroform for 16 hours (Scheme 5.41). <sup>1</sup>H NMR of the crude showed clean conversion to **7**.



Scheme 5.42

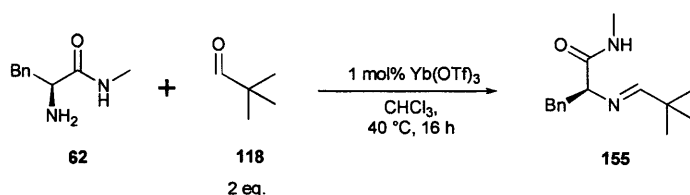
**62** and 2 equivalents of **101** were stirred with 1 mol% ytterbium(III) triflate in refluxing chloroform for 16 hours (Scheme 5.42).  $^1\text{H}$  NMR of the crude showed clean conversion once again, and established that 2 equivalents of **101** was sufficient for synthesis of **7**.

## 5.9 Temperature Screening



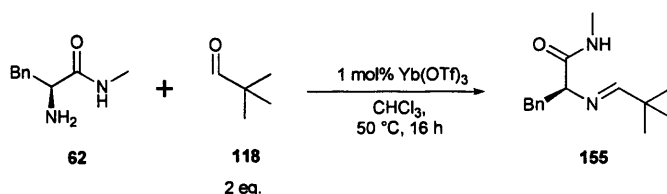
Scheme 5.43

Using the new conditions, **62** and 2 equivalents of **118** were stirred with 1 mol% ytterbium(III) triflate in refluxing chloroform for 16 hours (Scheme 5.43). Column chromatography provided **2** (28%, 97% ee) and **151** (57%, 99% ee). As the ee of the desired product **2** was too low, further optimization of conditions appeared necessary.



Scheme 5.44

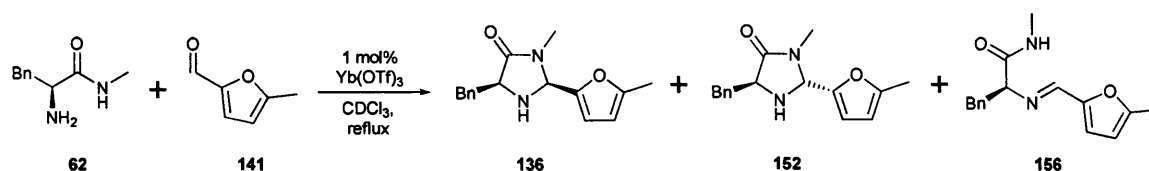
**62** and 2 equivalents of **118** were stirred with 1 mol% ytterbium(III) triflate in chloroform at 40 °C for 16 hours (Scheme 5.44).  $^1\text{H}$  NMR of the crude showed it to consist mainly of **155**, showing that the temperature was too low to induce cyclisation.



Scheme 5.45

**62** and 2 equivalents of **118** were stirred with 1 mol% ytterbium(III) triflate in chloroform at  $50\text{ }^\circ\text{C}$  for 16 hours (Scheme 5.45).  $^1\text{H}$  NMR of the crude showed it to consist mainly of **155**, with traces of **2** and **151**. Once again, the temperature appeared to be too low and it was deduced that no significant improvements could be made to product enantiopurity by tuning the temperature of the reaction system.

### 5.10 Reaction Time Optimization



Scheme 5.46

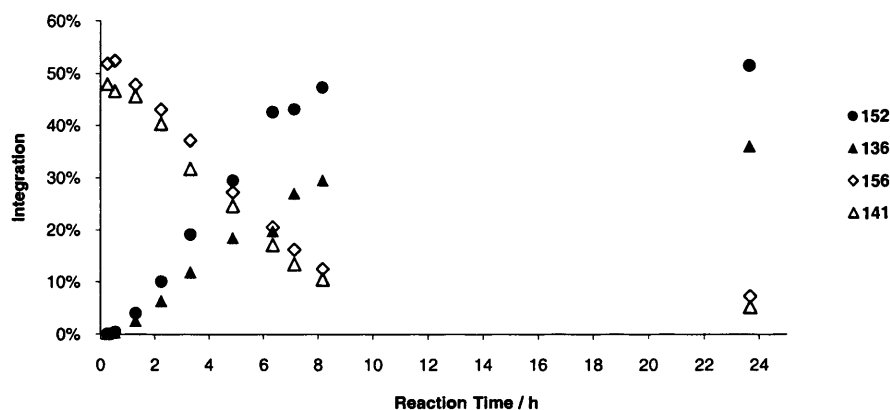
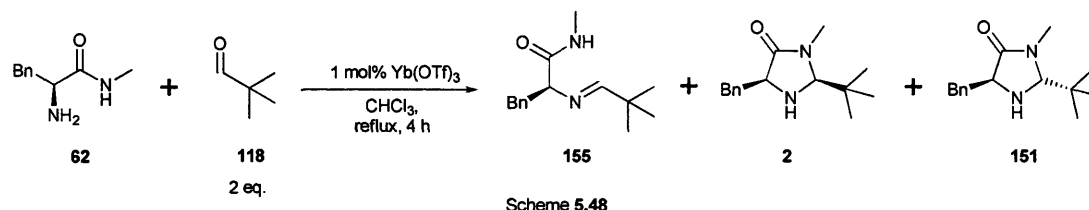


Figure 5.47

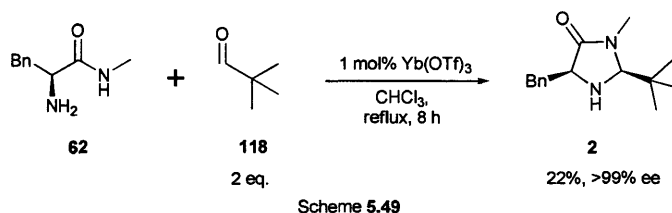
To gauge the effect of lowering the reaction time from 16 hours, the reaction between **62** and **141** was performed in deuterated chloroform and aliquots taken periodically and analysed by  $^1\text{H}$  NMR (Scheme 5.46). This reaction proved suitable for monitoring by  $^1\text{H}$  NMR as **141** is non-volatile, so can be used stoichiometrically, and presents clean signals for integration. Although the paramagnetic ytterbium(III) was present, its concentration was sufficiently low that the spectra could be interpreted without difficulty. For each spectra, signals of the compounds **62**, **141**, **136**, **152**, **156** were integrated, expressed as a percentage of the total, and plotted against the time at which the aliquot was taken (Figure 5.47). The

results suggested that the reaction was under thermodynamic control and showed that at the conclusion of the reaction, small amounts of **141** and **156** were present. Additionally, the reaction appeared close to equilibrium after 8 hours, suggesting that reducing reaction time may be a fruitful way to attain the desired levels of product enantiopurity.

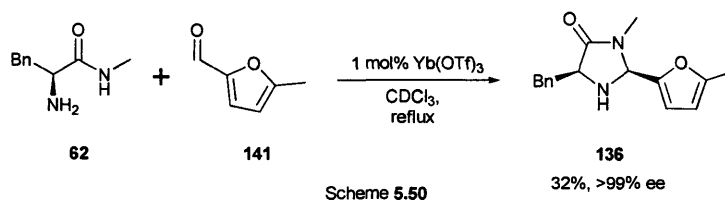


To see whether reducing reaction times may be fruitful with a different substrate, **62** and 2 equivalents of **118** were stirred with 1 mol% ytterbium(III) triflate in refluxing chloroform for 4 hours (Scheme 5.48). <sup>1</sup>H NMR showed the crude to contain **155**, **2** and **151** in a 1:1.8:6.3 ratio. This equated to an **2**:**151** ratio of 1:3.4, comparing unfavourably with the **2**:**151** isolated yield ratio, which was 1:2.0 in the comparable 16 hour reaction (Scheme 5.43). This suggested **151** to be the kinetic product.

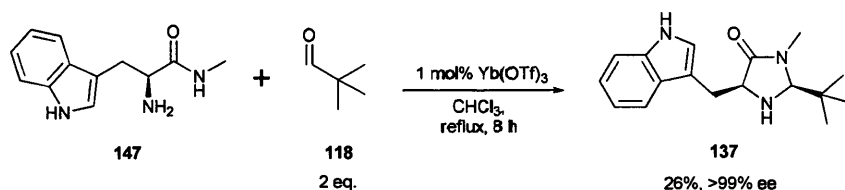
### 5.11 Final Conditions



As a 16 hour reaction time had induced unacceptable levels of epimerisation and a 4 hour reaction time had produced the desired product in low yields, an 8 hour reaction time appeared suitable. **62**, **118** and 1 mol% ytterbium(III) triflate were refluxed in chloroform for 8 hours (Scheme 5.49). Column chromatography provided **2** (22%, >99% ee).

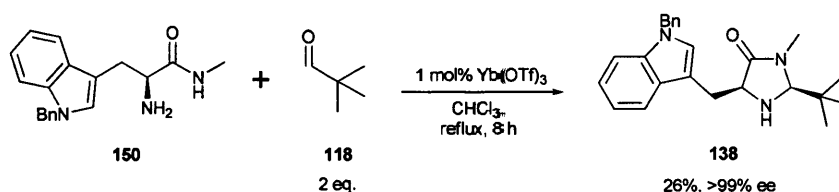


As expected, the reaction between **62** and **141** in the presence of 1 mol% ytterbium(III) triflate proceeded cleanly when refluxed in chloroform for 8 hours and column chromatography was used to provide **136** (32%, >99% ee) (Scheme 5.50).



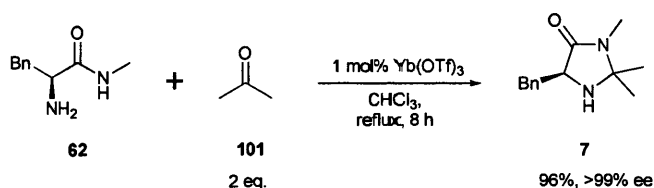
Scheme 5.51

**147**, **118** and 1 mol% ytterbium(III) triflate were refluxed in chloroform for 8 hours (Scheme 5.51). Column chromatography provided **137** (26%, >99% ee).



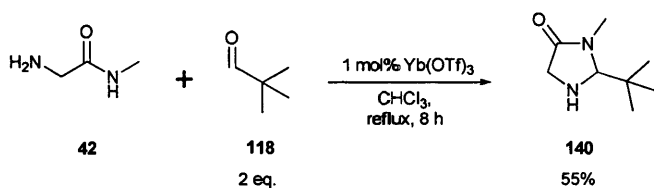
Scheme 5.52

**150**, **118** and 1 mol% ytterbium(III) triflate were refluxed in chloroform for 8 hours (Scheme 5.52). Column chromatography provided **138** (26%, >99% ee).



Scheme 5.53

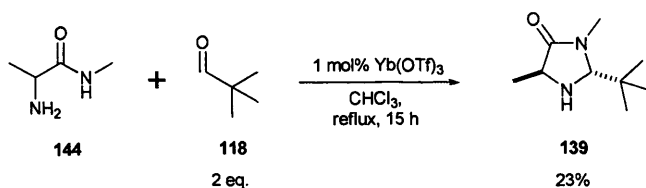
**62**, **101** and 1 mol% ytterbium(III) triflate were refluxed in chloroform for 8 hours (Scheme 5.53). Column chromatography provided **7** (96%, >99% ee).



Scheme 5.54

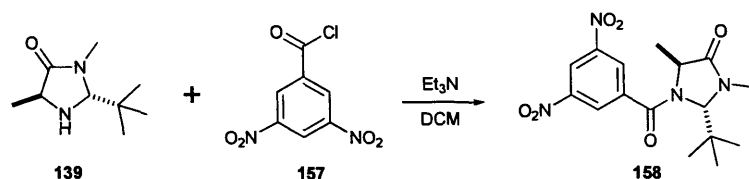
**42**, **118** and 1 mol% ytterbium(III) triflate were refluxed in chloroform for 8 hours (Scheme 5.54). Column chromatography provided **140** (55%) as a racemate.

## 5.12 UV active derivative synthesis



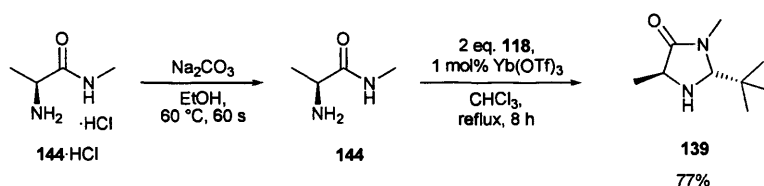
Scheme 5.55

Racemic **114** and 2 equivalents of **118** were stirred with 1 mol% ytterbium(III) triflate in chloroform at 50 °C for 15 hours (Scheme 5.55). After column chromatography, racemic **139** (23%) was obtained. Lacking the aromatic ring systems of **7**, **2**, **136–138**, UV absorbance was expected to be much weaker. UV-visible spectroscopy showed a maxima at 240 nm and HPLC separation was attempted with the detector set to this wavelength. Using a 199:1 hexanes:IPA mobile phase at 1.5 mL min<sup>-1</sup> on a Chiralcel OD column, partial separation of **139** was possible, but the weak signal rendered quantitative analysis impossible.



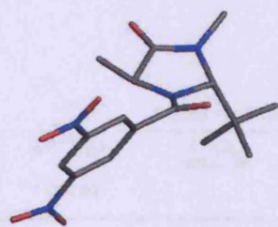
Scheme 5.56

To circumvent this problem, derivatisation of **139** was investigated. It was found that racemic **158**, produced from the condensation of racemic **139** and **157** (Scheme 5.56), absorbed strongly at 237 nm and would separate on a Chiralcel OD column with a 4:1 hexanes:IPA mobile phase running at 1.5 mL min<sup>-1</sup> ( $t = 20.1$  min, 27.1 min).



Scheme 5.57

**144·HCl** was heated in ethanol with sodium carbonate to around 60 °C for 1 minute and **144** isolated after filtration and evaporation of the solvent. **144**, **118** and 1 mol% ytterbium(III) triflate were refluxed in chloroform for 8 hours before the crude was subjected to column chromatography to provide **139** in 77% overall yield (Scheme 5.57). HPLC analysis of UV-active derivative **158** showed the material to have an ee of >99%.

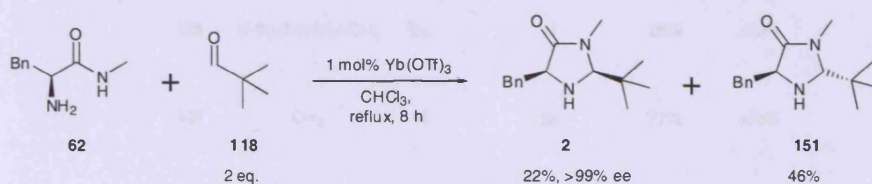


158

Figure 5.58

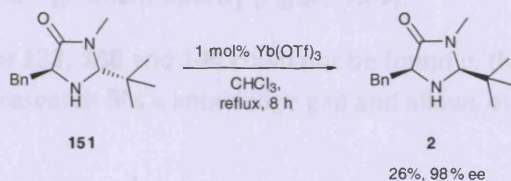
A sample of **158** was crystallised from IPA and submitted for X-ray crystallography. The solved structure served to confirm the stereochemistry of **158** and, by implication, **139** (Figure 5.58).

### 5.13 Scale-up and Recycling



Scheme 5.59

To prove that the methodology developed was amenable to scale-up, 5.0 g of **62** was refluxed with 2 equivalents of **118** and 1 mol% ytterbium(III) triflate for 8 hours in chloroform (Scheme 5.59). After column chromatography, **2** (22%, >99% ee) and **151** (46%) were obtained.



Scheme 5.60

**151** obtained in the previous reaction (Scheme 5.59) was refluxed with 1 mol% ytterbium(III) triflate for 8 hours in chloroform (Scheme 5.60). Column chromatography provided **2** (26%, 98% ee). This experiment showed the potential for unwanted diastereomers to be recycled, albeit with some loss of enantiopurity.



## 5.14 Conclusions

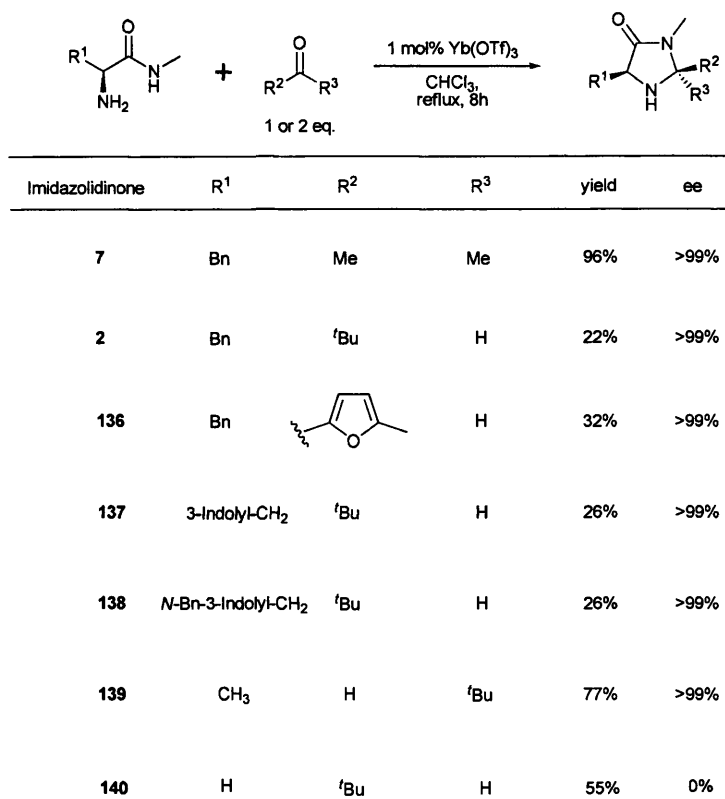


Figure 5.61

Utilising synthetic knowledge and techniques gained in previous chapters, a flexible, reliable and air insensitive synthesis has been developed that provides imidazolidinones **2**, **7**, **136–140** in good yields and high enantiopurity (Figure 5.61).

As preparations for **137**, **138** and **140** could not be found in the primary literature, it can also be said that this research fills a knowledge gap and allows other researchers easy access to these catalysts.

Finally, publicising the utility of ytterbium(III) triflate in imidazolidinone synthesis may allow other researchers to adapt this methodology to attain target compounds of their own design.

---

## **Chapter 6: Computer Modelling**

---

## 6 Computer Modelling

### 6.1 Introduction

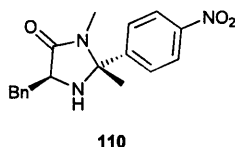


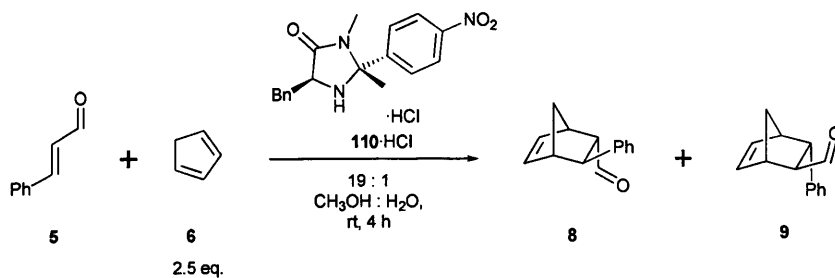
Figure 6.1

The overriding goal of this project was to develop an iminium ion organocatalyst that demonstrated both high performance and excellent levels of stereoselectivity. Efforts to improve the enantioselectivity of the high performance **110** catalyst had run into a dead end and experimental data suggested that its iminium ion geometric selectivity was lacking (Figure 6.1). To gain further insight, computer modelling was undertaken. The aim of the work documented within this chapter was to gain further understanding into iminium ion selectivity and move towards being able to design a catalyst with high turnover and good enantiocontrol.

Although modern computers have vast amounts of computational power, the difficulty involved in chemical modelling rendered the available processing power incapable of modelling systems of more than a few dozen atoms to the degree of accuracy deemed acceptable for this project. This mandated the design of a system that would at once be sufficiently simple as to be modelled on accessible computer hardware and yet sufficiently developed as to be able to explain catalyst performance and elucidate general principles for catalyst design.

### 6.2 Model Design

It has long been assumed that the transition state in the benchmark Diels-Alder reaction is bimolecular and occurs between an iminium ion and a molecule of cyclopentadiene **6**. The transition states are assumed to occur in the absence of the chloride counter-ion, which is assumed to be fully solvated in the protic solvent mixture.



Scheme 6.2

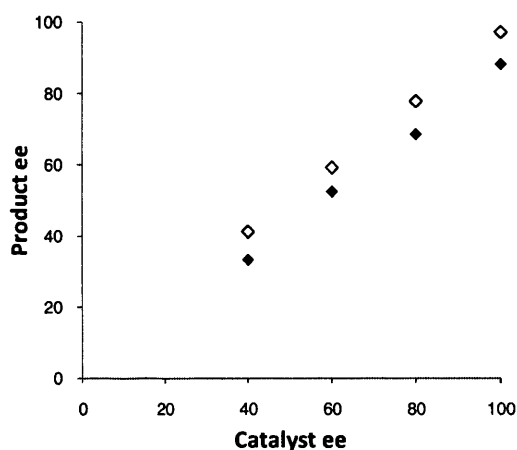


Figure 6.3

To investigate whether the reaction is bimolecular, the benchmark Diels-Alder reaction was performed using **110**-HCl and its enantiomer, mixed to attain overall **110**-HCl ee's of between 40% and 100% (Scheme 6.2). A linear correlation between catalyst ee and product ee was noted, indicating that the iminium ions react individually and not as aggregates (Figure 6.3).

Another longstanding assumption is that the only active species in iminium ion catalysed reactions are the iminium ions. While experiments documented in Chapter 4.3 showed a small degree of background reaction, this assumption was seen to hold largely true for the benchmark Diels-Alder reaction.

Additionally, in the presence of water, the iminium ion catalysed Diels-Alder reaction has been shown to be irreversible, meaning only the forward reaction needed to be considered.<sup>31</sup>

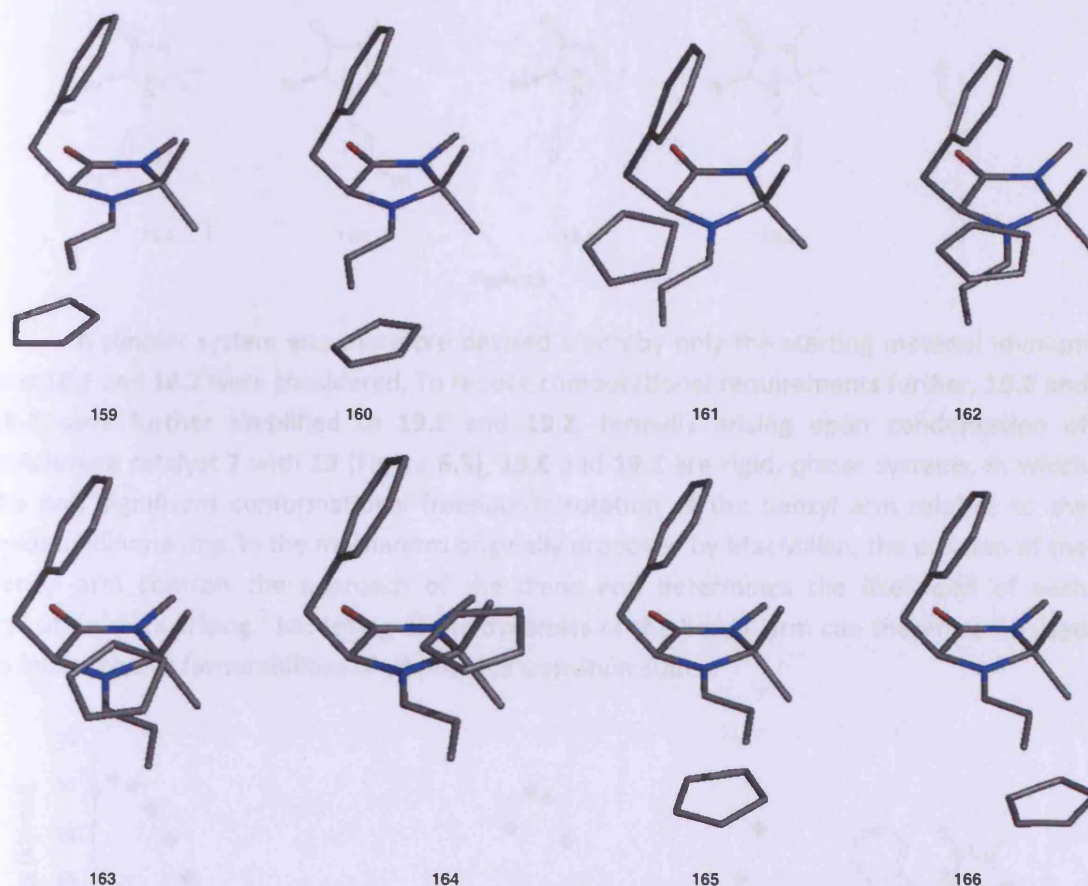


Figure 6.4

With these assumptions in mind, the stereocontrol exerted by **110** in the benchmark reaction may be understood in terms of the relative energies of all possible transition states. Assuming the position of the benzyl arm corresponds to its position in the lowest energy conformation of the free iminium ions, 8 transition states are possible. These are shown without the phenyl ring of the substrate for clarity in Figure 6.4. Reactions proceeding through transition states **160** and **163** will generate the major enantiomer of the *endo* adduct **8**, while reactions proceeding through states **159** and **164** will generate the major enantiomer of the *exo* adduct **9**. Transition states **162** and **165** give rise to the minor enantiomer of **8**, while **161** and **166** give rise to the minor enantiomer of **9**.

Taking into account the free rotation of the benzyl arm would increase the number of transition states that must be considered. When combined with the computational difficulty in determining transition states, this rendered transition state modelling infeasible for use within this project.

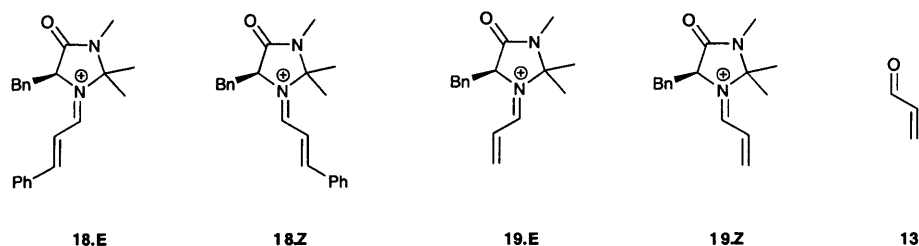


Figure 6.5

A simpler system was therefore devised whereby only the starting material iminium ions **18.E** and **18.Z** were considered. To reduce computational requirements further, **18.E** and **18.Z** were further simplified to **19.E** and **19.Z**, formally arising upon condensation of benchmark catalyst **7** with **13** (Figure 6.5). **19.E** and **19.Z** are rigid, planar systems, in which the only significant conformational freedom is rotation of the benzyl arm relative to the imidazolidinone ring. In the mechanism originally proposed by MacMillan, the position of the benzyl arm controls the approach of the diene and determines the likelihood of each transition state arising.<sup>2</sup> Modelling of the dynamics of the benzyl arm can therefore be used to intuit relative favourabilities of all possible transition states.

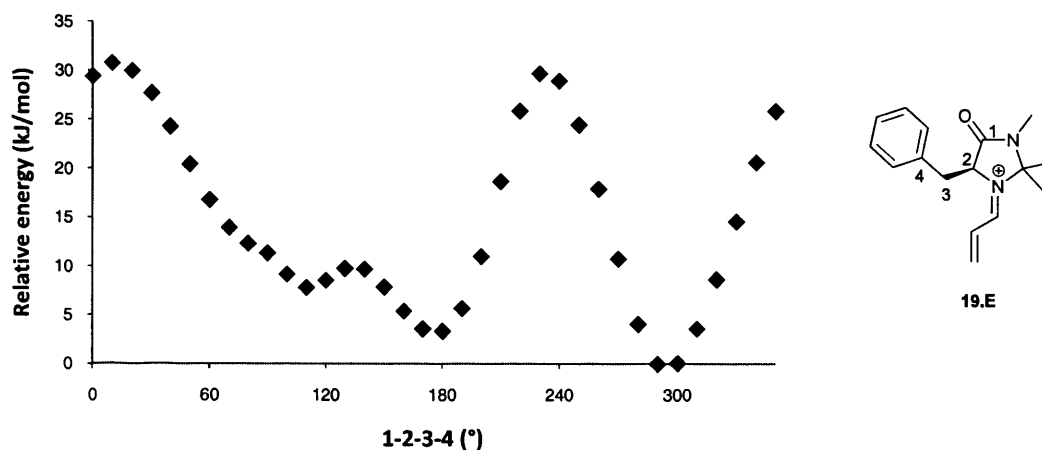


Figure 6.6

A potential energy surface scan was performed whereby the dihedral angles between atoms 1–4 of **19.E** were varied in units of 10 ° between 0 ° and 350 ° and the spatial arrangement of the rest of the iminium ions' atoms optimized at each step. This scan was performed using the Hartree-Fock function with the 6-31G\* basis set. When the conformational energy was plotted against the dihedral angle, 3 local minima were observed (Figure 6.6).

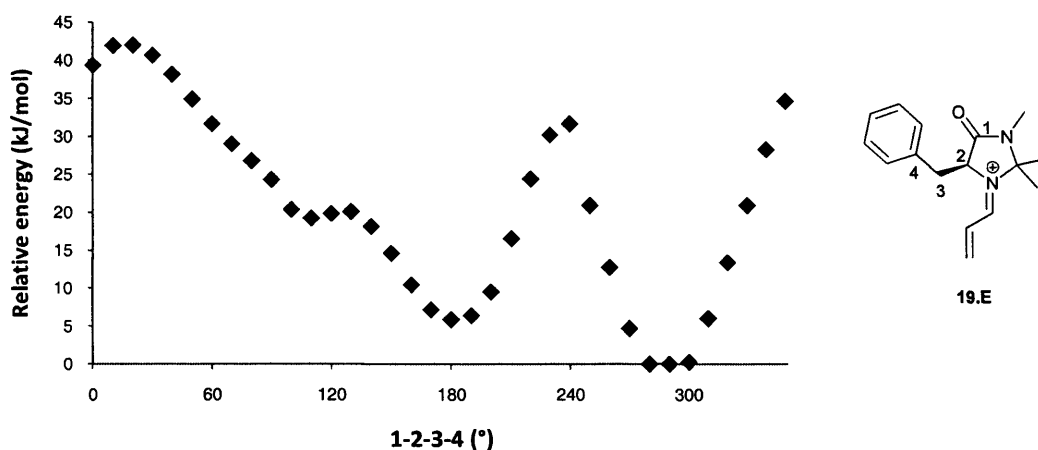


Figure 6.7

The scan was repeated for **19.E** using the more accurate and more computationally intensive Becke half-and-half function with the 6-31+G\*\* basis set.<sup>71</sup> This basis set has been shown to accurately model  $\pi$ -stacking interactions, believed to be important to the conformational preferences of **19E** and **19Z**.<sup>72</sup> 3 local minima were again observed (Figure 6.7). The minima were present at roughly the same dihedral angles, but had different relative energies.

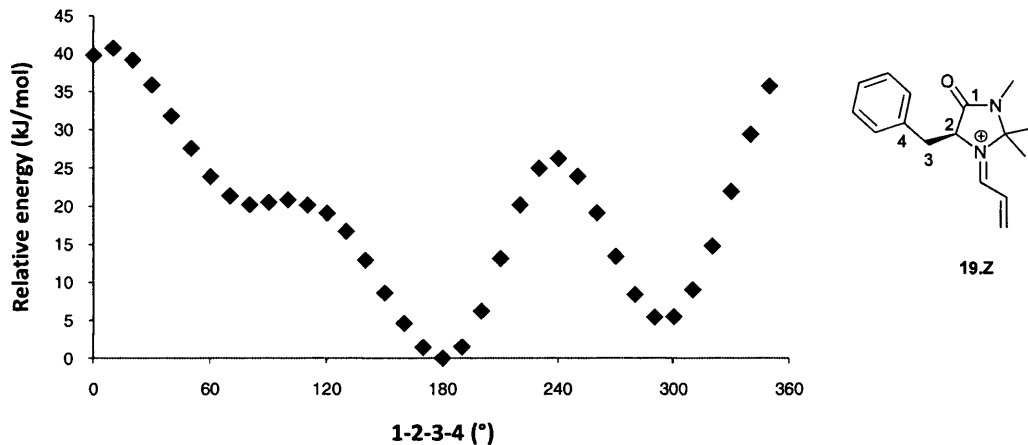


Figure 6.8

Using the Hartree-Fock function with the 6-31G\* basis set, a potential energy surface scan was performed whereby the dihedral angles between atoms 1–4 of **19.Z** were varied in units of 10 ° between 0 ° and 350 ° and the rest of the iminium ions' geometry optimized at each step. 3 local minima were observed at similar angles to those observed in Figure 6.6, but their relative energies were different (Figure 6.8).

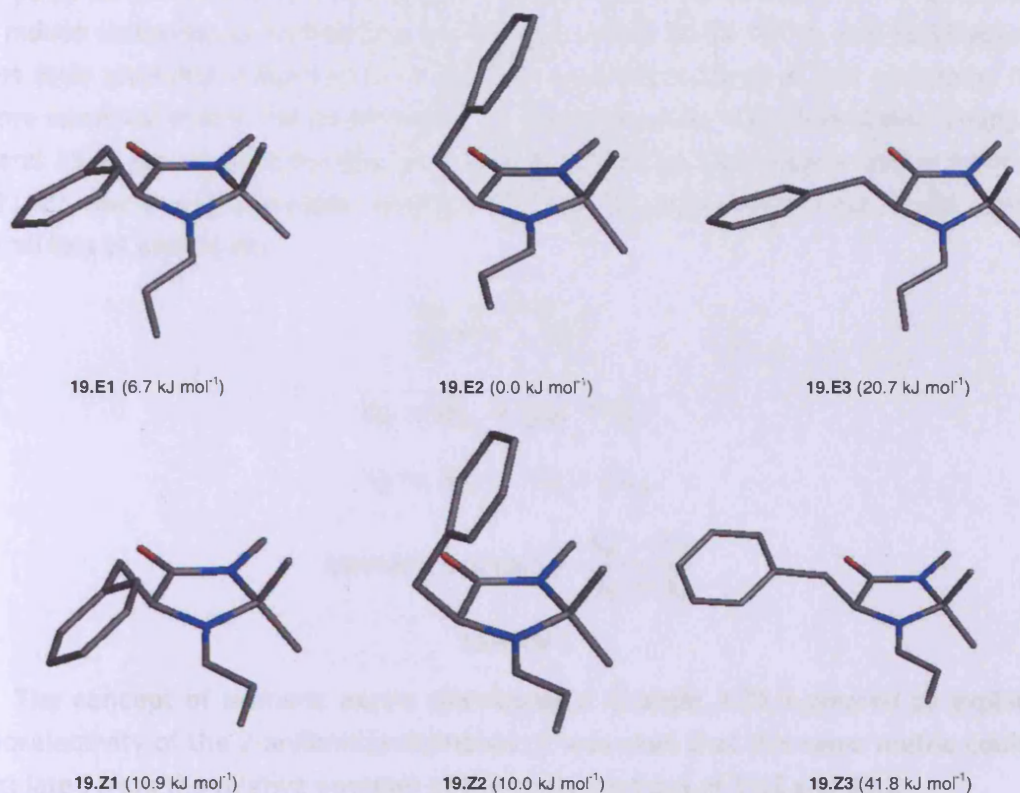


Figure 6.9

Using these minima as starting points, full geometry optimizations using the Becke half-and-half function with the 6-31+G\*\* basis set were performed, yielding conformations **19.E1–E3** and **19.Z1–Z3** (Figure 6.9). As **19.E** and **19.Z** are geometric isomers, the energies of their conformations may be compared directly and are given relative to the lowest energy conformation, **19.E2**.

In MacMillan's seminal paper, **19.E1** was stated to be the lowest energy conformation and **19.Z1** was stated to be disfavoured due to a steric clash between the proton  $\alpha$ - to the iminium carbon and the geminal dimethyl groups.<sup>2</sup> These results confirm the disfavouring of **19.Z1**, but show that the **19.E2** conformation is substantially lower in energy than the **19.E1** conformation, a result also found experimentally within the group.<sup>28</sup> This appears due to the close proximity of the benzyl arm to the carbon  $\alpha$ - to the iminium ion disfavouring **19.E1** and also due to the hydrogen bond between the  $\pi$  system of the benzyl arm and the closest proton of the geminal dimethyl groups stabilising **19.E2**.

Lacking a computational method for calculating the substrate shielding effect of each conformation, **19.E1–E3** and **19.Z1–Z3** were examined visually to ascertain the degree of shielding of the  $\alpha$ - and  $\beta$ - carbons of the substrate.



**19.E1** appeared to block the top face of the  $\alpha$ - and  $\beta$ -positions of the substrate, while **19.E2** appeared to block only the  $\alpha$ -position. **19.Z2** appeared to shield the  $\alpha$ -position, but would induce formation of undesired stereoisomers, while **19.E3**, **19.Z1**, and **19.Z3** appeared to exert little shielding influence on either the  $\alpha$ - or  $\beta$ -positions of the substrate. It was therefore surmised that in the benchmark Diels-Alder reaction, transition states arising from **19.E1** and **19.E2** would yield the desired products, while transition states arising from **19.E3** or **19.Z1–Z3** may give rise to either desired or undesired stereoisomers and would represent an overall loss of product ee.

$$\frac{N_i}{N} = e^{-E_i/k_B T}$$

$$N_E = N_{E1} + N_{E2} + N_{E3}$$

$$N_Z = N_{Z1} + N_{Z2} + N_{Z3}$$

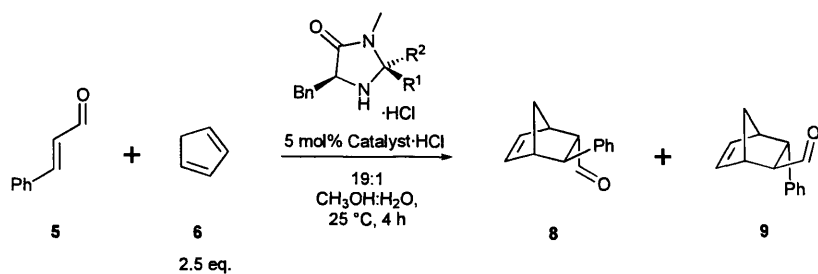
$$\text{isomeric excess} = \frac{N_E - N_Z}{N_E + N_Z}$$

Figure 6.10

The concept of isomeric excess developed in Chapter 4.21 appeared to explain the enantioselectivity of the 2-arylimidazolidinones. It was seen that this same metric could also be calculated from the relative energies of the conformations of **19.E** and **19.Z**.

Using the Boltzmann distribution function, a probability measure for each of the conformations **19.E1–E3** and **19.Z1–Z3** was calculated (Figure 6.10). Using the same function as is used for calculating ee's, these probability measures were used to calculate an isomeric excess for benchmark catalyst **7** (95%).

### 6.3 Acetophenone Catalysts Evaluated



Scheme 6.11

|            | R <sup>1</sup>   | R <sup>2</sup>   | calc. ie | exp. ie | 8 ee | 9 ee |
|------------|--|--|----------|---------|------|------|
| <b>7</b>   | CH <sub>3</sub>  | CH <sub>3</sub>  | 95       | 96      | 93   | 93   |
| <b>125</b> | CH <sub>3</sub>  | <i>p</i> -(NC)C <sub>6</sub> H <sub>4</sub>              | 76       | 75      | 83   | 73   |
| <b>121</b> | CH <sub>3</sub>  | C <sub>6</sub> H <sub>5</sub>                            | 75       | 72      | 96   | 82   |
| <b>110</b> | CH <sub>3</sub>  | <i>p</i> -NO <sub>2</sub> C <sub>6</sub> H <sub>4</sub>  | 75       | 80      | 97   | 87   |
| <b>119</b> | CH <sub>3</sub>  | <i>p</i> -CH <sub>3</sub> OC <sub>6</sub> H <sub>4</sub> | 65       | 67      | 95   | 84   |
| <b>123</b> | CH <sub>3</sub>  | <i>p</i> -ClC <sub>6</sub> H <sub>4</sub>                | 65       | 67      | 90   | 78   |
| <b>126</b> | <i>p</i> -(NC)C <sub>6</sub> H <sub>4</sub>              | CH <sub>3</sub>  | 23       | 59      | 52   | 42   |
| <b>124</b> | <i>p</i> -ClC <sub>6</sub> H <sub>4</sub>                | CH <sub>3</sub>  | 23       | 56      | 59   | 50   |
| <b>120</b> | <i>p</i> -CH <sub>3</sub> OC <sub>6</sub> H <sub>4</sub> | CH <sub>3</sub>  | 23       | 40      | 68   | 53   |
| <b>111</b> | <i>p</i> -NO <sub>2</sub> C <sub>6</sub> H <sub>4</sub>  | CH <sub>3</sub>  | 21       | 63      | 94   | 78   |
| <b>122</b> | C <sub>6</sub> H <sub>5</sub>                            | CH <sub>3</sub>  | 21       | 43      | 65   | 61   |

Figure 6.12

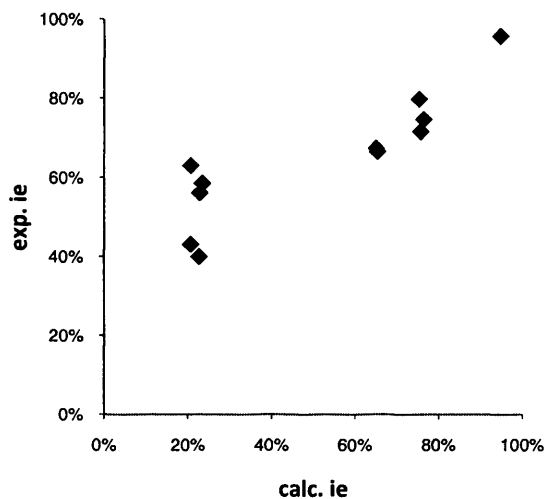


Figure 6.13: Experimentally-attained ie vs. calculated ie for each catalyst in Figure 6.12

Conformations for **110**, **111** and **119–126** were optimized and their relative energies calculated according to the previously described protocol (Figure 6.12). A strong correlation was noted between experimentally determined ie's (Chapter 4.21) and calculated ie's, indicating that the computational method for determining a catalyst ie is a good approximation of the experimental method (Figure 6.13).

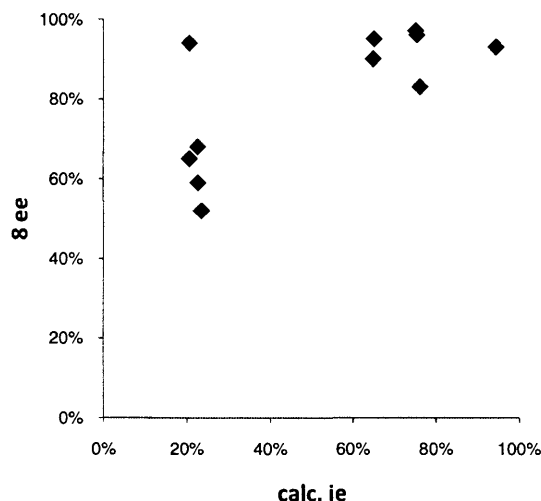


Figure 6.14

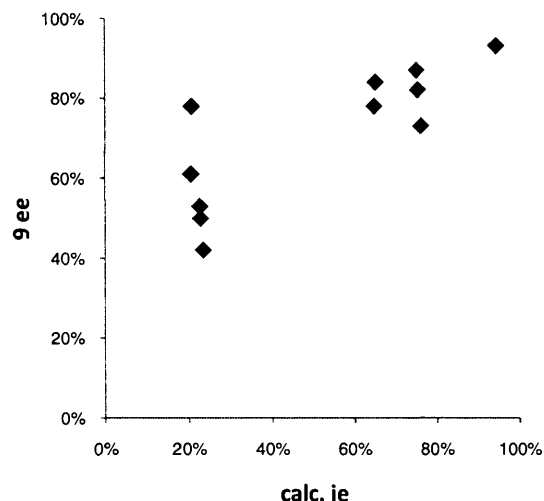


Figure 6.15

A correlation between calculated ie and 8 ee's attained in the benchmark Diels-Alder reaction for each catalyst in Figure 6.12 was noted (Figure 6.14). A correlation between calculated ie and 9 ee's for each catalyst in Figure 6.12 was also noted (Figure 6.15). The obvious outlier in both cases was **111**, which exhibited far stronger enantiocontrol than calculated ie's would suggest.

As the computational and experimental ie's matched closely, it appeared that the unexpectedly good enantiocontrol exhibited by **111** in the benchmark reaction was unlikely to be due to **111** possessing superior geometric control and that another mechanism may be responsible.

## 6.4 Conclusions

A computational model was developed for assaying the stereocontrol of iminium ion organocatalysts. Using this model, a catalyst may be characterised in terms of the relative energies of the six total conformations of the two geometric isomers of the iminium ion formed upon its condensation with **13**. This represented a substantial saving in computational time over the transition state model and rendered it a practical undertaking.

Previous work in this group had used the Hartree-Fock method exclusively due to the more limited computer hardware that was available at the time. This method was deemed unsuitable as it does not accurately model  $\pi$ -orbital interactions and could not be relied upon to generate the quality of results needed for this project. A more suitable model, the Becke half-and-half function was used instead. This algorithm rivals more computationally expensive models in terms of accuracy yet allows calculations on these systems to be performed in a reasonable time. When the energies of all the conformations of the two geometric isomers of an iminium ion were calculated in parallel using the university's Merlin cluster, results were returned in around 40 hours.

Calculated  $\Delta E$ 's were found to be a convenient measure of the iminium ion geometry selectivity of a catalyst, and were found to correlate with experimentally observed isomeric excesses and experimentally attained product ee's.

Finally, the data provided by this model provided further evidence that the 2-arylimidazolidinones attain low ee's in the benchmark Diels-Alder reaction due to poor iminium ion geometry control.

---

## **Chapter 7: Computer-Aided Catalyst Design**

---

## 7 Computer-Aided Catalyst Design

### 7.1 Introduction

The success of the theoretical model developed in the previous chapter in explaining the shortcomings of the acetophenone series catalysts increased interest in the use of computer modelling.

It had been a longstanding goal within the group to develop a reliable and accurate computational model of iminium ion organocatalysis that would allow catalyst structures to be evaluated *in silico*, thus reducing experimental workload and allowing for faster progress to be made.

At this stage in the project, there appeared to be 3 discrete factors influencing catalyst performance: EWG strength, iminium ion geometric selectivity, and substrate shielding ability of the dominant iminium ion.

### 7.2 Proton Affinity Calculation

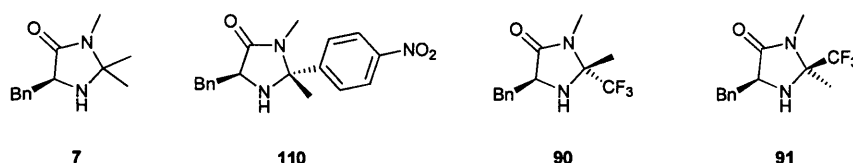


Figure 7.1

Research performed within the group had shown that the RDS in the benchmark Diels-Alder reaction catalysed by **7**·HCl was iminium ion formation, believed to be a second order reaction between the free amine and the aldehyde.<sup>31</sup> This suggested that the enhanced rate of **110**·HCl was attained due to a decreased proton affinity and an increased concentration of the free amine under reaction conditions. The upper limits for EWG strength in a functional catalyst appeared to have been exceeded in the case of **90** and **91**, which were seen not to catalyse the benchmark reaction.

$$PA = E(B) - E(BH^+) + ZPVE + \frac{5RT}{2}$$

ZPVE = zero-point vibrational energy

Figure 7.2

To gain understanding into the RDS of the benchmark reaction and generate an extra metric by which catalysts may be characterised, proton affinities (PA) were calculated. This

was performed in accordance with the method of Rao and Sastry using the B3LYP/6-31+G\* level of theory (Figure 7.2).<sup>73</sup>

|            | R <sup>1</sup>   | R <sup>2</sup>   | PA (kJ mol <sup>-1</sup> ) |
|------------|--|--|----------------------------|
| <b>33</b>  | H  | <i>p</i> -NO <sub>2</sub> C <sub>6</sub> H <sub>4</sub>  | 915                        |
| <b>104</b> | <i>p</i> -NO <sub>2</sub> C <sub>6</sub> H <sub>4</sub>  | H  | 917                        |
| <b>110</b> | CH <sub>3</sub>  | <i>p</i> -NO <sub>2</sub> C <sub>6</sub> H <sub>4</sub>  | 924                        |
| <b>111</b> | <i>p</i> -NO <sub>2</sub> C <sub>6</sub> H <sub>4</sub>  | CH <sub>3</sub>  | 927                        |
| <b>126</b> | <i>p</i> -(NC)C <sub>6</sub> H <sub>4</sub>              | CH <sub>3</sub>  | 927                        |
| <b>125</b> | CH <sub>3</sub>  | <i>p</i> -(NC)C <sub>6</sub> H <sub>4</sub>              | 928                        |
| <b>123</b> | CH <sub>3</sub>  | <i>p</i> -ClC <sub>6</sub> H <sub>4</sub>                | 950                        |
| <b>124</b> | <i>p</i> -ClC <sub>6</sub> H <sub>4</sub>                | CH <sub>3</sub>  | 951                        |
| <b>122</b> | C <sub>6</sub> H <sub>5</sub>                            | CH <sub>3</sub>  | 959                        |
| <b>121</b> | CH <sub>3</sub>  | C <sub>6</sub> H <sub>5</sub>                            | 960                        |
| <b>119</b> | CH <sub>3</sub>  | <i>p</i> -CH <sub>3</sub> OC <sub>6</sub> H <sub>4</sub> | 970                        |
| <b>120</b> | <i>p</i> -CH <sub>3</sub> OC <sub>6</sub> H <sub>4</sub> | CH <sub>3</sub>  | 972                        |

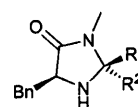


Figure 7.3

Amongst the 2-aryl imidazolidinones, a correlation between experimental catalyst performance and calculated proton affinity was observed within both the (2*S*,5*S*)- series and within the (2*R*,5*S*)- series (Figure 7.3). Comparison between these two series was not enlightening as proton affinity varied by no more than 3 kJ mol<sup>-1</sup> between diastereomers. Experimentally, the (2*R*,5*S*)- catalysts had shown substantial rate advantages over the (2*S*,5*S*)- catalysts (Chapter 4.14).

|            | R <sup>1</sup>                   | R <sup>2</sup>  | PA (kJ mol <sup>-1</sup> ) |
|------------|----------------------------------|-----------------|----------------------------|
| <b>115</b> | (CH <sub>2</sub> ) <sub>3</sub>  |                 | 942                        |
| <b>7</b>   | CH <sub>3</sub>                  | CH <sub>3</sub> | 945                        |
| <b>2</b>   | C(CH <sub>3</sub> ) <sub>3</sub> | H               | 948                        |
| <b>114</b> | (CH <sub>2</sub> ) <sub>4</sub>  |                 | 950                        |

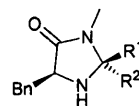


Figure 7.4

Very little spread was observed amongst the 2-alkyl catalysts (Figure 7.4). These results failed to explain why **2**, **7** and **115** had very similar experimentally observed turnovers, while **114** exhibited much lower performance. Additionally, the proton affinity of benchmark catalyst **7** would place it close to the median proton affinity of the 2-aryl catalysts, all of

which were found to be substantially higher performing in the benchmark Diels-Alder reaction (Chapter 4.4, 4.14).

|           | R <sup>1</sup>                | R <sup>2</sup>                | PA (kJ mol <sup>-1</sup> ) |
|-----------|-------------------------------|-------------------------------|----------------------------|
| <b>30</b> | CF <sub>3</sub>               | CF <sub>3</sub>               | 855                        |
| <b>91</b> | CF <sub>3</sub>               | CH <sub>3</sub>               | 898                        |
| <b>90</b> | CH <sub>3</sub>               | CF <sub>3</sub>               | 899                        |
| <b>89</b> | C <sub>6</sub> H <sub>5</sub> | CF <sub>3</sub>               | 917                        |
| <b>78</b> | CF <sub>3</sub>               | C <sub>6</sub> H <sub>5</sub> | 917                        |

Figure 7.5

All the trifluoromethyl-containing imidazolidinones evaluated (**30**, **78**, **89**, **90**, **91**) were found to have low proton affinities (Figure 7.5). These numbers alone did not explain the observed inability of **78** and **89** to form hydrochloride salts as their calculated proton affinities were very similar to **90** and **91**, which readily formed hydrochloride salts with pronounced catalytic activity. When the proton affinities of **7**, **91** and **30** were compared, the decrease in proton affinity appeared roughly proportional to the number of fluorine atoms in the molecule. This showed the potential for the basicity of imidazolidinones to be tuned by varying the degree of fluorination of alkyl groups at the 2-position and suggested that mono- or difluorination of **7** could result in a higher performance catalyst.

The calculation of proton affinities was undertaken as it appeared to provide a more logical handle on catalyst performance than LUMO energies previously relied upon within the group. It had been shown that while proton affinities may go some way to explaining catalyst performance, their utility in appraising the catalytic potential of novel structures was limited.

### 7.3 Substrate Shielding

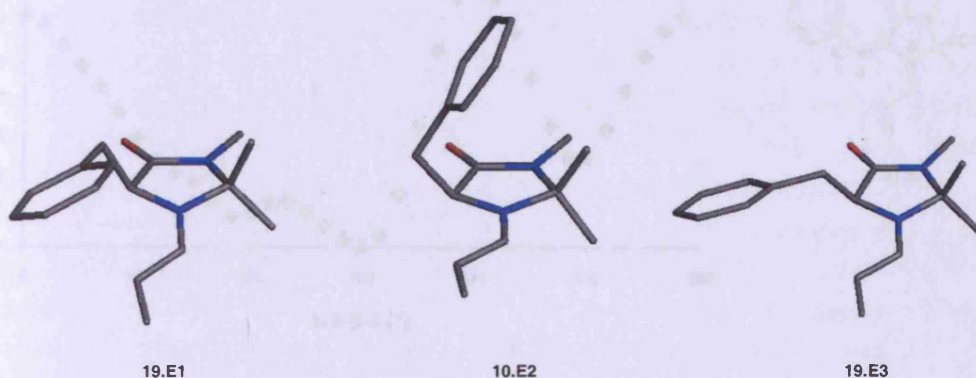


Figure 7.6



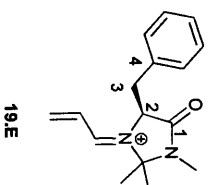
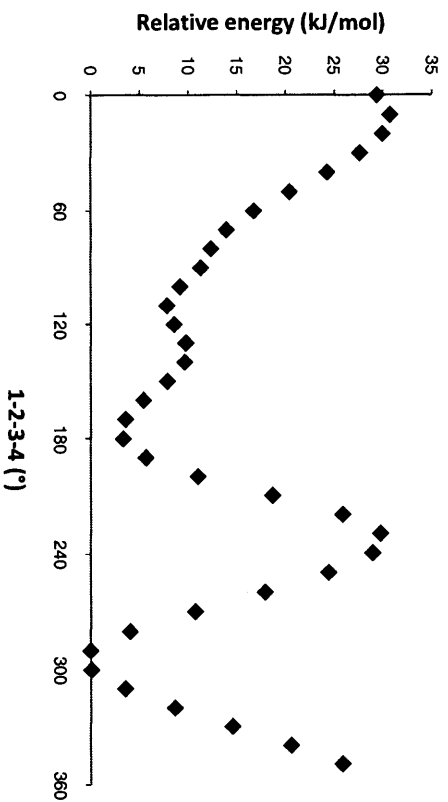


Figure 7.7

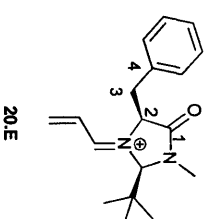
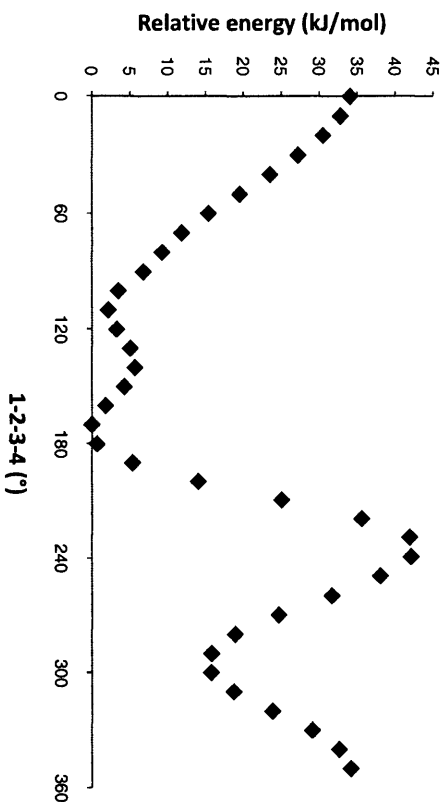


Figure 7.8

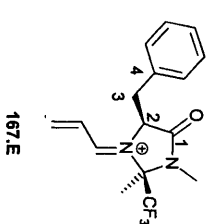
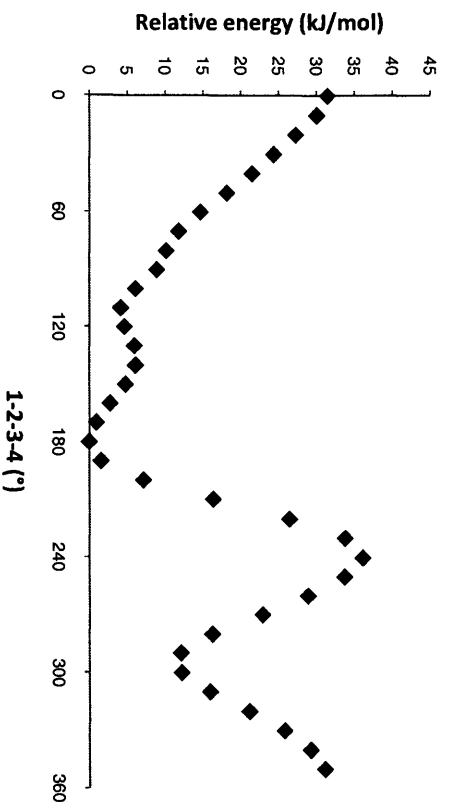


Figure 7.9

A potential energy surface scan was performed whereby the dihedral angles between atoms 1–4 of **20.E** and **167.E** were varied in units of 10 ° between 0 ° and 350 ° and the rest of the iminium ions' geometry optimized at each step. Figures 7.8 and 7.9 show conformational energy plotted against dihedral angle. These scans were performed using the Hartree-Fock function with the 6-31G\* basis set.

When compared to Figure 7.7, first generated in Chapter 6.2, Figures 7.8 and 7.9 indicated that the benzyl arm of **20.E** and **167.E** would be expected to spend little time in the **E2** conformation, due to the steric repulsion of the tertiary butyl group and the electronic repulsion of the trifluoromethyl group, respectively. The results also indicated that for both **20.E** and **167.E**, the **E3** conformation, in which the benzyl arm sits above the carbonyl of the amide, is less disfavoured and that substrate shielding may be compromised as a result.

| rel. energy (kJ mol <sup>-1</sup> ) | <b>19</b> | <b>20</b> | <b>167</b> |
|-------------------------------------|-----------|-----------|------------|
| <b>E1</b>                           | 6.7       | 0.0       | 0.0        |
| <b>E2</b>                           | 0.0       | 12.1      | 12.9       |
| <b>E3</b>                           | 20.7      | 10.7      | 14.6       |
| Z-E (kJ mol <sup>-1</sup> )         | 10.0      | 5.6       | 5.6        |

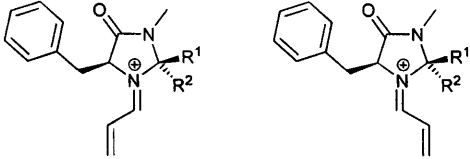
Figure 7.10

Using the minima on Figures 7.7, 7.8 and 7.9 as starting points, geometry optimizations and energy calculations were performed using the more accurate Becke half-and-half function with the 6-31+1G\*\* basis set (Figure 7.10). In all cases, these results showed much larger differences between the **E3** and **E1** conformations, indicating good benzyl arm control would be expected of these iminium ions. However, both **20.Z** and **167.Z** were found to have relatively low energies, implying the corresponding catalysts (**2** and **91**, respectively) would have poor iminium ion geometry control.

Experimentally, **7**, the parent amine of **19**, exhibits good enantiocontrol in the benchmark Diels-Alder reaction (93% *endo*- ee, 93% *exo*- ee), while **2**, the parent amine of **20**, shows very poor enantiocontrol (5% *endo*- ee, 55% *exo*- ee). **7** exerts a high degree of stereocontrol in other closed transition state reactions such as conjugate addition of pyrrole but is not used by MacMillan in open transition state reactions, suggesting a preference for the **E2** conformation. **2** has been used for conjugate addition, suggesting that **E1** is its preferred conformation, but generally at lower temperatures, suggesting that iminium ion geometry control may be an issue. **91**, the parent amine of **167**, has been reported to be catalytically inactive in the benchmark Diels-Alder reaction within this investigation (Chapter 2.8) but **167** was modelled as it manifested a novel method of benzyl arm control.

Two methods for controlling the rotation of benzyl arms at the 5-position of imidazolidinone rings, and hence substrate shielding, have been investigated: the steric method, and the electronic method. Both methods have shown good performance, as measured computationally. Unfortunately, no experimental methods for measuring conformations of imidazolidinone iminium ions have been established at this time.

#### 7.4 E/Z Selectivity



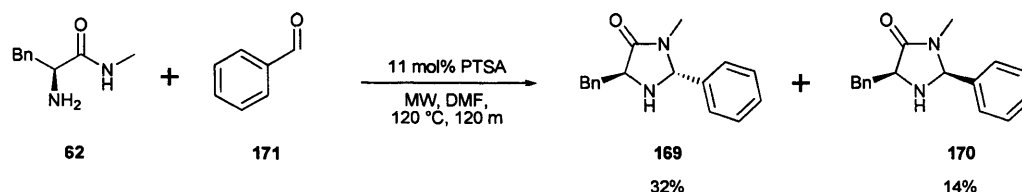
**168.E**
**168.Z**

| Parent<br>amine | R <sup>1</sup>                | R <sup>2</sup>                | E <sub>ZZ</sub> -E <sub>E2</sub><br>kJ mol <sup>-1</sup> |
|-----------------|-------------------------------|-------------------------------|--|
| <b>169</b>      | H                             | H                             | 0.0  |
|                 | H                             | CH <sub>3</sub>               | 5.9  |
|                 | H                             | C <sub>6</sub> H <sub>5</sub> | 10.0   |
| <b>7</b>        | CH <sub>3</sub>               | H                             | 1.0  |
|                 | CH <sub>3</sub>               | CH <sub>3</sub>               | 10.0   |
| <b>121</b>      | CH <sub>3</sub>               | C <sub>6</sub> H <sub>5</sub> | 0.9  |
| <b>170</b>      | C <sub>6</sub> H <sub>5</sub> | H                             | 2.2  |
| <b>122</b>      | C <sub>6</sub> H <sub>5</sub> | CH <sub>3</sub>               | 5.9  |
|                 | C <sub>6</sub> H <sub>5</sub> | C <sub>6</sub> H <sub>5</sub> | 0.2  |

Figure 7.11

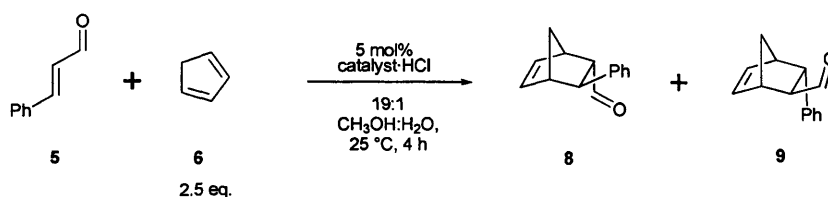
In an attempt to quantify the steric effects of the various possible substituents at the 2-position of the imidazolidinone ring, energies for the most favourable conformations of **168.E** and **168.Z** were calculated for each substitution pattern in Figure 7.11. In all cases, **E2** was found to be the lowest energy conformation of **168.E**, while **Z2** was found to be the lowest energy conformation of **168.Z**.

The results showed that **169** would be expected to have iminium ion geometric selectivity comparable to that of benchmark catalyst **7** and potentially high levels of enantiocontrol in the benchmark reaction.



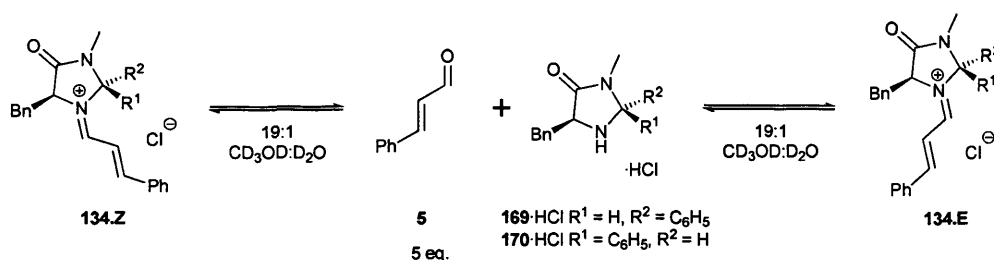
Scheme 7.12

**62**, **171** and 11 mol% PTSA in DMF were irradiated at 120 °C for 120 minutes (Scheme 7.12). After aqueous workup and column chromatography, **169** (32%) and **170** (14%) were isolated and converted to **169**·HCl (24% overall) and **170**·HCl (9% overall).



Scheme 7.13

In the benchmark Diels-Alder reaction, **169**·HCl was seen to exhibit good turnover but attained only 75% **8** ee and 22% **9** ee (Scheme 7.13). **170**·HCl also exhibited good turnover but attained 21% **8** ee and 44% **9** ee.



Scheme 7.14

When **169**·HCl was dissolved in 19:1 deuterated methanol:deuterium oxide with 5 equivalents **5**, a 2.0:1 **134.E**:**134.Z** ratio was observed (Scheme 7.14). The use of **170**·HCl under the same conditions gave rise to a 1.5:1 **134.E**:**134.Z** ratio.

Despite the promising computational results, **169** exhibited poor **134.E**:**134.Z** formation control and poor enantiocontrol in the benchmark Diels-Alder reaction. It appeared that calculated **134.E**:**134.Z** energy differences do not always correlate experimentally.

## 7.5 The H-bond Effect

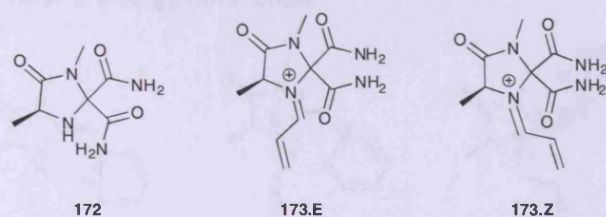


Figure 7.15

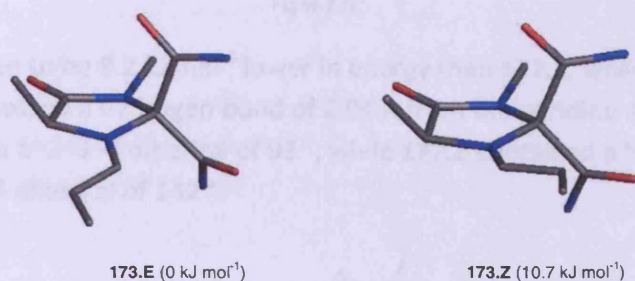


Figure 7.16

While performing a computational screening of potential EWGs, **172** was discovered to have an unexpectedly high **173.Z–173.E** energy difference of 10.7 kJ mol<sup>-1</sup>, giving a calculated ie of 96%. Upon closer inspection, it was found that **173.E** contained a hydrogen bond from one of the dihydroamidic oxygen atoms to the iminium proton (2.15 Å), whereas in the case of **173.Z**, the same oxygen atom had a hydrogen bond to the less positive α-proton atom (2.12 Å).

Suspecting that controlled formation of hydrogen bonds to the iminium proton may be a powerful mechanism for effecting iminium ion geometric selectivity, further *in silico* screening was performed.

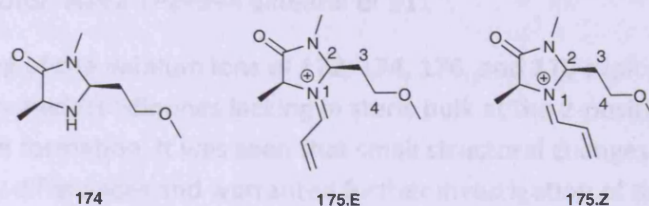


Figure 7.17

**174** was seen to exhibit a *Z–E* energy difference of 5.6 kJ mol<sup>-1</sup> and a calculated ie of 66%, substantial for a catalyst with very little steric bulk at the 2-position. **175.E** contains a hydrogen bond of 1.94 Å from the ethereal oxygen to the iminium proton, while **175.Z** contains a hydrogen bond of 2.09 Å from the ethereal oxygen to the α-proton. In **175.E** and **175.Z**, the 1–2–3–4 dihedral is 105 ° and 143 °, respectively. This shows that rotation

around this dihedral is necessary to allow formation of **175.Z** and that hindering this rotation may further increase the *Z-E* energy difference.

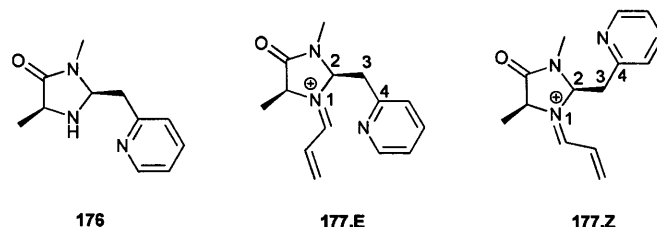


Figure 7.18

**177.E** was seen to be 8.2 kJ mol<sup>-1</sup> lower in energy than **177.Z**, while **176** had an overall ie of 86%. **177.E** possessed a hydrogen bond of 2.04 Å from the pyridine nitrogen atom to the iminium proton and a 1–2–3–4 dihedral of 93 °, while **177.Z** contained a hydrogen bond of 2.24 Å and a 1–2–3–4 dihedral of 142 °.

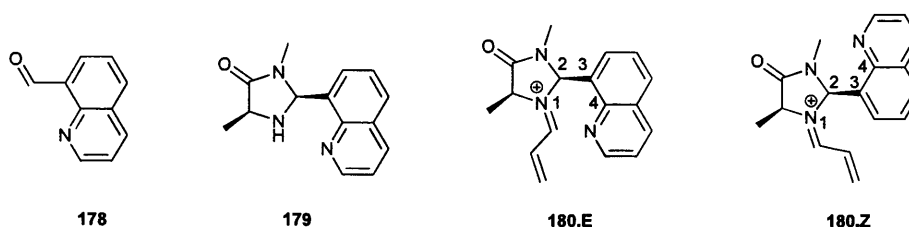


Figure 7.19

**176** looked promising but its synthesis was deemed potentially problematic. **179** was devised as a similar catalyst that may be obtained from commercially available **178**. The *Z-E* energy difference was found to be 7.7 kJ mol<sup>-1</sup> and overall ie found to be 88%. **180.E** exhibited a hydrogen bond of 2.18 Å from the quinolic nitrogen to the iminium proton and a 1–2–3–4 dihedral of 83 °, while **180.Z** exhibited a hydrogen bond of 2.09 Å from the quinolic nitrogen to the α-proton and a 1–2–3–4 dihedral of 111 °.

The modelling of the iminium ions of **172**, **174**, **176**, and **179** explored a theoretical mechanism by which imidazolidinones lacking in steric bulk at the 2-position may attain selective iminium ion formation. It was seen that small structural changes may result in significant selectivity differences and warranted further investigation of this effect.

It must be appreciated that the benchmark reaction is performed in methanol:water mixtures, which could be expected to disrupt any hydrogen bonding network. However, imidazolidinone catalysts have been used in aprotic solvents, and the possibility of greatly enhanced iminium geometry control made further investigations appear worthwhile.<sup>74</sup>

## 7.6 Fluorine H-bonders

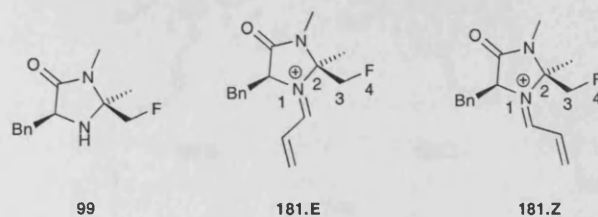


Figure 7.20

Since concluding the work within Chapter 2.8, **99** appeared to have potential for high catalytic performance and good enantiocontrol (Figure 7.20). To investigate the potential for a hydrogen bond between its fluorine atom and the iminium proton to enhance iminium ion selectivity, modelling work was undertaken. **181.E** was found to have a fluorine to iminium proton internuclear distance of 2.22 Å and a 1–2–3–4 dihedral of 64 °.

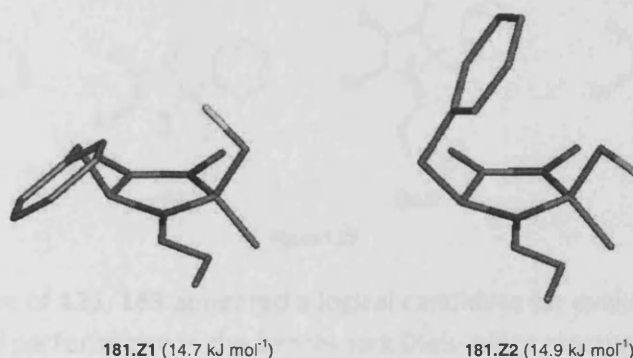


Figure 7.21

Interestingly, **181.Z** was seen to have two conformational minima with very similar energies, **181.Z1** and **181.Z2** (Figure 7.21). **181.Z1** was seen to have a marginally lower energy than **181.Z2** and featured a fluorine to benzylic proton distance of 2.33 Å, assumed to stabilise the conformation. **181.Z1** had a fluorine to α-proton distance of 2.06 Å and a 1–2–3–4 dihedral of 79 °. This showed the potential for unexpected interactions to stabilise otherwise unfavourable conformations. The overall calculated ie of **99** was found to be 99%.

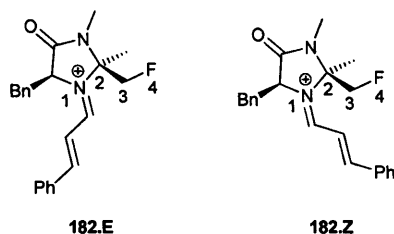


Figure 7.22

**99** appeared to be a very strong candidate for synthesis and experimental evaluation. Unfortunately, before this work could be carried out, Seebach released a publication detailing the mechanisms of iminium organocatalyst stereoselectivity. **99**·HPF<sub>6</sub> was stated to have a **182.E**:**182.Z** selectivity of >99:1 in deuterated acetone (Figure 7.22), but no further information was given.<sup>75</sup> Having lost the ability to claim **99** as a novel catalyst, no experimental evaluation was undertaken.

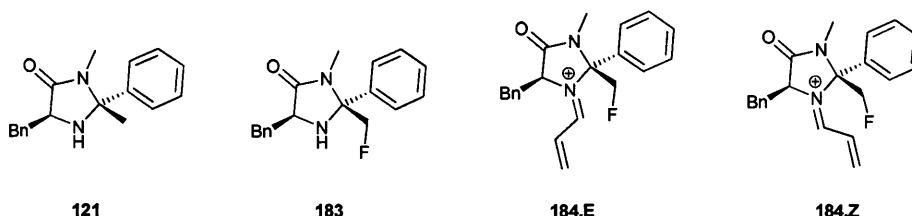
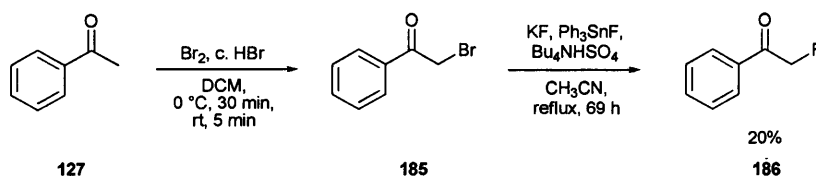


Figure 7.23

As a derivative of **121**, **183** appeared a logical candidate for evaluation (Figure 7.23). **121** had shown good performance in the benchmark Diels-Alder reaction while attaining reasonable levels of product ee (96% *endo*, 82% *exo*). **121** had shown a calculated ie of 75% and an experimental ie of 72%, indicating that improved iminium ion geometry selectivity should result in improved enantiocontrol.

**184.E** shows a fluorine – iminium proton distance of 2.32 Å, while **184.Z** shows a fluorine – α-proton distance of 2.28 Å. **183**'s calculated ie was determined to be 89%, suggesting that this catalyst may demonstrate very good levels of experimental enantiocontrol.



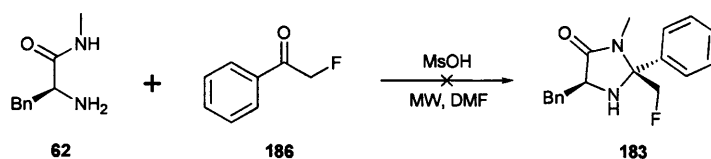
Scheme 7.24

To a solution of **127** and catalytic hydrogen bromide in DCM at 0 °C, bromine was added dropwise over the course of 30 minutes, resulting in copious evolution of hydrogen



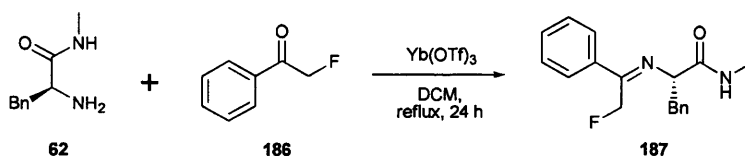
bromide (Scheme 7.24). After addition was complete, the mixture was stirred at room temperature for 5 minutes and then evaporated. **185** was obtained as a cream solid after multiple recrystallisations from hexanes (38%).

Using a literature procedure, **185** was stirred in refluxing acetonitrile with potassium fluoride, tetrabutylammonium bisulphate, and triphenyltin fluoride for 69 hours.<sup>76</sup> The mixture was poured into water, extracted twice with diethyl ether, dried, treated with pyridine, and refluxed for 20 minutes. An aqueous workup was then performed, after which distillation yielded **186**, a low melting point (23 °C) crystalline solid (52%, 20% overall).



Scheme 7.25

A solution of **62**, **186**, and 30 mol% MsOH in DMF was irradiated at 160 °C for 10 m (Scheme 7.25). Analysis of the reaction mixture revealed a number of compounds to be present but column chromatography failed to isolate **183**. The reaction was repeated at 150 °C for 30 minutes, at 140 °C for 19 minutes, and at 130 °C for 60 minutes. None of these attempts provided **183**.



Scheme 7.26

**62** and **186** were refluxed in DCM with ytterbium(III) triflate for 24 hours (Scheme 7.26). Column chromatography provided a compound suspected to be **187**. Attempts to cyclise this compound using copper(II) triflate under microwave irradiation failed and **183** could not be obtained.

Further synthetic efforts towards **183** were not undertaken due to time constraints.

## 7.7 2-(β-Acetamido)-Imidazolidinones

At this stage, the ability for well situated nitrogen, oxygen, and fluorine atoms to enhance iminium ion isomeric energy differences by selective hydrogen bond formation had been observed. Looking to enhance this effect, a search of the literature revealed that amides, sulfoxides, sulfones, phosphites and phosphates tended to be the strongest

hydrogen bond acceptors.<sup>77,78</sup> Of these functional groups, sulfones and amides appeared most suitable for incorporation into the imidazolidinone architecture.

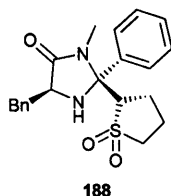
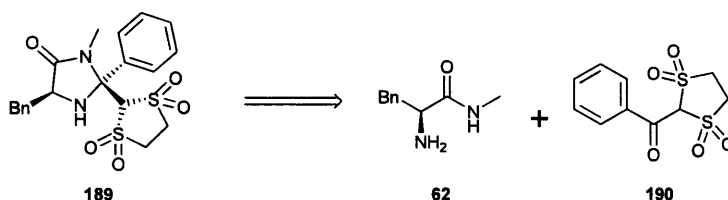


Figure 7.27

The iminium ions of **188** were found to have a *Z–E* energy difference of 23.6 kJ mol<sup>-1</sup> and an overall ie of 100% (Figure 7.27). In the *E*-iminium ion, a distance of 2.28 Å between the iminium proton and closest oxygen atom of the sulfone group was noted, while in the *Z*-iminium ion, a distance of 2.27 Å between the α-proton and the same oxygen atom was noted. **187** was found to have a calculated PA of 960 kJ mol<sup>-1</sup>.



Scheme 7.28

**188** looked promising, but the stereocenter α- to the sulfone was seen to be a likely point for epimerisation and also a source of synthetic difficulty. **189** was devised as a less stereocomplex sulfone-containing imidazolidinone (Scheme 7.28). **189** was seen to have an iminium ion *Z–E* difference of 17.0 kJ mol<sup>-1</sup>, an overall ie of 100% and a PA of 920 kJ mol<sup>-1</sup>. While the calculated results looked promising, it was imagined that the extreme acidity of the proton α to both sulfone groups could be problematic, especially in precursor **190**.

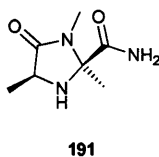


Figure 7.29

To investigate the positioning of an amidic carbonyl at the 2-position of the imidazolidinone ring, **191** was modelled (Figure 7.29). **191** was seen to have a *Z–E* difference of 12.7 kJ mol<sup>-1</sup> and an ie of 99%. The *E*-iminium ion was seen to have a distance of 2.32 Å between the iminium proton and amidic oxygen, while the *Z*-iminium ion showed a hydrogen bond between the α-proton and amidic oxygen of 2.07 Å.

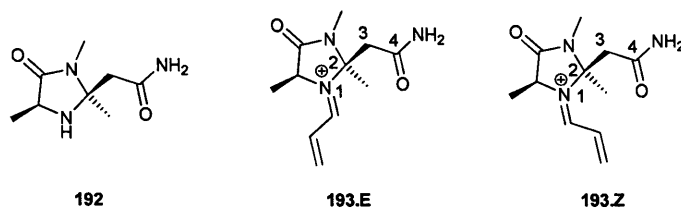


Figure 7.30

Formal insertion of a methylene group between the amidic carbonyl and imidazolidinone ring of **191** gave rise to **192** (Figure 7.30). **192** was seen to have a *Z-E* energy difference of 28.9 kJ mol<sup>-1</sup> and an ie of 100%. **193.E** was seen to have a distance of 1.93 Å between the amidic oxygen and iminium proton and a 1–2–3–4 dihedral of 68 °, while **193.Z** showed a hydrogen bond between the donor α-proton and acceptor amide of 1.91 Å and a 1–2–3–4 dihedral of 121 °. This showed that **193.Z** had to undergo greater geometric distortion in order to allow an intramolecular hydrogen bond to form and explained why it was found to be significantly higher in energy than **193.E**.

|            | R <sup>1</sup>                     | R <sup>2</sup>  | R <sup>3</sup>  | PA (kJ mol <sup>-1</sup> ) | <i>Z-E</i> (kJ mol <sup>-1</sup> ) |
|------------|------------------------------------|-----------------|-----------------|----------------------------|------------------------------------|
| <b>194</b> | H                                  | H               | CH <sub>3</sub> | 976                        | 33.4                               |
| <b>195</b> | CH <sub>3</sub>                    | CH <sub>3</sub> | CH <sub>3</sub> | 993                        | 32.7                               |
| <b>196</b> | -(CH <sub>2</sub> ) <sub>4</sub> - |                 | Ph              | 1010                       | 23.1                               |
| <b>197</b> | H                                  | H               | Ph              | 985                        | 22.3                               |
| <b>198</b> | Ph                                 | H               | Ph              | 991                        | 21.9                               |
| <b>199</b> | H                                  | H               | H               | 969                        | 18.4                               |

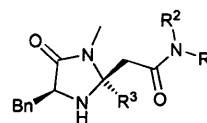
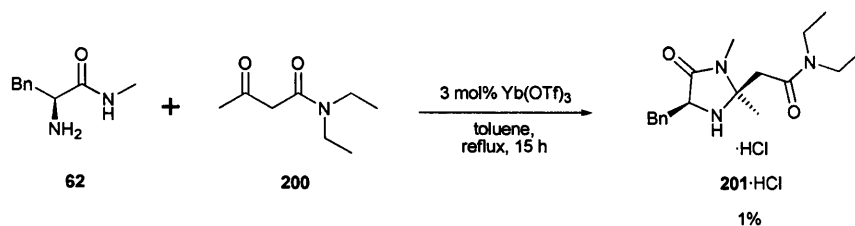


Figure 7.31

Further exploration of the 2-(β-acetamido) architecture was performed (Figure 7.31). All modelled systems had calculated iminium ion energy differences far above that of benchmark catalyst **7** (10.0 kJ mol<sup>-1</sup>). The choice of substituent on the lower face of the 2-position (R<sup>3</sup>) had a pronounced effect, comparable to those observed in Chapter 7.4. The choice of substituent on the amide appeared to have little effect on the relative iminium ion energies, but had a notable effect on proton affinity. This was of particular concern in the case of **196**, where its proton affinity was significantly higher than that of benchmark catalyst **7** (945 kJ mol<sup>-1</sup>) and was seen as a forewarning of potentially low performance.

It was felt that dihydroamides **194**, **197** and **199** may have solubility problems and as such, alkyl and aryl amides **195**, **196** and **198** would be better candidates for experimental evaluation.



As the ketone required to synthesise **195** was not commercially available, **200** was purchased instead. **62**, **200** and 3 mol% ytterbium(III) triflate were refluxed in toluene for 15 hours (Scheme 7.32). The crude was cooled and filtered to remove the majority of the ytterbium(III) residues, then treated with hydrogen chloride gas and filtered to yield a mixture of hydrochloride salts. Repeated recrystallisation yielded **201·HCl** (1%).

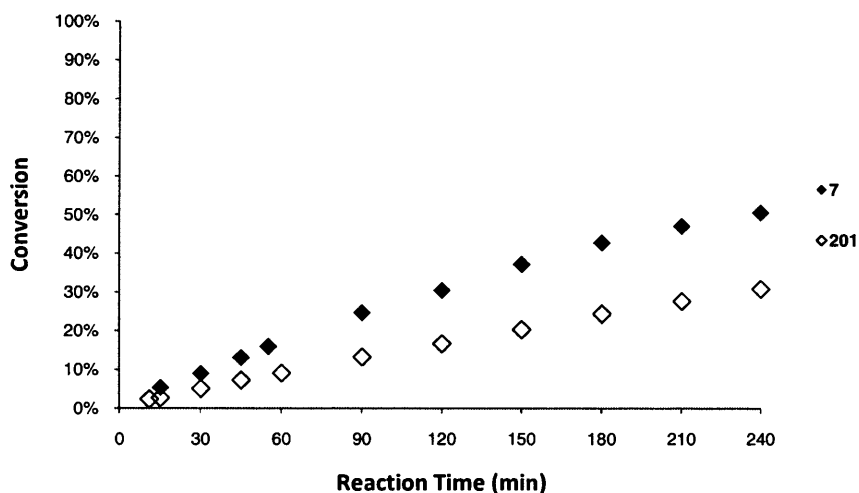
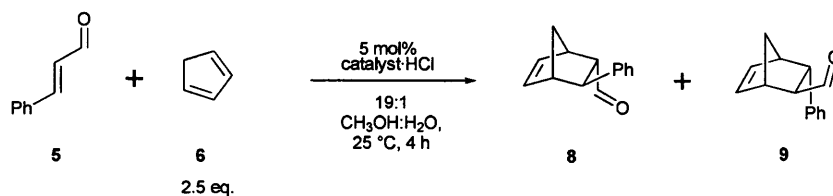


Figure 7.34

**201·HCl** was used at 5 mol% to catalyse the benchmark Diels-Alder reaction in 19:1 methanol:water at 25 °C (Scheme 7.33). As anticipated, its turnover was substantially lower than that of benchmark catalyst **7** (Figure 7.34). Product ee's were not measured.

This result demonstrated that the 2-(β-acetamido) moiety can be incorporated into a functioning imidazolidinone catalyst, albeit with a loss of performance. Although time restrictions on the project curtailed further experimental validation of the 2-(β-acetamido)

catalysts, the outstanding levels of iminium geometry control theoretically afforded by these catalysts warrants further synthetic effort.

## 7.8 Imidazolidinones with benzyl arm control

An investigation was undertaken to determine if the use of an amide hydrogen bond acceptor to control iminium ion geometry could be combined with a method for controlling the benzyl arm conformation, with the eventual aim of finding a catalyst capable of attaining good levels of stereocontrol in open transition state reactions.

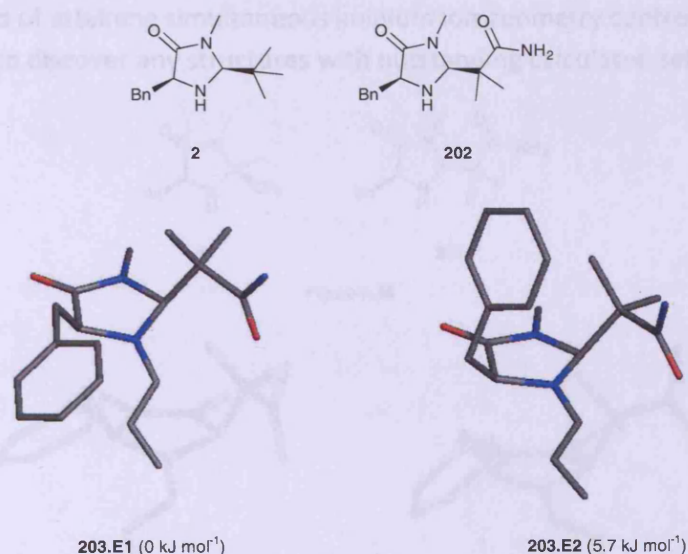


Figure 7.35

Using **2** as a template, **202** was devised (Figure 7.35). **202**'s *Z*–*E* energy difference was 12.2 kJ mol<sup>-1</sup> and its preferred conformation was found to be **203.E1**, 5.7 kJ mol<sup>-1</sup> lower in energy than **203.E2**.

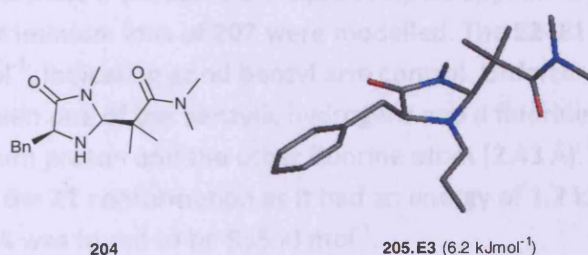
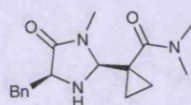


Figure 7.36

The *N,N*-dimethyl analogue of **202**, **204**, was found to have a *Z*–*E* energy difference of 18.2 kJ mol<sup>-1</sup> but had a low lying **E3** conformation at 6.2 kJ mol<sup>-1</sup> relative to the preferred **E1**.

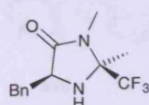


206

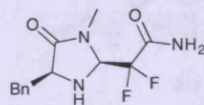
Figure 7.37

**206** can be seen as a subtle modification of **204** yet showed very different conformation energies. **204** was seen to have a *Z*–*E* energy difference of  $9.6 \text{ kJ mol}^{-1}$ , while its iminium ion's preferred conformation was **E2**.

The modelling of **202**, **204**, and **206** showed that mimicking the steric bulk of **2** may be a viable method of attaining simultaneous iminium ion geometry control and benzyl arm control but failed to discover any structures with outstanding calculated selectivity.

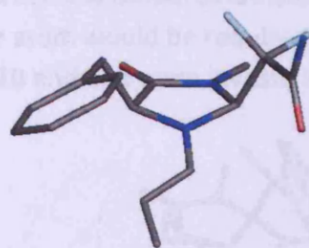


91

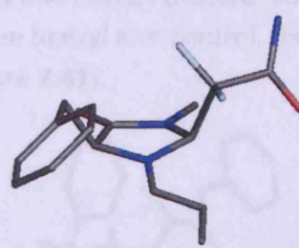


207

Figure 7.38



208.E1 ( $0 \text{ kJ mol}^{-1}$ )

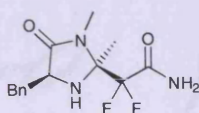


208.Z1 ( $1.2 \text{ kJ mol}^{-1}$ )

Figure 7.39

In Chapter 7.3, the ability of the trifluoromethyl group of **91** to direct the benzyl arm was observed. To determine if the same principle could be applied to amide hydrogen-bonding catalysts, the iminium ions of **207** were modelled. The **E2**–**E1** energy difference was found to be  $8.5 \text{ kJ mol}^{-1}$ , indicating good benzyl arm control. Unfortunately, **208.Z1** featured close proximity between one of the benzylic hydrogens and a fluorine atom ( $2.33 \text{ \AA}$ ), as well as between the iminium proton and the other fluorine atom ( $2.43 \text{ \AA}$ ). These interactions appeared to stabilise the **Z1** conformation as it had an energy of  $1.2 \text{ kJ mol}^{-1}$  relative to the preferred **E1**. **207**'s PA was found to be  $935 \text{ kJ mol}^{-1}$ .

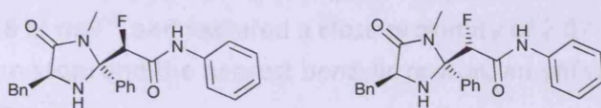




209

Figure 7.40

In an attempt to increase the *Z*–*E* energy difference of **207**, a methyl group was added to the 2-position. **209** was found to have a *Z*–*E* energy difference of 16.6 kJ mol<sup>−1</sup> and showed **E1** to be its preferred conformation (Figure 7.40). The second most stable conformation, **E2**, was found to have a relative energy of 7.1 kJ mol<sup>−1</sup>. **209**'s PA was found to be 942 kJ mol<sup>−1</sup>, showing a slight increase arising from the addition of the 2-methyl group.

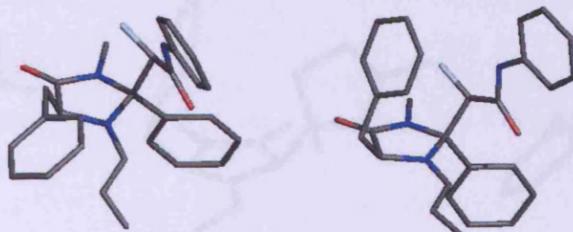


210

211

Figure 7.41

During the study of **207**, it was seen how the **Z1** conformation was stabilised by interactions between the difluoromethylene moiety and nearby protons. As it appeared that only one fluorine atom would be required to achieve benzyl arm control, the iminium ions of diastereomers **210** and **211** were investigated (Figure 7.41).



212.E1 (0 kJ mol<sup>−1</sup>)

212.E2 (13.0 kJ mol<sup>−1</sup>)

Figure 7.42

**212** was found to have a *Z*–*E* energy difference of 14.4 kJ mol<sup>−1</sup> and an **E2** conformation that lay 13.0 kJ mol<sup>−1</sup> above the preferred **E1** conformation (Figure 7.42). Preferred conformation **212.E1** was seen to be stabilised by a hydrogen bond of 2.35 Å between the fluorine atom and closest benzylic proton as well as a hydrogen bond between the iminium proton and amidic oxygen (2.28 Å). **212.E2** was seen to be stabilised by a hydrogen bond of 2.03 Å between the iminium proton and amidic oxygen but was also destabilised by close proximity between the fluorine atom and the  $\pi$ -system of the benzyl arm, as evidenced by an angle at the benzylic carbon between the imidazolidinone ring and phenyl ring of 115°. **210**'s PA was found to be 966 kJ mol<sup>−1</sup>.

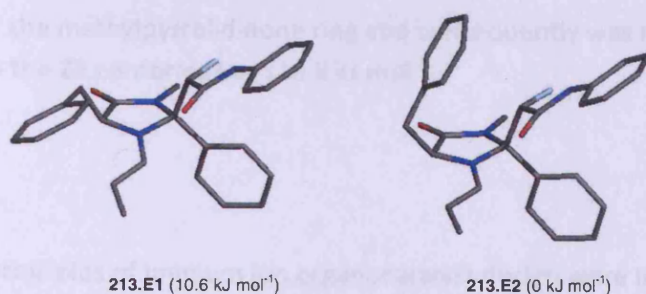


Figure 7.43

**213** was found to have a higher *Z-E* energy difference of 22.3 kJ mol<sup>-1</sup> but showed preference for **213.E2**, which was seen to be stabilised by an interaction between the benzyl arm and proton geminal to the fluorine atom (Figure 7.43). **213.E1** was seen to have a relative energy of 10.6 kJ mol<sup>-1</sup>, and featured a close proximity of 2.07 Å between the proton geminal to the fluorine atom and the nearest benzylic proton, an unfavourable interaction. **211**'s PA was 971 kJ mol<sup>-1</sup>.

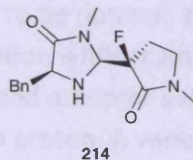


Figure 7.44

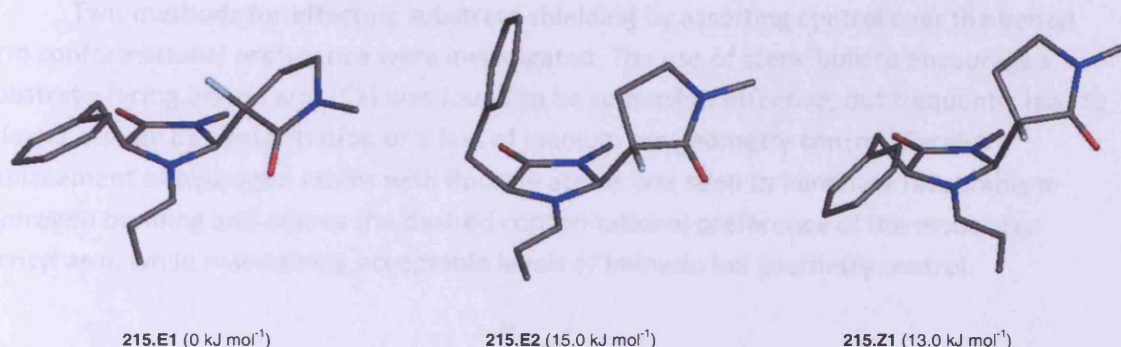


Figure 7.45

Applying the principals examined in the study of **210** and **211**, **214** was devised (Figure 7.45). **215** was seen to have a *Z-E* energy difference of 13.0 kJ mol<sup>-1</sup>, notable for a 2-monosubstituted imidazolidinone. **215.E1** was found to be the lowest energy conformation, stabilised both by a hydrogen bond from a benzylic proton to the fluorine atom (2.26 Å) and by a hydrogen bond from the iminium proton to the amidic oxygen (1.94 Å). **215.E2** showed a rotation of the methylpyrrolidinone ring so as to remove the  $\pi$ -fluorine repulsive interaction and attain a  $\pi$ -hydrogen bond. This rotation meant that the amidic oxygen pointed away from the rest of the iminium ion and was not engaged in hydrogen bonding. **215.Z1** showed



the same rotation of the methylpyrrolidinone ring and consequently was not that much lower in energy than the **Z2** conformation (18.8 kJ mol<sup>-1</sup>).

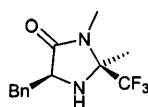
## 7.9 Conclusions

Three basic principles of iminium ion organocatalyst design were investigated independently and the findings combined to design catalysts theoretically capable of unparalleled performance.

Calculated proton affinities were found to be unsuitable for quantitative comparisons amongst structurally diverse catalysts but were found to serve adequately as a rough indicator of catalytic potential.

The substitution pattern at the 2-position of imidazolidinones was varied and the effect upon the resultant catalysts' iminium ion geometric selectivity investigated. The 2,2-dimethyl substitution pattern was seen to be optimal, both in theory and in practice. The ability to alter substitution at the 2-position while maintaining good iminium ion geometry control was attained when hydrogen-bond acceptor substituents were employed to effect a selective hydrogen bond to the iminium proton. A variety of hydrogen bond acceptors were evaluated and amidic oxygen atoms found to be most suitable.

Two methods for effecting substrate shielding by asserting control over the benzyl arm conformational preference were investigated. The use of steric bulk to encourage a substrate-facing benzyl arm (**E1**) was found to be somewhat effective, but frequently lead to a lower energy **E3** conformation or a loss of iminium ion geometry control. Careful replacement of hydrogen atoms with fluorine atoms was seen to eliminate favourable  $\pi$ -hydrogen bonding and induce the desired conformational preference of the associated benzyl arm, while maintaining acceptable levels of iminium ion geometry control.



**91**

Figure 7.46

As evidenced by the catalytic impotence of **91**·HCl, fluorine atoms have very pronounced electron withdrawing effects and are best used in moderation (**Figure 7.46**). Accordingly, selective monofluorination of a 2-alkyl group would seem the most promising approach towards developing a functional catalyst based on the theoretical principals explored within this chapter.

## 7.10 Future Work

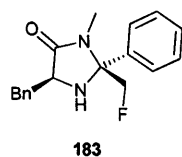


Figure 7.47

Experimental evaluation of **183** should be at the forefront of any further research into imidazolidinone catalyst development (Figure 7.47). **183** holds promise as a high performance highly stereoselective iminium organocatalyst.

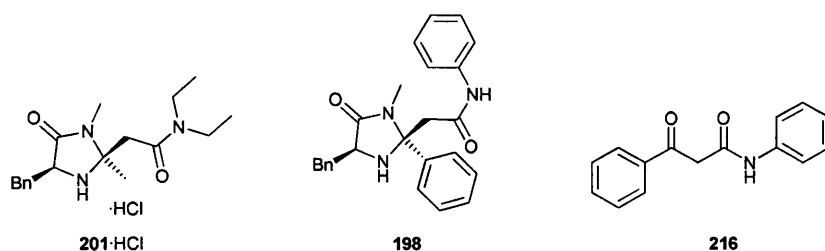


Figure 7.48

The synthesis and evaluation of **201·HCl** in the benchmark Diels-Alder reaction showed that incorporation of the 2-( $\beta$ -acetamido) moiety into an imidazolidinone catalyst may be expected to reduce turnover but does not eliminate catalyst activity completely. As the incorporation of a 2-aryl group has been shown to give rise to higher performance imidazolidinone catalysts, **198** appeared a good target for future experimental work. **198** may theoretically be obtained from commercially available **216**.

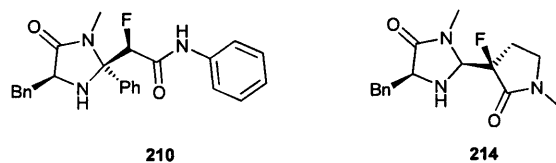


Figure 7.49

Finally, a catalyst with a pronounced theoretical preference for the **E1** conformation, such as **210** and **214**, should be evaluated in conjugate addition reactions.

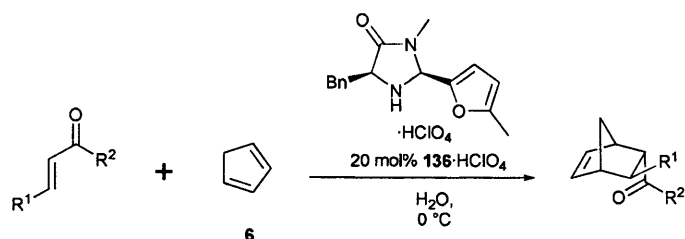
---

## **Chapter 8: C<sub>2</sub>-Symmetric Catalysts**

---

## 8 C<sub>2</sub>-Symmetric Catalysts

### 8.1 Introduction



|            | R <sup>1</sup>  | R <sup>2</sup>  | Yield (%) | ee (%) |
|------------|-----------------|-----------------|-----------|--------|
| <b>217</b> | CH <sub>3</sub> | CH <sub>3</sub> | 85        | 61     |
| <b>218</b> | CH <sub>3</sub> | Et              | 89        | 90     |
| <b>219</b> | CH <sub>3</sub> | <i>n</i> -Bu    | 83        | 92     |
| <b>220</b> | CH <sub>3</sub> | <i>i</i> -Am    | 86        | 92     |
| <b>221</b> | CH <sub>3</sub> | <i>i</i> -Pr    | 24        | 0      |
| <b>222</b> | <i>n</i> -Pr    | Et              | 84        | 92     |
| <b>223</b> | <i>i</i> -Pr    | Et              | 78        | 90     |

Scheme 8.1

Work performed so far in this project had centered around the development of catalysts for  $\alpha,\beta$ -unsaturated aldehyde substrates. To further leverage the understanding in catalyst design developed in this project, the possibility of developing imidazolidinone organocatalysts for use with  $\alpha,\beta$ -unsaturated ketones was investigated. MacMillan describes the use of **136**·HClO<sub>4</sub> in catalysing the Diels-Alder reaction between a range of  $\alpha,\beta$ -unsaturated ketones and **6** (Scheme 8.1).<sup>63</sup>

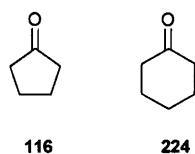


Figure 8.2

As seen in Scheme 8.1, **136** did not achieve good stereocontrol when used with **217** or **221**. Poor enantiocontrol was also observed with **116** (48% ee) and **224** (63% ee) (Figure 8.2). This showed that **136** had pronounced substrate specificity.

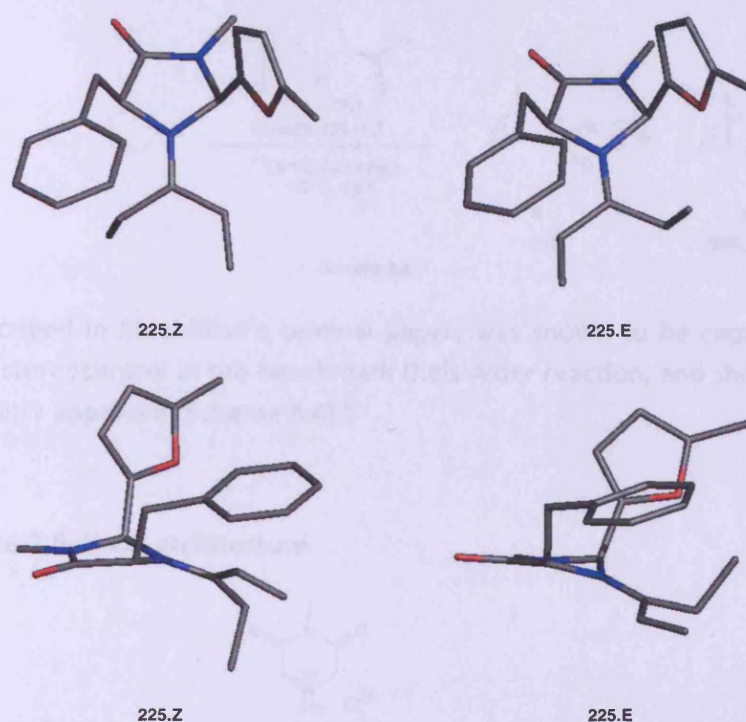
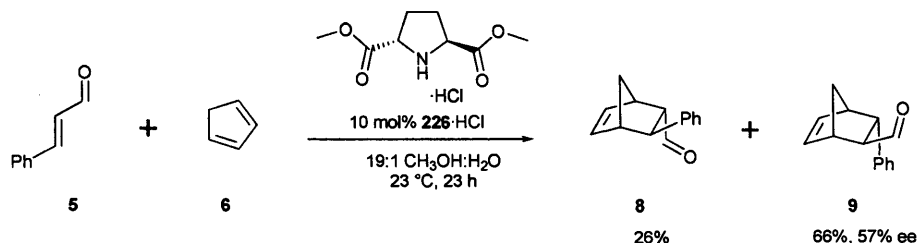


Figure 8.3

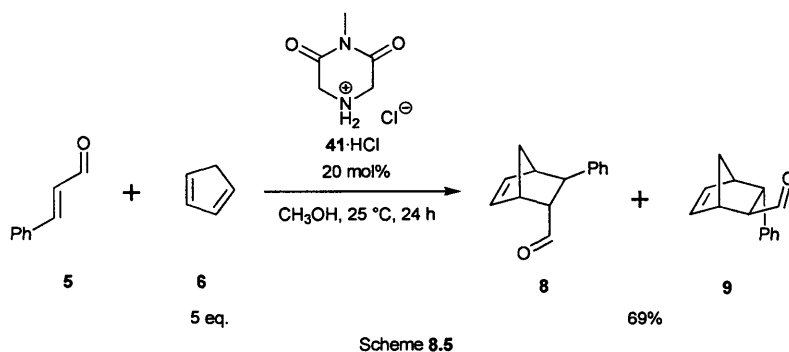
Condensation of **136** and **218** gives rise to **225.E** and **225.Z** (Figure 8.3). In the mechanism postulated by MacMillan, the methyl group  $\alpha$ - to the iminium carbon bends out of the plane of the  $\pi$ -system.<sup>63</sup> In both **225.E** and **225.Z**, the methyl group shields the *Re* face, while leaving the *Si* face exposed. Stereocontrol was therefore said to be achieved with either **225.E** or **225.Z** and geometric selectivity in iminium ion formation was not necessary.

The stereocontrol mechanism employed by **136** was seen to limit substrate scope and alternatives were sought. One alternative appeared to be catalysts with  $C_2$  rotational symmetry running through the active nitrogen atom. Such catalysts would not give rise to geometric isomers upon condensation with a substrate enone and may demonstrate a more general purpose technique for effecting stereocontrol.

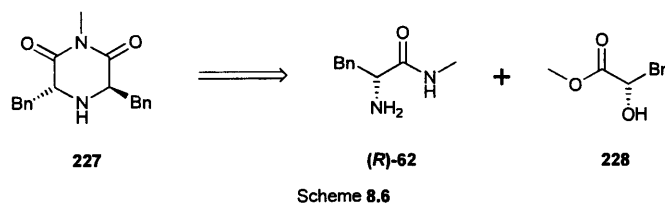


**226**, described in MacMillan's seminal paper, was shown to be capable of exerting some degree of stereocontrol in the benchmark Diels-Alder reaction, and showed precedent for the  $C_2$  symmetry approach (Scheme 8.4).<sup>2</sup>

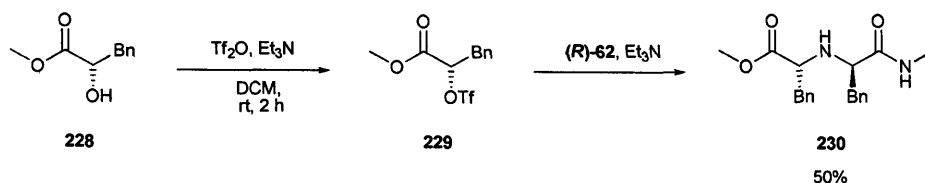
## 8.2 Piperazine-2,6-dione architecture



One of the key catalysts discovered during previous investigations within the group, **41**·HCl, attained 69% conversion after 24 hours in the benchmark Diels-Alder reaction when used at 20 mol% in methanol (Scheme 8.5).<sup>30</sup> The piperazine-2,6-dione architecture had been investigated within the group by previous members and was thought to hold promise as the foundation around which a  $C_2$ -symmetric catalyst capable of catalyzing the reactions of ketones as well as aldehydes could be constructed.

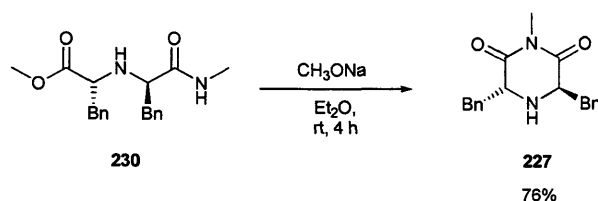


The formal addition of two benzyl arms to **41** yielded **227**, which appeared to be obtainable from (*R*)-**62** and **228** (Scheme 8.6).



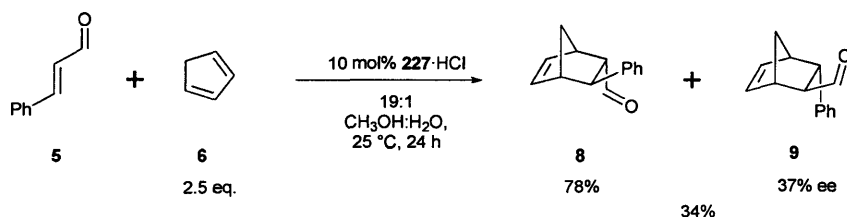
Scheme 8.7

A solution of **228** and triethylamine in DCM was treated with triflic anhydride and the solution allowed to react over the course of 2 hours (Scheme 8.7). The DCM was evaporated and the residue extracted 6 times petroleum ether, yielding **229**. **229**, (*R*)-**62** and triethylamine were stirred in DCM for 19 hours at room temperature. Aqueous workup and column chromatography yielded **230** (50%).



Scheme 8.8

**230** was stirred with sodium methoxide in diethyl ether at room temperature for 4 hours then subjected to aqueous workup and column chromatography to provide **227** (76%) (Scheme 8.8). **227**·HCl was formed by the usual method (53% overall).



Scheme 8.9

**227**·HCl was found to be a very low performance catalyst in the benchmark Diels-Alder reaction, attaining only 34% conversion when used at 10 mol% in 19:1 methanol:water at 25 °C for 24 hours (Scheme 8.9). Enantiocontrol was also lacking, with ee's of 78% (**8**) and 37% (**9**) noted. Experimental evaluation with an enone substrate was not performed.

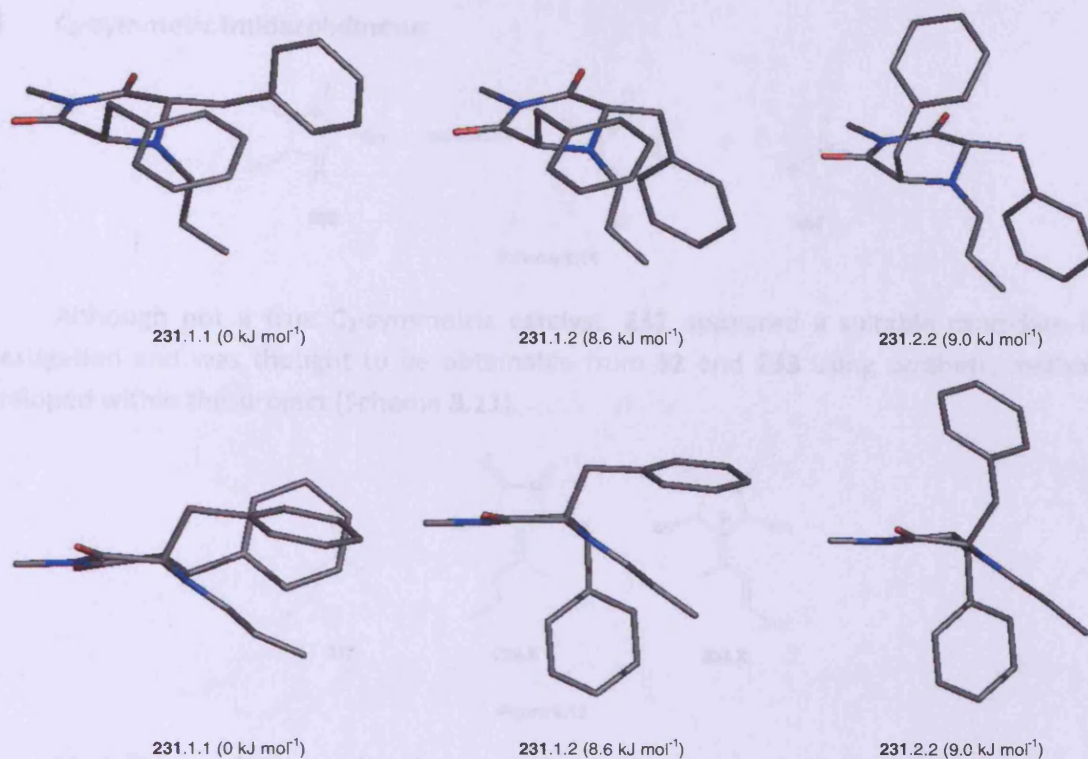


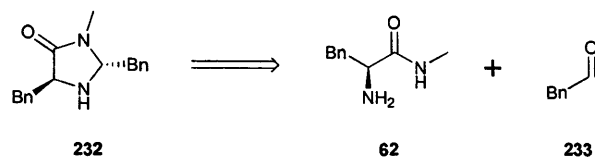
Figure 8.10

**227** was subjected to the standard computer modelling regime and its iminium ion (**231**) found to exhibit 3 low energy conformations (<19 kJ mol<sup>-1</sup>) (Figure 8.10). The preferred conformation, **231.1.1**, could be expected to effectively shield the top face of the substrate, while leaving the bottom face exposed. **231.1.2** may also shield the top face of the substrate but may disfavour a bottom-face *endo*-transition state. **231.2.2** appears to not fully shield the upper face of the substrate, as the nonplanarity of the piperazine-2,6-dione ring allows the substrate to bend away from the upper shielding arm. Particularly low ee's were noted for the *endo*-product, **8**. This could be explained by the furthest benzyl arm partially blocking the bottom face of the substrate of **231.1.2** and **231.2.2** and selectively disfavouring the *endo*-transition state.

Perhaps due to the nonplanarity of its iminium ion, **227** was found to exert poor enantiocontrol in the benchmark Diels-Alder reaction. Turnover was also seen to be lacking. While synthetically accessible, the piperazine-2,6-dione architecture appeared to hold little promise as the scaffold around which a high performance C<sub>2</sub>-symmetric catalyst could be constructed and further investigations were not performed.



### 8.3 C<sub>2</sub>-symmetric imidazolidinone



Scheme 8.11

Although not a true C<sub>2</sub>-symmetric catalyst, **232** appeared a suitable candidate for investigation and was thought to be obtainable from **62** and **233** using synthetic methods developed within this project (Scheme 8.11).

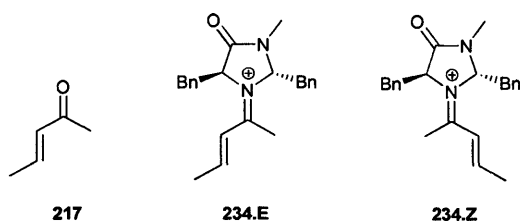


Figure 8.12

Modelling work was undertaken to estimate the stereoselectivity of **232**. As the goal of the work performed within this chapter was to develop a catalyst for use with enones, **217** was used as a substrate, giving rise to **234.E** and **234.Z** (Figure 8.12).

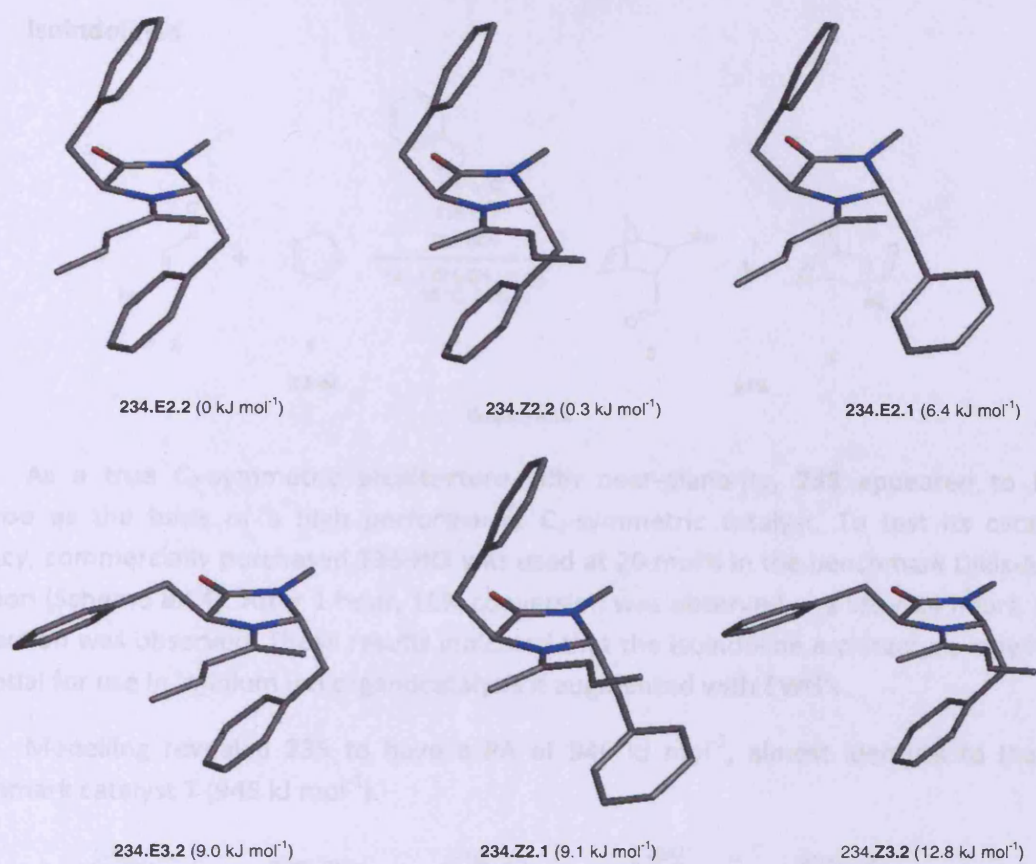


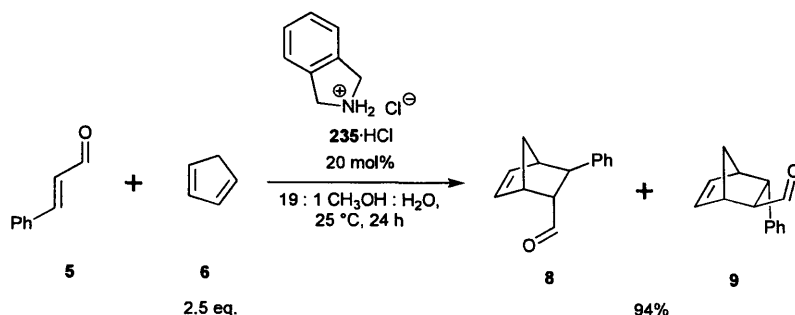
Figure 8.13

The *pseudo*-isosteric pair of iminium ions **234.E2.2** and **234.Z2.2** were found to have the lowest energies (Figure 8.13). Unfortunately, in both cases, the benzyl arms appeared to block the top and bottom faces of the substrate thus equally disfavoured both desired and undesired transition states. The same lack of facial discrimination was apparent in **234.E2.1**, **234.E3.2** and **234.Z2.1**. **234.Z3.2** appeared to selectively block the lower face but was considered too high in energy relative to the other conformations to be significant.

Having observed the inability of **232**'s iminium ions to exhibit effective substrate shielding through modelling, it was considered that **232** would most likely show very poor enantiocontrol under experimental conditions and that its synthesis was not a worthwhile undertaking.

The modelling of **232** showed that a far greater degree of control over benzyl arm positioning would be required for any *pseudo*- or fully- *C*<sub>2</sub>-symmetric catalyst to achieve good stereocontrol than for an asymmetric catalyst with good iminium ion geometry selectivity.

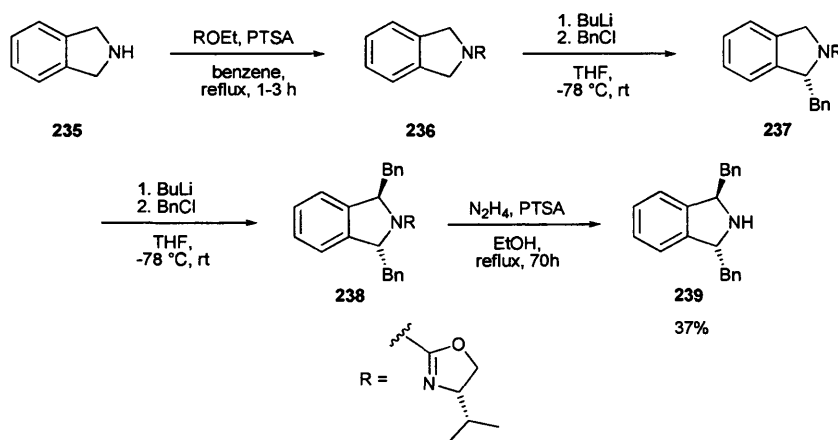
## 8.4 Isoindolines



Scheme 8.14

As a true  $\text{C}_2$ -symmetric architecture with near-planarity, **235** appeared to hold promise as the basis of a high performance  $\text{C}_2$ -symmetric catalyst. To test its catalytic efficacy, commercially purchased **235**·HCl was used at 20 mol% in the benchmark Diels-Alder reaction (Scheme 8.14). After 1 hour, 16% conversion was observed and after 24 hours, 94% conversion was observed. These results indicated that the isoindoline architecture may have potential for use in iminium ion organocatalysis if augmented with EWG's.

Modelling revealed **235** to have a PA of  $946 \text{ kJ mol}^{-1}$ , almost identical to that of benchmark catalyst **7** ( $945 \text{ kJ mol}^{-1}$ ).



Scheme 8.15

Publications were found in which **239** was obtained by deprotonation of an *N*-protected **235** derivative and quenching of the resultant anion with benzyl halides.<sup>79,80</sup> In the method of Gawley *et. al.*, **235** was protected with a chiral auxiliary, alkylated at the 2- and 7-positions, then deprotected to give **239** in 37% overall yield (Scheme 8.15).

Satisfied that the isoindoline architecture was both synthetically accessible and catalytically active, theoretical studies were undertaken to assess its potential for effecting enantiocontrol.

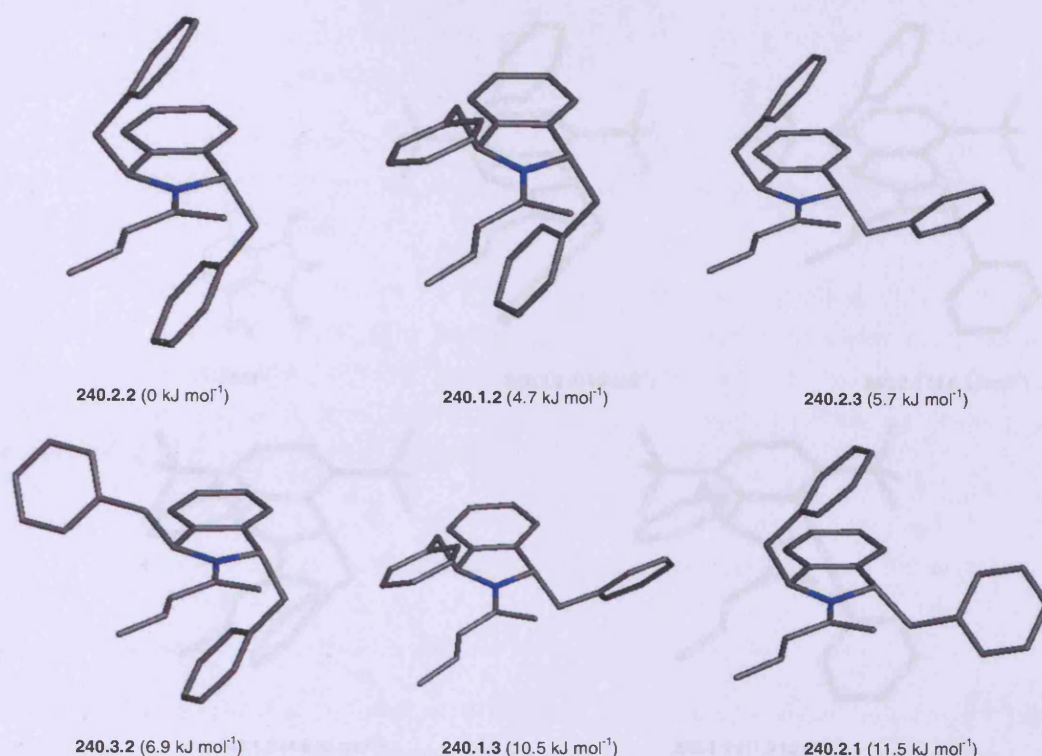


Figure 8.16

The iminium ion arising from condensation of **239** and **217** was seen to have 9 conformations, corresponding to the 3 non-eclipsing positions of each benzyl arm, of which 6 have relative energies of <15 kJ mol<sup>-1</sup> (Figure 8.16). The lowest energy conformation **240.2.2** appeared to block both the top and bottom face of the substrate  $\alpha$ - to the iminium carbon atom. This indicated that open transition state reactions would proceed freely but with no enantiocontrol, while closed transition state reactions would proceed slowly, if at all. **240.1.2** and **240.3.2** exhibited uneven facial shielding but would still be expected react very slowly *via* closed transition states. **240.2.3** showed effective shielding of the top face of the substrate and allowed free approach towards the lower face of the substrate. This was also seen to be the case with **240.1.3** and **240.2.1**.

As 3 of the 6 lowest energy conformations demonstrated the desired substrate shielding pattern, and the other 3 low energy conformations appeared unamenable towards closed transition state reactions, it was thought that **239** may have potential for use in the Diels-Alder reaction between **217** and **6**.

The proton affinity of **239** was found to be 1010 kJ mol<sup>-1</sup>, higher than **235**'s proton affinity of 946 kJ mol<sup>-1</sup>, and was seen as a forewarning of performance problems.



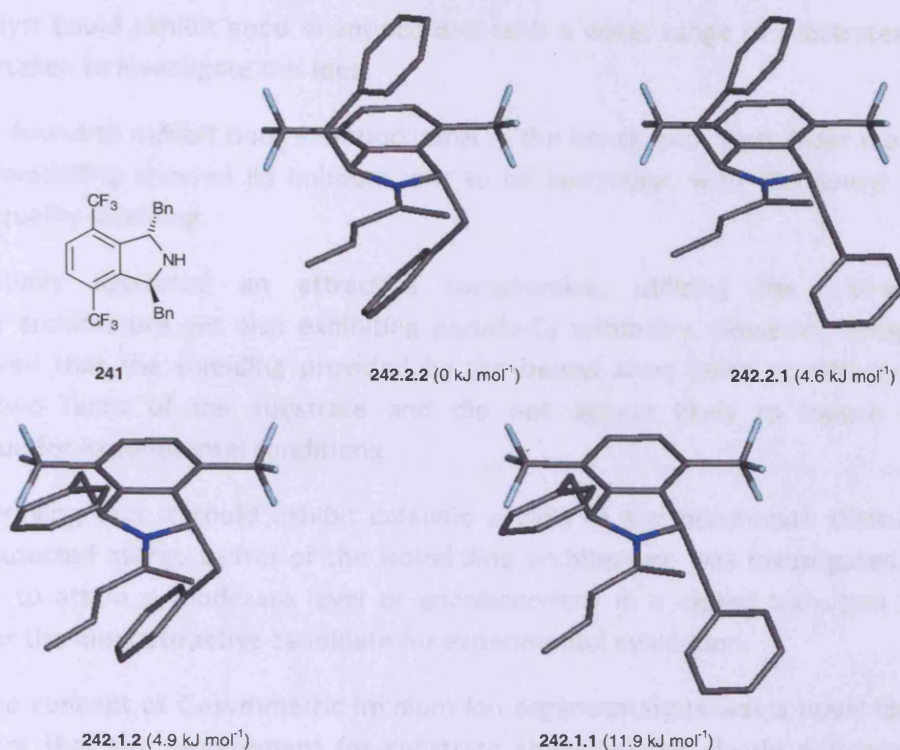


Figure 8.17

As **235** had shown a high PA ( $946 \text{ kJ mol}^{-1}$ ) and a low turnover in the benchmark Diels-Alder reaction, it appeared that the isoindoline architecture may require EWG's to exhibit good performance. The formal addition of two trifluoromethyl groups to **239** (PA:  $1010 \text{ kJ mol}^{-1}$ ) yielded **241**, which was seen to have a PA of  $967 \text{ kJ mol}^{-1}$  (Figure 8.17). This indicated that EWG's should be positioned closer to the active nitrogen.

All of **242**'s 4 lowest energy conformations ( $<24 \text{ kJ mol}^{-1}$ ) appeared unselective towards open transition state reactions and unfavourable for closed transition state reactions. **241** therefore did not appear to have potential as an iminium ion organocatalyst.

## 8.5 Conclusions

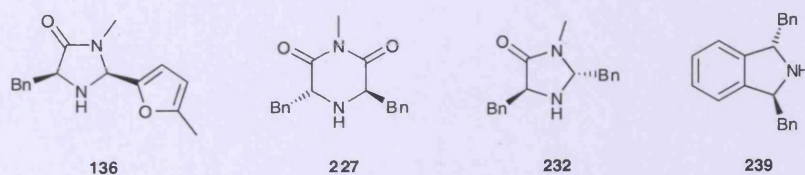


Figure 8.18

**136**, the catalyst used by MacMillan for the Diels-Alder reaction with enones, attains good stereocontrol only with certain substrates (Figure 8.18). It was imagined that a  $\text{C}_2$ -

symmetric catalyst could exhibit good enantiocontrol with a wider range of substrates and work was undertaken to investigate this idea.

**227** was found to exhibit poor enantiocontrol in the benchmark Diels-Alder reaction and computer modelling showed its iminium ions to be nonplanar, with the benzyl arms providing poor quality shielding.

**232** initially appeared an attractive compromise, utilising the well-tested imidazolidinone architecture yet also exhibiting *pseudo*-C<sub>2</sub> symmetry. However, computer modelling showed that the shielding provided by the benzyl arms failed to differentiate between the two faces of the substrate and did not appear likely to induce good enantiocontrol under experimental conditions.

After verifying that it could exhibit catalytic activity in the benchmark Diels-Alder reaction, the expected stereocontrol of the isoindoline architecture was investigated. **239** appeared likely to attain a moderate level of enantiocontrol in a closed transition state reaction and was the most attractive candidate for experimental evaluation.

While the concept of C<sub>2</sub>-symmetric iminium ion organocatalysts was a novel idea, it became apparent that the requirement for substrate shielding that clearly differentiates between the upper and lower faces of a substrate rendered its implementation a difficult undertaking. It is now thought that progress may be realised more easily by focussing on the design of structural features able to induce iminium ion geometry selectivity with enone substrates and using a single benzyl arm for substrate shielding.

---

## **Chapter 9: Conclusions and Future Work**

---

## 9 Conclusions and Future Work

### 9.1 Overview

At the outset of this project, 3 primary limitations of iminium organocatalysis were identified:

- High catalyst loadings
- Low temperature requirements for conjugate additions
- Specificity for aldehyde substrates

Accordingly, this project aimed to develop catalysts with (i) increased efficiency, (ii) the ability to perform conjugate additions at ambient temperature, and (iii) the ability to accelerate the reactions of enone as well as enal substrates.

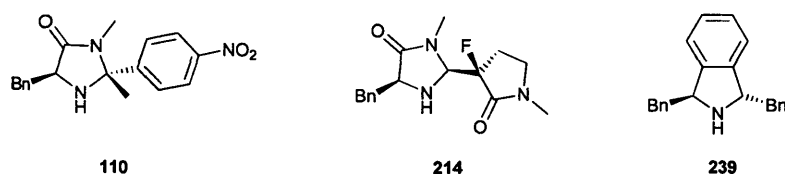


Figure 9.1

The first goal was realised with the synthesis and evaluation of **110**, a catalyst capable of attaining very high performance in the Benchmark reaction, while still exhibiting good stereocontrol.

The second goal was not realised experimentally, although modelling work investigated the structural features required for such a catalyst and arrived at likely candidates for experimental evaluation, such as **214**.

The third goal was also not realised experimentally. However, theoretical investigations elucidated structures with potential for use with enones, such as **239**.



## 9.2 Architectural Comparisons

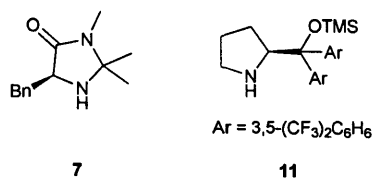


Figure 9.2

Before this work was performed, no direct comparison between imidazolidinone and prolinol ether organocatalysts in the Diels-Alder reaction had been performed. The work in Chapter 3.5 showed that **7** outperformed **11** in the benchmark Diels-Alder reaction, under the conditions examined. This result filled a gap in the literature and validated this project's focus on the imidazolidinone architecture.

## 9.3 EWG Investigation

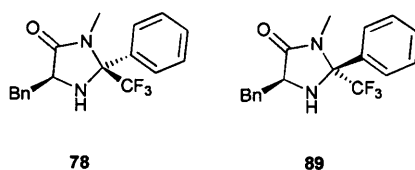


Figure 9.3

In Chapters 2 and 4, an investigation into the ability of EWGs to improve the rate of reaction catalysed by imidazolidinones was undertaken. **78** and **89** were synthesised, but could not be converted to their hydrochloride salts. **78** and **89** both failed to exhibit catalytic activity when used in the benchmark reaction with 1 equivalent of hydrochloric acid.

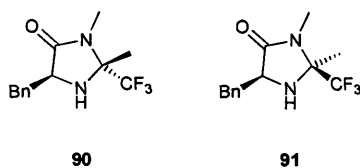


Figure 9.4

**90**·HCl and **91**·HCl were synthesised but found to be catalytically inactive, presumably due to the vastly reduced nucleophilicity of the free amines. Reinforcing this hypothesis was the observation that both **90**·HCl and **91**·HCl readily revert to the corresponding free amines when dried *in vacuo*. Before this project was undertaken, no upper limits to the strength of an EWG on an iminium organocatalyst had been envisaged. It has now been shown that positioning very strong EWG's close to the active nitrogen can render an imidazolidinone catalytically inactive.

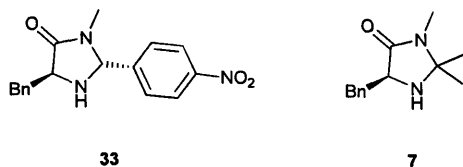
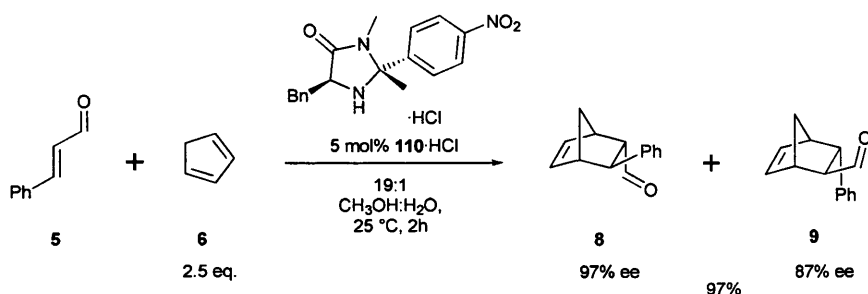


Figure 9.5

**33** had previously been discovered and evaluated within the group and was found to exhibit far higher performance than benchmark catalyst **7**, but lower levels of stereocontrol. Starting out with the postulate that increasing steric bulk at the 2-position of the imidazolidinone ring may improve iminium geometry selectivity and enhance overall stereocontrol, ten imidazolidinones were synthesised and their hydrochloride salts evaluated in the benchmark reaction.

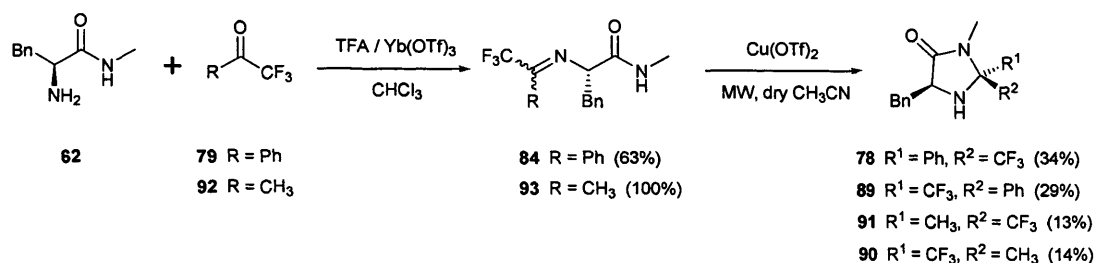


Scheme 9.6

5 mol% **110**·HCl was seen to catalyse 97% conversion in the benchmark reaction after 2 h. When optically pure catalyst was used, product ee's of 97% (**8**) and 87% (**9**) were observed. When **110**·HCl was used at 1 mol%, the benchmark reaction ran to completion overnight at room temperature, attaining 95% (**8**) and 88% (**9**) ee.

**110**·HCl was the first imidazolidinone catalyst able to attain substantially higher performance than benchmark catalyst **7** while still maintaining comparable levels of stereocontrol. It is possible that further screening of conditions and co-acids (such as TFA, found particularly effective in Chapter 3.5) could further boost **110**'s enantiocontrol.

## 9.4 Synthetic Development



Scheme 9.7

A search of the literature revealed only 4 reports of 2-fluoroalkylimidazolidin-4-ones. Three of these reports attained the products *via* inflexible mineral acid-based syntheses; the fourth provided no experimental details.<sup>81–83,1</sup> The synthetic methodology developed in Chapter 2.5 and Chapter 2.7 thus represents the first potentially general purpose synthetic route to this class of compound, using relatively mild conditions and delivering the products in reasonable yields (Scheme 9.7).

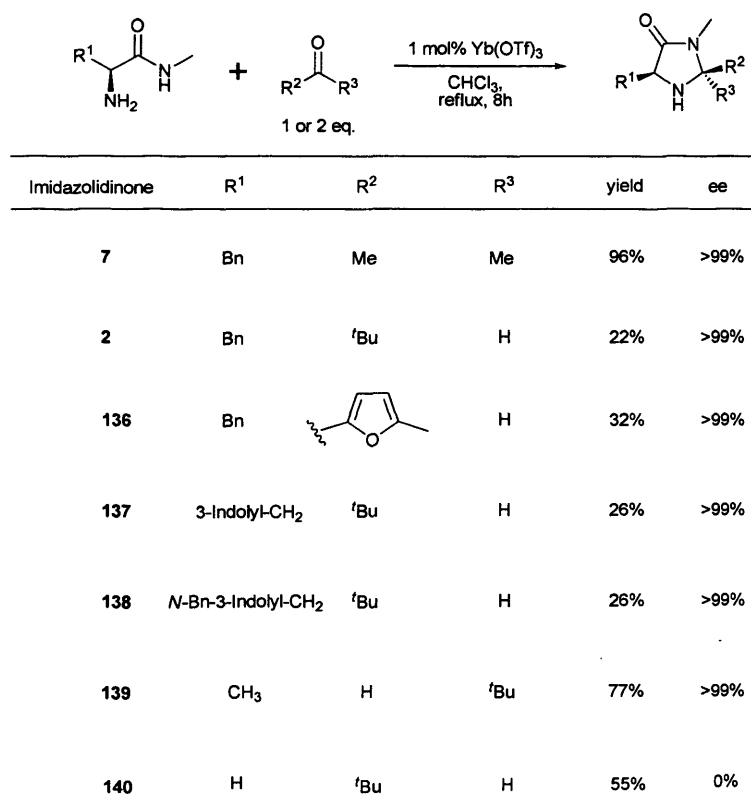
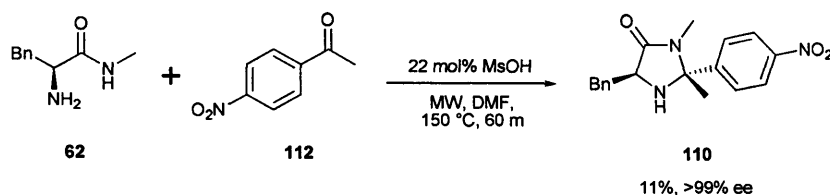


Figure 9.8

The use of Lewis acids such as ytterbium(III) triflate for synthesis of imidazolidinones was investigated. This research lead to a general purpose air- and water-insensitive one-step

reaction, allowing widely used imidazolidinone catalysts to be obtained in good yields with negligible loss of optical purity (Figure 9.8).



Scheme 9.9

While attempting to boost the stereocontrol of **110**, it was found that the use of ytterbium(III) triflate induced loss of enantiopurity both when used under thermal and microwave conditions. Alternative methods of synthesis were investigated and a method arrived upon that allowed **110** to be synthesised in one step under microwave conditions in 11% yield with 99% ee (Scheme 9.9)

While not the primary goal of this project, development of synthetic methodology was found to be a necessary prerequisite to investigation of the catalytic activity of promising target structures. The methodology developed has allowed the evaluation of novel catalysts and has also opened up synthetic access to the imidazolidinone architecture, removing impediments to future investigations both from within and also from outside the group.

## 9.5 Improved Stereocontrol

In Chapter 4.21, The development of  $^1\text{H}$  NMR analysis of a thermodynamic distribution of iminium ions as a tool for discerning the geometric selectivity of an iminium ion organocatalyst was developed. In Chapter 6.3, a computational method for calculating the same metric was developed and found to achieve good agreement with the experimental method.

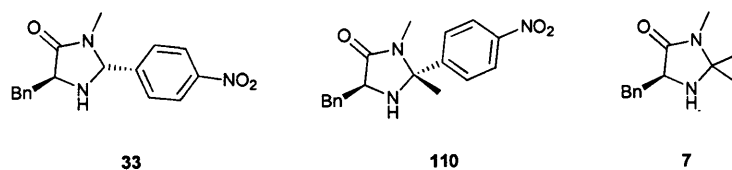


Figure 9.10

These techniques showed that **110** attained far greater geometric selectivity than **33** yet still fell short of the geometric selectivity attained by benchmark catalyst **7** (Figure 9.10). A good agreement between geometric selectivity and stereocontrol in the benchmark Diels-Alder reaction was noted, suggesting that for an iminium ion organocatalyst to attain good levels of stereocontrol, it must first attain good levels of iminium ion geometry control.

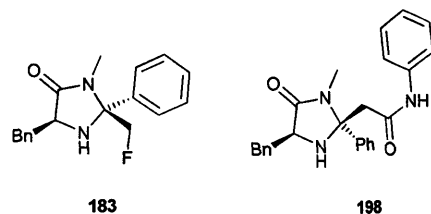


Figure 9.11

A thorough computational investigation of the structural motifs that may be used to effect iminium ion geometry control was performed. This investigation showed that limited control may be achieved by relying upon the use of steric hindrance and that the use of tactically positioned hydrogen bond acceptors appears more effective and allows greater flexibility in catalyst design. This principle was used in the design of **183** and **198** (Figure 9.11).

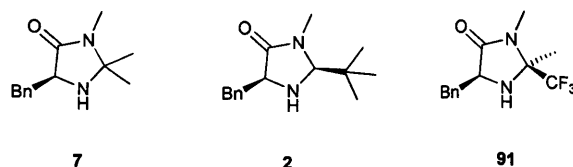


Figure 9.12

Modelling work was undertaken to establish the role of the benzyl arm feature of imidazolidinone catalysts in effecting stereocontrol. The favoured position of the benzyl arm was found to correlate with a catalyst's ability to attain stereocontrol in open and closed transition state reactions. The modelling of **7**, **2** and **91** showed the different conformational preferences of **7** vs. **2** and **91** and elucidated two mechanism by which benzyl arm position may be controlled (Figure 9.12). As the steric method of benzyl arm control, embodied by **2**, appeared less effective and had detrimental effects on calculated iminium ion geometry control, the electronic method embodied in **91** appeared to have the greatest potential for incorporation into a useful catalyst.

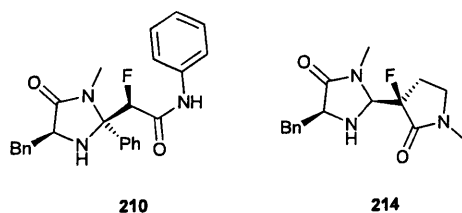
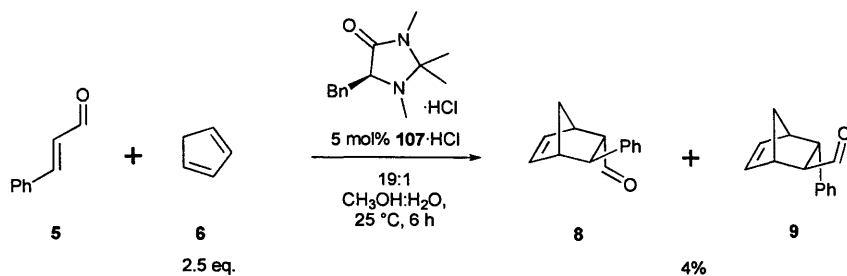


Figure 9.13

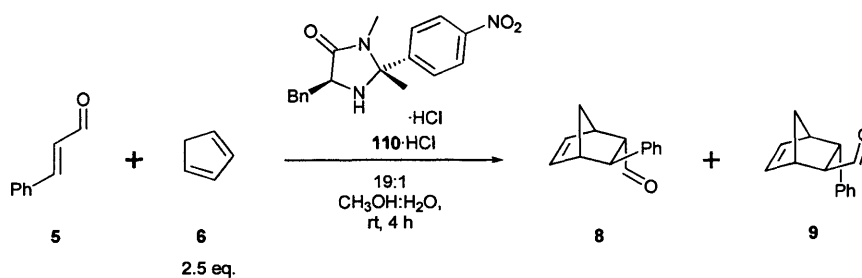
The electronic method of benzyl arm control was used in designing **210** and **214**, both of which are expected to exhibit good stereocontrol in open transition state reactions, such as the conjugate addition of indoles to  $\alpha,\beta$ -unsaturated aldehydes.

## 9.6 Background Reaction



Scheme 9.14

In Chapter 4.3, 5 mol% **107**·HCl was found to attain 4% conversion after 6 hours in the benchmark Diels-Alder reaction at 25 °C (Scheme 9.14). As **107**·HCl was incapable of forming iminium ions, one or more alternative mechanisms must have been responsible for formation of **8** and **9**.



Scheme 9.15

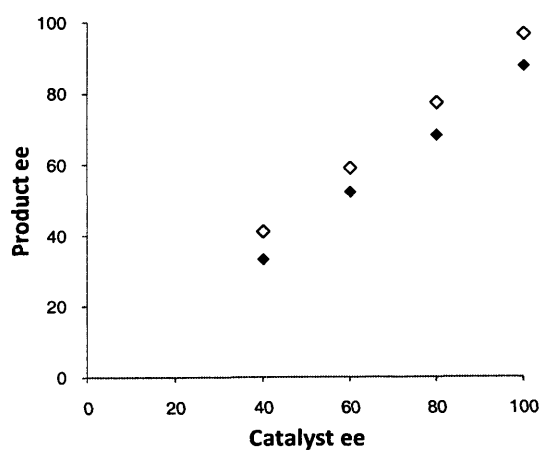


Figure 9.16

| <b>110 ee – 8 ee</b> | <b>110 ee – 9 ee</b> |
|----------------------|----------------------|
| %                    | %                    |
| 3                    | 12                   |
| 2                    | 12                   |
| 1                    | 8                    |
| -1                   | 7                    |

Figure 9.17

When the benchmark Diels-Alder reaction was run multiple times with **110**·HCl of differing enantiopurity, a correlation between the ee of each product and catalyst ee was noted (Figure 9.16, 9.17). Within the relatively large margins of error in these experiments, **8** ee roughly matched the ee of **110**·HCl, indicating that the reactions giving rise to **8** were exclusively bimolecular reactions proceeding through the iminium ion. **9** ee's appeared, within error margins, to be lower than **110** ee's by a consistent amount. This indicated that a non-stereoselective side reaction was occurring and was responsible for approximately 9% conversion.

As **107**·HCl effected only 4% formation of **8** and **9** in 6 hours, it can be said that the side reaction occurring in the presence of **110**·HCl is substantially faster than the dominant reaction occurring in the presence of **107**·HCl. As **110**·HCl is suspected to be more acidic than **107**·HCl, it appeared possible that acid catalysis was the mechanism in both cases. This suggested that careful tuning of catalyst acidity and counterion basicity may minimise side reactions and allow greater stereoselectivity to be attained in the iminium ion organocatalysed Diels-Alder reaction.

## 9.7 Future work

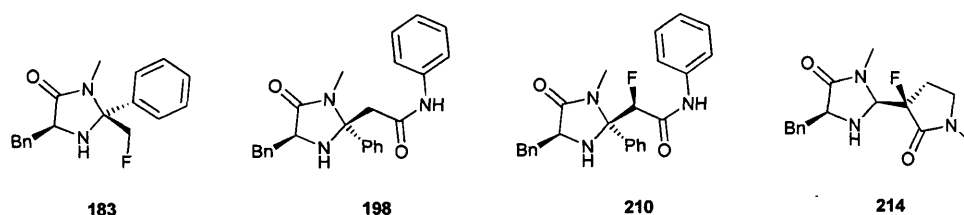


Figure 9.18

Having identified structural motifs that may be used to enhance iminium geometry control and substrate shielding, multiple target structures incorporating these motifs were posited for experimental evaluation (Figure 9.18). Unfortunately, due to time constraints, no experimental evaluation of these target structures could be performed. Future work should

therefore focus first on experimental appraisal of the theoretical work performed in Chapter 7, before additional modelling work is undertaken.

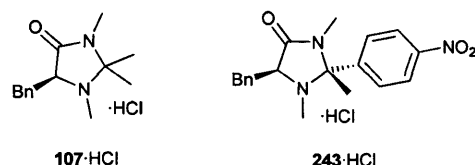


Figure 9.19

Investigations into background reaction rates in the benchmark Diels-Alder reaction showed that side reactions appeared to be occurring and that acid catalysis was a likely mechanism. To investigate further, **243**·HCl could be synthesised and used in the benchmark Diels-Alder reaction. **243**·HCl is predicted to induce greater conversion than **107**·HCl and produce products with extremely low ee's.

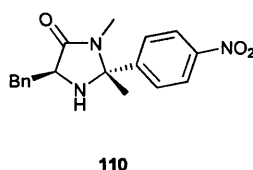


Figure 9.20

Screening of co-acids for use with **110** would be a quick and easy way to explore the potential of this imidazolidinone. As the analysis in Chapter 9.6 makes the case that a loss in enantiopurity in the benchmark reaction may be occurring largely through an acid-catalysed reaction, there is a good chance that use of an alternative co-acid could boost **110**'s enantiocontrol beyond the levels demonstrated by benchmark catalyst **7**.

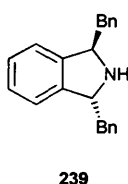


Figure 9.21

Finally, theoretical inroads were made towards targeting enone substrates. The isoindoline architecture showed some promise for use with enones in closed transition state reactions, with **239** being worthy of experimental evaluation.

The concept of C<sub>2</sub>-symmetric iminium catalysts appeared valid but was shown to require very well defined substrate shielding to be effective. Hence, future work should focus on the elucidation of structural motifs able to control iminium geometry with enone substrates.



---

## **Chapter 10: Experimental**

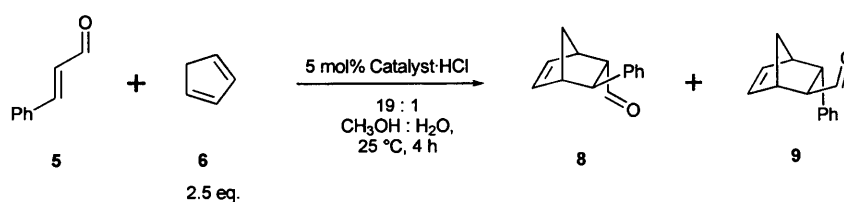
---

## 10 Experimental

### 10.1 General Procedures

Commercially available solvents and reagents were used without further purification. Petroleum ether refers to the fraction with bp 40–60 °C and ether refers to diethyl ether. Flash chromatography was carried out using Merck Kieselgel 60 H silica or Matrex silica 60. Analytical thin layer chromatography was carried out using aluminium-backed plates coated with Merck Kieselgel 60 GF<sub>254</sub> that were visualized under UV light (at 254 and/or 360 nm). Infra-red (IR) spectra were recorded in the range 4000–600 cm<sup>-1</sup> using KBr disks for solid samples and thin films between NaCl plates for liquid samples or as a nujol mull and are reported in cm<sup>-1</sup>. Nuclear magnetic resonance (NMR) spectra were recorded in CDCl<sub>3</sub> at 21 °C and were reported in ppm; *J* values were recorded in Hz and multiplicities were expressed by the usual conventions. Low-resolution mass spectra (MS) were determined using electrospray ionization (ES) unless otherwise stated. APCI refers to atmospheric pressure chemical ionization, CI refers to chemical ionization (ammonia) and EI refers to electron ionization. High-resolution mass spectra were obtained courtesy of the EPSRC Mass Spectrometry Service at University of Wales, Swansea, U.K. using the ionization methods specified. *In vacuo* refers to evaporation at reduced pressure using a rotary evaporator and diaphragm pump, followed by the removal of trace volatiles using a vacuum (oil) pump.

### 10.2 Benchmark Reaction Development



Scheme 10.1

As part of this project, a catalyst benchmarking reaction was developed, based on the Diels-Alder described by MacMillan in his seminal publication. A lower catalyst loading of 5 mol% was used to allow more accurate monitoring of high performance catalysts, while a slightly lesser excess of freshly distilled **6** was found necessary to avoid biphasic formation under certain conditions (Scheme 10.1). The temperature was conveniently fixed at 25 °C, and reactions were run for 4 hours. To hydrolyse dimethylacetals and ensure that **5**, **8** and **9** were not present in other forms, crude reaction mixtures were stirred vigorously with TFA, water, and chloroform for 2 hours at room temperature. Shorter hydrolysis periods were

investigated, but were found not to reliably hydrolyse all species. Extended hydrolysis periods of up to 6 hours were found not to alter the **8:9** ratio or ee of either product. To monitor the relative concentrations of **5**, **8** and **9** with respect to time, periodic aliquots were removed from the reaction, hydrolysed, and after basic workup, subjected to  $^1\text{H}$  NMR.

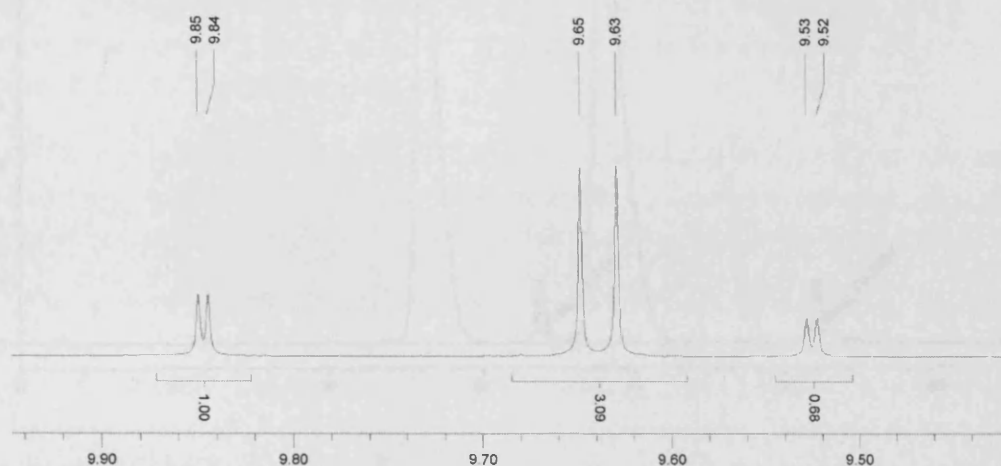
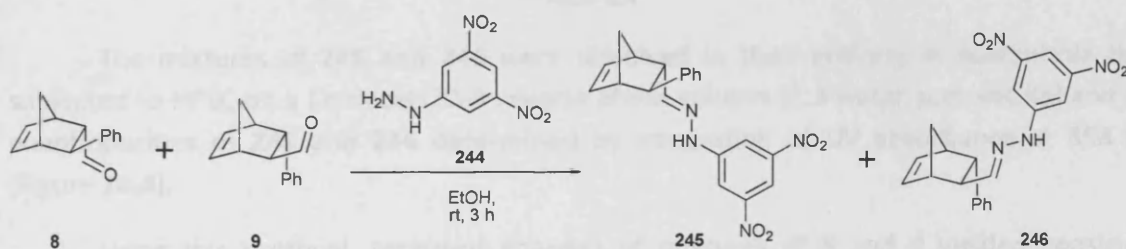


Figure 10.2

As the species of interest were all present as aldehydes, integration of the aldehyde region of the  $^1\text{H}$  NMR spectra was found the most suitable technique for assaying relative abundances (Figure 10.2). Using this technique, results could be obtained with an estimated error margin of <1%.



Scheme 10.3

To assay the enantiopurities of **8** and **9**, a technique previously developed within the group was used (Scheme 10.3). The crude reaction mixture was subjected to column chromatography (1:9 ethyl acetate:petroleum ether) to isolate a mixture of **8** and **9**. The aldehydes were then stirred with an excess of **244** in ethanol for 3 hours at room temperature before the ethanol was evaporated and column chromatography (1:3 ethyl acetate:petroleum ether) used to provide a mixture of **245** and **246** as an air-stable yellow solid.

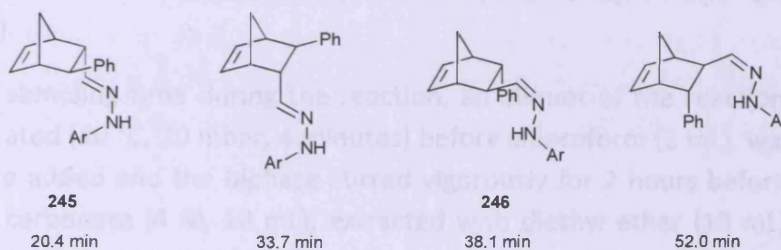
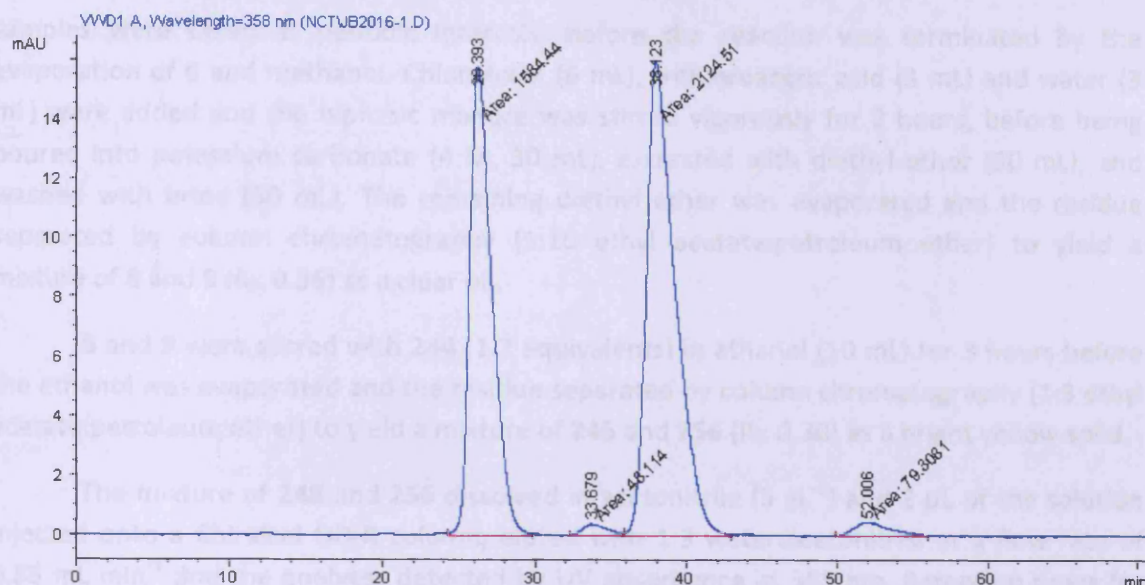


Figure 10.4

The mixtures of **245** and **246** were dissolved in their entirety in acetonitrile then subjected to HPLC on a Chiralcel OD-R reverse phase column (1:3 water:acetonitrile) and the enantiopurities of **245** and **246** determined by integration of UV absorbance at 358 nm (Figure 10.4).

Using this protocol, repeated analyses of mixtures of **8** and **9** yielded consistent results, with overall variations of <1%.

### 10.3 Final Benchmark Reaction

The catalyst freebase or hydrochloride salt (1.0 mmol) was dried by heating at 50 °C for 60 minutes under high vacuum (1 mbar). The reaction solvent, either toluene (5 mL), or methanol (4.75 mL) and water (0.25 mL), was then added, followed by TFA (0.148 mL, 0.228 g, 2.0 mmol) if required. **5** (0.630 mL, 0.661 g, 5.00 mmol) was added and the mixture was stirred at 25 °C for 10 minutes. The timer was started as freshly distilled **6** (0.995 mL, 0.826 g, 12.5 mmol) was added. Stirring was continued at 25 °C for 6 hours, during which time

samples were taken at periodic intervals, before the reaction was terminated by the evaporation of **6** and methanol. Chloroform (6 mL), trifluoroacetic acid (3 mL) and water (3 mL) were added and the biphasic mixture was stirred vigorously for 2 hours, before being poured into potassium carbonate (4 M, 30 mL), extracted with diethyl ether (30 mL), and washed with brine (30 mL). The remaining diethyl ether was evaporated and the residue separated by column chromatography (1:10 ethyl acetate:petroleum ether) to yield a mixture of **8** and **9** ( $R_f$ : 0.36) as a clear oil.

**8** and **9** were stirred with **244** (1.2 equivalents) in ethanol (10 mL) for 3 hours before the ethanol was evaporated and the residue separated by column chromatography (1:3 ethyl acetate:petroleum ether) to yield a mixture of **245** and **256** ( $R_f$ : 0.30) as a bright yellow solid.

The mixture of **245** and **256** dissolved in acetonitrile (5 gL<sup>-1</sup>) and 2  $\mu$ L of the solution injected onto a Chiralcel OD-R column, eluted with 1:3 water:acetonitrile at a flow rate of 0.85 mL min<sup>-1</sup> and the analytes detected by UV absorbance at 358 nm. Retention times for the hydrazones were: 20.4 min (major **245**), 33.7 min (minor **245**), 38.1 min (major **246**), 52.0 min (minor **246**).

At each sampling time during the reaction, an aliquot of the reaction mixture (0.15 mL) was evaporated (40 °C, 20 mbar, 4 minutes) before chloroform (2 mL), water (1 mL), and TFA (1 mL) were added and the biphasic mixture stirred vigorously for 2 hours before being poured into potassium carbonate (4 M, 10 mL), extracted with diethyl ether (10 mL), washed with brine (10 mL) then evaporated (40 °C, 20 mbar, 4 minutes) and the residue taken up in CDCl<sub>3</sub> (0.7 mL) for analysis by <sup>1</sup>H NMR.

#### 10.4 Standard Preparation A: 2-Aryl-imidazolidinones

| Solvent                  |            | R <sub>f</sub> | % Yield |            | R <sub>f</sub> | % Yield |
|--------------------------|------------|----------------|---------|------------|----------------|---------|
| 3:1 ethyl acetate:petrol | <b>33</b>  | 0.37           | 41*     | <b>104</b> | 0.15           | 35*     |
| ethyl acetate            | <b>110</b> | 0.47           | 36      | <b>111</b> | 0.21           | 35      |
| 3:1 ethyl acetate:petrol | <b>119</b> | 0.38           | 29      | <b>120</b> | 0.11           | 39      |
| ethyl acetate            | <b>121</b> | 0.46           | 33      | <b>122</b> | 0.24           | 28      |
| ethyl acetate            | <b>123</b> | 0.53           | 36      | <b>124</b> | 0.25           | 36      |
| ethyl acetate            | <b>125</b> | 0.43           | 21**    | <b>126</b> | 0.19           | 19**    |
| 2:1 ethyl acetate:petrol | <b>169</b> | 0.34           | 32      | <b>170</b> | 0.15           | 14      |

\*Prepared under microwave conditions \*\*As the hydrochloride salt

Figure 10.5

2-Aryl imidazolidinones were formed accordingly: A toluene solution of L-Phenylalanine *N*-methylamide **62** (0.6 M), the appropriate carbonyl compound (0.9 eq.), and ytterbium(III) trifluoromethanesulfonate (0.05 eq.) were refluxed in toluene for 16–69 h. Diethyl ether (2 vol.) was added and the solution washed with 4 M potassium carbonate (0.3 vol.), water (0.3 vol.), and brine (0.3 vol.), then evaporated and the desired products obtained by column chromatography (Figure 10.5).

#### 10.5 Standard Preparation B: MacMillan imidazolidinones

| Solvent                    |            | R <sub>f</sub> | % Yield |            | R <sub>f</sub> | % Yield |
|----------------------------|------------|----------------|---------|------------|----------------|---------|
| ethyl acetate              | <b>7</b>   | 0.32           | 96      | -          | -              | -       |
| 3:1 ethyl acetate:petrol   | <b>2</b>   | 0.22           | 22      | <b>151</b> | 0.36           | 46      |
| ethyl acetate              | <b>136</b> | 0.22           | 32      | <b>152</b> | 0.46           | 58*     |
| ethyl acetate              | <b>137</b> | 0.15           | 26      | <b>153</b> | 0.35           | 36*     |
| ethyl acetate              | <b>138</b> | 0.14           | 26      | <b>247</b> | 0.46           | -       |
| ethyl acetate              | <b>139</b> | 0.16           | 77      | n.d        | -              | -       |
| 4:1 ethyl acetate:methanol | <b>140</b> | 0.3            | 55      | -          | -              | -       |

\*Not using final reaction conditions

Figure 10.6

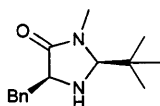
MacMillan imidazolidinones were formed accordingly: A chloroform solution of the amino amide (0.6 M), the appropriate aldehyde or acetone (2 eq.), and ytterbium(III) trifluoromethanesulfonate (0.01 eq.) was refluxed for 16 hours, after which the solvent was evaporated and the products isolated *via* column chromatography (Figure 10.6).

## 10.6 Standard Preparation C: hydrochloride salts

Hydrochloride salts were formed as follows: a solution of the amine in diethyl ether was treated with hydrogen chloride gas for 10 minutes before the precipitate was filtered, washed with diethyl ether and petroleum ether, then dried *in vacuo*.

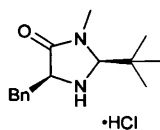
## 10.7 Compounds

### (2S,5S)-5-Benzyl-2-*tert*-butyl-3-methylimidazolidin-4-one 2



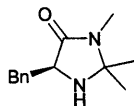
Prepared according to Standard Preparation B.  $\nu_{\max}$  (NaCl disk)/ $\text{cm}^{-1}$  3354, 2975, 1676, 1392, 1340, 1106;  $^1\text{H}$  NMR (500 MHz,  $\text{CDCl}_3$ )  $\delta_{\text{H}}$  7.24–7.14 (5H, m, ArH), 3.99 (1H, s,  $\text{CH}_3\text{NCH}$ ), 3.64 (1H, dd,  $J = 7.3$  Hz, 3.9 Hz,  $\text{COCH}$ ), 3.08 (1H, dd,  $J = 13.7$  Hz, 3.9 Hz,  $\text{CH}_2$ ), 2.87 (1H, dd,  $J = 13.7$  Hz, 7.3 Hz,  $\text{CH}_2$ ), 2.85 (3H, s,  $\text{NCH}_3$ ), 0.76 (9H, s,  $\text{CCH}_3$ );  $^{13}\text{C}$  NMR (125 MHz,  $\text{CDCl}_3$ )  $\delta_{\text{C}}$  175.3 (C), 137.9 (C), 129.6 (CH), 128.6 (CH), 126.6 (CH), 82.5 (CH), 59.4 (CH), 38.3 ( $\text{CH}_2$ ), 35.0 (C), 30.7 ( $\text{CH}_3$ ), 25.3 ( $\text{CH}_3$ ); LRMS  $m/z$  ( $\text{ES}^+$ )  $[\text{M}+\text{H}]^+ = 247.2$ ; HRMS  $m/z$  ( $\text{ES}^+$ )  $[\text{M}+\text{H}]^+ = 247.1803$ ; HRMS  $m/z$  calc.  $[\text{M}+\text{H}]^+ = 247.1810$ ; Mpt. 78–80 °C;  $[\alpha]_{\text{D}}^{30} -48.6$  (c 0.1,  $\text{CH}_3\text{OH}$ ).<sup>13</sup>

### (2S,5S)-5-Benzyl-2-*tert*-butyl-3-methylimidazolidin-4-one hydrochloride 2·HCl



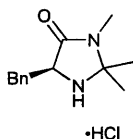
Prepared according to Standard Preparation C.  $\nu_{\max}$  (NaCl disk)/ $\text{cm}^{-1}$  3423, 1723, 1478, 1412, 1261, 1083; LRMS  $m/z$  ( $\text{AP}^+$ )  $[\text{M}-\text{Cl}]^+ = 247.2$ ; HRMS  $m/z$  ( $\text{ES}^+$ )  $[\text{M}-\text{Cl}]^+ = 247.1801$ ; HRMS  $m/z$  calc.  $[\text{M}-\text{Cl}]^+ = 247.1810$ ; Mpt. 124–126 °C;  $[\alpha]_{\text{D}}^{34} -23.0$  (c 0.1,  $\text{CH}_3\text{OH}$ ).

**(S)-5-Benzyl-2,2,3-trimethylimidazolidin-4-one 7**



L-Phenylalanine *N*-methylamide **62** (0.467 g, 2.62 mmol), acetone (1.92 mL, 1.52 g, 26.1 mmol) and ytterbium(III) trifluoromethanesulfonate (0.016 g, 0.026 mmol) were refluxed in chloroform (26 mL) for 16 hours, poured into diethyl ether (50 mL), washed with potassium carbonate (4 M, 25 mL), water (25 mL), and brine (25 mL), then evaporated to yield the desired product, a clear oil (0.503 g, 2.31 mmol, 88%).  $\nu_{\max}$  (NaCl disk)/cm<sup>-1</sup> 3318, 2975, 1682, 1428, 1400, 1148, 1090, 748, 702; <sup>1</sup>H NMR (500 MHz, CDCl<sub>3</sub>)  $\delta_{\text{H}}$  7.29 (2H, t,  $J$  = 7.2 Hz, ArH), 7.23–7.20 (3H, m, ArH), 3.79 (1H, dd,  $J$  = 6.8 Hz, 4.5 Hz, COCH), 3.14 (1H, dd,  $J$  = 14.2 Hz, 4.5 Hz, CH<sub>2</sub>), 3.00 (1H, dd,  $J$  = 14.2 Hz, 6.8 Hz, CH<sub>2</sub>), 2.74 (1H, s, NCH<sub>3</sub>), 1.25 (3H, s, CCH<sub>3</sub>), 1.15 (3H, s, CCH<sub>3</sub>); <sup>13</sup>C NMR (125 MHz, CDCl<sub>3</sub>)  $\delta_{\text{C}}$  173.4 (C), 137.2 (C), 129.5 (CH), 128.6 (CH), 126.8 (CH), 75.6 (C), 59.3 (CH), 37.2 (CH<sub>2</sub>), 27.2 (CH<sub>3</sub>), 25.3 (CH<sub>3</sub>), 25.2 (CH<sub>3</sub>); LRMS  $m/z$  (ES<sup>+</sup>) [M+H]<sup>+</sup> = 219.1; HRMS  $m/z$  (ES<sup>+</sup>) [M+H]<sup>+</sup> = 219.1492; HRMS  $m/z$  calc. [M+H]<sup>+</sup> = 219.1497; [ $\alpha$ ]<sub>D</sub><sup>30</sup> –57.8 (c 0.1, CH<sub>3</sub>OH).<sup>2</sup>

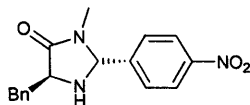
**(S)-5-Benzyl-2,2,3-trimethylimidazolidin-4-one hydrochloride 7·HCl**



Prepared according to Standard Preparation C.  $\nu_{\max}$  (NaCl disk)/cm<sup>-1</sup> 3403, 1711, 1455, 1428, 1396, 1273, 1159, 1061; <sup>1</sup>H NMR (500 MHz, CD<sub>3</sub>OD)  $\delta_{\text{H}}$  7.34 (2H, d,  $J$  = 7.2 Hz, *o*-ArH), 7.30 (2H, t,  $J$  = 7.8 Hz, *m*-ArH), 7.22 (1H, t,  $J$  = 7.3 Hz, *p*-ArH), 4.57 (1H, dd,  $J$  = 10.7 Hz, 3.5 Hz, COCH), 3.43 (1H, dd,  $J$  = 15.2 Hz, 3.5 Hz, CH<sub>2</sub>), 2.99 (1H, dd,  $J$  = 15.2 Hz, 10.7 Hz, CH<sub>2</sub>), 2.82 (3H, s, NCH<sub>3</sub>), 1.65 (3H, s, CCH<sub>3</sub>), 1.50 (3H, s, CCH<sub>3</sub>); <sup>13</sup>C NMR (125 MHz, CD<sub>3</sub>OD)  $\delta_{\text{C}}$  167.7 (C), 136.6 (C), 130.3 (CH), 130.2 (CH), 128.8 (CH), 79.1 (C), 59.8 (CH), 35.0 (CH<sub>2</sub>), 25.7 (CH<sub>3</sub>), 24.3 (CH<sub>3</sub>), 22.2 (CH<sub>3</sub>); LRMS  $m/z$  (ES<sup>+</sup>) [M+H]<sup>+</sup> = 219.1; Mpt. 133–134 °C; [ $\alpha$ ]<sub>D</sub><sup>30</sup> –60.6 (c 0.1, CH<sub>3</sub>OH).<sup>2</sup>

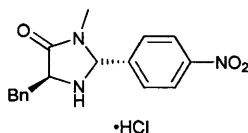


**(2*R*,5*S*)-5-Benzyl-3-methyl-2-(4-nitrophenyl)imidazolidin-4-one 33**



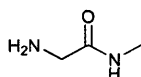
Prepared according to Standard Preparation A.  $\nu_{\max}$  (NaCl disk)/ $\text{cm}^{-1}$  1699, 1522, 1349;  $^1\text{H}$  NMR (500 MHz,  $\text{CDCl}_3$ )  $\delta_{\text{H}}$  8.15 (2H, td,  $J = 6.9$  Hz, 1.8 Hz, ArH), 7.26–7.17 (7H, m, ArH), 4.88 (1H, s,  $\text{NCH}_3$ ), 4.98–5.00 (1H, m, COCH), 3.06 (1H, dd,  $J = 13.8$  Hz, 4.2 Hz,  $\text{CH}_2$ ), 2.94 (1H, dd,  $J = 13.8$  Hz, 6.9 Hz,  $\text{CH}_2$ ), 2.52 (3H, s,  $\text{NCH}_3$ );  $^{13}\text{C}$  NMR (125 MHz,  $\text{CDCl}_3$ )  $\delta_{\text{C}}$  174.0 (C), 148.5 (C), 146.5 (C), 137.0 (C), 129.6 (CH), 128.6 (CH), 127.8 (CH), 127.0 (CH), 124.3 (CH), 76.6 (CH), 59.7 (CH), 38.6 ( $\text{CH}_2$ ), 28.3 ( $\text{CH}_3$ ); LRMS  $m/z$  ( $\text{EI}^+$ )  $[\text{M}]^+ = 311.0$ ; HRMS  $m/z$  ( $\text{EI}^+$ )  $[\text{M}]^+ = 311.1260$ ; HRMS  $m/z$  calc.  $[\text{M}]^+ = 311.1270$ ;  $[\alpha]_{\text{D}}^{32} 21.8$  (c 0.1,  $\text{CH}_2\text{Cl}_2$ ).<sup>30</sup>

**(2*S*,5*S*)-5-Benzyl-3-methyl-2-(4-nitrophenyl)imidazolidin-4-one hydrochloride 33·HCl**



Prepared according to Standard Preparation C (85%).  $\nu_{\max}$  (NaCl disk)/ $\text{cm}^{-1}$  1739, 1555, 1514, 1349;  $^1\text{H}$  NMR (500 MHz,  $\text{CD}_3\text{OD}$ )  $\delta_{\text{H}}$  8.40 (2H, dt,  $J = 8.8$  Hz, 2.5 Hz,  $o\text{-NO}_2\text{ArH}$ ), 7.79 (2H, dt,  $J = 8.8$  Hz, 2.5 Hz,  $m\text{-NO}_2\text{ArH}$ ), 7.45 (2H, d,  $J = 7.2$  Hz,  $o\text{-CH}_2\text{ArH}$ ), 7.40 (2H, t,  $J = 7.8$  Hz,  $m\text{-CH}_2\text{ArH}$ ), 7.33 (1H, tt,  $J = 7.3$  Hz, 2.13 Hz,  $p\text{-CH}_2\text{ArH}$ ), 6.10 (1H, s, ArCH), 4.72 (1H, dd,  $J = 10.3$  Hz, 3.6 Hz, COCH), 3.59 (1H, dd,  $J = 15.1$  Hz, 3.6 Hz,  $\text{CH}_2$ ), 3.21 (1H, dd,  $J = 15.1$  Hz, 10.3 Hz,  $\text{CH}_2$ ), 2.88 (3H, s,  $\text{CH}_3$ );  $^{13}\text{C}$  NMR (125 MHz,  $\text{CD}_3\text{OD}$ )  $\delta_{\text{C}}$  170.0 (C), 149.2 (C), 137.0 (C), 131.1 (CH), 129.6 (CH), 128.9 (CH), 127.2 (CH), 124.2 (CH), 73.3 (CH), 59.2 (CH), 35.0 ( $\text{CH}_2$ ), 28.3 ( $\text{CH}_3$ ); LRMS  $m/z$  ( $\text{ES}^+$ )  $[\text{M}-\text{Cl}]^+ = 312.1$ ; HRMS  $m/z$  ( $\text{ES}^+$ )  $[\text{M}-\text{Cl}]^+ = 312.1345$ ; HRMS  $m/z$  calc.  $[\text{M}-\text{Cl}]^+ = 312.1348$ ; decomp. 132–135 °C;  $[\alpha]_{\text{D}}^{34} 2.2$  (c 0.1,  $\text{CH}_3\text{OH}$ ).<sup>30</sup>

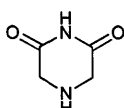
**Glycine *N*-methylamide 42**



Glycine ethyl ester hydrochloride (5.23 g, 37.5 mmol) was stirred in a 33% w/w ethanolic solution of methylamine (25 mL, 6.24 g, 201 mmol) at 50 °C for 30 minutes before sodium hydroxide (1.61 g, 40.4 mmol) was added and stirring continued for 3 minutes. The mixture was evaporated to give a slurry then extracted with ethyl acetate (2 x 50 mL), which was filtered and removed *in vacuo* to yield the desired product, a clear oil (2.56 g, 29.1 mmol,

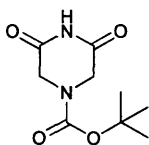
77%).  $\nu_{\max}$  (NaCl disk)/ $\text{cm}^{-1}$  3353, 3101, 2947, 1659, 1564, 1414, 1312, 1161;  $^1\text{H}$  NMR (500 MHz,  $\text{DMSO-d}_6$ )  $\delta_{\text{H}}$  7.79 (1H, bs, CONH), 3.06 (2H, s,  $\text{CH}_2$ ), 2.61 (3H, d,  $J = 4.7$  Hz,  $\text{CH}_3$ ), 1.89 (2H, s,  $\text{NH}_2$ );  $^{13}\text{C}$  NMR (125 MHz,  $\text{DMSO-d}_6$ )  $\delta_{\text{C}}$  173.6 (C), 45.3 ( $\text{CH}_2$ ), 25.7 ( $\text{CH}_3$ ); LRMS  $m/z$  ( $\text{EI}^+$ )  $[\text{M}]^+ = 88.1$ ; HRMS  $m/z$  ( $\text{EI}^+$ )  $[\text{M}]^+ = 88.0634$ ; HRMS  $m/z$  calc.  $[\text{M}]^+ = 88.0637$ .<sup>69</sup>

#### Piperazine-2,6-dione 46



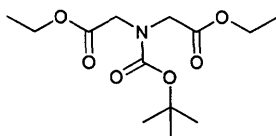
Glycine methyl ester hydrochloride (10.0 g, 79.1 mmol), 2-bromoacetamide (11.0 g, 79.7 mmol) and potassium bicarbonate (20.0 g, 200 mmol) were refluxed in acetonitrile (600 mL) for 23 hours then stirred at room temperature for 42 hours. The solution was evaporated and the residue dissolved in methanol (100 mL). Diethyl ether (100 mL) was then added and the precipitate filtered and washed with diethyl ether (100 mL) then dried to yield the desired product, a white solid (2.0 g, 18 mmol, 23%).  $\nu_{\max}$  (NaCl disk)/ $\text{cm}^{-1}$  3434, 1644;  $^1\text{H}$  NMR (400 MHz,  $\text{DMSO-d}_6$ )  $\delta_{\text{H}}$  10.85 (1H, bs, CONH), 3.37 (4H, d,  $J = 7.0$  Hz,  $\text{CH}_2$ ), 3.08 (1H, t,  $J = 8.4$  Hz,  $\text{CH}_2\text{NH}$ );  $^{13}\text{C}$  NMR (62.5 MHz,  $\text{DMSO-d}_6$ )  $\delta_{\text{C}}$  173.3 (C), 48.4 ( $\text{CH}_2$ ); LRMS  $m/z$  ( $\text{EI}^+$ )  $[\text{M}]^+ = 114.0$ ; HRMS  $m/z$  ( $\text{EI}^+$ )  $[\text{M}]^+ = 114.0424$ ; HRMS  $m/z$  calc.  $[\text{M}]^+ = 114.0429$ ; decomp. 158 °C.

#### tert-Butyl 3,5-dioxopiperazine-1-carboxylate 50



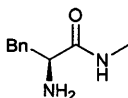
Piperazine-2,6-dione **46** (1.04 g, 9.11 mmol) and di-*tert*-butyl dicarbonate (1.97 g, 9.02 mmol) were stirred for 17 hours in DMF (15 mL). Water (25 mL) was then added and the mixture extracted with diethyl ether (2 x 50 mL). The combined diethyl ether was then washed with water (4 x 50 mL) and brine (50 mL) then evaporated to yield the desired product, a white solid (1.05 g, 4.90 mmol, 54%).  $\nu_{\max}$  (NaCl disk)/ $\text{cm}^{-1}$  3429, 2981, 1736, 1700;  $^1\text{H}$  NMR (500 MHz,  $\text{CDCl}_3$ )  $\delta_{\text{H}}$  9.05 (1H, bs, NH), 4.24 (4H, s,  $\text{CH}_2$ ), 1.41 (9H, s,  $\text{CH}_3$ );  $^{13}\text{C}$  NMR (125 MHz,  $\text{CDCl}_3$ )  $\delta_{\text{C}}$  168.7 (C), 153.1 (C), 82.4 (C), 46.5 ( $\text{CH}_2$ ), 28.2 ( $\text{CH}_3$ ); LRMS  $m/z$  ( $\text{EI}^+$ )  $[\text{M}]^+ = 214.1$ ; HRMS  $m/z$  ( $\text{EI}^+$ )  $[\text{M}]^+ = 214.0950$ ; HRMS  $m/z$  calc.  $[\text{M}]^+ = 214.0954$ ; Mpt. 124–126 °C.

### Diethyl 2,2'-(*tert*-butoxycarbonylazanediy)diacetate 56



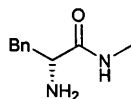
Diethyliminodiacetate (3.0 g, 16 mmol) and di-*tert*-butyl dicarbonate (3.2 g, 15 mmol) were stirred in THF (10 mL) for 26 hours then evaporated to give a residue, which was dissolved in ethyl acetate (40 mL) and washed with citric acid (1 M, 2 x 30 mL) and brine (30 mL) then evaporated to yield the desired product, a clear oil (4.4 g, 15 mmol, 100%).  $\nu_{\max}$  (NaCl disk)/ $\text{cm}^{-1}$  3433, 2980, 1750, 1706, 1646, 1191;  $^1\text{H}$  NMR (500 MHz,  $\text{CDCl}_3$ )  $\delta_{\text{H}}$  4.12 (4H, m,  $\text{CH}_3\text{CH}_2$ ), 4.04 (2H, s,  $\text{NCH}_2$ ), 3.93 (2H, s,  $\text{NCH}_2$ ), 1.37 (9H, s,  $\text{CCH}_3$ ), 1.21 (6H, q,  $J = 7.3$  Hz,  $\text{CH}_2\text{CH}_3$ );  $^{13}\text{C}$  NMR (125 MHz,  $\text{CDCl}_3$ )  $\delta_{\text{C}}$  169.7 (C), 169.6 (C), 155.0 (C), 80.8 (C), 61.0 ( $\text{CH}_2$ ), 60.9 ( $\text{CH}_2$ ), 49.6 ( $\text{CH}_2$ ), 49.0 ( $\text{CH}_2$ ), 28.0 ( $\text{CH}_3$ ), 14.1 ( $\text{CH}_3$ ), 14.0 ( $\text{CH}_3$ ); LRMS  $m/z$  ( $\text{ES}^+$ )  $[\text{M}+\text{H}]^+ = 290.2$ ; HRMS  $m/z$  ( $\text{ES}^+$ )  $[\text{M}+\text{NH}_4]^+ = 307.1860$ ; HRMS  $m/z$  calc.  $[\text{M}+\text{NH}_4]^+ = 307.1869$ .

### L-Phenylalanine *N*-methylamide 62



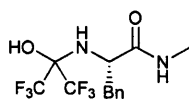
L-Phenylalanine ethyl ester hydrochloride (100.80 g, 439 mmol) was stirred in a 33% w/w ethanolic solution of methylamine (300 mL, 74.8 g, 2.41 mol) for 95h. The solution was evaporated and the residue dissolved in sodium hydrogen carbonate solution (saturated, 200 mL) then extracted with chloroform (4 x 100 mL). The combined extracts were dried over sodium carbonate and evaporated to give the crude product, a white solid (52.41 g, 294 mmol, 67%). This was recrystallised from ethyl acetate:hexanes (1:2, 600 mL) and dried *in vacuo* to give the pure product as white crystals (42.67 g, 240 mmol, 55%).  $\nu_{\max}$  (NaCl disk)/ $\text{cm}^{-1}$  3358, 1651, 1573, 1496, 1454, 1412;  $^1\text{H}$  NMR (500 MHz,  $\text{CDCl}_3$ )  $\delta_{\text{H}}$  7.34–7.22 (5H, m,  $\text{ArH}$ ), 3.61 (1H, dd,  $J = 9.5$  Hz, 4.0 Hz,  $\text{COCH}$ ), 3.29 (1H, dd,  $J = 13.7$  Hz, 4.0 Hz,  $\text{CH}_2$ ), 2.82 (3H, d,  $J = 5.0$  Hz,  $\text{NCH}_3$ ), 2.68 (1H, dd,  $J = 13.7$  Hz, 9.5 Hz,  $\text{CH}_2$ ), 1.44 (2H, s,  $\text{NH}_2$ );  $^{13}\text{C}$  NMR (125 MHz,  $\text{CDCl}_3$ )  $\delta_{\text{C}}$  174.8 (C), 138.0 (C), 129.3 (CH), 128.7 (CH), 126.8 (CH), 56.5 (CH), 41.1 ( $\text{CH}_2$ ), 25.8 ( $\text{CH}_3$ ); LRMS  $m/z$  ( $\text{ES}^+$ )  $[\text{M}+\text{H}]^+ = 179.1$ ; HRMS  $m/z$  ( $\text{ES}^+$ )  $[\text{M}+\text{H}]^+ = 179.1181$ ; HRMS  $m/z$  calc.  $[\text{M}+\text{H}]^+ = 179.1184$ ; Mpt. 58–60 °C;  $[\alpha]_{\text{D}}^{25} 72.6$  (c 0.1,  $\text{CH}_2\text{Cl}_2$ ).

### D-Phenylalanine *N*-methylamide (*R*)-**62**



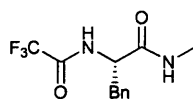
Prepared as **62**, from D-phenylalanine ethyl ester hydrochloride.  $[\alpha]_D^{32}$  82.8 (*c* 0.1, CH<sub>2</sub>Cl<sub>2</sub>).

### (*S*)-2-(1,1,1,3,3,3-Hexafluoro-2-hydroxypropan-2-ylamino)-*N*-methyl-3-phenylpropanamide **64**



Anhydrous hexafluoroacetone (ca. 57 mmol) was bubbled through a solution of phenylalanine *N*-methylamide **62** (3.0 g, 17 mmol) in DCM (25 mL) held at  $-78\text{ }^{\circ}\text{C}$  for 90 minutes. The solution was allowed to warm to room temperature and was evaporated to yield the desired product, a white solid (5.4 g, 16 mmol, 93 %).  $\nu_{\text{max}}$  (NaCl disk)/ $\text{cm}^{-1}$  3412, 1651, 1551, 1308, 1220, 957;  $^1\text{H}$  NMR (500 MHz, CDCl<sub>3</sub>)  $\delta_{\text{H}}$  7.38–7.28 (4H, m, ArH, CF<sub>3</sub>CNH), 7.20 (2H, d, *J* = 6.9 Hz, ArH), 6.83 (1H, d, *J* = 4.8 Hz, CH<sub>3</sub>NH), 6.32 (1H, s, OH), 4.04 (1H, dd, *J* = 11.7 Hz, 5.5 Hz, COCH), 3.14 (1H, dd, *J* = 13.8 Hz, 5.5 Hz, CH<sub>2</sub>), 3.04 (1H, dd, *J* = 13.8 Hz, 7.03 Hz, CH<sub>2</sub>), 2.79 (3H, d, *J* = 4.8 Hz, CH<sub>3</sub>);  $^{13}\text{C}$  NMR (125 MHz, CDCl<sub>3</sub>)  $\delta_{\text{C}}$  175.2 (C), 135.7 (C), 129.3 (CH), 129.0 (CH), 127.6 (CH), 122.1 (CF<sub>3</sub>, *J* = 289 Hz), 121.9 (CF<sub>3</sub>, *J* = 286 Hz), 83.4 (C, *J* = 30 Hz), 55.6 (CH), 39.3 (CH<sub>2</sub>), 26.2 (CH<sub>3</sub>); LRMS *m/z* (EI<sup>+</sup>) [*M*–H<sub>2</sub>O]<sup>+</sup> = 326.1; Mpt. 71–74  $^{\circ}\text{C}$ ;  $[\alpha]_D^{30}$  –28.8 (*c* 0.1, CH<sub>2</sub>Cl<sub>2</sub>).

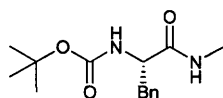
### (*S*)-*N*-Methyl-3-phenyl-2-(2,2,2-trifluoroacetamido)propanamide **65**



L-Phenylalanine *N*-methylamide **62** (0.51 g, 2.9 mmol), TFAA (0.55 mL, 0.83 g, 4.0 mmol) and potassium bicarbonate (0.65 g, 6.5 mmol) were stirred in acetonitrile (8 mL) for 32 hours and then evaporated to give a sludge, which was taken up in aqueous potassium carbonate (saturated) and extracted with ethyl acetate (15 mL). The ethyl acetate was washed with hydrochloric acid (2 M, 15 mL) and brine (15 mL) then evaporated to give a yellow solid which was washed with 1:1 diethyl ether:petroleum ether (3 x 10 mL) and 3:1 diethyl ether:petroleum ether (3 x 10 mL) to yield the desired product, a white solid (0.34 g, 1.2 mmol, 46%).  $\nu_{\text{max}}$  (NaCl disk)/ $\text{cm}^{-1}$  3312, 2358, 1701, 1655, 1554, 1182;  $^1\text{H}$  NMR (500 MHz,

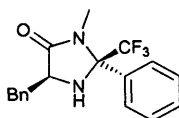
DMSO- $d_6$ )  $\delta_H$  9.69 (1H, d,  $J$  = 8.5 Hz,  $CF_3CONH$ ), 8.20 (1H, d,  $J$  = 4.4 Hz,  $CH_3NH$ ), 7.29–7.24 (4H, m, ArH), 7.18–7.22 (1H, m, ArH), 4.47–5.53 (1H, m,  $COCH$ ), 3.08 (1H, dd,  $J$  = 13.6 Hz, 4.25 Hz,  $CH_2$ ), 2.91 (1H, dd,  $J$  = 13.6 Hz, 10.9 Hz,  $CH_2$ ), 2.62 (3H, d,  $J$  = 4.4 Hz,  $NCH_3$ );  $^{13}C$  NMR (125 MHz, DMSO- $d_6$ )  $\delta_C$  170.3 (C), 156.6 (C,  $J$  = 38 Hz), 138.0 (C), 129.5 (CH), 128.6 (CH), 126.9 (CH), 116.2 ( $CF_3$ ,  $J$  = 286 Hz), 55.3 (CH), 37.3 ( $CH_2$ ), 26.1 ( $CH_3$ ); LRMS  $m/z$  ( $AP^+$ )  $[M+H]^+$  = 275.1; HRMS  $m/z$  ( $ES^+$ )  $[M+NH_4]^+$  = 292.1270; HRMS  $m/z$  calc.  $[M+NH_4]^+$  = 292.1273; Mpt. 158–160 °C;  $[\alpha]_D^{34}$  24.6 (c 0.1,  $CH_3OH$ ).

**(S)-tert-Butyl 1-(methylamino)-1-oxo-3-phenylpropan-2-ylcarbamate 75**

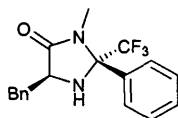


L-Phenylalanine *N*-methylamide **62** (1.34g, 17.5 mmol) and di-*tert*-butyl dicarbonate (1.54g, 7.05 mmol) were stirred in DCM (15 mL) for 24 hours then poured into ethyl acetate (30 mL) and washed with hydrochloric acid (3 x 40 mL) and brine (40 mL) then evaporated to yield the desired product, a pure white solid (1.70 g, 6.12 mmol, 81%).  $\nu_{max}$  (NaCl disk)/ $cm^{-1}$  3340, 1686, 1657, 1523, 1169;  $^1H$  NMR (500 MHz,  $CDCl_3$ )  $\delta_H$  7.24–7.12 (5H, m, ArH), 5.77 (1H, bs,  $CH_3NH$ ), 5.02 (1H, bs,  $OCONH$ ), 4.20–4.26 (1H, m,  $COCH$ ), 2.98 (2H, m,  $CH_2$ ), 2.65 (3H, d,  $J$  = 6.4 Hz,  $CH_3$ ), 1.33 (9H, s,  $CCH_3$ );  $^{13}C$  NMR (125 MHz,  $CDCl_3$ )  $\delta_C$  136.9 (C), 129.3 (CH), 128.6 (CH), 126.9 (CH), 56.1 (CH), 38.8 ( $CH_2$ ), 28.3 ( $CH_3$ ), 26.1 ( $CH_3$ ); LRMS  $m/z$  ( $El^+$ )  $[M]^+$  = 270.0; HRMS  $m/z$  ( $ES^+$ )  $[M+H]^+$  = 279.1706; HRMS  $m/z$  calc.  $[M+H]^+$  = 279.1709; Mpt. 122–125 °C;  $[\alpha]_D^{32}$  11.2 (c 0.1,  $CH_2Cl_2$ ).

**(2S,5S)-5-Benzyl-3-methyl-2-phenyl-2-(trifluoromethyl)imidazolidin-4-one and (2R,5S)-5-benzyl-3-methyl-2-phenyl-2-(trifluoromethyl)imidazolidin-4-one 78 and 89**



**78**

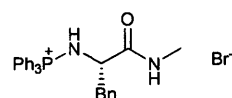


**89**

Pre-dried (*S*)-*N*-methyl-3-phenyl-2-(2,2,2-trifluoro-1-phenylethylideneamino)propanamide **84** (0.95 g, 2.85 mmol) and copper(II) trifluoromethanesulfonate (0.52 g, 1.43 mmol) were dissolved in 15 mL dry acetonitrile and subjected to microwave irradiation at 125 °C for 90 minutes (200 W initial power). The acetonitrile was evaporated and the resultant residue taken up in diethyl ether (60 mL) and washed with water (3 x 30 mL) and brine then evaporated. The resultant oil was subjected to column chromatography (3:1 petroleum ether:ethyl acetate) to give **78** ( $R_f$ : 0.45), a yellow solid (0.33 g, 0.98 mmol, 34%), and **89** ( $R_f$ :

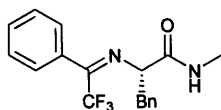
0.27), an orange solid (0.28 g, 0.83 mmol, 29%). **78**  $\nu_{\max}$  (NaCl disk)/ $\text{cm}^{-1}$  3346, 1717, 1388, 1161, 699;  $^1\text{H}$  NMR (500 MHz,  $\text{CDCl}_3$ )  $\delta_{\text{H}}$  7.29–7.19 (4H, m, ArH), 7.13–7.10 (4H, m, ArH), 6.67 (2H, d,  $J$  = 7.9 Hz, ArH), 3.97 (1H, t,  $J$  = 4.6 Hz, COCH), 3.30 (1H, dd,  $J$  = 14.2, 4.6 Hz, CH<sub>2</sub>), 2.97 (1H, dd,  $J$  = 14.2, 5.1 Hz, CH<sub>2</sub>), 2.53 (3H, s, NCH<sub>3</sub>), 2.12 (1H, bs, NH);  $^{13}\text{C}$  NMR (125 MHz,  $\text{CDCl}_3$ )  $\delta_{\text{C}}$  174.5 (C), 135.8 (C), 134.3 (C), 130.1 (CH), 129.6 (CH), 129.2 (CH), 129.0 (CH), 127.3 (CH), 126.6 (CH), 81.7 (q,  $J$  = 29 Hz,  $\text{CF}_3$ ), 59.5 (CH), 36.4 (CH<sub>2</sub>), 27.4 (CH<sub>3</sub>);  $^{19}\text{F}$  NMR (282 MHz,  $\text{CDCl}_3$ )  $\delta_{\text{F}}$  73.3(C); LRMS  $m/z$  (EI)  $[\text{M}+\text{H}]^+ = 335.1$ ; HRMS  $m/z$  (ES<sup>+</sup>)  $[\text{M}+\text{H}]^+ = 335.1360$ ; HRMS  $m/z$  calc.  $[\text{M}+\text{H}]^+ = 335.1371$ ; Mpt. 85–87 °C;  $[\alpha]_{\text{D}}^{30} -72.4$  (c 0.1,  $\text{CH}_2\text{Cl}_2$ ). **89**  $\nu_{\max}$  (NaCl disk)/ $\text{cm}^{-1}$  3393, 1712, 1389, 1163, 698;  $^1\text{H}$  NMR (500 MHz,  $\text{CDCl}_3$ )  $\delta_{\text{H}}$  7.33–7.28 (5H, m, ArH), 7.19–7.10 (5H, m, ArH), 3.92 (1H, dd,  $J$  = 10.7, 2.6 Hz, COCH), 3.16 (1H, dd,  $J$  = 13.4, 2.6 Hz, CH<sub>2</sub>), 2.75 (3H, s, NCH<sub>3</sub>), 2.69 (1H, dd,  $J$  = 13.4, 5.7 Hz, CH<sub>2</sub>), 2.19 (d,  $J$  = 8.3 Hz, NH);  $^{13}\text{C}$  NMR (125 MHz,  $\text{CDCl}_3$ )  $\delta_{\text{C}}$  173.9 (C), 138.5 (C), 135.8 (C), 129.8 (CH), 129.5 (CH), 129.4 (CH), 128.4 (CH), 126.5 (CH), 125.9 (CH), 125.4 (CH), 81.7 (q,  $J$  = 30 Hz,  $\text{CF}_3$ ), 59.5 (CH), 39.9 (CH<sub>2</sub>), 27.4 (CH<sub>3</sub>);  $^{19}\text{F}$  NMR (282 MHz,  $\text{CDCl}_3$ )  $\delta_{\text{F}}$  73.9(C); LRMS  $m/z$  (EI)  $[\text{M}+\text{H}]^+ = 335.2$ ; HRMS  $m/z$  (ES<sup>+</sup>)  $[\text{M}+\text{H}]^+ = 335.1367$ ; HRMS  $m/z$  calc.  $[\text{M}+\text{H}]^+ = 335.1371$ ; Mpt. 80–83 °C;  $[\alpha]_{\text{D}}^{30} -32.6$  (c 0.1,  $\text{CH}_2\text{Cl}_2$ ).

**(S)-(1-(Methylamino)-1-oxo-3-phenylpropan-2-ylamino)triphenylphosphonium bromide 82**



To a solution of triphenylphosphine (5.04 g, 19.2 mmol) in dry DCM (100 mL) stirred over potassium carbonate (7.86 g, 56.8 mmol) at 0 °C was added bromine (0.950 mL, 2.96 g, 18.5 mmol) in dry DCM (20 mL). The mixture was allowed to warm to room temperature over the course of an hour before L-phenylalanine *N*-methanamide **62** (3.65 g, 20.5 mmol) in dry DCM (30 mL) was added, dropwise, and the mixture refluxed for 19 hours then filtered and evaporated. The residue was purified *via* column chromatography (9:1 DCM:methanol) and recrystallised from DCM/THF to yield the desired product, a cream solid (4.28 g, 8.24 mmol, 45%).  $\nu_{\max}$  (NaCl disk)/ $\text{cm}^{-1}$  3426, 1657, 1439, 1116, 727, 691;  $^1\text{H}$  NMR (500 MHz,  $\text{CDCl}_3$ )  $\delta_{\text{H}}$  8.85–8.89 (1H, m, PNH), 7.82 (1H, t,  $J$  = 10.7 Hz, *p*-CArH), 7.72 (3H, td,  $J$  = 7.4 Hz, 1.6 Hz, *p*-PArH), 7.55–7.51 (6H, m, PArH), 7.48–7.44 (6H, m, PArH), 7.33–7.31 (2H, m, CArH), 7.26–7.24 (3H, m, CArH, CH<sub>3</sub>NH), 3.72–3.80 (1H, m, COCH), 3.60 (1H, t,  $J$  = 11.9 Hz, CH<sub>2</sub>), 3.16 (1H, dt,  $J$  = 14.0 Hz, 3.8 Hz, CH<sub>2</sub>), 2.65 (3H, d,  $J$  = 4.7 Hz, CH<sub>3</sub>);  $^{13}\text{C}$  NMR (125 MHz,  $\text{CDCl}_3$ )  $\delta_{\text{C}}$  172.6 (C), 137.6 (C), 134.8 (CH,  $J$  = 3 Hz), 133.7 (CH,  $J$  = 11 Hz), 130.2 (CH), 129.8 (CH,  $J$  = 13 Hz), 128.5 (CH), 126.8 (CH), 120.4 (C,  $J$  = 103 Hz), 61.1 (CH), 39.7 (CH<sub>2</sub>), 25.8 (CH<sub>3</sub>); LRMS  $m/z$  (ES<sup>+</sup>)  $[\text{M}-\text{Br}]^+ = 439.2$ ; HRMS  $m/z$  (ES<sup>+</sup>)  $[\text{M}-\text{Br}]^+ = 439.1929$ ; HRMS  $m/z$  calc.  $[\text{M}-\text{Br}]^+ = 439.1939$ ; Mpt. 200–201 °C;  $[\alpha]_{\text{D}}^{30} -47.6$  (c 0.1,  $\text{CH}_2\text{Cl}_2$ ).

**(S)-N-Methyl-3-phenyl-2-(2,2,2-trifluoro-1-phenylethylideneamino)propanamide 84**



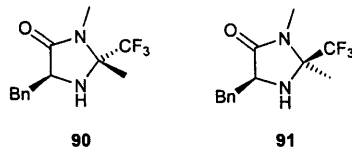
L-Phenylalanine *N*-methylamide **62** (1.12 g, 6.29 mmol), 2,2,2-trifluoroacetophenone (0.85 mL, 1.05 g, 6.05 mmol), and ytterbium(III) trifluoromethanesulfonate (0.17 g, 0.28 mmol) were refluxed in chloroform (20 mL) over 3Å molecular sieves for 16 h. The mixture was filtered and column chromatography (1:1 petroleum ether:ethyl acetate) was used to provide the desired product (*R*<sub>f</sub>: 0.47), a pale yellow solid (1.27 g, 3.81 mmol, 63%).  $\nu_{\text{max}}$  (NaCl disk)/cm<sup>-1</sup> 3362, 1667, 1538, 1199, 1134; <sup>1</sup>H NMR (500 MHz, CDCl<sub>3</sub>)  $\delta_{\text{H}}$  7.36 (1H, t, *J* = 1.4 Hz, ArH), 7.29–7.19 (5H, m, ArH), 6.99 (2H, dd, *J* = 7.3, 1.4 Hz, ArH), 6.65 (1H, bs, NH), 6.40 (2H, d, *J* = 7.3 Hz, ArH), 4.18 (1H, dd, *J* = 10.1, 2.9 Hz, COCH), 3.25 (1H, dd, *J* = 13.3, 2.9 Hz, CH<sub>2</sub>), 2.95 (1H, dd, *J* = 13.3, 10.1 Hz, CH<sub>2</sub>), 2.91 (3H, d, *J* = 4.9 Hz, NCH<sub>3</sub>); <sup>13</sup>C NMR (125 MHz, CDCl<sub>3</sub>)  $\delta_{\text{C}}$  171.2 (C), 160.2 (q, *J* = 34 Hz, CCF<sub>3</sub>), 136.5 (C), 130.0 (CH), 128.9 (CH), 128.5 (CH), 128.4 (CH), 127.2 (CH), 126.9 (CH), 119.3 (q, *J* = 228 Hz, CF<sub>3</sub>), 67.4 (CH), 41.0 (CH<sub>2</sub>), 26.1 (CH<sub>3</sub>); <sup>19</sup>F NMR (282 MHz, CDCl<sub>3</sub>)  $\delta_{\text{F}}$  71.1 (C); LRMS *m/z* (EI) [M+H]<sup>+</sup> = 335.1; HRMS *m/z* (ES<sup>+</sup>) [M+H]<sup>+</sup> = 335.1630; HRMS *m/z* calc. [M+H]<sup>+</sup> = 335.1371; Mpt. 95–97 °C; [ $\alpha$ ]<sub>D</sub><sup>30</sup> 24.6 (c 0.1, CH<sub>2</sub>Cl<sub>2</sub>).

**Gallium(III) trifluoromethanesulfonate 86**

Gallium (3.2 g, 45 mmol) and trifluoromethanesulfonic acid (30 mL, 50.9 g, 339 mmol) were heated together at 160 °C for 96 hours then cooled to room temperature and poured into water (150 mL), filtered, and the filtrate evaporated and dried *in vacuo* at 180 °C to yield the desired product, a light grey powder (15.6g, 30 mmol, 66%).

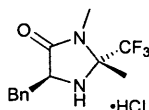
**(2*R*,5*S*)-5-Benzyl-3-methyl-2-phenyl-2-(trifluoromethyl)imidazolidin-4-one 89:** See 78.

**(2R,5S)-5-Benzyl-2,3-dimethyl-2-(trifluoromethyl)imidazolidin-4-one and (2S,5S)-5-benzyl-2,3-dimethyl-2-(trifluoromethyl)imidazolidin-4-one **90** and **91****



Pre-dried (S)-N-methyl-3-phenyl-2-(1,1,1-trifluoropropan-2-ylideneamino)propanamide **93** (8.1 g, 29.8 mmol) and copper(II) trifluoromethanesulfonate (2.59 g, 7.16 mmol) were dissolved in dry acetonitrile (40 mL) and subjected to microwave irradiation at 140 °C for 60 minutes (200 W initial power). The acetonitrile was evaporated and the resultant residue taken up in diethyl ether (60 mL) and washed with water (3 x 30 mL) and brine then evaporated. The resultant oil was subjected to column chromatography (3:1 petroleum ether:ethyl acetate) to give **90** ( $R_f$ : 0.46), a yellow solid (1.13 g, 4.16 mmol, 14%), and **91** ( $R_f$ : 0.29), an orange solid (0.88 g, 3.23 mmol, 13%). **90**  $\nu_{\max}$  (NaCl disk)/ $\text{cm}^{-1}$  3323, 2926, 1708, 1429, 1396, 1308, 1278, 1152, 1098;  $^1\text{H}$  NMR (500 MHz,  $\text{CDCl}_3$ )  $\delta_{\text{H}}$  7.24 (2H, tt,  $J = 7.5$  Hz, 1.4 Hz,  $m\text{-ArH}$ ), 7.18 (1H, tt,  $J = 7.50$  Hz, 2.6 Hz,  $p\text{-ArH}$ ), 7.10 (2H, d,  $J = 6.9$  Hz,  $o\text{-ArH}$ ), 3.84 (1H, at,  $J = 5.3$  Hz,  $\text{COCH}$ ), 3.06 (1H, dd,  $J = 14.2$  Hz, 5.3 Hz,  $\text{CH}_2$ ), 2.98 (1H, dd,  $J = 14.2$  Hz, 5.0 Hz,  $\text{CH}_2$ ), 2.76 (3H, s,  $\text{NCH}_3$ ), 1.77 (1H, bs,  $\text{NH}$ ), 1.08 (3H, s,  $\text{CCH}_3$ );  $^{13}\text{C}$  NMR (125 MHz,  $\text{CDCl}_3$ )  $\delta_{\text{C}}$  174.1 (C), 136.0 (C), 129.6 (CH), 128.8 (CH), 127.2 (CH), 125.2 (q,  $J = 289$  Hz,  $\text{CF}_3$ ), 77.2 (q,  $J = 30$  Hz,  $\text{CCF}_3$ ), 58.8 (CH), 37.2 ( $\text{CH}_2$ ), 26.3 ( $\text{CH}_3$ ), 19.0 ( $\text{CH}_3$ ); LRMS  $m/z$  ( $\text{ES}^+$ )  $[\text{M}+\text{H}]^+ = 273.1$ ; HRMS  $m/z$  ( $\text{ES}^+$ )  $[\text{M}+\text{H}]^+ = 273.1212$ ; HRMS  $m/z$  calc.  $[\text{M}+\text{H}]^+ = 273.1215$ ;  $[\alpha]_{\text{D}}^{20} -22.6$  (c 0.1,  $\text{CHCl}_3$ ). **91**  $\nu_{\max}$  (NaCl disk)/ $\text{cm}^{-1}$  3344, 2930, 1701, 1428, 1397, 1154, 1097;  $^1\text{H}$  NMR (500 MHz,  $\text{CDCl}_3$ )  $\delta_{\text{H}}$  7.23 (2H, t,  $J = 7.31$  Hz,  $m\text{-ArH}$ ), 7.19–7.14 (3H, m,  $\text{ArH}$ ), 3.77 (1H, d,  $J = 10.59$  Hz,  $\text{COCH}$ ), 3.09 (1H, dd,  $J = 13.48$  Hz, 2.91 Hz,  $\text{CH}_2$ ), 2.85 (3H, s,  $\text{NCH}_3$ ), 2.59 (1H, dd,  $J = 13.38$  Hz, 11.15 Hz,  $\text{CH}_2$ ), 1.95 (1H, bs,  $\text{NH}$ ), 1.46 (3H, s,  $\text{CCH}_3$ );  $^{13}\text{C}$  NMR (125 MHz,  $\text{CDCl}_3$ )  $\delta_{\text{C}}$  173.4 (C), 138.6 (C), 129.5 (CH), 128.5 (CH), 126.5 (CH), 124.3 (q,  $J = 287$  Hz,  $\text{CF}_3$ ), 77.1 (q,  $J = 31$  Hz,  $\text{CCF}_3$ ), 59.6 (CH), 39.6 ( $\text{CH}_2$ ), 26.5 (q,  $J = 1$  Hz,  $\text{H}_3\text{CCCF}_3$ ), 19.7 ( $\text{CH}_3$ ); LRMS  $m/z$  ( $\text{EI}^+$ )  $[\text{M}]^+ = 272.1$ ; HRMS  $m/z$  ( $\text{ES}^+$ )  $[\text{M}+\text{H}]^+ = 273.1210$ ; HRMS  $m/z$  calc.  $[\text{M}+\text{H}]^+ = 273.1215$ ; Mpt. 99–102 °C;  $[\alpha]_{\text{D}}^{20} -116.4$  (c 0.1,  $\text{CHCl}_3$ ).

**(2R,5S)-5-Benzyl-2,3-dimethyl-2-(trifluoromethyl)imidazolidin-4-one hydrochloride **90**·HCl**



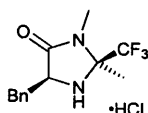
Prepared according to Standard Preparation C.  $\nu_{\max}$  (NaCl disk)/ $\text{cm}^{-1}$  3318, 2927, 1706, 1397, 1152, 1098;  $^1\text{H}$  NMR (500 MHz,  $\text{CDCl}_3$ )  $\delta_{\text{H}}$  7.33–7.23 (5H, m,  $\text{ArH}$ ), 3.94–3.98 (1H, m,  $\text{COCH}$ ), 3.14 (1H, dd,  $J = 14.50$  Hz, 4.34 Hz,  $\text{CH}_2$ ), 3.01 (1H, dd,  $J = 14.50$  Hz, 6.93 Hz,  $\text{CH}_2$ ), 2.86 (3H, s,



NCH<sub>3</sub>), 1.39 (3H, s, CCH<sub>3</sub>); <sup>13</sup>C NMR (125 MHz, CDCl<sub>3</sub>) δ<sub>c</sub> 176.6 (C), 138.7 (C), 131.6 (CH), 139.6 (CH), 129.1 (CH), 127.5 (q, *J* = 289 Hz, C<sub>2</sub>CF<sub>3</sub>), 80.1 (q, *J* = 30 Hz, C<sub>1</sub>CF<sub>3</sub>), 61.7 (CH), 39.0 (CH<sub>2</sub>), 27.8 (q, *J* = 2 Hz, H<sub>3</sub>C<sub>2</sub>CF<sub>3</sub>), 19.6 (CH<sub>3</sub>); LRMS *m/z* (AP<sup>+</sup>) [M–Cl]<sup>+</sup> = 273.1; HRMS *m/z* (ES<sup>+</sup>) [M–Cl]<sup>+</sup> = 273.1207; HRMS *m/z* calc. [M–Cl]<sup>+</sup> = 273.1215; decomp. 55 °C; [α]<sub>D</sub><sup>22</sup> 58.6 (c 0.1, CH<sub>3</sub>OH).

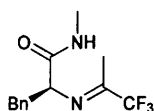
**(2S,5S)-5-Benzyl-2,3-dimethyl-2-(trifluoromethyl)imidazolidin-4-one 91:** See 90.

**(2S,5S)-5-Benzyl-2,3-dimethyl-2-(trifluoromethyl)imidazolidin-4-one hydrochloride 91·HCl**



Prepared according to Standard Preparation C. *v*<sub>max</sub> (NaCl disk)/cm<sup>−1</sup> 3328, 2926, 1700, 1398, 1154, 1136; <sup>1</sup>H NMR (500 MHz, CDCl<sub>3</sub>) δ<sub>H</sub> 7.21–7.06 (5H, m, ArH), 3.80 (1H, dd, *J* = 10.4 Hz, 2.2 Hz, COCH), 2.95 (1H, dd, *J* = 13.4 Hz, 10.7 Hz, CH<sub>2</sub>), 2.80 (3H, s, NCH<sub>3</sub>), 2.51 (1H, dd, *J* = 13.2 Hz, 10.7 Hz, CH<sub>2</sub>), 1.44 (3H, s, CCH<sub>3</sub>); <sup>13</sup>C NMR (125 MHz, CDCl<sub>3</sub>) δ<sub>c</sub> 175.0 (C), 138.7 (C), 129.1 (CH), 127.8 (CH), 125.9 (CH), 125.4 (q, *J* = 286 Hz, C<sub>2</sub>CF<sub>3</sub>), 78.1 (q, *J* = 30 Hz, C<sub>1</sub>CF<sub>3</sub>), 59.6 (CH), 39.4 (CH<sub>2</sub>), 25.3 (CH<sub>3</sub>), 17.4 (CH<sub>3</sub>); LRMS *m/z* (AP<sup>+</sup>) [M–Cl]<sup>+</sup> = 273.1; HRMS *m/z* (ES<sup>+</sup>) [M–Cl]<sup>+</sup> = 273.1208; HRMS *m/z* calc. [M–Cl]<sup>+</sup> = 273.1215; decomp. 80 °C; [α]<sub>D</sub><sup>22</sup> 83.2 (c 0.025, CH<sub>3</sub>OH).

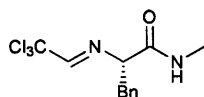
**(S)-N-Methyl-3-phenyl-2-(1,1,1-trifluoropropan-2-ylideneamino)propanamide 93**



L-Phenylalanine *N*-methylamide **62** (5.28 g, 29.6 mmol), 1,1,1-trifluoroacetone (7.26 g, 64.8 mmol) and TFA (1 drop) were stirred in chloroform (25 mL) at room temperature for 17 hours. The reaction mixture was evaporated to yield the desired product, a cream solid (8.1 g, 100%). *v*<sub>max</sub> (NaCl disk)/cm<sup>−1</sup> 3415, 3031, 2931, 1676, 1533, 1339, 1200, 1120; <sup>1</sup>H NMR (500 MHz, CDCl<sub>3</sub>) δ<sub>H</sub> 7.29–7.22 (3H, m, ArH), 7.11 (2H, d, *J* = 6.6 Hz, *o*-ArH), 6.87 (1H, bs, NH), 4.20 (1H, dd, *J* = 10.6 Hz, 2.7 Hz, COCH), 3.46 (1H, dd, *J* = 13.2 Hz, 2.7 Hz, CH<sub>2</sub>), 2.88 (3H, d, *J* = 5.0 Hz, NCH<sub>3</sub>), 2.80 (1H, dd, *J* = 13.2 Hz, 10.6 Hz, CH<sub>2</sub>), 1.19 (3H, s, CCH<sub>3</sub>); <sup>13</sup>C NMR (100 MHz, CDCl<sub>3</sub>) δ<sub>c</sub> 171.4 (C), 157.9 (q, *J* = 33 Hz, C<sub>2</sub>CF<sub>3</sub>), 136.7 (C), 129.9 (CH), 128.6 (CH), 127.0 (CH), 119.3 (q, *J* = 279 Hz, C<sub>1</sub>CF<sub>3</sub>), 66.2 (CH), 40.4 (CH<sub>2</sub>), 26.0 (CH<sub>3</sub>), 12.4 (CH<sub>3</sub>); LRMS *m/z* (AP<sup>+</sup>) [M+H]<sup>+</sup>

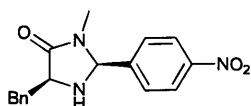
= 273.2; HRMS  $m/z$  ( $ES^+$ )  $[M+H]^+ = 273.1210$ ; HRMS  $m/z$  calc.  $[M+H]^+ = 273.1215$ ; Mpt. 93–95 °C;  $[\alpha]_D^{20}$  42.0 ( $c$  0.1,  $CHCl_3$ ).

**(*S,E*)-*N*-Methyl-3-phenyl-2-(2,2,2-trichloroethylideneamino)propanamide 98**



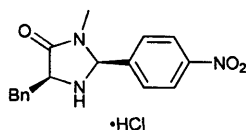
L-Phenylalanine *N*-methylamide **62** (1.15 g, 6.47 mmol), anhydrous chloral (0.720 mL, 1.09 g, 7.42 mmol) and *p*-toluenesulfonic acid monohydrate (0.12 g, 0.61 mmol) were stirred in DCM (10 mL) for 66 hours then poured into diethyl ether (20 mL) and washed with potassium carbonate (2 M, 40 mL) and brine (40 mL) then evaporated to give an oil, which was purified *via* column chromatography (diethyl ether) to yield the desired product ( $R_f$ : 0.44), an orange oil (0.71 g, 2.31 mmol, 36%).  $\nu_{max}$  (NaCl disk)/ $cm^{-1}$  3408, 1668, 1538, 809, 739, 701;  $^1H$  NMR (500 MHz,  $CDCl_3$ )  $\delta_H$  7.26 (2H, t,  $J = 7.4$  Hz, *m*-ArH), 7.19 (1H, t,  $J = 7.4$  Hz, *p*-ArH), 7.08 (2H, d,  $J = 7.0$  Hz, *o*-ArH), 6.99 (1H, s,  $Cl_3CCH$ ), 6.80 (1H, d,  $J = 4.5$  Hz, NH), 4.01 (1H, dd,  $J = 10.5$  Hz, 3.1 Hz, COCH), 3.45 (1H, dd,  $J = 13.6$  Hz, 3.1 Hz,  $CH_2$ ), 2.86 (3H, d,  $J = 4.5$  Hz,  $CH_3$ ), 2.84 (1H, dd,  $J = 13.6$  Hz, 4.3 Hz,  $CH_2$ );  $^{13}C$  NMR (125 MHz,  $CDCl_3$ )  $\delta_C$  171.1 (C), 157.7 (C), 136.1 (C), 130.0 (CH), 128.7 (CH), 127.0 (CH), 93.0 (C), 71.7 (CH), 40.5 ( $CH_2$ ), 26.1 ( $CH_3$ ); LRMS  $m/z$  ( $El^+$ )  $[M]^+ = 306.0$ ; HRMS  $m/z$  ( $El^+$ )  $[M]^+ = 306.0088$ ; HRMS  $m/z$  calc.  $[M]^+ = 306.0093$ ;  $[\alpha]_D^{34}$  -1.6 ( $c$  0.1,  $CH_2Cl_2$ ).

**(2*S*,5*S*)-5-Benzyl-3-methyl-2-(4-nitrophenyl)imidazolidin-4-one 104**



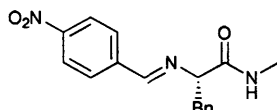
Prepared according to Standard Preparation A.  $\nu_{max}$  (NaCl disk)/ $cm^{-1}$  1698, 1523, 1349;  $^1H$  NMR (500 MHz,  $CDCl_3$ )  $\delta_H$  8.02 (2H, td,  $J = 6.83$  Hz, 1.92 Hz, ArH), 7.26–7.23 (3H, m, ArH), 7.15 (2H, m, ArH), 6.90 (2H, td,  $J = 6.8$  Hz, 1.9 Hz, ArH), 5.19 (1H, d,  $J = 1.4$  Hz,  $NCH_3CH$ ), 3.86–3.89 (1H, m, COCH), 3.19 (1H, dd,  $J = 14.0$  Hz, 5.5 Hz,  $CH_2$ ), 3.03 (1H, dd,  $J = 14.0$  Hz, 4.6 Hz,  $CH_2$ ), 2.48 (3H, s,  $NCH_3$ );  $^{13}C$  NMR (125 MHz,  $CDCl_3$ )  $\delta_C$  173.9 (C), 148.6 (C), 145.9 (C), 136.7 (C), 130.0 (CH), 128.9 (CH), 128.3 (CH), 127.1 (CH), 124.2 (CH), 76.4 (CH), 60.1 (CH), 37.2 ( $CH_2$ ), 27.4 ( $CH_3$ ); LRMS  $m/z$  ( $El^+$ )  $[M]^+ = 311.0$ ; HRMS  $m/z$  ( $El^+$ )  $[M]^+ = 311.1262$ ; HRMS  $m/z$  calc.  $[M]^+ = 311.1270$ ;  $[\alpha]_D^{32}$  -78.2 ( $c$  0.1,  $CH_2Cl_2$ ).

**(2*R*,5*S*)-5-Benzyl-3-methyl-2-(4-nitrophenyl)imidazolidin-4-one hydrochloride 104·HCl**



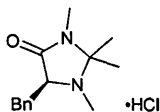
Prepared according to Standard Preparation C (85%).  $\nu_{\max}$  (NaCl disk)/ $\text{cm}^{-1}$  2590, 1729, 1524, 1351;  $^1\text{H}$  NMR (500 MHz,  $\text{CD}_3\text{OD}$ )  $\delta_{\text{H}}$  8.40 (2H, d,  $J = 8.8$  Hz,  $o\text{-NO}_2\text{ArH}$ ), 7.79 (2H, d,  $J = 8.8$  Hz,  $m\text{-NO}_2\text{ArH}$ ), 7.45 (2H, d,  $J = 7.4$  Hz,  $o\text{-ArH}$ ), 7.40 (2H, t,  $J = 7.4$  Hz,  $m\text{-ArH}$ ), 7.32 (1H, tt,  $J = 7.4$  Hz, 1.2 Hz,  $p\text{-ArH}$ ), 6.10 (1H, s, CONCH), 4.72 (1H, dd,  $J = 10.3$  Hz, 3.6 Hz, COCH), 3.21 (1H, dd,  $J = 15.1$  Hz, 10.3 Hz,  $\text{CH}_2$ ), 2.88 (3H, s,  $\text{NCH}_3$ ), 3.59 (1H, dd,  $J = 15.1$  Hz, 3.6 Hz,  $\text{CH}_2$ );  $^{13}\text{C}$  NMR (125 MHz,  $\text{CD}_3\text{OD}$ )  $\delta_{\text{C}}$  LRMS  $m/z$  ( $\text{ES}^+$ )  $[\text{M}-\text{Cl}]^+ = 312.1$ ; HRMS  $m/z$  ( $\text{ES}^+$ )  $[\text{M}-\text{Cl}]^+ = 312.1342$ ; HRMS  $m/z$  calc.  $[\text{M}-\text{Cl}]^+ = 312.1348$ ; decomp. 130–132 °C;  $[\alpha]_{\text{D}}^{32} -12.0$  ( $c$  0.1,  $\text{CH}_3\text{OH}$ ).

**(*S*,*E*)-*N*-Methyl-2-(4-nitrobenzylideneamino)-3-phenylpropanamide 106**



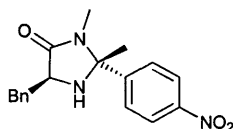
L-Phenylalanine *N*-methylamide **62** (5.07 g, 28.5 mmol) and 4-nitrobenzaldehyde (4.29g, 28.4 mmol) were stirred over 3 Å molecular sieves under nitrogen in DCM (50 mL) for 68 hours to give the desired product in quantitative yield.  $\nu_{\max}$  (NaCl disk)/ $\text{cm}^{-1}$  1676, 1526, 1348, 1265;  $^1\text{H}$  NMR (500 MHz,  $\text{CDCl}_3$ )  $\delta_{\text{H}}$  8.18 (2H, d,  $J = 8.4$  Hz,  $\text{NO}_2\text{CCH}$ ), 7.69 (2H, d,  $J = 8.4$  Hz,  $\text{NO}_2\text{CCCH}$ ), 7.51 (1H, s,  $\text{ArCH}$ ), 7.16–7.10 (3H, m,  $\text{ArH}$ ), 6.99 (2H, d,  $J = 6.9$  Hz,  $\text{ArH}$ ), 6.77 (1H, s,  $\text{NH}$ ), 3.96 (1H, dd,  $J = 10.1$  Hz, 3.0 Hz, COCH), 3.40 (1H, dd,  $J = 13.5$  Hz, 3.0 Hz,  $\text{CH}_2$ ), 2.85 (1H, dd,  $J = 13.5$  Hz, 10.1 Hz,  $\text{CH}_2$ ), 2.84 (3H, d,  $J = 4.9$  Hz,  $\text{CH}_3$ );  $^{13}\text{C}$  NMR (100 MHz,  $\text{CDCl}_3$ )  $\delta_{\text{C}}$  172.2 (C), 160.4 (C), 149.3 (C), 140.6 (C), 137.1 (C), 130.0 (CH), 128.9 (CH), 128.3 (CH), 126.8 (CH), 124.0 (CH), 75.4 (CH), 41.1 ( $\text{CH}_2$ ), 26.1 ( $\text{CH}_3$ ); LRMS  $m/z$  ( $\text{ES}^+$ )  $[\text{M}+\text{H}]^+ = 312.1$ ; HRMS  $m/z$  ( $\text{ES}^+$ )  $[\text{M}+\text{H}]^+ = 312.1343$ ; HRMS  $m/z$  calc.  $[\text{M}+\text{H}]^+ = 312.1348$ ;  $[\alpha]_{\text{D}}^{34} -152.4$  ( $c$  0.1,  $\text{CH}_2\text{Cl}_2$ ).

**(S)-5-Benzyl-1,2,2,3-tetramethylimidazolidin-4-one hydrochloride 107·HCl**



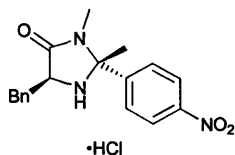
(S)-5-benzyl-2,2,3-trimethylimidazolidin-4-one hydrochloride **7**·HCl (0.549 g, 2.16 mmol) and sodium cyanoborohydride (0.490 g, 7.81 mmol) were stirred in aqueous formaldehyde (37%, 6 mL, 37 mmol) for 67 hours then poured into diethyl ether (30 mL) and washed with potassium carbonate (4 M, 30 mL), water (30 mL), and brine (30 mL) then evaporated. The residual oil was taken up in diethyl ether (30 mL), treated with anhydrous hydrogen chloride then filtered and the residue washed with diethyl ether (10 mL) and dried to yield the desired product, a white powder (0.470 g, 1.75 mmol, 81%).  $\nu_{\max}$  (NaCl disk)/ $\text{cm}^{-1}$  3422, 1715, 1396, 1288, 1157, 751, 706;  $^1\text{H}$  NMR (500 MHz,  $\text{CD}_3\text{OD}$ )  $\delta_{\text{H}}$  7.37 (2H, d,  $J = 7.5$  Hz, *o*-ArH), 7.29 (2H, t,  $J = 7.5$  Hz, *m*-ArH), 7.22 (1H, t,  $J = 7.5$  Hz, *p*-ArH), 4.44 (1H, dd,  $J = 9.0$  Hz, 4.3 Hz, CH), 3.48 (1H, dd,  $J = 15.4$  Hz, 4.3 Hz,  $\text{CH}_2$ ), 3.12 (1H, dd,  $J = 15.4$  Hz, 9.0 Hz,  $\text{CH}_2$ ), 2.86 (3H, s,  $\text{CHNCH}_3$ ), 2.59 (3H, s,  $\text{CONCH}_3$ ), 1.71 (3H, s,  $\text{CCH}_3$ ), 1.46 (3H, s,  $\text{CCH}_3$ );  $^{13}\text{C}$  NMR (125 MHz,  $\text{CD}_3\text{OD}$ )  $\delta_{\text{C}}$  165.7 (C), 135.7 (C), 128.9 (CH), 128.7 (CH), 127.3 (CH), 83.2 (C), 67.5 ( $\text{CH}_2$ ), 65.3 (CH), 33.8 ( $\text{CH}_3$ ), 25.0 ( $\text{CH}_3$ ), 20.5 ( $\text{CH}_3$ ), 17.2 ( $\text{CH}_3$ ); LRMS  $m/z$  ( $\text{AP}^+$ )  $[\text{M}-\text{Cl}]^+ = 233.2$ ; HRMS  $m/z$  ( $\text{ES}^+$ )  $[\text{M}-\text{Cl}]^+ = 233.1643$ ; HRMS  $m/z$  calc.  $[\text{M}-\text{Cl}]^+ = 233.1654$ ; decomp. 167 °C;  $[\alpha]_{\text{D}}^{34} -48.0$  (c 0.1,  $\text{CH}_3\text{OH}$ ).

**(2R,5S)-5-Benzyl-2,3-dimethyl-2-(4-nitrophenyl)imidazolidin-4-one 110**



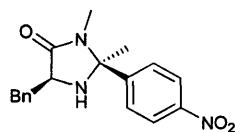
Prepared according to Standard Preparation A.  $\nu_{\max}$  (NaCl disk)/ $\text{cm}^{-1}$  3306, 2922, 1694, 1519, 1396, 1350, 857, 734, 701;  $^1\text{H}$  NMR (500 MHz,  $\text{CDCl}_3$ )  $\delta_{\text{H}}$  8.19 (2H, d,  $J = 8.8$  Hz, ArH), 7.46 (2H, d,  $J = 8.8$  Hz, ArH), 7.33–7.29 (2H, m, ArH), 7.26–7.23 (3H, m, ArH), 3.82 (1H, dd,  $J = 6.3$  Hz, 4.6 Hz, COCH), 3.16 (1H, dd,  $J = 14.1$  Hz, 4.6 Hz,  $\text{CH}_2$ ), 3.09 (1H, dd,  $J = 14.1$  Hz, 6.3 Hz,  $\text{CH}_2$ ), 2.79 (3H, s,  $\text{NCH}_3$ ), 1.56 (3H, s,  $\text{CCH}_3$ );  $^{13}\text{C}$  NMR (125 MHz,  $\text{CDCl}_3$ )  $\delta_{\text{C}}$  173.6 (C), 149.9 (C), 147.6 (C), 136.8 (C), 129.6 (CH), 128.7 (CH), 127.0 (CH), 126.4 (CH), 124.0 (CH), 78.1 (C), 59.0 (CH), 37.6 ( $\text{CH}_2$ ), 26.3 ( $\text{CH}_3$ ), 26.0 ( $\text{CH}_3$ ); LRMS  $m/z$  ( $\text{ES}^+$ )  $[\text{M}+\text{H}]^+ = 326.2$ ; HRMS  $m/z$  ( $\text{ES}^+$ )  $[\text{M}+\text{H}]^+ = 326.1503$ ; HRMS  $m/z$  calc.  $[\text{M}+\text{H}]^+ = 326.1505$ ;  $[\alpha]_{\text{D}}^{34} 31.0$  (c 0.1,  $\text{CH}_2\text{Cl}_2$ ).

**(2R,5S)-5-Benzyl-2,3-dimethyl-2-(4-nitrophenyl)imidazolidin-4-one hydrochloride 110·HCl**



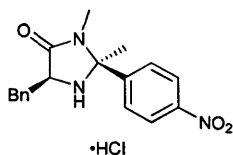
Prepared according to Standard Preparation C.  $\nu_{\text{max}}$  (NaCl disk)/ $\text{cm}^{-1}$  2462, 1721, 1523, 1352, 857, 698;  $^1\text{H}$  NMR (500 MHz,  $\text{CD}_3\text{OD}$ )  $\delta_{\text{H}}$  8.26 (2H, dt,  $J = 9.0$  Hz, 2.0 Hz,  $o\text{-NO}_2\text{ArH}$ ), 7.61 (2H, dt,  $J = 9.0$  Hz, 2.0 Hz,  $m\text{-NO}_2\text{ArH}$ ), 7.27–7.18 (5H, m,  $\text{CH}_2\text{ArH}$ ), 4.32 (1H, dd,  $J = 9.6$  Hz, 3.9 Hz,  $\text{CH}$ ), 3.44 (1H, dd,  $J = 15.2$  Hz, 3.9 Hz,  $\text{CH}_2$ ), 3.02 (1H, dd,  $J = 15.2$  Hz, 9.6 Hz,  $\text{CH}_2$ ), 2.83 (3H, s,  $\text{NCH}_3$ ), 2.06 (3H, s,  $\text{CCH}_3$ );  $^{13}\text{C}$  NMR (125 MHz,  $\text{CD}_3\text{OD}$ )  $\delta_{\text{C}}$  174.5 (C), 149.2 (C), 141.3 (C), 135.1 (C), 128.9 (CH), 128.6 (CH), 128.0 (CH), 127.3 (CH), 124.2 (CH), 79.2 (C), 58.3 (CH), 34.7 ( $\text{CH}_2$ ), 25.5 ( $\text{CH}_3$ ), 22.5 ( $\text{CH}_3$ ); LRMS  $m/z$  ( $\text{AP}^+$ )  $[\text{M}-\text{Cl}]^+ = 326.2$ ; HRMS  $m/z$  ( $\text{ES}^+$ )  $[\text{M}-\text{Cl}]^+ = 326.1497$ ; HRMS  $m/z$  calc.  $[\text{M}-\text{Cl}]^+ = 326.1505$ ; Mpt. 108 °C;  $[\alpha]_{\text{D}}^{34}$  48.4 (c 0.1,  $\text{CH}_3\text{OH}$ ). See Appendix A for X-ray crystallography data.

**(2S,5S)-5-Benzyl-2,3-dimethyl-2-(4-nitrophenyl)imidazolidin-4-one 111**



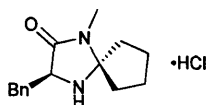
Prepared according to Standard Preparation A.  $\nu_{\text{max}}$  (NaCl disk)/ $\text{cm}^{-1}$  3327, 2921, 1694, 1519, 1396, 1350, 856, 750, 701;  $^1\text{H}$  NMR (500 MHz,  $\text{CDCl}_3$ )  $\delta_{\text{H}}$  7.97 (2H, d,  $J = 8.9$  Hz,  $\text{ArH}$ ), 7.25–7.22 (3H, m,  $\text{ArH}$ ), 7.13–7.11 (2H, m,  $\text{ArH}$ ), 6.96 (2H, d,  $J = 8.9$  Hz,  $\text{ArH}$ ), 3.90 (1H, t,  $J = 5.0$  Hz,  $\text{COCH}$ ), 3.19 (1H, dd,  $J = 14.0$  Hz, 5.0 Hz,  $\text{CH}_2$ ), 2.98 (1H, dd,  $J = 14.0$  Hz, 5.0 Hz,  $\text{CH}_2$ ), 2.47 (3H, s,  $\text{NCH}_3$ ), 1.69 (3H, s,  $\text{CCH}_3$ );  $^{13}\text{C}$  NMR (125 MHz,  $\text{CDCl}_3$ )  $\delta_{\text{C}}$  173.3 (C), 149.2 (C), 147.8 (C), 136.7 (C), 130.0 (CH), 128.9 (CH), 127.3 (CH), 127.1 (CH), 123.8 (CH), 78.2 (C), 59.3 (CH), 36.7 ( $\text{CH}_2$ ), 26.1 ( $\text{CH}_3$ ), 23.2 ( $\text{CH}_3$ ); LRMS  $m/z$  ( $\text{AP}^+$ )  $[\text{M}+\text{H}]^+ = 326.2$ ; HRMS  $m/z$  ( $\text{ES}^+$ )  $[\text{M}+\text{H}]^+ = 326.1496$ ; HRMS  $m/z$  calc.  $[\text{M}+\text{H}]^+ = 326.1505$ ;  $[\alpha]_{\text{D}}^{34}$  -138.0 (c 0.1,  $\text{CH}_2\text{Cl}_2$ ).

**(2S,5S)-5-Benzyl-2,3-dimethyl-2-(4-nitrophenyl)imidazolidin-4-one hydrochloride 111·HCl**



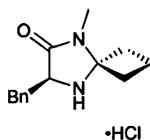
Prepared according to Standard Preparation C.  $\nu_{\max}$  (NaCl disk)/ $\text{cm}^{-1}$  2354, 1718, 1524, 1393, 1352, 699;  $^1\text{H}$  NMR (500 MHz,  $\text{CD}_3\text{OD}$ )  $\delta_{\text{H}}$  8.25 (2H, dt,  $J = 9.0$  Hz, 2.0 Hz,  $o\text{-NO}_2\text{ArH}$ ), 7.60 (2H, dt,  $J = 9.0$  Hz, 2.0 Hz,  $m\text{-NO}_2\text{ArH}$ ), 7.29–7.16 (5H, m,  $\text{CH}_2\text{ArH}$ ), 4.62 (1H, dd,  $J = 9.2$  Hz, 3.8 Hz,  $\text{CH}$ ), 3.39 (1H, dd,  $J = 15.2$  Hz, 3.8 Hz,  $\text{CH}_2$ ), 2.99 (1H, dd,  $J = 15.2$  Hz, 9.2 Hz,  $\text{CH}_2$ ), 2.71 (3H, s,  $\text{NCH}_3$ ), 2.02 (3H, s,  $\text{CCH}_3$ );  $^{13}\text{C}$  NMR (125 MHz,  $\text{CD}_3\text{OD}$ )  $\delta_{\text{C}}$  179.0 (C), 149.1 (C), 135.2 (C), 129.0 (CH), 128.7 (CH), 128.5 (CH), 127.3 (CH), 124.0 (CH), 122.9 (C), 79.6 (C), 58.8 (CH), 34.6 ( $\text{CH}_2$ ), 26.0 ( $\text{CH}_3$ ), 19.8 ( $\text{CH}_3$ ); LRMS  $m/z$  ( $\text{ES}^+$ )  $[\text{M}-\text{Cl}]^+ = 326.2$ ; HRMS  $m/z$  ( $\text{ES}^+$ )  $[\text{M}-\text{Cl}]^+ = 326.1501$ ; HRMS  $m/z$  calc.  $[\text{M}-\text{Cl}]^+ = 326.1505$ ; Mpt. 106 °C;  $[\alpha]_{\text{D}}^{34} -106.6$  (c 0.1,  $\text{CH}_3\text{OH}$ ).

**(S)-3-Benzyl-1-methyl-1,4-diazaspiro[4.4]nonan-2-one hydrochloride 114·HCl**



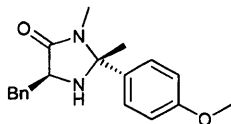
L-Phenylalanine *N*-methylamide **62** (1.12 g, 6.28 mmol), cyclopentanone (0.510 mL, 0.485 g, 5.77 mmol) and *p*-toluenesulfonic acid monohydrate (0.065 g, 0.34 mmol) were refluxed in isopropanol (16 mL) for 18 hours. The solvent was evaporated and the residue taken up in diethyl ether (45 mL) then washed with potassium carbonate (4 M, 20 mL) and brine (20 mL), dried over sodium carbonate, and evaporated to give an oil which was separated by column chromatography (1:1 petroleum ether:ethyl acetate) to yield the free amine ( $R_f$ : 0.14), a brown oil (0.679 g, 2.78 mmol, 48%). The amine was dissolved in diethyl ether (75 mL), treated with anhydrous hydrogen chloride, filtered, and the residue washed with diethyl ether (20 mL) and dried to yield the desired product, a cream solid (0.534 g, 2.19 mmol, 38%).  $\nu_{\max}$  (NaCl disk)/ $\text{cm}^{-1}$  3414, 1716, 1455, 1425, 1402, 1341, 1259;  $^1\text{H}$  NMR (500 MHz,  $\text{CD}_3\text{OD}$ )  $\delta_{\text{H}}$  7.33 (2H, d,  $J = 7.4$  Hz,  $o\text{-ArH}$ ), 7.29 (2H, t,  $J = 7.4$  Hz,  $m\text{-ArH}$ ), 7.22 (1H, t,  $J = 7.4$  Hz,  $p\text{-ArH}$ ), 4.49 (1H, dd,  $J = 10.3$  Hz, 3.8 Hz,  $\text{COCH}$ ), 3.41 (1H, dd,  $J = 15.1$  Hz, 3.8 Hz,  $\text{ArCH}_2$ ), 2.99 (1H, dd,  $J = 15.1$  Hz, 10.3 Hz,  $\text{ArCH}_2$ ), 2.83 (3H, s,  $\text{CH}_3$ ), 2.23–2.29 (1H, m,  $\text{CH}_2\text{CH}_2$ ), 2.06–1.96 (2H, m,  $\text{CH}_2\text{CH}_2$ ), 1.87–1.94 (1H, m,  $\text{CH}_2\text{CH}_2$ ), 1.82–1.65 (4H, m,  $\text{CH}_2\text{CH}_2$ );  $^{13}\text{C}$  NMR (125 MHz,  $\text{CD}_3\text{OD}$ )  $\delta_{\text{C}}$  165.1 (C), 133.6 (C), 127.5 (CH), 127.3 (CH), 125.9 (CH), 85.6 (C), 57.1 (CH), 32.3 ( $\text{CH}_2$ ), 32.2 ( $\text{CH}_2$ ), 30.6 ( $\text{CH}_2$ ), 23.1 ( $\text{CH}_3$ ), 22.3 ( $\text{CH}_2$ ), 22.0 ( $\text{CH}_2$ ); LRMS  $m/z$  ( $\text{ES}^+$ )  $[\text{M}-\text{Cl}]^+ = 245.2$ ; HRMS  $m/z$  ( $\text{ES}^+$ )  $[\text{M}-\text{Cl}]^+ = 245.1650$ ; HRMS  $m/z$  calc.  $[\text{M}-\text{Cl}]^+ = 245.1654$ ; Mpt. 133–135 °C;  $[\alpha]_{\text{D}}^{30} -104.0$  (c 0.1,  $\text{CH}_3\text{OH}$ ).

**(S)-7-Benzyl-5-methyl-5,8-diazaspiro[3.4]octan-6-one hydrochloride 115·HCl**



L-Phenylalanine *N*-methylamide **62** (0.940 g, 5.28 mmol), cyclobutanone (0.360 mL, 0.338 g, 4.82 mmol) and *p*-toluenesulfonic acid monohydrate (0.218 g, 1.15 mmol) in DMF (7 mL) were subjected to microwave irradiation at 140 °C for 50 minutes with an initial power of 100 W. The reaction mixture was then poured into diethyl ether (70 mL), shaken with potassium carbonate (4 M, 20 mL) and the top layer washed with water (2 x 20 mL) and brine (20 mL) then evaporated and the resultant oil separated by column chromatography (ethyl acetate) to yield the free amine (*R*<sub>f</sub>: 0.22), a yellow oil (0.441 g, 1.92 mmol, 40%). The free amine was taken up in diethyl ether (60 mL), treated with anhydrous hydrogen chloride, filtered, and the residue washed with diethyl ether (20 mL) and dried to yield the desired product, a pink solid (0.387 g, 1.45 mmol, 30%).  $\nu_{\max}$  (NaCl disk)/cm<sup>-1</sup> 3415, 1715, 1400, 1327, 1292, 1257, 1119, 1034; <sup>1</sup>H NMR (500 MHz, CD<sub>3</sub>OD)  $\delta_{\text{H}}$  7.32–7.28 (4H, m, ArH), 7.21–7.24 (1H, m, *p*-ArH), 4.41 (1H, dd, *J* = 9.8 Hz, 3.9 Hz, CH), 3.36 (1H, dd, *J* = 15.1 Hz, 3.9 Hz, ArCH<sub>2</sub>), 3.00 (1H, dd, *J* = 15.1 Hz, 9.8 Hz, ArCH<sub>2</sub>), 2.95 (3H, s, CH<sub>3</sub>), 2.65–2.72 (1H, m, CH<sub>2</sub>CH<sub>2</sub>), 2.54–2.61 (1H, m, CH<sub>2</sub>CH<sub>2</sub>), 2.47–2.36 (2H, m, CH<sub>2</sub>CH<sub>2</sub>), 1.91–1.78 (2H, m, CH<sub>2</sub>CH<sub>2</sub>); <sup>13</sup>C NMR (125 MHz, CD<sub>3</sub>OD)  $\delta_{\text{C}}$  166.6 (C), 134.8 (C), 129.0 (CH), 128.8 (CH), 127.5 (CH), 79.6 (C), 58.4 (CH), 33.7 (CH<sub>2</sub>), 29.6 (CH<sub>2</sub>), 29.4 (CH<sub>2</sub>), 24.7 (CH<sub>2</sub>), 11.6 (CH<sub>3</sub>); LRMS *m/z* (ES<sup>+</sup>) [M–Cl]<sup>+</sup> = 231.2; HRMS *m/z* (ES<sup>+</sup>) [M–Cl]<sup>+</sup> = 231.1489; HRMS *m/z* calc. [M–Cl]<sup>+</sup> = 231.1497; Mpt. 135–137 °C; [ $\alpha$ ]<sub>D</sub><sup>30</sup> –57.8 (c 0.1, CH<sub>3</sub>OH).

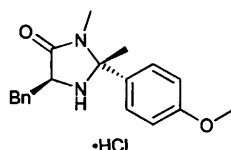
**(2R,5S)-5-Benzyl-2-(4-methoxyphenyl)-2,3-dimethylimidazolidin-4-one 119**



Prepared according to Standard Preparation A.  $\nu_{\max}$  (NaCl disk)/cm<sup>-1</sup> 3360, 2933, 1690, 1608, 1510, 1397, 1252, 1181, 1031, 833, 701; <sup>1</sup>H NMR (500 MHz, CDCl<sub>3</sub>)  $\delta_{\text{H}}$  7.23–7.08 (7H, m, ArH), 6.78 (2H, d, *J* = 8.9 Hz, ArH), 3.81 (1H, dd, *J* = 7.2 Hz, 4.2 Hz, COCH), 3.71 (3H, s, OCH<sub>3</sub>), 3.08 (1H, dd, *J* = 13.9 Hz, 4.2 Hz, CH<sub>2</sub>), 2.93 (1H, dd, *J* = 13.9 Hz, 7.2 Hz, CH<sub>2</sub>), 2.64 (3H, s, NCH<sub>3</sub>), 1.46 (3H, s, CCH<sub>3</sub>); <sup>13</sup>C NMR (125 MHz, CDCl<sub>3</sub>)  $\delta_{\text{C}}$  173.6 (C), 159.4 (C), 137.7 (C), 134.9 (C), 129.7 (CH), 128.5 (CH), 126.7 (CH), 126.5 (CH), 114.1 (CH), 78.4 (C), 59.4 (CH), 55.3 (CH<sub>3</sub>), 38.4

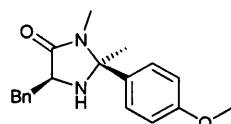
(CH<sub>2</sub>), 26.4 (CH<sub>3</sub>), 26.1 (CH<sub>3</sub>); LRMS *m/z* (ES<sup>+</sup>) [M+H]<sup>+</sup> = 311.2; HRMS *m/z* (ES<sup>+</sup>) [M+H]<sup>+</sup> = 311.1753; HRMS *m/z* calc. [M+H]<sup>+</sup> = 311.1760; [α]<sub>D</sub><sup>30</sup> (c 0.1, CH<sub>2</sub>Cl<sub>2</sub>).

**(2*R*,5*S*)-5-Benzyl-2-(4-methoxyphenyl)-2,3-dimethylimidazolidin-4-one** **hydrochloride**  
**119·HCl**



Prepared according to Standard Preparation C (66%). *v*<sub>max</sub> (NaCl disk)/cm<sup>-1</sup> 3418, 1715, 1608, 1515, 1393, 1258, 1183, 1025; <sup>13</sup>C NMR (125 MHz, CD<sub>3</sub>OD) δ<sub>c</sub> 165.8 (C), 160.1 (C), 133.4 (C), 127.3 (CH), 127.1 (CH), 126.3 (CH), 125.8 (CH), 123.6 (C), 113.1 (CH), 78.5 (C), 55.4 (CH), 53.1 (CH<sub>3</sub>), 32.4 (CH<sub>2</sub>), 23.9 (CH<sub>3</sub>), 20.1 (CH<sub>3</sub>); LRMS *m/z* (ES<sup>+</sup>) [M–Cl]<sup>+</sup> = 311.2; HRMS *m/z* (ES<sup>+</sup>) [M–Cl]<sup>+</sup> = 311.1753; HRMS *m/z* calc. [M–Cl]<sup>+</sup> = 311.1760; Mpt. 117–119 °C; [α]<sub>D</sub><sup>30</sup> 36.0 (c 0.1, CH<sub>3</sub>OH). See Appendix A for X-ray crystallography data.

**(2*S*,5*S*)-5-Benzyl-2-(4-methoxyphenyl)-2,3-dimethylimidazolidin-4-one** **120**

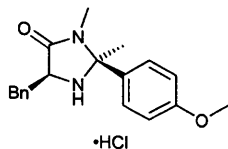


Prepared according to Standard Preparation A. *v*<sub>max</sub> (NaCl disk)/cm<sup>-1</sup> 3323, 2933, 1694, 1610, 1513, 1395, 1254; <sup>1</sup>H NMR (500 MHz, CDCl<sub>3</sub>) δ<sub>H</sub> 7.24–7.20 (3H, m, ArH), 7.15–7.14 (2H, m, ArH), 6.67–6.61 (4H, m, ArH), 3.84 (1H, t, *J* = 4.9 Hz, COCH), 3.70 (3H, s, OCH<sub>3</sub>), 3.23 (1H, dd, *J* = 14.0 Hz, 5.2 Hz, CH<sub>2</sub>), 2.99 (1H, dd, *J* = 14.0 Hz, 4.9 Hz, CH<sub>2</sub>), 2.42 (3H, s, NCH<sub>3</sub>), 1.59 (3H, s, CCH<sub>3</sub>); <sup>13</sup>C NMR (125 MHz, CDCl<sub>3</sub>) δ<sub>c</sub> 173.6 (C), 159.6 (C), 136.7 (C), 133.8 (C), 130.0 (CH), 128.9 (CH), 127.4 (CH), 126.9 (CH), 113.9 (CH), 78.7 (C), 59.4 (CH), 55.3 (CH<sub>3</sub>), 36.3 (CH<sub>2</sub>), 26.1 (CH<sub>3</sub>), 22.8 (CH<sub>3</sub>); LRMS *m/z* (ES<sup>+</sup>) [M+H]<sup>+</sup> = 311.2; HRMS *m/z* (ES<sup>+</sup>) [M+H]<sup>+</sup> = 311.1755; HRMS *m/z* calc. [M+H]<sup>+</sup> = 311.1760; [α]<sub>D</sub><sup>30</sup> –121.0 (c 0.1, CH<sub>2</sub>Cl<sub>2</sub>).



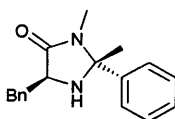
**(2S,5S)-5-Benzyl-2-(4-methoxyphenyl)-2,3-dimethylimidazolidin-4-one**  
**120·HCl**

**hydrochloride**



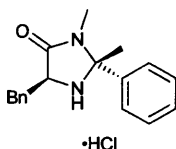
Prepared according to Standard Preparation C (80%).  $\nu_{\max}$  (NaCl disk)/ $\text{cm}^{-1}$  3420, 1710, 1515, 1391, 1257, 1184;  $^{13}\text{C}$  NMR (125 MHz,  $\text{CD}_3\text{OD}$ )  $\delta_{\text{C}}$  167.5 (C), 161.8 (C), 134.9 (C), 129.1 (CH), 128.9 (CH), 128.8 (CH), 128.6 (CH), 125.8 (C), 114.6 (CH), 80.5 (C), 58.4 (CH), 54.7 ( $\text{CH}_3$ ), 37.4 ( $\text{CH}_2$ ), 26.0 ( $\text{CH}_3$ ), 19.3 ( $\text{CH}_3$ ); LRMS  $m/z$  ( $\text{ES}^+$ )  $[\text{M}-\text{Cl}]^+ = 311.2$ ; HRMS  $m/z$  ( $\text{ES}^+$ )  $[\text{M}-\text{Cl}]^+ = 311.1756$ ; HRMS  $m/z$  calc.  $[\text{M}-\text{Cl}]^+ = 311.1760$ ; Mpt. 115–117 °C;  $[\alpha]_{\text{D}}^{30} -117.6$  (c 0.1,  $\text{CH}_3\text{OH}$ ).

**(2R,5S)-5-Benzyl-2,3-dimethyl-2-phenylimidazolidin-4-one 121**



Prepared according to Standard Preparation A.  $\nu_{\max}$  (NaCl disk)/ $\text{cm}^{-1}$  1693, 1454, 1396, 1080, 745, 699;  $^1\text{H}$  NMR (500 MHz,  $\text{CDCl}_3$ )  $\delta_{\text{H}}$  7.23 (2H, t,  $J = 6.2$  Hz,  $\text{ArH}$ ), 7.20–7.09 (8H, m,  $\text{ArH}$ ), 3.76 (1H, dd,  $J = 7.1$  Hz, 4.2 Hz,  $\text{COCH}$ ), 3.05 (1H, dd,  $J = 13.9$  Hz, 4.2 Hz,  $\text{CH}_2$ ), 2.91 (1H, dd,  $J = 13.9$  Hz, 7.1 Hz,  $\text{CH}_2$ ), 2.63 (3H, s,  $\text{NCH}_3$ ), 1.45 (3H, s,  $\text{CCH}_3$ );  $^{13}\text{C}$  NMR (125 MHz,  $\text{CDCl}_3$ )  $\delta_{\text{C}}$  173.7 (C), 142.8 (C), 137.6 (C), 129.7 (CH), 128.9 (CH), 128.5 (CH), 128.1 (CH), 126.7 (CH), 125.1 (CH), 78.6 (C), 59.3 (CH), 38.3 (CH), 26.3 ( $\text{CH}_3$ ), 26.2 ( $\text{CH}_3$ ); LRMS  $m/z$  ( $\text{ES}^+$ )  $[\text{M}+\text{H}]^+ = 281.2$ ; HRMS  $m/z$  ( $\text{ES}^+$ )  $[\text{M}+\text{H}]^+ = 281.1646$ ; HRMS  $m/z$  calc.  $[\text{M}+\text{H}]^+ = 281.1654$ ;  $[\alpha]_{\text{D}}^{30} 3.0$  (c 0.1,  $\text{CH}_2\text{Cl}_2$ ).

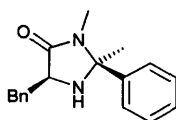
**(2R,5S)-5-Benzyl-2,3-dimethyl-2-phenylimidazolidin-4-one hydrochloride 121·HCl**



Prepared according to Standard Preparation C (89%).  $\nu_{\max}$  (NaCl disk)/ $\text{cm}^{-1}$  3412, 2096, 1644, 1393, 1220;  $^1\text{H}$  NMR (500 MHz,  $\text{CD}_3\text{OD}$ )  $\delta_{\text{H}}$  7.60–7.55 (3H, m,  $\text{CArH}$ ), 7.50–7.46 (2H, m,  $\text{CArH}$ ), 7.41 (2H, d,  $J = 7.6$  Hz,  $o\text{-CH}_2\text{ArH}$ ), 7.36 (2H, t,  $J = 7.6$  Hz,  $m\text{-CH}_2\text{ArH}$ ), 7.30 (1H, tt,  $J = 7.60$  Hz, 2.4 Hz,  $p\text{-CH}_2\text{ArH}$ ), 4.44 (1H, dd,  $J = 9.7$  Hz, 4.0 Hz,  $\text{CH}$ ), 3.57 (1H, dd,  $J = 15.2$  Hz, 4.0 Hz,  $\text{CH}_2$ ),

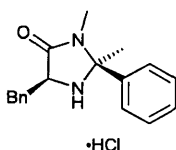
3.24 (1H, dd,  $J = 15.2$  Hz, 9.7 Hz,  $\text{CH}_2$ ), 2.94 (3H, s,  $\text{NCH}_3$ ), 2.21 (3H, s,  $\text{CCH}_3$ );  $^{13}\text{C}$  NMR (125 MHz,  $\text{CD}_3\text{OD}$ )  $\delta_{\text{C}}$  167.6 (C), 134.9 (C), 134.3 (C), 130.8 (CH), 129.5 (CH), 129.0 (CH), 128.8 (CH), 127.4 (CH), 126.9 (CH), 80.5 (C), 58.6 (CH), 34.0 ( $\text{CH}_2$ ), 26.2 ( $\text{CH}_3$ ), 19.4 ( $\text{CH}_3$ ); LRMS  $m/z$  ( $\text{ES}^+$ )  $[\text{M}-\text{Cl}]^+ = 281.2$ ; HRMS  $m/z$  ( $\text{ES}^+$ )  $[\text{M}-\text{Cl}]^+ = 281.1646$ ; HRMS  $m/z$  calc.  $[\text{M}-\text{Cl}]^+ = 281.1654$ ; Mpt. 139–141 °C;  $[\alpha]_{\text{D}}^{34} 7.6$  (c 0.1,  $\text{CH}_2\text{Cl}_2$ ). See Appendix A for X-ray crystallography data.

**(2S,5S)-5-Benzyl-2,3-dimethyl-2-phenylimidazolidin-4-one 122**



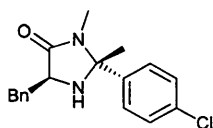
Prepared according to Standard Preparation A.  $\nu_{\text{max}}$  (NaCl disk)/ $\text{cm}^{-1}$  3319, 2928, 1690, 1427, 1396, 764, 700;  $^1\text{H}$  NMR (500 MHz,  $\text{CDCl}_3$ )  $\delta_{\text{H}}$  7.21–7.10 (8H, m,  $\text{ArH}$ ), 6.77 (2H, d,  $J = 7.6$  Hz,  $\text{ArH}$ ), 3.83 (1H, t,  $J = 5.0$  Hz,  $\text{COCH}$ ), 3.19 (1H, dd,  $J = 14.0$  Hz, 5.0 Hz,  $\text{CH}_2$ ), 2.99 (1H, dd,  $J = 14.2$  Hz, 5.0 Hz,  $\text{CH}_2$ ), 2.43 (3H, s,  $\text{NCH}_3$ ), 1.61 (3H, s,  $\text{NCH}_3$ );  $^{13}\text{C}$  NMR (125 MHz,  $\text{CDCl}_3$ )  $\delta_{\text{C}}$  173.7 (C), 141.9 (C), 136.7 (C), 129.9 (CH), 128.9 (CH), 128.7 (CH), 128.5 (CH), 126.9 (CH), 126.0 (CH), 79.0 (C), 59.5 (CH), 36.4 (CH), 26.2 ( $\text{CH}_3$ ), 22.8 ( $\text{CH}_3$ ); LRMS  $m/z$  ( $\text{ES}^+$ )  $[\text{M}+\text{H}]^+ = 281.2$ ; HRMS  $m/z$  ( $\text{ES}^+$ )  $[\text{M}+\text{H}]^+ = 281.1644$ ; HRMS  $m/z$  calc.  $[\text{M}+\text{H}]^+ = 281.1654$ ;  $[\alpha]_{\text{D}}^{30} -114.4$  (c 0.1,  $\text{CH}_3\text{OH}$ ).

**(2S,5S)-5-Benzyl-2,3-dimethyl-2-phenylimidazolidin-4-one hydrochloride 122·HCl**



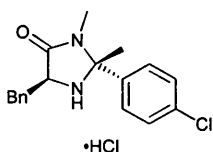
Prepared according to Standard Preparation C (82%).  $\nu_{\text{max}}$  (NaCl disk)/ $\text{cm}^{-1}$  3882, 2434, 1716, 1393, 700;  $^1\text{H}$  NMR (500 MHz,  $\text{CD}_3\text{OD}$ )  $\delta_{\text{H}}$  7.61–7.59 (3H, m,  $\text{ArH}$ ), 7.54–7.51 (2H, m,  $\text{ArH}$ ), 7.41–7.33 (5H, m,  $\text{ArH}$ ), 3.55 (1H, dd,  $J = 15.3$  Hz, 3.9 Hz,  $\text{CH}$ ), 3.55 (1H, dd,  $J = 15.3$  Hz, 3.9 Hz,  $\text{CH}_2$ ), 3.12 (1H, dd,  $J = 15.3$  Hz, 9.5 Hz,  $\text{CH}_2$ ), 2.83 (3H, s,  $\text{NCH}_3$ ), 2.15 (3H, s,  $\text{CCH}_3$ );  $^{13}\text{C}$  NMR (125 MHz,  $\text{CD}_3\text{OD}$ )  $\delta_{\text{C}}$  167.6 (C), 134.9 (C), 134.3 (C), 130.8 (CH), 129.5 (CH), 128.9 (CH), 128.8 (CH), 127.4 (CH), 126.9 (CH), 80.5 (C), 58.6 (CH), 34.0 ( $\text{CH}_2$ ), 26.1 ( $\text{CH}_3$ ), 19.3 ( $\text{CH}_3$ ); LRMS  $m/z$  ( $\text{ES}^+$ )  $[\text{M}-\text{Cl}]^+ = 281.2$ ; HRMS  $m/z$  ( $\text{ES}^+$ )  $[\text{M}-\text{Cl}]^+ = 281.1648$ ; HRMS  $m/z$  calc.  $[\text{M}-\text{Cl}]^+ = 281.1654$ ; Mpt. 132–134 °C;  $[\alpha]_{\text{D}}^{34} -95.6$  (c 0.1,  $\text{CH}_3\text{OH}$ ).

**(2R,5S)-5-Benzyl-2-(4-chlorophenyl)-2,3-dimethylimidazolidin-4-one 123**



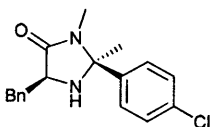
Prepared according to Standard Preparation A.  $\nu_{\max}$  (NaCl disk)/ $\text{cm}^{-1}$  3316, 2720, 1704, 1493, 1398, 1096;  $^1\text{H}$  NMR (500 MHz,  $\text{CDCl}_3$ )  $\delta_{\text{H}}$  7.23–7.19 (4H, m, ArH), 7.16–7.14 (3H, m, ArH), 7.13–7.09 (2H, m, ArH), 3.76 (1H, dd,  $J = 6.9$  Hz, 4.3 Hz, COCH), 3.06 (1H, dd,  $J = 14.0$  Hz, 4.3 Hz, CH<sub>2</sub>), 2.95 (1H, dd,  $J = 14.0$  Hz, 6.9 Hz, CH<sub>2</sub>), 2.64 (3H, s, NCH<sub>3</sub>), 1.44 (3H, s, CCH<sub>3</sub>);  $^{13}\text{C}$  NMR (125 MHz,  $\text{CDCl}_3$ )  $\delta_{\text{C}}$  173.5 (C), 141.4 (C), 137.3 (C), 134.1 (C), 129.7 (CH), 129.0 (CH), 128.6 (CH), 126.8 (CH), 126.7 (CH), 78.2 (C), 59.2 (CH), 38.0 (CH<sub>2</sub>), 26.2 (CH<sub>3</sub>), 21.0 (CH<sub>3</sub>); LRMS  $m/z$  ( $\text{ES}^+$ )  $[\text{M}+\text{H}]^+ = 315.1$ ; HRMS  $m/z$  ( $\text{ES}^+$ )  $[\text{M}+\text{H}]^+ = 315.1253$ ; HRMS  $m/z$  calc.  $[\text{M}+\text{H}]^+ = 315.1264$ ;  $[\alpha]_{\text{D}}^{30}$  5.2 ( $c$  0.1,  $\text{CH}_3\text{OH}$ ).

**(2R,5S)-5-Benzyl-2-(4-chlorophenyl)-2,3-dimethylimidazolidin-4-one hydrochloride 123·HCl**



Prepared according to Standard Preparation C.  $\nu_{\max}$  (NaCl disk)/ $\text{cm}^{-1}$  3414, 1720, 1495, 1398, 1099, 1011, 830;  $^1\text{H}$  NMR (500 MHz,  $\text{CD}_3\text{OD}$ )  $\delta_{\text{H}}$  7.58 (2H, dt,  $J = 8.8$  Hz, 1.9 Hz,  $o\text{-ClArH}$ ), 7.47 (2H, dt,  $J = 8.8$  Hz, 1.9 Hz,  $m\text{-ClArH}$ ), 7.42 (2H, d,  $J = 7.4$  Hz,  $o\text{-CH}_2\text{ArH}$ ), 7.36 (2H, t,  $J = 7.4$  Hz,  $m\text{-CH}_2\text{ArH}$ ), 7.30 (1H, t,  $J = 7.4$  Hz,  $p\text{-CH}_2\text{ArH}$ ), 4.46 (1H, dd,  $J = 9.7$  Hz, 4.0 Hz, COCH), 3.57 (1H, dd,  $J = 15.2$  Hz, 4.0 Hz, CH<sub>2</sub>), 3.25 (1H, dd,  $J = 15.24$  Hz, 9.7 Hz, CH<sub>2</sub>), 2.93 (3H, s, NCH<sub>3</sub>), 2.20 (3H, s, CCH<sub>3</sub>);  $^{13}\text{C}$  NMR (125 MHz,  $\text{CD}_3\text{OD}$ )  $\delta_{\text{C}}$  167.3 (C), 136.8 (C), 134.9 (C), 132.4 (C), 129.6 (CH), 129.0 (CH), 128.7 (CH), 128.2 (CH), 127.3 (CH), 79.6 (C), 58.0 (CH), 33.8 (CH<sub>2</sub>), 25.5 (CH<sub>3</sub>), 22.2 (CH<sub>3</sub>); LRMS  $m/z$  ( $\text{AP}^+$ )  $[\text{M}-\text{Cl}]^+ = 315.1$ ; HRMS  $m/z$  ( $\text{ES}^+$ )  $[\text{M}-\text{Cl}]^+ = 315.1257$ ; HRMS  $m/z$  calc.  $[\text{M}-\text{Cl}]^+ = 315.1264$ ; Mpt. 133–135 °C;  $[\alpha]_{\text{D}}^{30}$  38.0 ( $c$  0.1,  $\text{CH}_3\text{OH}$ ).

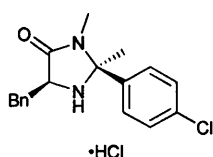
**(2S,5S)-5-Benzyl-2-(4-chlorophenyl)-2,3-dimethylimidazolidin-4-one 124**



Prepared according to Standard Preparation A.  $\nu_{\max}$  (NaCl disk)/ $\text{cm}^{-1}$  3328, 2929, 1694, 1396, 1097, 1012, 702;  $^1\text{H}$  NMR (500 MHz,  $\text{CDCl}_3$ )  $\delta_{\text{H}}$  7.24–7.22 (3H, m, CH<sub>2</sub>ArH), 7.14–7.12 (2H, m,

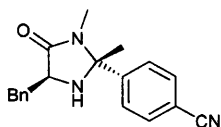
CH<sub>2</sub>ArH), 7.09 (2H, dt, *J* = 8.7 Hz, 2.0 Hz, *o*-ClArH), 6.68 (2H, dt, *J* = 8.7 Hz, 2.0 Hz, *m*-ClArH), 3.85 (1H, t, *J* = 4.8 Hz, COCH), 3.22 (1H, dd, *J* = 14.0 Hz, 5.2 Hz, CH<sub>2</sub>), 2.98 (1H, dd, *J* = 14.0 Hz, 4.8 Hz, CH<sub>2</sub>), 2.43 (3H, s, NCH<sub>3</sub>), 1.61 (3H, s, CCH<sub>3</sub>); <sup>13</sup>C NMR (125 MHz, CDCl<sub>3</sub>) δ<sub>c</sub> 173.4 (C), 140.5 (C), 136.6 (C), 134.6 (C), 129.7 (CH), 128.9 (CH), 128.9 (CH), 127.6 (CH), 127.0 (CH), 78.4 (C), 59.4 (CH), 36.4 (CH<sub>2</sub>), 26.1 (CH<sub>3</sub>), 22.9 (CH<sub>3</sub>); LRMS *m/z* (ES<sup>+</sup>) [M+H]<sup>+</sup> = 315.1; HRMS *m/z* (ES<sup>+</sup>) [M+H]<sup>+</sup> = 315.1256; HRMS *m/z* calc. [M+H]<sup>+</sup> = 315.1264; [α]<sub>D</sub><sup>30</sup> -82.0 (c 0.1, CH<sub>3</sub>OH).

**(2*S*,5*S*)-5-Benzyl-2-(4-chlorophenyl)-2,3-dimethylimidazolidin-4-one hydrochloride 124·HCl**



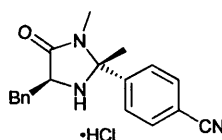
Prepared according to Standard Preparation C. *v*<sub>max</sub> (NaCl disk)/cm<sup>-1</sup> 3414, 1720, 1494, 1392, 1097, 1011, 827; <sup>1</sup>H NMR (500 MHz, CD<sub>3</sub>OD) δ<sub>H</sub> 7.34 (2H, dt, *J* = 8.8 Hz, 2.0 Hz, *o*-ClArH), 7.34 (2H, dt, *J* = 8.8 Hz, 2.0 Hz, *m*-ClArH), 7.29 (2H, d, *J* = 7.5 Hz, *o*-CH<sub>2</sub>ArH), 7.23 (2H, t, *J* = 7.5 Hz, *m*-CH<sub>2</sub>ArH), 7.17 (1H, t, *J* = 7.5 Hz, *p*-CH<sub>2</sub>ArH), 4.33 (1H, dd, *J* = 9.7 Hz, 4.0 Hz, COCH), 3.44 (1H, dd, *J* = 15.2 Hz, 4.0 Hz, CH<sub>2</sub>), 3.12 (1H, dd, *J* = 15.2 Hz, 9.7 Hz, CH<sub>2</sub>), 2.80 (3H, s, NCH<sub>3</sub>), 2.07 (3H, s, CCH<sub>3</sub>); <sup>13</sup>C NMR (125 MHz, CD<sub>3</sub>OD) δ<sub>c</sub> 167.3 (C), 136.8 (C), 134.9 (C), 132.4 (C), 129.6 (CH), 129.0 (CH), 128.7 (CH), 128.2 (CH), 127.3 (CH), 79.6 (C), 58.0 (CH), 33.8 (CH<sub>2</sub>), 25.5 (CH<sub>3</sub>), 22.2 (CH<sub>3</sub>); LRMS *m/z* (ES<sup>+</sup>) [M-Cl]<sup>+</sup> = 315.1; HRMS *m/z* (ES<sup>+</sup>) [M-Cl]<sup>+</sup> = 315.1254; HRMS *m/z* calc. [M-Cl]<sup>+</sup> = 315.1264; Mpt. 118–120 °C; [α]<sub>D</sub><sup>30</sup> -102.6 (c 0.1, CH<sub>3</sub>OH).

**(2*R*,5*S*)-5-Benzyl-2,3-dimethyl-2-(4-cyanophenyl)imidazolidin-4-one 125**



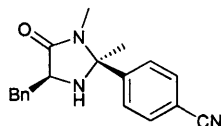
Prepared according to Standard Preparation A. *v*<sub>max</sub> (NaCl disk)/cm<sup>-1</sup> 2228, 1695, 1424, 1396, 1077; <sup>1</sup>H NMR (500 MHz, CDCl<sub>3</sub>) δ<sub>H</sub> 7.57 (2H, dt, *J* = 10.4 Hz, 1.7 Hz, ArH), 7.31 (2H, dt, *J* = 10.4 Hz, 1.7 Hz, ArH), 7.24 (2H, t, *J* = 7.5 Hz, ArH), 7.20–7.15 (3H, m, ArH), 3.72 (1H, dd, *J* = 6.3 Hz, 4.7 Hz, COCH), 3.07 (1H, dd, *J* = 14.1 Hz, 4.7 Hz, CH<sub>2</sub>), 3.00 (1H, dd, *J* = 14.1 Hz, 6.3 Hz, CH<sub>2</sub>), 2.99 (3H, s, NCH<sub>3</sub>), 1.94 (1H, s, NH), 1.45 (3H, s, CCH<sub>3</sub>); <sup>13</sup>C NMR (125 MHz, CDCl<sub>3</sub>) δ<sub>c</sub> 173.6 (C), 147.9 (C), 136.8 (C), 132.7 (CH), 129.6 (CH), 128.7 (CH), 127.0 (CH), 126.1 (CH), 118.3 (C), 112.1 (C), 78.2 (C), 59.0 (CH), 37.6 (CH<sub>2</sub>), 26.3 (CH<sub>3</sub>), 25.8 (CH<sub>3</sub>); LRMS *m/z* (AP<sup>+</sup>) [M+H]<sup>+</sup> = 306.2; HRMS *m/z* (ES<sup>+</sup>) [M+H]<sup>+</sup> = 306.1600; HRMS *m/z* calc. [M+H]<sup>+</sup> = 306.1606; [α]<sub>D</sub><sup>22</sup> 41.8 (c 0.1, CH<sub>3</sub>OH).

**(2*R*,5*S*)-5-Benzyl-2,3-dimethyl-2-(4-cyanophenyl)imidazolidin-4-one hydrochloride 125·HCl**



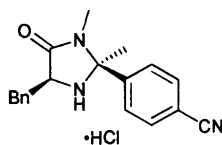
Prepared according to Standard Preparation C.  $\nu_{\max}$  (NaCl disk)/ $\text{cm}^{-1}$  3415, 2534, 2231, 1722, 1395, 1259, 1016;  $^1\text{H}$  NMR (500 MHz,  $\text{CD}_3\text{OD}$ )  $\delta_{\text{H}}$  7.91 (2H, d,  $J$  = 8.6 Hz, ArH), 7.65 (2H, d,  $J$  = 8.6 Hz, ArH), 7.40 (2H, d,  $J$  = 7.5 Hz, ArH), 7.34 (2H, t,  $J$  = 7.5 Hz, ArH), 7.28 (1H, t,  $J$  = 7.5 Hz, ArH), 4.44 (1H, dd,  $J$  = 9.6 Hz, 3.9 Hz, COCH), 3.55 (1H, dd,  $J$  = 15.2 Hz, 3.9 Hz, CH<sub>2</sub>), 3.23 (1H, dd,  $J$  = 15.2 Hz, 9.6 Hz, CH<sub>2</sub>), 2.93 (3H, s, NCH<sub>3</sub>), 2.21 (3H, s, CCH<sub>3</sub>);  $^{13}\text{C}$  NMR (125 MHz,  $\text{CD}_3\text{OD}$ )  $\delta_{\text{C}}$  167.4 (C), 138.7 (C), 134.9 (C), 133.2 (CH), 129.0 (CH), 128.7 (CH), 127.7 (CH), 127.3 (CH), 117.3 (C), 114.5 (C), 79.3 (C), 58.1 (CH), 33.8 (CH<sub>2</sub>), 25.6 (CH<sub>3</sub>), 22.1 (CH<sub>3</sub>); LRMS  $m/z$  (AP<sup>+</sup>)  $[\text{M}-\text{Cl}]^+ = 306.1$ ; HRMS  $m/z$  (ES<sup>+</sup>)  $[\text{M}+\text{H}]^+ = 306.1597$ ; HRMS  $m/z$  calc.  $[\text{M}-\text{Cl}]^+ = 306.1606$ ; Mpt. 109–111 °C;  $[\alpha]_{\text{D}}^{22} +43.6$  (c 0.1,  $\text{CH}_3\text{OH}$ ).

**(2*S*,5*S*)-5-Benzyl-2,3-dimethyl-2-(4-cyanophenyl)imidazolidin-4-one 126**



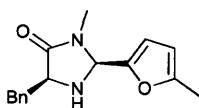
Prepared according to Standard Preparation A.  $\nu_{\max}$  (NaCl disk)/ $\text{cm}^{-1}$  3328, 2228, 1696, 1496, 1395, 1232, 1101;  $^1\text{H}$  NMR (500 MHz,  $\text{CDCl}_3$ )  $\delta_{\text{H}}$  7.42 (2H, d,  $J$  = 8.3 Hz, ArH), 7.23–7.21 (3H, m, ArH), 7.12–7.10 (2H, m, ArH), 6.90 (2H, d,  $J$  = 8.3 Hz, ArH), 3.86–3.90 (1H, m, COCH), 3.17 (1H, dd,  $J$  = 14.0 Hz, 5.4 Hz, CH<sub>2</sub>), 2.97 (1H, dd,  $J$  = 14.0 Hz, 4.7 Hz, CH<sub>2</sub>), 2.45 (3H, s, NCH<sub>3</sub>), 1.90 (1H, s, NH), 1.65 (3H, s, CCH<sub>3</sub>);  $^{13}\text{C}$  NMR (125 MHz,  $\text{CDCl}_3$ )  $\delta_{\text{C}}$  173.3 (C), 147.4 (C), 136.7 (C), 132.5 (CH), 130.0 (CH), 128.9 (CH), 127.0 (CH), 118.2 (C), 112.4 (C), 78.2 (C), 59.3 (CH), 36.7 (CH<sub>2</sub>), 26.1 (CH<sub>3</sub>), 23.0 (CH<sub>3</sub>); LRMS  $m/z$  (AP<sup>+</sup>)  $[\text{M}+\text{H}]^+ = 306.1$ ; HRMS  $m/z$  (ES<sup>+</sup>)  $[\text{M}+\text{H}]^+ = 306.1600$ ; HRMS  $m/z$  calc.  $[\text{M}+\text{H}]^+ = 306.1606$ ;  $[\alpha]_{\text{D}}^{22} -104.6$  (c 0.1,  $\text{CH}_3\text{OH}$ ).

**(2S,5S)-5-Benzyl-2,3-dimethyl-2-(4-cyanophenyl)imidazolidin-4-one hydrochloride 126·HCl**



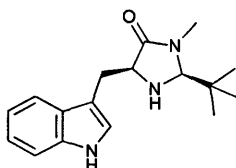
Prepared according to Standard Preparation C.  $\nu_{\max}$  (NaCl disk)/ $\text{cm}^{-1}$  2601, 2230, 1722, 1559, 1394, 1269;  $^1\text{H}$  NMR (500 MHz,  $\text{CD}_3\text{OD}$ )  $\delta_{\text{H}}$  7.81 (2H, d,  $J = 8.5$  Hz, ArH), 7.52 (2H, d,  $J = 8.5$  Hz, ArH), 7.35–7.28 (5H, m, ArH), 4.56 (1H, dd,  $J = 8.3$  Hz, 4.0 Hz, COCH), 3.36 (1H, dd,  $J = 14.9$  Hz, 4.0 Hz, CH<sub>2</sub>), 3.09 (1H, dd,  $J = 14.9$  Hz, 8.3 Hz, CH<sub>2</sub>), 2.73 (3H, s, NCH<sub>3</sub>), 2.02 (3H, s, CCH<sub>3</sub>);  $^{13}\text{C}$  NMR (125 MHz,  $\text{CD}_3\text{OD}$ )  $\delta_{\text{C}}$  168.2 (C), 140.0 (C), 135.0 (C), 133.1 (CH), 129.1 (CH), 128.7 (CH), 128.1 (CH), 127.3 (CH), 117.4 (C), 114.3 (C), 79.9 (C), 58.9 (CH), 34.3 (CH<sub>2</sub>), 26.1 (CH<sub>3</sub>), 19.7 (CH<sub>3</sub>); LRMS  $m/z$  ( $\text{AP}^+$ )  $[\text{M}-\text{Cl}]^+ = 306.1$ ; HRMS  $m/z$  ( $\text{ES}^+$ )  $[\text{M}-\text{Cl}]^+ = 306.1597$ ; HRMS  $m/z$  calc.  $[\text{M}-\text{Cl}]^+ = 306.1606$ ; Mpt. 84–86 °C;  $[\alpha]_{\text{D}}^{22} -124.0$  (c 0.1,  $\text{CH}_3\text{OH}$ ).

**(2S,5S)-5-Benzyl-3-methyl-2-(5-methylfuran-2-yl)imidazolidin-4-one 136**



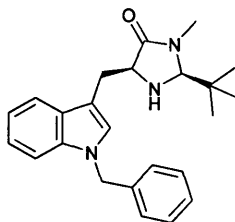
Prepared according to Standard Preparation B.  $\nu_{\max}$  (NaCl disk)/ $\text{cm}^{-1}$  3331, 2920, 1694, 1454, 791, 702;  $^1\text{H}$  NMR (500 MHz,  $\text{CDCl}_3$ )  $\delta_{\text{H}}$  7.20 (2H, t,  $J = 7.3$  Hz, PhH), 7.16–7.11 (3H, m, PhH), 6.02 (1H, d,  $J = 3.1$  Hz, OCCH), 5.80 (1H, dd,  $J = 3.1$  Hz, 0.9 Hz, OCCH), 5.09 (1H, s, ArCH), 3.68 (1H, dd,  $J = 7.6$  Hz, 4.2 Hz, COCH), 3.15 (1H, dd,  $J = 14.2$  Hz, 4.2 Hz, CH<sub>2</sub>), 2.99 (1H, dd,  $J = 14.2$  Hz, 7.6 Hz, CH<sub>2</sub>), 2.54 (3H, s, NCH<sub>3</sub>), 2.11 (1H, s, NH), 2.11 (3H, s, ArCH<sub>3</sub>);  $^{13}\text{C}$  NMR (125 MHz,  $\text{CDCl}_3$ )  $\delta_{\text{C}}$  173.7 (C), 153.3 (C), 148.7 (C), 137.2 (C), 129.4 (CH), 128.6 (CH), 126.7 (CH), 110.8 (CH), 106.4 (CH), 70.9 (CH), 60.1 (CH), 37.6 (CH<sub>2</sub>), 26.9 (CH<sub>3</sub>), 13.5 (CH<sub>3</sub>); LRMS  $m/z$  ( $\text{ES}^+$ )  $[\text{M}+\text{H}]^+ = 271.2$ ; HRMS  $m/z$  ( $\text{ES}^+$ )  $[\text{M}+\text{H}]^+ = 271.1444$ ; HRMS  $m/z$  calc.  $[\text{M}+\text{H}]^+ = 271.1447$ ;  $[\alpha]_{\text{D}}^{30} -151.0$  (c 0.1,  $\text{CH}_3\text{OH}$ ).<sup>63</sup>

**(2S,5S)-5-((1H-Indol-3-yl)methyl)-2-tert-butyl-3-methylimidazolidin-4-one 137**



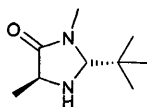
Prepared according to Standard Preparation B.  $\nu_{\max}$  (NaCl disk)/ $\text{cm}^{-1}$  3299, 2960, 1682, 1481, 1432, 1400, 1103;  $^1\text{H}$  NMR (500 MHz,  $\text{CDCl}_3$ )  $\delta_{\text{H}}$  8.38 (1H, s, ArH), 7.62 (1H, d,  $J = 7.8$  Hz, ArH), 7.27 (1H, d,  $J = 7.8$  Hz, ArH), 7.11 (1H, td,  $J = 7.8$  Hz, 0.8 Hz, ArH), 7.05 (1H, td,  $J = 7.8$  Hz, 0.8 Hz, ArH), 7.01 (1H, d,  $J = 2.2$  Hz, ArH), 3.93 (1H, s,  $\text{CH}_3\text{CCH}$ ), 3.64–3.67 (1H, m,  $\text{COCH}$ ), 3.27 (1H, dd,  $J = 14.7$  Hz, 4.2 Hz,  $\text{CH}_2$ ), 3.08 (1H, dd,  $J = 14.7$  Hz, 6.4 Hz,  $\text{CH}_2$ ), 2.81 (3H, s,  $\text{NCH}_3$ ), 1.74 (1H, bs, NH), 0.63 (9H, s,  $\text{CCH}_3$ );  $^{13}\text{C}$  NMR (125 MHz,  $\text{CDCl}_3$ )  $\delta_{\text{C}}$  176.2 (C), 136.3 (C), 128.1 (C), 123.2 (CH), 122.1 (CH), 119.6 (CH), 118.9 (CH), 111.2 (C), 111.2 (CH), 82.6 (CH), 59.5 (CH), 34.7 (C), 30.7 ( $\text{CH}_3$ ), 27.0 ( $\text{CH}_2$ ), 25.3 ( $\text{CH}_3$ ); LRMS  $m/z$  ( $\text{ES}^+$ )  $[\text{M}+\text{H}]^+ = 286.2$ ; HRMS  $m/z$  ( $\text{ES}^+$ )  $[\text{M}+\text{H}]^+ = 286.1925$ ; HRMS  $m/z$  calc.  $[\text{M}+\text{H}]^+ = 268.1919$ ; Mpt. 178–181 °C;  $[\alpha]_{\text{D}}^{30} -85.8$  (c 0.1,  $\text{CH}_3\text{OH}$ ).

**(2R,5S)-5-((1-Benzyl-1H-indol-3-yl)methyl)-2-tert-butyl-3-methylimidazolidin-4-one 138**



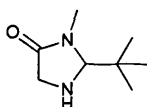
Prepared according to Standard Preparation B.  $\nu_{\max}$  (NaCl disk)/ $\text{cm}^{-1}$  2962, 1720, 1468, 1397, 1262, 740;  $^1\text{H}$  NMR (500 MHz,  $\text{CDCl}_3$ )  $\delta_{\text{H}}$  7.63 (1H, d,  $J = 7.7$  Hz, ArH), 7.21–7.14 (4H, m, ArH), 7.09 (1H, td,  $J = 8.2$  Hz, 1.03 Hz, ArH), 7.05–7.02 (3H, m, ArH), 6.97 (1H, s, ArH), 5.17 (2H, s,  $\text{PhCH}_2$ ), 3.91 (1H, s,  $\text{CH}_3\text{CCH}$ ), 3.63 (1H, t,  $J = 5.0$  Hz,  $\text{COCH}$ ), 3.25 (1H, dd,  $J = 14.7$  Hz, 5.0 Hz,  $\text{CH}_2$ ), 3.09 (1H, dd,  $J = 14.7$  Hz, 5.0 Hz,  $\text{CH}_2$ ), 2.79 (3H, s,  $\text{NCH}_3$ ), 0.60 (9H, s,  $\text{CCH}_3$ );  $^{13}\text{C}$  NMR (125 MHz,  $\text{CDCl}_3$ )  $\delta_{\text{C}}$  176.2 (C), 137.6 (C), 136.6 (C), 128.8 (CH), 128.7 (C), 127.6 (CH), 127.3 (CH), 126.9 (CH), 121.9 (CH), 119.4 (CH), 119.2 (CH), 110.4 (C), 109.7 (CH), 82.6 (CH), 59.4 (CH), 50.0 ( $\text{CH}_2$ ), 34.6 (C), 30.6 ( $\text{CH}_3$ ), 26.9 ( $\text{CH}_2$ ), 25.3 ( $\text{CH}_3$ ); LRMS  $m/z$  ( $\text{ES}^+$ )  $[\text{M}+\text{H}]^+ = 376.2$ ; HRMS  $m/z$  ( $\text{ES}^+$ )  $[\text{M}+\text{H}]^+ = 376.2380$ ; HRMS  $m/z$  calc.  $[\text{M}+\text{H}]^+ = 376.2389$ ;  $[\alpha]_{\text{D}}^{30} -11.4$  (c 0.1,  $\text{CH}_3\text{OH}$ ).

**(2*R*,5*S*)-5-Methyl-2-*tert*-butyl-3-methylimidazolidin-4-one 139**



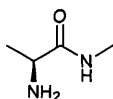
Prepared according to Standard Preparation B.  $\nu_{\max}$  (NaCl disk)/ $\text{cm}^{-1}$  3419, 2981, 1664, 1479, 1404;  $^1\text{H}$  NMR (500 MHz,  $\text{CD}_3\text{OD}$ )  $\delta_{\text{H}}$  4.92 (1H, s,  $\text{CH}_3\text{CCH}$ ), 4.29 (1H, d,  $J = 7.1$  Hz,  $\text{COCH}$ ), 3.08 (3H, s,  $\text{NCH}_3$ ), 1.58 (1H, d,  $J = 7.1$  Hz,  $\text{CHCH}_3$ ), 1.18 (9H, s,  $\text{CHCCH}_3$ );  $^{13}\text{C}$  NMR (125 MHz,  $\text{CD}_3\text{OD}$ )  $\delta_{\text{C}}$  174.7 (C), 84.5 (CH), 49.2 ( $\text{CH}_2$ ), 37.8 (C), 31.1 ( $\text{CH}_3$ ), 25.9 ( $\text{CH}_3$ ); LRMS  $m/z$  ( $\text{AP}^+$ )  $[\text{M}+\text{H}]^+ = 171.2$ ; HRMS  $m/z$  ( $\text{ES}^+$ )  $[\text{M}+\text{H}]^+ = 171.1492$ ; HRMS  $m/z$  calc.  $[\text{M}+\text{H}]^+ = 171.1497$ ;  $[\alpha]_{\text{D}}^{25} -1.8$  ( $c$  0.1,  $\text{CH}_3\text{OH}$ ).

**2-*tert*-Butyl-3-methylimidazolidin-4-one 140**



Prepared according to Standard Preparation B.  $\nu_{\max}$  (NaCl disk)/ $\text{cm}^{-1}$  3339, 2957, 1694, 1483, 1432, 1400, 1322, 1260;  $^1\text{H}$  NMR (500 MHz,  $\text{DMSO}-d_6$ )  $\delta_{\text{H}}$  4.05 (1H, s,  $\text{CH}$ ), 3.21 (2H, s,  $\text{CH}_2$ ), 2.82 (3H, s,  $\text{NCH}_3$ ), 0.89 (9H, s,  $\text{CCH}_3$ );  $^{13}\text{C}$  NMR (125 MHz,  $\text{DMSO}-d_6$ )  $\delta_{\text{C}}$  174.6 (C), 84.5 (CH), 49.2 ( $\text{CH}_2$ ), 37.8 ( $\text{CH}_3$ ), 25.8 ( $\text{CH}_3$ ); LRMS  $m/z$  ( $\text{ES}^+$ )  $[\text{M}+\text{H}]^+ = 157.1$ ; HRMS  $m/z$  ( $\text{ES}^+$ )  $[\text{M}+\text{H}]^+ = 157.1334$ ; HRMS  $m/z$  calc.  $[\text{M}+\text{H}]^+ = 157.1341$ .

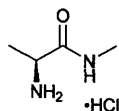
**L-Alanine *N*-methylamide 144**



L-Alanine ethyl ester hydrochloride (8.05 g, 52.4 mmol) was stirred in an ethanolic methylamine solution (36 mL, 289 mmol) for 97 hours then evaporated. The residue was taken up in potassium carbonate (4 M, 30 mL) and sodium bicarbonate (saturated, 20 mL) then extracted with chloroform (5 x 25 mL) which was dried over sodium carbonate and evaporated to yield the desired product, a red oil (3.62 g, 35.5 mmol, 68%).  $\nu_{\max}$  (NaCl disk)/ $\text{cm}^{-1}$  3364, 1646, 1575, 1456, 1413, 1375, 1318, 1272, 1160;  $^1\text{H}$  NMR (500 MHz,  $\text{CDCl}_3$ )  $\delta_{\text{H}}$  7.37 (1H, bs,  $\text{NH}$ ), 3.34 (1H, q,  $J = 7.0$  Hz,  $\text{CH}$ ), 2.66 (3H, d,  $J = 5.0$  Hz,  $\text{NCH}_3$ ), 1.39 (2H, bs,  $\text{NH}_2$ ), 1.17 (3H, d,  $J = 7.0$  Hz,  $\text{CHCH}_3$ );  $^{13}\text{C}$  NMR (125 MHz,  $\text{CDCl}_3$ )  $\delta_{\text{C}}$  176.5 (C), 50.6 (CH), 25.7 ( $\text{CH}_2$ ), 21.6 ( $\text{CH}_3$ ); LRMS  $m/z$  ( $\text{EI}^+$ )  $[\text{M}]^+ = 102.1$ ; HRMS  $m/z$  ( $\text{EI}^+$ )  $[\text{M}]^+ = 102.0788$ ; HRMS  $m/z$  calc.  $[\text{M}]^+ = 102.0793$ ;  $[\alpha]_{\text{D}}^{34} 2.0$  ( $c$  0.1,  $\text{CH}_2\text{Cl}_2$ ).

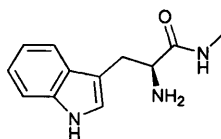


### L-Alanine *N*-methylester hydrochloride **144**·HCl



Hydrogen chloride gas was bubbled through a solution of L-Alanine *N*-methylester **144** (1.90 g, 18.5 mmol) in diethyl ether (200 mL) for 10 minutes before the product was removed by filtration, and washed with diethyl ether to yield the desired product, a clear crystalline solid (2.21 g, 16.0 mmol, 86%). The product was further purified by recrystallisation from ethanol and hexane.  $\nu_{\max}$  (NaCl disk)/ $\text{cm}^{-1}$  3408, 1674, 1514, 1417, 1275, 1169;  $^1\text{H}$  NMR (400 MHz,  $\text{D}_2\text{O}$ )  $\delta_{\text{H}}$  3.85 (1H, q,  $J = 7.1$  Hz,  $\text{CH}$ ), 2.60 (3H, s,  $\text{NCH}_3$ ), 1.32 (3H, d,  $J = 7.1$  Hz,  $\text{CCH}_3$ );  $^{13}\text{C}$  NMR (100 MHz,  $\text{D}_2\text{O}$ )  $\delta_{\text{C}}$  174.1 (C), 51.2 (CH), 28.5 ( $\text{CH}_3$ ), 19.2 ( $\text{CH}_3$ ); LRMS  $m/z$  ( $\text{ES}^+$ )  $[\text{M}-\text{Cl}]^+ = 103.1$ ; HRMS  $m/z$  ( $\text{ES}^+$ )  $[\text{M}-\text{Cl}]^+ = 103.0867$ ; HRMS  $m/z$  calc.  $[\text{M}-\text{Cl}]^+ = 103.0871$ ; Mpt. 213–215 °C;  $[\alpha]_{\text{D}}^{25}$  19.6 (c 0.1,  $\text{CH}_3\text{OH}$ ).

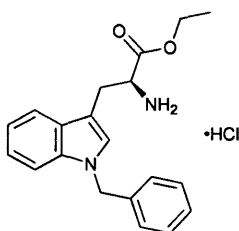
### L-Tryptophan *N*-methylester **147**



Thionyl chloride (10.0 mL, 16.3 g, 134 mmol) was added dropwise to ethanol (130 mL). The solution was cooled to room temperature before L-tryptophan (9.73 g, 47.6 mmol) was added and the mixture stirred for 24 hours then evaporated. The residue was washed with ethyl acetate (1 x 300 mL, 1 x 100 mL) and petroleum ether (ca. 100 mL) then dried to yield a cream solid. The solid was stirred in an ethanolic solution of methylamine (70 mL, 560 mmol) for 120 hours then evaporated, taken up in sodium bicarbonate (saturated, 100 mL) and extracted with chloroform (4 x 40 mL). The combined chloroform was dried over sodium carbonate and evaporated to yield the desired product, a yellow solid (6.1 g, 28 mmol, 59%).  $\nu_{\max}$  (NaCl disk)/ $\text{cm}^{-1}$  3282, 1650, 1537, 1457, 1411, 1342, 1232, 1101;  $^1\text{H}$  NMR (500 MHz,  $\text{DMSO}-d_6$ )  $\delta_{\text{H}}$  10.85 (1H, bs,  $\text{ArH}$ ), 7.79–7.82 (1H, m,  $\text{ArH}$ ), 7.34 (1H, d,  $J = 8.1$  Hz,  $\text{ArH}$ ), 7.15 (1H, d,  $J = 2.2$  Hz,  $\text{ArH}$ ), 7.06 (1H, td,  $J = 7.0$  Hz, 0.9 Hz,  $\text{ArH}$ ), 6.97 (1H, td,  $J = 7.0$  Hz, 0.9 Hz,  $\text{ArH}$ ), 3.41 (1H, dd,  $J = 8.0$  Hz, 4.8 Hz,  $\text{COCH}$ ), 3.06 (1H, dd,  $J = 14.2$  Hz, 4.8 Hz,  $\text{CH}_2$ ), 2.75 (1H, dd,  $J = 14.2$  Hz, 8.0 Hz,  $\text{CH}_2$ ), 2.58 (3H, d,  $J = 4.7$  Hz,  $\text{CH}_3$ ), 1.62 (1H, bs,  $\text{NH}_2$ );  $^{13}\text{C}$  NMR (125 MHz,  $\text{DMSO}-d_6$ )  $\delta_{\text{C}}$  175.7 (C), 136.7 (C), 128.0 (C), 124.2 (CH), 121.3 (CH), 119.0 (CH), 118.7 (CH), 111.8 (CH), 111.3 (C), 56.0 (CH), 31.7 ( $\text{CH}_2$ ), 26.0 ( $\text{CH}_3$ ); LRMS  $m/z$  ( $\text{ES}^+$ )  $[\text{M}+\text{H}]^+ = 218.1$ ;

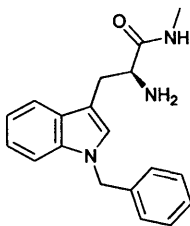
HRMS  $m/z$  ( $ES^+$ )  $[M+H]^+ = 218.1285$ ; HRMS  $m/z$  calc.  $[M+H]^+ = 218.1293$ ; Mpt. 123–125 °C;  $[\alpha]_D^{34} 32.0$  (c 0.1,  $CH_3OH$ ).

### 1-Benzyl-L-tryptophan ethyl ester hydrochloride 149·HCl



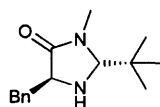
Iron(III) nitrate nonahydrate (0.31 g, 0.78 mmol) was dissolved in liquid ammonia (500 mL). Sodium (3.95 g, 172 mmol) was dissolved and the ammonia was kept at reflux for 1 hour before L-tryptophan (15.4 g, 75.4 mmol) was added, along with anhydrous diethyl ether (10 mL). The reaction was refluxed for 60 minutes and benzyl chloride was added dropwise (12.0 mL, 13.2 g, 104 mmol). The reaction mixture was then allowed to evaporate slowly overnight and quenched by the addition of water (600 mL) then heated to precipitate a solid, which was removed by filtration. The filtrate was treated with glacial acetic acid (65 mL), cooled to around 10 °C and the resultant white precipitate filtered, washed with water (500 mL), ethanol (200 mL), and 40–60 °C petroleum ether (200 mL) then dried *in vacuo*. It was then refluxed for 23 hours in an ethanolic solution of hydrogen chloride formed by the cautious addition of thionyl chloride (30 mL) to ethanol (1.1 L). The solution was then evaporated and the residue washed with 1:1 ethyl acetate:diethyl ether (300 mL) and copious diethyl ether then dried to give the desired product, a fluffy white solid (17.7 g, 43.4 mmol, 58%).  $\nu_{\max}$  (NaCl disk)/ $cm^{-1}$  1736, 1507, 1238, 734, 699;  $^1H$  NMR (500 MHz,  $DMSO-d_6$ )  $\delta_H$  8.81 (3H, s,  $NH_3^+$ ), 7.62 (1H, d,  $J = 7.5$  Hz, ArH), 7.42 (1H, d,  $J = 7.5$  Hz, ArH), 7.39 (1H, s, ArH), 7.31 (2H, t,  $J = 7.5$  Hz, ArH), 7.25 (1H, t,  $J = 7.1$  Hz, ArH), 7.21 (2H, d,  $J = 7.1$  Hz, ArH), 7.12 (1H, t,  $J = 7.1$  Hz, ArH), 7.05 (1H, t,  $J = 7.1$  Hz, ArH), 5.39 (2H, t,  $J = 16.5$  Hz,  $PhCH_2$ ), 4.15 (1H, dd,  $J = 7.9$  Hz, 5.3 Hz, COCH), 4.08 – 3.95 (2H, m,  $CH_3CH_2$ ), 3.41 (1H, dd,  $J = 14.6$  Hz, 5.3 Hz,  $CHCH_2$ ), 3.27 (1H, dd,  $J = 14.6$  Hz, 7.9 Hz,  $CHCH_2$ ), 1.00 (3H, t,  $J = 7.1$  Hz,  $CH_2CH_3$ );  $^{13}C$  NMR (125 MHz,  $DMSO-d_6$ )  $\delta_C$  169.8 (C), 138.6 (C), 136.5 (C), 128.9 (CH), 128.1 (C), 127.8 (CH), 127.5 (CH), 122.0 (CH), 119.4 (CH), 119.0 (CH), 110.7 (CH), 107.3 (C), 62.0 ( $CH_2$ ), 53.3 (CH), 49.5 ( $CH_2$ ), 26.7 ( $CH_2$ ), 14.1 ( $CH_3$ ); LRMS  $m/z$  (EI)  $[M-Cl]^+ = 323.2$ ; HRMS  $m/z$  ( $ES^+$ )  $[M-Cl]^+ = 323.1758$ ; HRMS  $m/z$  calc.  $[M-Cl]^+ = 323.1760$ ; Mpt. 192–195 °C;  $[\alpha]_D^{25} 4.6$  (c 0.1,  $CH_2Cl_2$ ).

### 1-Benzyl-L-tryptophan *N*-methanamide 150



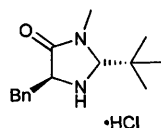
1-Benzyltryptophan ethyl ester hydrochloride **149**·HCl (5.34 g, 14.9 mmol) was taken up in potassium carbonate (4 M, 100 mL) and extracted with chloroform (3 x 50 mL). The chloroform was evaporated and the residue was stirred in an ethanolic methanamine solution (25 mL, 201 mmol) for 62 hours then evaporated and dried to yield the desired product, a cream solid (3.71 g, 12.1 mmol, 86%).  $\nu_{\max}$  (NaCl disk)/ $\text{cm}^{-1}$  3362, 3059, 2935, 1655, 1537, 1467, 1333, 1178;  $^1\text{H}$  NMR (500 MHz,  $\text{CDCl}_3$ )  $\delta_{\text{H}}$  7.61 (1H, d,  $J = 7.9$  Hz, ArH), 7.23–7.16 (5H, m, ArH, NH), 7.11 (1H, td,  $J = 8.2$  Hz, 1.0 Hz, ArH), 7.06–7.02 (3H, m, ArH), 6.91 (1H, s, ArH), 5.19 (2H, s,  $\text{PhCH}_2$ ), 3.62 (1H, dd,  $J = 8.8$  Hz, 3.9 Hz, COCH), 3.30 (1H, dd,  $J = 14.5$  Hz, 3.9 Hz, CHCH<sub>2</sub>), 2.84 (1H, dd,  $J = 14.5$  Hz, 8.8 Hz, CHCH<sub>2</sub>), 2.70 (3H, d,  $J = 5.0$  Hz, CH<sub>3</sub>), 1.40 (2H, bs, NH<sub>2</sub>);  $^{13}\text{C}$  NMR (125 MHz,  $\text{CDCl}_3$ )  $\delta_{\text{C}}$  175.5 (C), 137.6 (C), 136.9 (C), 128.8 (CH), 128.4 (C), 127.7 (CH), 127.2 (CH), 126.9 (CH), 122.1 (CH), 119.4 (CH), 119.3 (CH), 111.1 (C), 109.9 (CH), 55.8 (CH), 49.9 (CH<sub>2</sub>), 30.9 (CH<sub>2</sub>), 25.8 (CH<sub>3</sub>); LRMS  $m/z$  ( $\text{ES}^+$ )  $[\text{M}+\text{H}]^+ = 308.2$ ; HRMS  $m/z$  ( $\text{ES}^+$ )  $[\text{M}+\text{H}]^+ = 308.1756$ ; HRMS  $m/z$  calc.  $[\text{M}+\text{H}]^+ = 308.1763$ ; Mpt. 80–82 °C;  $[\alpha]_{\text{D}}^{34} -51.8$  (c 0.1,  $\text{CH}_2\text{Cl}_2$ ).

### (2*R*,5*S*)-5-Benzyl-2-*tert*-butyl-3-methylimidazolidin-4-one 151



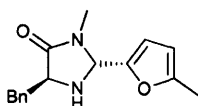
Prepared according to Standard Preparation B.  $\nu_{\max}$  (NaCl disk)/ $\text{cm}^{-1}$  2956, 1691, 1454, 1397, 1104, 702;  $^1\text{H}$  NMR (500 MHz,  $\text{CDCl}_3$ )  $\delta_{\text{H}}$  7.30 (2H, t,  $J = 7.1$  Hz, ArH), 7.25–7.22 (3H, m, ArH), 3.84–3.87 (1H, m, COCH), 3.81 (1H, d,  $J = 1.8$  Hz, CH<sub>3</sub>CCH), 3.11 (1H, dd,  $J = 14.0$  Hz, 4.2 Hz, CH<sub>2</sub>), 2.90 (1H, dd,  $J = 14.0$  Hz, 7.1 Hz, CH<sub>2</sub>), 2.89 (3H, s, NCH<sub>3</sub>), 0.90 (9H, s, CCH<sub>3</sub>);  $^{13}\text{C}$  NMR (125 MHz,  $\text{CDCl}_3$ )  $\delta_{\text{C}}$  175.3 (C), 137.5 (C), 129.5 (CH), 128.5 (CH), 126.7 (CH), 83.4 (CH), 59.5 (CH), 38.6 (CH<sub>2</sub>), 37.7 (C), 41.3 (CH<sub>3</sub>), 25.6 (CH<sub>3</sub>); LRMS  $m/z$  ( $\text{ES}^+$ )  $[\text{M}+\text{H}]^+ = 247.2$ ; HRMS  $m/z$  ( $\text{ES}^+$ )  $[\text{M}+\text{H}]^+ = 247.1802$ ; HRMS  $m/z$  calc.  $[\text{M}+\text{H}]^+ = 247.1810$ ; Mpt. 86–88 °C;  $[\alpha]_{\text{D}}^{30} -51.2$  (c 0.1,  $\text{CH}_3\text{OH}$ ).

**(2*R*,5*S*)-5-Benzyl-2-*tert*-butyl-3-methylimidazolidin-4-one hydrochloride 151·HCl**



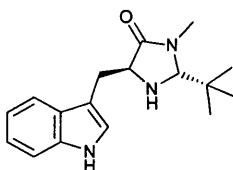
Prepared according to Standard Preparation C.  $\nu_{\max}$  (NaCl disk)/ $\text{cm}^{-1}$  1704, 1458, 1398, 1338, 1064;  $^1\text{H}$  NMR (500 MHz,  $\text{CD}_3\text{OD}$ )  $\delta_{\text{H}}$  7.34 (2H, t,  $J = 7.5$  Hz, ArH), 7.28 (2H, t,  $J = 7.5$  Hz, ArH), 7.22 (1H, t,  $J = 7.5$  Hz, *p*-ArH), 4.59 (1H, s,  $\text{CH}_3\text{CCH}$ ), 4.37 (1H, dd,  $J = 8.6$  Hz, 4.6 Hz, COCH), 3.34 (1H, dd,  $J = 15.0$  Hz, 4.6 Hz,  $\text{CH}_2$ ), 3.05 (1H, dd,  $J = 15.0$  Hz, 8.6 Hz,  $\text{CH}_2$ ), 2.96 (3H, s,  $\text{NCH}_3$ ), 1.01 (9H, s,  $\text{CCH}_3$ );  $^{13}\text{C}$  NMR (125 MHz,  $\text{CD}_3\text{OD}$ )  $\delta_{\text{C}}$  168.4 (C), 134.7 (C), 129.3 (CH), 128.7 (CH), 127.4 (CH), 81.2 (CH), 58.9 (CH), 36.2 (C), 35.2 ( $\text{CH}_3$ ), 31.1 (C), 23.9 ( $\text{CH}_3$ ); LRMS  $m/z$  ( $\text{ES}^+$ )  $[\text{M}-\text{Cl}]^+ = 247.2$ ; HRMS  $m/z$  ( $\text{ES}^+$ )  $[\text{M}-\text{Cl}]^+ = 247.1801$ ; HRMS  $m/z$  calc.  $[\text{M}-\text{Cl}]^+ = 247.1810$ ; decomp. 145 °C;  $[\alpha]_{\text{D}}^{34} -72.2$  (*c* 0.1,  $\text{CH}_3\text{OH}$ ).

**(2*R*,5*S*)-5-Benzyl-3-methyl-2-(5-methylfuran-2-yl)imidazolidin-4-one 152**



Prepared according to Standard Preparation B.  $\nu_{\max}$  (NaCl disk)/ $\text{cm}^{-1}$  3354, 1697, 1454, 1400, 1334, 1262, 1217, 1094, 1021;  $^1\text{H}$  NMR (500 MHz,  $\text{CDCl}_3$ )  $\delta_{\text{H}}$  7.20–7.18 (4H, m, PhH), 7.12–7.16 (1H, m, PhH), 6.09 (1H, d,  $J = 3.1$  Hz, OCCH), 5.80 (1H, d,  $J = 2.4$  Hz, OCCH), 4.85 (1H, s, ArCH), 3.94 (1H, dd,  $J = 7.3$  Hz, 4.0 Hz, COCH), 3.05 (1H, dd,  $J = 13.8$  Hz, 4.0 Hz,  $\text{CH}_2$ ), 2.85 (1H, dd,  $J = 13.8$  Hz, 7.3 Hz,  $\text{CH}_2$ ), 2.55 (3H, s,  $\text{NCH}_3$ ), 2.14 (3H, s, ArCH<sub>3</sub>), 2.26 (1H, bs, NH);  $^{13}\text{C}$  NMR (125 MHz,  $\text{CDCl}_3$ )  $\delta_{\text{C}}$  173.7 (C), 153.3 (C), 149.2 (C), 137.7 (C), 129.6 (CH), 128.4 (CH), 126.6 (CH), 110.2 (CH), 106.3 (CH), 70.9 (CH), 59.7 (CH), 38.3 ( $\text{CH}_2$ ), 27.0 ( $\text{CH}_3$ ), 13.6 ( $\text{CH}_3$ ); LRMS  $m/z$  ( $\text{AP}^+$ )  $[\text{M}+\text{H}]^+ = 271.1$ ; HRMS  $m/z$  ( $\text{ES}^+$ )  $[\text{M}+\text{H}]^+ = 271.1443$ ; HRMS  $m/z$  calc.  $[\text{M}+\text{H}]^+ = 271.1447$ ;  $[\alpha]_{\text{D}}^{30} 29.2$  (*c* 0.1,  $\text{CH}_3\text{OH}$ ).

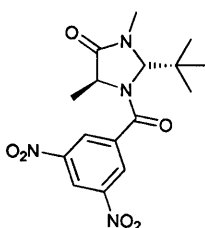
**(2*S*,5*S*)-5-((1*H*-Indol-3-yl)methyl)-2-*tert*-butyl-3-methylimidazolidin-4-one 153**



Prepared according to Standard Preparation B.  $\nu_{\max}$  (NaCl disk)/ $\text{cm}^{-1}$  3298, 2957, 1678, 1457, 1400, 1258, 1100;  $^1\text{H}$  NMR (500 MHz,  $\text{CDCl}_3$ )  $\delta_{\text{H}}$  8.32 (1H, s, ArH), 7.58 (1H, d,  $J = 8.0$  Hz, ArH),

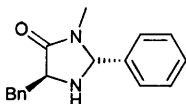
7.28 (ArH, d,  $J = 8.0$  Hz, ArH), 7.12 (1H, td,  $J = 7.6$  Hz, 0.96 Hz, ArH), 7.04 (1H, td,  $J = 7.6$  Hz, 0.7 Hz, ArH), 7.01 (1H, d,  $J = 2.3$  Hz, ArH), 3.82 (1H, t,  $J = 5.2$  Hz, COCH), 3.69 (1H, d,  $J = 1.57$  Hz, CH<sub>3</sub>CCH), 3.21 (1H, dd,  $J = 15.0$  Hz, 5.2 Hz, CH<sub>2</sub>), 3.03 (1H, dd,  $J = 15.0$  Hz, 5.2 Hz, CH<sub>2</sub>), 2.80 (3H, s, NCH<sub>3</sub>), 0.81 (3H, s, CCH<sub>3</sub>); <sup>13</sup>C NMR (125 MHz, CDCl<sub>3</sub>)  $\delta_c$  176.1 (C), 136.3 (C), 128.0 (C), 123.3 (CH), 122.1 (CH), 119.6 (CH), 119.0 (CH), 111.2 (CH), 110.9 (C), 83.4 (CH), 59.2 (CH), 37.9 (C), 31.4 (CH<sub>3</sub>), 27.7 (CH<sub>2</sub>), 25.7 (CH<sub>3</sub>); LRMS  $m/z$  (AP<sup>+</sup>) [M+H]<sup>+</sup> = 286.2; HRMS  $m/z$  (ES<sup>+</sup>) [M+H]<sup>+</sup> = 286.1911; HRMS  $m/z$  calc. [M+H]<sup>+</sup> = 286.1919; [ $\alpha$ ]<sub>D</sub><sup>30</sup> -64.4 (c 0.1, CH<sub>3</sub>OH).

**(2R,5S)-2-*tert*-Butyl-1-(3,5-dinitrobenzoyl)-3,5-dimethylimidazolidin-4-one 158**



(2R,5S)-5-Methyl-2-*tert*-butyl-3-methylimidazolidin-4-one **139** (0.028 g, 0.16 mmol), 3,5-dinitrobenzoyl chloride (0.060 g, 0.26 mmol) and triethylamine (0.040 mL, 0.030 g, 0.30 mmol) were stirred in DCM (2 mL) for 1 hour, before sodium hydroxide (4 M, 2 mL) was added and stirring was continued for 10 minutes. The mixture was poured into sodium bicarbonate (saturated, 20 mL), extracted with chloroform (20 mL), dried over sodium carbonate, and column chromatography (1:1 petroleum ether:ethyl acetate) used to obtain the desired product ( $R_f$ : 0.38), a cream solid.  $\nu_{\max}$  (NaCl disk)/cm<sup>-1</sup> 3403, 1695, 1651, 1537, 1345; <sup>1</sup>H NMR (500 MHz, CDCl<sub>3</sub>)  $\delta_H$  9.20 (1H, t,  $J = 2.0$  Hz, *p*-ArH), 8.75 (2H, s, *o*-ArH), 5.69 (1H, s, (CH<sub>3</sub>)<sub>3</sub>CCH), 4.36 (1H, q,  $J = 6.5$  Hz, COCH), 4.35 (3H, s, NCH<sub>3</sub>), 4.34 (9H, s, (CH<sub>3</sub>)<sub>3</sub>C), 1.09 (3H, s, COCCH<sub>3</sub>); <sup>13</sup>C NMR (125 MHz, CDCl<sub>3</sub>)  $\delta_c$  170.8 (C), 166.2 (C), 148.9 (C), 140.3 (C), 127.5 (CH), 121.1 (CH), 80.3 (CH), 56.8 (CH), 40.8 (C), 32.3 (CH<sub>3</sub>), 26.4 (CH<sub>3</sub>), 20.3 (CH<sub>3</sub>); LRMS  $m/z$  (AP<sup>+</sup>) [M+H]<sup>+</sup> = 365.2; HRMS  $m/z$  (AP<sup>+</sup>) [M+H]<sup>+</sup> = 365.1445; HRMS  $m/z$  calc. [M+H]<sup>+</sup> = 365.1461; Mpt. 209–210 °C; [ $\alpha$ ]<sub>D</sub><sup>25</sup> 140 (c 0.01, CH<sub>3</sub>CN).

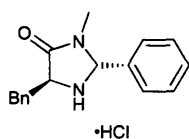
**(2R,5S)-5-Benzyl-3-methyl-2-phenylimidazolidin-4-one 169**



Prepared according to Standard Preparation A.  $\nu_{\max}$  (NaCl disk)/cm<sup>-1</sup> 3326, 2920, 1694, 1455, 1400, 754, 700; <sup>1</sup>H NMR (500 MHz, CDCl<sub>3</sub>)  $\delta_H$  7.28–7.24 (3H, m, ArH), 7.21–7.18 (4H, m, ArH), 7.15–7.11 (3H, m, ArH), 4.77 (1H, d,  $J = 1.5$  Hz, NCH<sub>3</sub>CH), 3.94–3.97 (1H, m, COCH), 3.03 (1H,

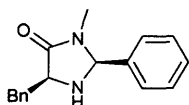
dd,  $J = 13.7$  Hz, 4.0 Hz,  $\text{CH}_2$ ), 2.86 (1H, dd,  $J = 13.7$  Hz, 7.4 Hz,  $\text{CH}_2$ ), 2.48 (3H, s,  $\text{NCH}_3$ );  $^{13}\text{C}$  NMR (125 MHz,  $\text{CDCl}_3$ )  $\delta_{\text{C}}$  174.2 (C), 139.4 (C), 137.8 (C), 129.7 (CH), 129.3 (CH), 129.1 (CH), 128.6 (CH), 128.4 (CH), 126.7 (CH), 77.8 (CH), 60.1 (CH), 38.8 ( $\text{CH}_2$ ), 27.2 ( $\text{CH}_3$ ); LRMS  $m/z$  ( $\text{EI}^+$ )  $[\text{M}]^+ = 266.1$ ; HRMS  $m/z$  ( $\text{EI}^+$ )  $[\text{M}]^+ = 266.1412$ ; HRMS  $m/z$  calc.  $[\text{M}]^+ = 266.1419$ ;  $[\alpha]_{\text{D}}^{34} 31.0$  (c 0.1,  $\text{CH}_2\text{Cl}_2$ ).

**(2R,5S)-5-Benzyl-3-methyl-2-phenylimidazolidin-4-one 169·HCl**



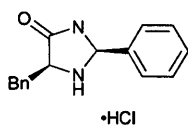
Prepared according to Standard Preparation C (64%).  $\nu_{\text{max}}$  (NaCl disk)/ $\text{cm}^{-1}$  2478, 1716, 1457, 1402, 699;  $^1\text{H}$  NMR (500 MHz,  $\text{CD}_3\text{OD}$ )  $\delta_{\text{H}}$  7.60–7.57 (3H, m,  $\text{ArH}$ ), 7.52–7.50 (2H, m,  $\text{ArH}$ ), 7.46 (2H, d,  $J = 7.3$  Hz,  $\text{ArH}$ ), 7.39 (2H, t,  $J = 7.3$  Hz,  $\text{ArH}$ ), 7.33 (1H, t,  $J = 7.3$  Hz,  $\text{ArH}$ ), 5.93 (1H, s,  $\text{ArCH}$ ), 4.70 (1H, dd,  $J = 10.0$  Hz, 3.8 Hz,  $\text{COCH}$ ), 3.57 (1H, dd,  $J = 15.1$  Hz, 3.8 Hz,  $\text{CH}_2$ ), 3.24 (1H, dd,  $J = 15.1$  Hz, 10.0 Hz,  $\text{CH}_2$ ), 2.84 (3H, s,  $\text{CH}_3$ );  $^{13}\text{C}$  NMR (125 MHz,  $\text{CD}_3\text{OD}$ )  $\delta_{\text{C}}$  167.4 (C), 134.7 (C), 131.4 (CH), 130.5 (C), 129.6 (CH), 128.9 (CH), 128.8 (CH), 127.7 (CH), 127.5 (CH), 74.0 (CH), 58.0 (CH), 34.3 ( $\text{CH}_2$ ), 26.7 ( $\text{CH}_3$ ); LRMS  $m/z$  ( $\text{AP}^+$ )  $[\text{M}-\text{Cl}]^+ = 267.2$ ; HRMS  $m/z$  ( $\text{ES}^+$ )  $[\text{M}-\text{Cl}]^+ = 267.1490$ ; HRMS  $m/z$  calc.  $[\text{M}-\text{Cl}]^+ = 267.1497$ ; Mpt. 130–132 °C;  $[\alpha]_{\text{D}}^{34} 11.8$  (c 0.1,  $\text{CH}_3\text{OH}$ ).

**(2S,5S)-5-Benzyl-3-methyl-2-phenylimidazolidin-4-one 170**



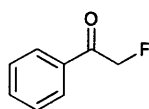
Prepared according to Standard Preparation A.  $\nu_{\text{max}}$  (NaCl disk)/ $\text{cm}^{-1}$  3328, 3030, 1690, 1458, 1401, 1097;  $^1\text{H}$  NMR (500 MHz,  $\text{CDCl}_3$ )  $\delta_{\text{H}}$  7.34–7.24 (8H, m,  $\text{ArH}$ ), 6.85 (2H, d,  $J = 7.3$  Hz,  $\text{ArH}$ ), 5.14 (1H, s,  $\text{NCH}_3\text{CH}$ ), 3.88 (1H, t,  $J = 5.1$  Hz,  $\text{COCH}$ ), 3.25 (1H, dd,  $J = 14.1$  Hz, 5.1 Hz,  $\text{CH}_2$ ), 3.15 (1H, dd,  $J = 14.1$  Hz, 4.1 Hz,  $\text{CH}_2$ ), 2.56 (3H, s,  $\text{NCH}_3$ );  $^{13}\text{C}$  NMR (125 MHz,  $\text{CDCl}_3$ )  $\delta_{\text{C}}$  174.4 (C), 138.5 (C), 136.8 (C), 129.8 (CH), 129.5 (CH), 129.0 (CH), 128.8 (CH), 127.1 (CH), 126.9 (CH), 77.6 (CH), 60.5 (CH), 37.0 ( $\text{CH}_2$ ), 27.3 ( $\text{CH}_3$ ); LRMS  $m/z$  ( $\text{EI}^+$ )  $[\text{M}]^+ = 266.1$ ; HRMS  $m/z$  ( $\text{EI}^+$ )  $[\text{M}]^+ = 266.1414$ ; HRMS  $m/z$  calc.  $[\text{M}]^+ = 266.1419$ ;  $[\alpha]_{\text{D}}^{34} -138.0$  (c 0.1,  $\text{CH}_2\text{Cl}_2$ ).

**(2S,5S)-5-Benzyl-3-methyl-2-phenylimidazolidin-4-one hydrochloride 170·HCl**



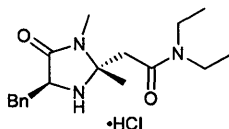
Prepared according to Standard Preparation C (75%).  $\nu_{\max}$  (NaCl disk)/ $\text{cm}^{-1}$  3381, 2517, 1719, 1462, 1419, 699;  $^1\text{H}$  NMR (500 MHz,  $\text{CD}_3\text{OD}$ )  $\delta_{\text{H}}$  7.64–7.57 (3H, m, ArH), 7.50–7.48 (2H, m, ArH), 7.43–7.38 (4H, m, ArH), 7.36–7.34 (1H, m, ArH), 5.90 (1H, s, ArCH), 4.63 (1H, dd,  $J = 9.9$  Hz, 3.7 Hz, COCH), 3.57 (1H, dd,  $J = 15.4$  Hz, 3.7 Hz, CH<sub>2</sub>), 3.18 (1H, dd,  $J = 15.4$  Hz, 9.9 Hz, CH<sub>2</sub>), 2.82 (3H, s, CH<sub>3</sub>);  $^{13}\text{C}$  NMR (125 MHz,  $\text{CD}_3\text{OD}$ )  $\delta_{\text{C}}$  168.4 (C), 135.0 (C), 131.5 (CH), 129.9 (C), 129.5 (CH), 128.8 (CH), 128.4 (CH), 127.4 (CH), 74.2 (CH), 59.9 (CH), 33.8 (CH<sub>2</sub>), 27.3 (CH<sub>3</sub>); LRMS  $m/z$  (AP<sup>+</sup>)  $[\text{M}-\text{Cl}]^+ = 267.2$ ; HRMS  $m/z$  (ES<sup>+</sup>)  $[\text{M}-\text{Cl}]^+ = 267.1493$ ; HRMS  $m/z$  calc.  $[\text{M}-\text{Cl}]^+ = 267.1497$ ;  $[\alpha]_{\text{D}}^{25} -54.0$  ( $c$  0.1,  $\text{CH}_3\text{OH}$ ).

**2-Fluoroacetophenone 186**



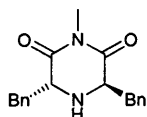
To a solution of acetophenone (130.9 g, 1089 mmol) and 45% hydrogen bromide in acetic acid (1.2 mL) in DCM (370 mL) at  $-8^\circ\text{C}$  was added bromine (56 mL, 174 g, 1.09 mol) dropwise over the course of 30 minutes. The mixture was allowed to warm to room temperature and was stirred for 5 minutes, before being evaporated and the residue recrystallised from hexanes to yield 2-bromoacetophenone as a cream solid (81.8 g, 410 mmol, 38%). 2-bromoacetophenone (31.8 g, 160 mmol), potassium fluoride (44.6, 768 mmol), tetrabutylammonium bisulfate (7.47, 22.0 mmol) and triphenyltin fluoride (6.61 g, 17.9 mmol) in acetonitrile (120 mL) were refluxed for 69 hours before being cooled, filtered and evaporated. The residue was taken up in water (400 mL), extracted with diethyl ether (1 x 200 mL, 2 x 100 mL), dried over magnesium sulfate, treated with pyridine (10 mL) and refluxed for 20 minutes. The reaction mixture was washed with hydrochloric acid (4 M, 2 x 100 mL), dried over magnesium sulfate and evaporated and the desired product isolated by distillation ( $105^\circ\text{C}$ , 1 mbar) as a clear crystalline solid (11.53 g, 83.5 mmol, 52%).  $\nu_{\max}$  (NaCl disk)/ $\text{cm}^{-1}$  1707, 1598, 1451, 1233, 1089, 968, 757;  $^1\text{H}$  NMR (400 MHz,  $\text{CDCl}_3$ )  $\delta_{\text{H}}$  7.89 (2H, d,  $J = 7.6$  Hz,  $o\text{-ArH}$ ), 7.63 (1H, t,  $J = 7.6$  Hz,  $p\text{-ArH}$ ), 7.50 (2H, t,  $J = 7.6$  Hz,  $m\text{-ArH}$ ), 5.55 (2H, d,  $J = 46.8$  Hz, CH<sub>2</sub>F);  $^{13}\text{C}$  NMR (100 MHz,  $\text{CDCl}_3$ )  $\delta_{\text{C}}$  193.4 (C, d,  $J = 15$  Hz), 134.2 (CH), 133.6 (C), 129.0 (CH), 127.8 (CH, d,  $J = 22$  Hz), 83.5 (CH<sub>2</sub>, d,  $J = 182$  Hz); LRMS  $m/z$  (EI<sup>+</sup>)  $[\text{M}]^+ = 138.0$ ; HRMS  $m/z$  (EI<sup>+</sup>)  $[\text{M}]^+ = 138.0476$ ; HRMS  $m/z$  calc.  $[\text{M}]^+ = 138.0481$ ; Mpt.  $25\text{--}27^\circ\text{C}$ .<sup>76</sup>

**2-((2R,4S)-4-Benzyl-1,2-dimethyl-5-oxoimidazolidin-2-yl)-N,N-diethylacetamide hydrochloride 201·HCl**



L-Phenylalanine *N*-methylamide **62** (7.94 g, 44.6 mmol), *N,N*-diethylacetoacetamide (7.69 g, 48.9 mmol) and ytterbium(III) trifluoromethanesulfonate (0.85 g, 1.4 mmol) were refluxed in toluene (300 mL) for 15 hours, cooled to room temperature, filtered, and the clear solution treated with hydrogen chloride gas for 30 minutes. The mixed hydrochloride salts were isolated by filtration, washed with diethyl ether and recrystallised repeatedly from acetonitrile:chloroform:diethyl ether:ethyl acetate and DCM:hexanes to provide the desired product as clear crystals (0.12 g, 0.34 mmol, 1%).  $\nu_{\max}$  (NaCl disk)/ $\text{cm}^{-1}$  2909, 2380, 1717, 1616, 1456, 1394, 1354, 1265;  $^1\text{H}$  NMR (500 MHz,  $\text{CH}_3\text{OD}$ )  $\delta_{\text{H}}$  7.41–7.37 (4H, m, ArH), 7.32 (1H, t,  $J$  = 6.4 Hz, ArH), 4.73 (1H, dd,  $J$  = 8.7 Hz, 4.8 Hz, COCH), 3.49–3.37 (5H, m, PhCH<sub>2</sub>, NCH<sub>2</sub>), 3.26–3.19 (2H, m, PhCH<sub>2</sub>, COCH<sub>2</sub>), 3.09 (1H, d,  $J$  = 17.1 Hz, COCH<sub>2</sub>), 2.91 (3H, s, NCH<sub>3</sub>), 1.67 (3H, s, CCH<sub>3</sub>), 1.21 (3H, t,  $J$  = 7.1 Hz, CH<sub>2</sub>CH<sub>3</sub>), 1.10 (3H, t,  $J$  = 7.1 Hz, CH<sub>2</sub>CH<sub>3</sub>);  $^{13}\text{C}$  NMR (125 MHz,  $\text{CDCl}_3$ )  $\delta_{\text{C}}$  166.6 (C), 165.8 (C), 133.4 (C), 127.2 (CH), 127.1 (CH), 125.8 (CH), 76.9 (C), 56.7 (CH), 40.6 (CH<sub>2</sub>), 38.9 (CH<sub>2</sub>), 33.6 (CH<sub>2</sub>), 32.5 (CH<sub>2</sub>), 23.2 (CH<sub>3</sub>), 20.7 (CH<sub>3</sub>), 11.5 (CH<sub>3</sub>), 10.1 (CH<sub>3</sub>); HRMS  $m/z$  ( $\text{ES}^+$ ) [ $\text{M}-\text{Cl}$ ] $^+$  = 318.2178; HRMS  $m/z$  calc. [ $\text{M}-\text{Cl}$ ] $^+$  = 318.2182; decomp. 158 °C;  $[\alpha]_{\text{D}}^{22}$  21.2 ( $c$  0.1,  $\text{CH}_3\text{OH}$ ).

**(3R,5R)-3,5-Dibenzyl-1-methylpiperazine-2,6-dione 227**

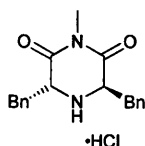


(*R*)-Methyl-2-((*R*)-1-(methylamino)-1-oxo-3-phenylpropan-2-ylamino)-3-phenylpropanoate **230** (0.480 g, 1.41 mmol) was dissolved in diethyl ether (25 mL) and sodium methoxide (0.062 g, 1.15 mmol) was added. The suspension was stirred for four hours at room temperature then washed with brine (2 x 30 mL) and evaporated to yield an off-white solid that was purified *via* column chromatography (1:1 petroleum ether:diethyl ether) to give the desired product **16** ( $R_{\text{f}}$ : 0.38) as a white solid (0.33 g, 1.07 mmol, 76%).  $\nu_{\max}$  (NaCl disk)/ $\text{cm}^{-1}$  3401, 3321, 1728, 1675, 1296, 1118;  $^1\text{H}$  NMR (500 MHz,  $\text{CDCl}_3$ )  $\delta_{\text{H}}$  7.24 – 7.19 (6H, m, ArH), 7.00 (4H, dd,  $J$  = 7.1 Hz,  $J$  = 1.1 Hz, ArH), 3.89 (2H, dd,  $J$  = 10.6 Hz,  $J$  = 3.3 Hz, COCH), 3.29 (2H, dd,  $J$  = 13.7 Hz,  $J$  = 3.3 Hz, CH<sub>2</sub>), 3.23 (3H, s, NCH<sub>3</sub>), 2.87 (2H, dd,  $J$  = 13.7 Hz,  $J$  = 10.7 Hz, CH<sub>2</sub>);  $^{13}\text{C}$  NMR (125 MHz,  $\text{CDCl}_3$ )  $\delta_{\text{C}}$  172.4 (C), 136.7 (C), 129.1 (CH), 128.9 (CH), 126.8 (CH), 57.1 (CH), 36.2 (CH<sub>2</sub>), 26.4 (CH<sub>3</sub>); LRMS  $m/z$  ( $\text{ES}^+$ ) [ $\text{M}+\text{H}$ ] $^+$  = 309.2; HRMS  $m/z$  ( $\text{ES}^+$ )



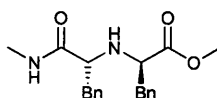
$[M+H]^+ = 309.1601$ ; HRMS  $m/z$  calc.  $[M+H]^+ = 309.1603$ ; Mpt. 70–72 °C;  $[\alpha]_D^{32} 54.6$  (c 0.1, CH<sub>2</sub>Cl<sub>2</sub>).

**(3*R*,5*R*)-3,5-Dibenzyl-1-methylpiperazine-2,6-dione hydrochloride 227·HCl**



Prepared according to Standard Preparation C (70%).  $\nu_{\max}$  (NaCl disk)/cm<sup>-1</sup> 2354, 1692, 1427, 1300, 1137, 749, 700; <sup>1</sup>H NMR (500 MHz, CD<sub>3</sub>OD)  $\delta_H$  7.39–7.28 (10H, m, ArH), 4.62 (2H, t,  $J = 6.8$  Hz, CH), 3.53 (2H, dd,  $J = 14.6$  Hz, 6.8 Hz, CH<sub>2</sub>), 3.29 (2H, dd,  $J = 14.6$  Hz, 7.8 Hz, CH<sub>2</sub>), 3.24 (3H, s, CH<sub>3</sub>); <sup>13</sup>C NMR (125 MHz, CD<sub>3</sub>OD)  $\delta_C$  166.4 (C), 134.0 (C), 129.2 (CH), 128.9 (CH), 127.7 (CH), 55.9 (CH), 34.1 (CH<sub>2</sub>), 26.0 (CH<sub>3</sub>); LRMS  $m/z$  (AP<sup>+</sup>)  $[M-Cl]^+ = 309.2$ ; HRMS  $m/z$  (ES<sup>+</sup>)  $[M-Cl]^+ = 309.1600$ ; HRMS  $m/z$  calc.  $[M-Cl]^+ = 309.1603$ ; Mpt. 87–89 °C;  $[\alpha]_D^{34} 31.2$  (c 0.1, CH<sub>2</sub>Cl<sub>2</sub>).

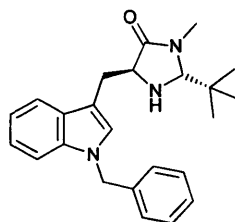
**(*R*)-Methyl 2-((*R*)-1-(methylanino)-1-oxo-3-phenylpropan-2-ylamino)-3-phenylpropanoate 230**



To a solution of trifluoromethanesulfonic anhydride (1.0 mL, 1.68 g, 5.96 mmol) in dichloromethane (6 mL) at –42 °C was added a solution of methyl L-3-phenyllactate (1.09 g, 6.07 mmol) and triethylamine (1.0 mL, 0.72 g, 7.11 mmol) in dichloromethane (6 mL) dropwise. The combined solution was allowed to warm slowly to room temperature and stirred for 2 hours, before it was evaporated and the residual oil extracted with petroleum ether (6 x 10 mL). The combined extracts were evaporated and a solution of D-Phenylalanine *N*-methanide (1.14 g, 6.38 mmol) and triethylamine (1.0 mL, 0.72g, 7.11 mmol) in dichloromethane (15 mL) was added and the mixture stirred for 19 hours at room temperature. The mixture was then evaporated and the residue taken up in ethyl acetate (30 mL), washed with 4M potassium carbonate (20 mL) and brine (20 mL), and then evaporated. The resultant oil was taken up in diethyl ether (70 mL), washed with 4M potassium carbonate (40 mL), water (2 x 40 mL) and brine (20 mL) then evaporated to yield an oil which was subjected to column chromatography (diethyl ether) to yield the desired product ( $R_f$ : 0.27) as a pale green oil (1.01 g, 2.97 mmol, 50%).  $\nu_{\max}$  (NaCl disk)/cm<sup>-1</sup> 3371, 2949, 1737, 1667, 1530; <sup>1</sup>H NMR (500 MHz, CDCl<sub>3</sub>)  $\delta_H$  7.28–7.19 (6H, m, ArH), 7.12 (4H, d,  $J = 7.0$  Hz, ArH), 6.00 (1H,

s, CONH), 3.43 (3H, s, OCH<sub>3</sub>), 3.18–3.04 (1H, m, COCH), 2.06–2.40 (2H, m, CH/CH<sub>2</sub>); <sup>13</sup>C NMR (125 MHz, CDCl<sub>3</sub>) δ<sub>c</sub> 137.0 (C), 129.6 (CH), 129.3 (CH), 128.6 (CH), 128.5 (CH), 126.9 (CH), 126.9 (CH), 62.6 (CH), 62.4 (CH), 52.0 (CH<sub>3</sub>), 39.8 (CH<sub>2</sub>), 39.7 (CH<sub>2</sub>), 25.6 (CH<sub>3</sub>); LRMS *m/z* (EI) [M<sup>+</sup>] = 340; HRMS *m/z* (ES<sup>+</sup>) [M+H]<sup>+</sup> = 341.1863; HRMS *m/z* calc. [M+H]<sup>+</sup> = 341.1865; [α]<sub>D</sub><sup>32</sup> 83.4 (c 0.1, CH<sub>2</sub>Cl<sub>2</sub>).

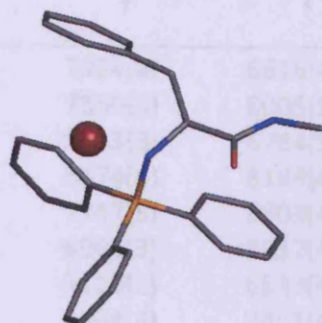
**(2S,5S)-5-((1-Benzyl-1H-indol-3-yl)methyl)-2-tert-butyl-3-methylimidazolidin-4-one 247**



Prepared according to Standard Preparation B. *v*<sub>max</sub> (NaCl disk)/cm<sup>-1</sup> 3474, 3356, 2956, 1694, 1454, 1396, 740; <sup>1</sup>H NMR (500 MHz, CDCl<sub>3</sub>) δ<sub>H</sub> 7.59 (1H, d, *J* = 7.9 Hz, ArH), 7.21–7.14 (4H, m, ArH), 7.10 (1H, td, *J* = 7.9 Hz, 1.1 Hz, ArH), 7.04 (1H, td, *J* = 7.9 Hz, 1.1 Hz, ArH), 7.00 (2H, d, *J* = 7.9 Hz, ArH), 6.94 (1H, s, ArH), 5.18 (2H, dd, *J* = 24.2 Hz, 16.0 Hz, PhCH<sub>2</sub>), 3.79 (1H, t, *J* = 5.0 Hz, COCH), 3.61 (1H, s, CH<sub>3</sub>CCH), 3.18 (1H, dd, *J* = 14.9 Hz, 5.0 Hz, CHCH<sub>2</sub>), 3.05 (1H, dd, *J* = 14.9 Hz, 5.0 Hz, CHCH<sub>2</sub>), 2.72 (3H, s, NCH<sub>3</sub>), 1.90 (1H, bs, NH), 0.79 (9H, s, CH<sub>3</sub>); <sup>13</sup>C NMR (125 MHz, CDCl<sub>3</sub>) δ<sub>c</sub> 176.0 (C), 137.7 (C), 136.6 (C), 128.8 (CH), 128.8 (C), 127.6 (CH), 127.3 (CH), 126.8 (CH), 121.9 (CH), 119.4 (CH), 119.2 (CH), 110.1 (C), 109.7 (CH), 83.4 (CH), 59.3 (CH), 49.9 (CH<sub>2</sub>), 31.3 (CH<sub>3</sub>), 27.4 (CH<sub>2</sub>), 25.7 (CH<sub>3</sub>); LRMS *m/z* (ES<sup>+</sup>) [M+H]<sup>+</sup> = 376.2; HRMS *m/z* (ES<sup>+</sup>) [M+H]<sup>+</sup> = 376.2384; HRMS *m/z* calc. [M+H]<sup>+</sup> = 376.2389; [α]<sub>D</sub><sup>30</sup> -48.0 (c 0.1, CH<sub>3</sub>OH).

## 11 Appendix A

### 11.1 X-ray data for 82



|                                   |  |                    |
|-----------------------------------|--|--------------------|
| Identification code               | nct0809  |                    |
| Empirical formula                 | C <sub>28</sub> H <sub>30</sub> Br N <sub>2</sub> O <sub>2</sub> P |                    |
| Formula weight                    | 537.42   |                    |
| Temperature                       | 150(2) K   |                    |
| Wavelength                        | 0.71073 Å  |                    |
| Crystal system                    | Monoclinic   |                    |
| Space group                       | P2 <sub>1</sub>  |                    |
| Unit cell dimensions              | a = 9.1420(3) Å  | α = 90°.           |
|                                   | b = 14.8200(5) Å   | β = 113.0440(10)°. |
|                                   | c = 10.7260(4) Å   | γ = 90°.           |
| Volume                            | 1337.25(8) Å <sup>3</sup>  |                    |
| Z                                 | 2  |                    |
| Density (calculated)              | 1.335 Mg/m <sup>3</sup>  |                    |
| Absorption coefficient            | 1.623 mm <sup>-1</sup>   |                    |
| F(000)                            | 556  |                    |
| Crystal size                      | 0.36 x 0.22 x 0.11 mm <sup>3</sup>                                 |                    |
| Theta range for data collection   | 2.48 to 27.55°.  |                    |
| Index ranges                      | -11 ≤ h ≤ 11, -18 ≤ k ≤ 19, -13 ≤ l ≤ 13                           |                    |
| Reflections collected             | 5237   |                    |
| Independent reflections           | 5237 [R(int) = 0.0000]   |                    |
| Completeness to theta = 27.55°    | 99.2 %   |                    |
| Max. and min. transmission        | 0.8416 and 0.5926  |                    |
| Refinement method                 | Full-matrix least-squares on F <sup>2</sup>                        |                    |
| Data / restraints / parameters    | 5237 / 4 / 316   |                    |
| Goodness-of-fit on F <sup>2</sup> | 1.079  |                    |
| Final R indices [I > 2σ(I)]       | R <sub>1</sub> = 0.0472, wR <sub>2</sub> = 0.0846                  |                    |
| R indices (all data)              | R <sub>1</sub> = 0.0629, wR <sub>2</sub> = 0.0913                  |                    |
| Absolute structure parameter      | 0.010(9)   |                    |
| Largest diff. peak and hole       | 0.318 and -0.379 e.Å <sup>-3</sup>                                 |                    |

Table 2. Atomic coordinates ( $\times 10^4$ ) and equivalent isotropic displacement parameters ( $\text{\AA}^2 \times 10^3$ )

for nct0809.  $U(\text{eq})$  is defined as one third of the trace of the orthogonalized  $U_{ij}$  tensor.

|       | x        | y       | z       | $U(\text{eq})$ |
|-------|----------|---------|---------|----------------|
| C(1)  | 4589(4)  | 7024(2) | 6616(4) | 23(1)          |
| C(2)  | 4151(6)  | 7856(3) | 6005(5) | 36(1)          |
| C(3)  | 4384(6)  | 8633(3) | 6784(5) | 51(1)          |
| C(4)  | 5057(6)  | 8574(4) | 8189(4) | 44(1)          |
| C(5)  | 5509(6)  | 7747(3) | 8803(4) | 38(1)          |
| C(6)  | 5281(5)  | 6968(3) | 8037(4) | 29(1)          |
| C(7)  | 5511(4)  | 5128(2) | 6523(4) | 22(1)          |
| C(8)  | 5245(5)  | 4568(3) | 7451(4) | 26(1)          |
| C(9)  | 6342(5)  | 3901(3) | 8101(4) | 32(1)          |
| C(10) | 7699(5)  | 3802(3) | 7862(4) | 35(1)          |
| C(11) | 7981(6)  | 4363(3) | 6962(5) | 43(1)          |
| C(12) | 6895(5)  | 5028(3) | 6287(4) | 32(1)          |
| C(13) | 4158(4)  | 6175(2) | 4025(4) | 22(1)          |
| C(14) | 5298(5)  | 6722(3) | 3844(4) | 27(1)          |
| C(15) | 5369(5)  | 6781(3) | 2582(5) | 37(1)          |
| C(16) | 4312(5)  | 6294(3) | 1511(4) | 39(1)          |
| C(17) | 3172(5)  | 5767(3) | 1672(4) | 38(1)          |
| C(18) | 3096(5)  | 5692(3) | 2938(4) | 31(1)          |
| C(19) | 1136(4)  | 6265(3) | 5591(4) | 24(1)          |
| C(20) | -500(4)  | 5893(3) | 4682(4) | 26(1)          |
| C(21) | -754(4)  | 5833(3) | 3203(4) | 30(1)          |
| C(22) | -711(5)  | 6607(3) | 2492(4) | 28(1)          |
| C(23) | -979(5)  | 6555(3) | 1124(4) | 36(1)          |
| C(24) | -1281(6) | 5729(3) | 471(5)  | 51(1)          |
| C(25) | -1309(7) | 4972(4) | 1170(5) | 62(2)          |
| C(26) | -1058(6) | 5017(3) | 2538(5) | 47(1)          |
| C(27) | 1248(5)  | 6370(3) | 7052(4) | 28(1)          |
| C(28) | 450(8)   | 7324(4) | 8544(6) | 67(2)          |
| N(1)  | 2385(3)  | 5651(2) | 5566(3) | 22(1)          |
| N(2)  | 571(5)   | 7120(3) | 7253(4) | 41(1)          |
| O(1)  | 1875(4)  | 5814(2) | 7940(3) | 40(1)          |
| O(2)  | 2170(5)  | 3938(2) | 8632(4) | 53(1)          |
| P(1)  | 4118(1)  | 5998(1) | 5669(1) | 19(1)          |
| Br(1) | 1376(1)  | 3477(1) | 5363(1) | 40(1)          |

Table 3. Bond lengths [Å] and angles [°] for nct0809.

|                |          |
|----------------|----------|
| C(1)-C(2)      | 1.380(5) |
| C(1)-C(6)      | 1.406(5) |
| C(1)-P(1)      | 1.785(4) |
| C(2)-C(3)      | 1.390(6) |
| C(3)-C(4)      | 1.389(6) |
| C(4)-C(5)      | 1.376(7) |
| C(5)-C(6)      | 1.385(6) |
| C(7)-C(8)      | 1.389(5) |
| C(7)-C(12)     | 1.392(5) |
| C(7)-P(1)      | 1.792(4) |
| C(8)-C(9)      | 1.386(6) |
| C(9)-C(10)     | 1.369(6) |
| C(10)-C(11)    | 1.373(6) |
| C(11)-C(12)    | 1.385(6) |
| C(13)-C(18)    | 1.389(5) |
| C(13)-C(14)    | 1.392(5) |
| C(13)-P(1)     | 1.797(4) |
| C(14)-C(15)    | 1.383(6) |
| C(15)-C(16)    | 1.380(6) |
| C(16)-C(17)    | 1.366(6) |
| C(17)-C(18)    | 1.391(6) |
| C(19)-N(1)     | 1.469(5) |
| C(19)-C(20)    | 1.533(5) |
| C(19)-C(27)    | 1.537(6) |
| C(20)-C(21)    | 1.513(6) |
| C(21)-C(26)    | 1.376(6) |
| C(21)-C(22)    | 1.386(6) |
| C(22)-C(23)    | 1.392(6) |
| C(23)-C(24)    | 1.382(6) |
| C(24)-C(25)    | 1.356(7) |
| C(25)-C(26)    | 1.395(7) |
| C(27)-O(1)     | 1.220(5) |
| C(27)-N(2)     | 1.330(5) |
| C(28)-N(2)     | 1.463(6) |
| N(1)-P(1)      | 1.628(3) |
|                |          |
| C(2)-C(1)-C(6) | 119.5(4) |
| C(2)-C(1)-P(1) | 122.0(3) |
| C(6)-C(1)-P(1) | 118.2(3) |
| C(1)-C(2)-C(3) | 120.5(4) |
| C(4)-C(3)-C(2) | 119.9(5) |
| C(5)-C(4)-C(3) | 119.9(4) |
| C(4)-C(5)-C(6) | 120.8(4) |
| C(5)-C(6)-C(1) | 119.5(4) |

|                   |            |
|-------------------|------------|
| C(8)-C(7)-C(12)   | 119.5(4)   |
| C(8)-C(7)-P(1)    | 120.5(3)   |
| C(12)-C(7)-P(1)   | 119.9(3)   |
| C(9)-C(8)-C(7)    | 119.5(4)   |
| C(10)-C(9)-C(8)   | 120.8(4)   |
| C(9)-C(10)-C(11)  | 120.0(4)   |
| C(10)-C(11)-C(12) | 120.3(4)   |
| C(11)-C(12)-C(7)  | 119.9(4)   |
| C(18)-C(13)-C(14) | 119.8(4)   |
| C(18)-C(13)-P(1)  | 118.2(3)   |
| C(14)-C(13)-P(1)  | 121.7(3)   |
| C(15)-C(14)-C(13) | 119.9(4)   |
| C(16)-C(15)-C(14) | 119.7(4)   |
| C(17)-C(16)-C(15) | 120.9(4)   |
| C(16)-C(17)-C(18) | 120.1(4)   |
| C(13)-C(18)-C(17) | 119.6(4)   |
| N(1)-C(19)-C(20)  | 109.8(3)   |
| N(1)-C(19)-C(27)  | 109.8(3)   |
| C(20)-C(19)-C(27) | 110.1(3)   |
| C(21)-C(20)-C(19) | 113.5(3)   |
| C(26)-C(21)-C(22) | 119.0(4)   |
| C(26)-C(21)-C(20) | 120.8(4)   |
| C(22)-C(21)-C(20) | 120.2(4)   |
| C(21)-C(22)-C(23) | 120.2(4)   |
| C(24)-C(23)-C(22) | 120.0(4)   |
| C(25)-C(24)-C(23) | 119.7(4)   |
| C(24)-C(25)-C(26) | 120.7(5)   |
| C(21)-C(26)-C(25) | 120.2(5)   |
| O(1)-C(27)-N(2)   | 123.0(4)   |
| O(1)-C(27)-C(19)  | 123.4(4)   |
| N(2)-C(27)-C(19)  | 113.6(4)   |
| C(19)-N(1)-P(1)   | 123.1(3)   |
| C(27)-N(2)-C(28)  | 122.6(4)   |
| N(1)-P(1)-C(1)    | 108.62(17) |
| N(1)-P(1)-C(7)    | 106.58(17) |
| C(1)-P(1)-C(7)    | 110.91(18) |
| N(1)-P(1)-C(13)   | 111.90(16) |
| C(1)-P(1)-C(13)   | 109.92(17) |
| C(7)-P(1)-C(13)   | 108.88(17) |

---

Symmetry transformations used to generate equivalent atoms:

Table 4. Anisotropic displacement parameters ( $\text{\AA}^2 \times 10^3$ ) for nct0809. The anisotropic displacement factor exponent takes the form:  $-2\pi^2 [h^2 a^{*2} U_{11} + \dots + 2 h k a^* b^* U_{12}]$

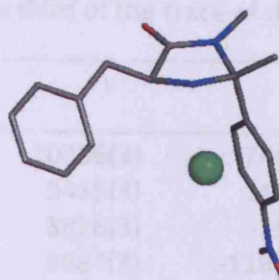
|       | U <sub>11</sub> | U <sub>22</sub> | U <sub>33</sub> | U <sub>23</sub> | U <sub>13</sub> | U <sub>12</sub> |
|-------|-----------------|-----------------|-----------------|-----------------|-----------------|-----------------|
| C(1)  | 23(2)           | 18(2)           | 25(2)           | -3(2)           | 7(2)            | -3(2)           |
| C(2)  | 55(3)           | 22(2)           | 30(2)           | 1(2)            | 14(2)           | -1(2)           |
| C(3)  | 84(4)           | 18(3)           | 49(3)           | 1(2)            | 24(3)           | -4(2)           |
| C(4)  | 65(3)           | 28(3)           | 39(2)           | -12(3)          | 18(2)           | -13(3)          |
| C(5)  | 46(3)           | 35(2)           | 27(2)           | -5(2)           | 8(2)            | -6(2)           |
| C(6)  | 32(2)           | 24(2)           | 30(2)           | -2(2)           | 12(2)           | 0(2)            |
| C(7)  | 23(2)           | 18(2)           | 21(2)           | -3(2)           | 5(2)            | 1(2)            |
| C(8)  | 24(2)           | 27(2)           | 26(2)           | -2(2)           | 8(2)            | -6(2)           |
| C(9)  | 37(3)           | 26(2)           | 24(2)           | 4(2)            | 1(2)            | -4(2)           |
| C(10) | 39(3)           | 31(2)           | 26(2)           | 3(2)            | 2(2)            | 12(2)           |
| C(11) | 35(3)           | 53(3)           | 39(3)           | 7(2)            | 13(2)           | 22(2)           |
| C(12) | 29(2)           | 36(2)           | 34(2)           | 11(2)           | 17(2)           | 8(2)            |
| C(13) | 19(2)           | 22(2)           | 24(2)           | 1(2)            | 9(2)            | 7(2)            |
| C(14) | 22(2)           | 29(2)           | 31(2)           | 6(2)            | 13(2)           | 7(2)            |
| C(15) | 39(3)           | 39(3)           | 41(3)           | 17(2)           | 25(2)           | 14(2)           |
| C(16) | 42(3)           | 52(3)           | 30(2)           | 11(2)           | 21(2)           | 19(2)           |
| C(17) | 40(3)           | 48(3)           | 24(2)           | 0(2)            | 10(2)           | 14(2)           |
| C(18) | 24(2)           | 38(3)           | 27(2)           | -5(2)           | 7(2)            | 1(2)            |
| C(19) | 24(2)           | 21(2)           | 29(2)           | 5(2)            | 14(2)           | 2(2)            |
| C(20) | 20(2)           | 27(2)           | 33(2)           | 5(2)            | 12(2)           | 5(2)            |
| C(21) | 13(2)           | 35(2)           | 33(2)           | 8(2)            | 0(2)            | 4(2)            |
| C(22) | 24(2)           | 28(2)           | 31(2)           | 1(2)            | 11(2)           | 4(2)            |
| C(23) | 36(3)           | 41(3)           | 29(2)           | 3(2)            | 11(2)           | 4(2)            |
| C(24) | 58(3)           | 53(3)           | 24(2)           | -7(2)           | -3(2)           | 10(3)           |
| C(25) | 85(4)           | 37(3)           | 35(3)           | -11(2)          | -9(3)           | -6(3)           |
| C(26) | 44(3)           | 36(3)           | 34(3)           | 1(2)            | -12(2)          | -5(2)           |
| C(27) | 32(2)           | 26(2)           | 31(2)           | 2(2)            | 18(2)           | 5(2)            |
| C(28) | 118(6)          | 54(3)           | 49(3)           | 2(3)            | 52(4)           | 27(4)           |
| N(1)  | 20(2)           | 16(1)           | 32(2)           | 0(1)            | 12(1)           | 0(1)            |
| N(2)  | 67(3)           | 35(2)           | 29(2)           | 10(2)           | 28(2)           | 21(2)           |
| O(1)  | 58(2)           | 32(2)           | 30(2)           | 9(2)            | 18(2)           | 13(2)           |
| O(2)  | 68(3)           | 39(2)           | 48(2)           | 16(2)           | 20(2)           | 9(2)            |
| P(1)  | 17(1)           | 19(1)           | 21(1)           | 0(1)            | 7(1)            | -1(1)           |
| Br(1) | 47(1)           | 21(1)           | 39(1)           | 1(1)            | 2(1)            | -7(1)           |

Table 5. Hydrogen coordinates (  $\times 10^4$ ) and isotropic displacement parameters ( $\text{\AA}^2 \times 10^3$ ) for nct0809.

|        | x        | y        | z        | U(eq)   |
|--------|----------|----------|----------|---------|
| H(2)   | 3688     | 7898     | 5045     | 44      |
| H(3)   | 4082     | 9204     | 6357     | 61      |
| H(4)   | 5206     | 9103     | 8724     | 53      |
| H(5)   | 5983     | 7710     | 9763     | 45      |
| H(6)   | 5591     | 6399     | 8469     | 35      |
| H(8)   | 4319     | 4641     | 7638     | 32      |
| H(9)   | 6150     | 3508     | 8720     | 39      |
| H(10)  | 8445     | 3345     | 8319     | 42      |
| H(11)  | 8926     | 4295     | 6801     | 51      |
| H(12)  | 7094     | 5415     | 5665     | 38      |
| H(14)  | 6027     | 7053     | 4585     | 32      |
| H(15)  | 6142     | 7155     | 2453     | 44      |
| H(16)  | 4377     | 6326     | 650      | 47      |
| H(17)  | 2431     | 5451     | 919      | 46      |
| H(18)  | 2324     | 5313     | 3058     | 37      |
| H(19)  | 1286     | 6869     | 5242     | 29      |
| H(20A) | -626     | 5284     | 5006     | 32      |
| H(20B) | -1332    | 6286     | 4768     | 32      |
| H(22)  | -498     | 7174     | 2940     | 33      |
| H(23)  | -954     | 7087     | 639      | 43      |
| H(24)  | -1468    | 5693     | -463     | 61      |
| H(25)  | -1502    | 4404     | 724      | 75      |
| H(26)  | -1097    | 4482     | 3013     | 56      |
| H(28A) | 158      | 6776     | 8903     | 101     |
| H(28B) | -364     | 7788     | 8403     | 101     |
| H(28C) | 1477     | 7546     | 9191     | 101     |
| H(1)   | 2188     | 5068     | 5492     | 27      |
| H(2A)  | 180      | 7508     | 6583     | 49      |
| H(10)  | 2180(50) | 4536(7)  | 8540(40) | 26(11)  |
| H(20)  | 1830(80) | 3710(30) | 7790(20) | 110(30) |



## 11.2 X-ray data for 110-HCl



|                                   |  |          |
|-----------------------------------|--|----------|
| Identification code               | nct0807  |          |
| Empirical formula                 | C <sub>18</sub> H <sub>20</sub> Cl N <sub>3</sub> O <sub>3</sub> |          |
| Formula weight                    | 361.82   |          |
| Temperature                       | 200(2) K   |          |
| Wavelength                        | 0.71073 Å  |          |
| Crystal system                    | Orthorhombic   |          |
| Space group                       | P2 <sub>1</sub> 2 <sub>1</sub> 2 <sub>1</sub>                    |          |
| Unit cell dimensions              | a = 7.5840(2) Å  | α = 90°. |
|                                   | b = 10.4830(3) Å   | β = 90°. |
|                                   | c = 23.1960(6) Å   | γ = 90°. |
| Volume                            | 1844.15(9) Å <sup>3</sup>  |          |
| Z                                 | 4  |          |
| Density (calculated)              | 1.303 Mg/m <sup>3</sup>  |          |
| Absorption coefficient            | 0.229 mm <sup>-1</sup>   |          |
| F(000)                            | 760  |          |
| Crystal size                      | 0.40 x 0.15 x 0.04 mm <sup>3</sup>                               |          |
| Theta range for data collection   | 3.21 to 27.48°.  |          |
| Index ranges                      | -9 ≤ h ≤ 9, -13 ≤ k ≤ 13, -29 ≤ l ≤ 30                           |          |
| Reflections collected             | 4216   |          |
| Independent reflections           | 4216 [R(int) = 0.0000]   |          |
| Completeness to theta = 27.48°    | 99.6 %   |          |
| Max. and min. transmission        | 0.9909 and 0.9141  |          |
| Refinement method                 | Full-matrix least-squares on F <sup>2</sup>                      |          |
| Data / restraints / parameters    | 4216 / 0 / 228   |          |
| Goodness-of-fit on F <sup>2</sup> | 1.044  |          |
| Final R indices [I > 2σ(I)]       | R1 = 0.0601, wR2 = 0.1054  |          |
| R indices (all data)              | R1 = 0.0992, wR2 = 0.1198  |          |
| Absolute structure parameter      | 0.06(9)  |          |
| Largest diff. peak and hole       | 0.229 and -0.255 e.Å <sup>-3</sup>                               |          |

Table 2. Atomic coordinates ( $\times 10^4$ ) and equivalent isotropic displacement parameters ( $\text{\AA}^2 \times 10^3$ )

for nct0807.  $U(\text{eq})$  is defined as one third of the trace of the orthogonalized  $U_{ij}$  tensor.

|       | x        | y        | z        | $U(\text{eq})$ |
|-------|----------|----------|----------|----------------|
| C(1)  | 4602(4)  | 10336(3) | -746(1)  | 25(1)          |
| C(2)  | 5718(4)  | 9455(3)  | 143(1)   | 24(1)          |
| C(3)  | 3980(4)  | 8826(3)  | -29(1)   | 25(1)          |
| C(4)  | 5848(4)  | 9684(3)  | -1182(1) | 26(1)          |
| C(5)  | 7021(4)  | 10424(3) | -1499(1) | 32(1)          |
| C(6)  | 8244(4)  | 9849(4)  | -1857(1) | 37(1)          |
| C(7)  | 8237(5)  | 8553(4)  | -1903(1) | 42(1)          |
| C(8)  | 7065(5)  | 7789(4)  | -1609(1) | 49(1)          |
| C(9)  | 5859(5)  | 8378(3)  | -1243(1) | 38(1)          |
| C(10) | 3707(4)  | 11521(3) | -984(1)  | 34(1)          |
| C(11) | 1731(4)  | 9074(3)  | -798(1)  | 37(1)          |
| C(12) | 5878(4)  | 9655(3)  | 787(1)   | 29(1)          |
| C(13) | 7705(4)  | 9940(3)  | 1020(1)  | 29(1)          |
| C(14) | 7891(5)  | 10143(4) | 1609(1)  | 48(1)          |
| C(15) | 9512(5)  | 10443(4) | 1844(2)  | 56(1)          |
| C(16) | 10973(5) | 10552(3) | 1504(2)  | 43(1)          |
| C(17) | 10810(5) | 10334(3) | 922(1)   | 37(1)          |
| C(18) | 9191(4)  | 10023(3) | 685(1)   | 31(1)          |
| O(1)  | 3300(3)  | 7928(2)  | 220(1)   | 34(1)          |
| O(2)  | 10692(5) | 8552(4)  | -2491(2) | 96(1)          |
| O(3)  | 9393(8)  | 6789(4)  | -2357(2) | 160(3)         |
| N(1)  | 5666(3)  | 10657(2) | -212(1)  | 23(1)          |
| N(2)  | 3343(3)  | 9439(2)  | -497(1)  | 26(1)          |
| N(3)  | 9553(6)  | 7925(5)  | -2273(2) | 74(1)          |
| Cl(1) | 9070(1)  | 12173(1) | -509(1)  | 32(1)          |

Table 3. Bond lengths [Å] and angles [°] for nct0807.

|              |          |
|--------------|----------|
| C(1)-N(2)    | 1.460(4) |
| C(1)-N(1)    | 1.517(3) |
| C(1)-C(10)   | 1.519(4) |
| C(1)-C(4)    | 1.543(4) |
| C(2)-N(1)    | 1.505(4) |
| C(2)-C(12)   | 1.514(4) |
| C(2)-C(3)    | 1.527(4) |
| C(2)-H(2)    | 1.0000   |
| C(3)-O(1)    | 1.219(3) |
| C(3)-N(2)    | 1.350(4) |
| C(4)-C(9)    | 1.376(4) |
| C(4)-C(5)    | 1.391(4) |
| C(5)-C(6)    | 1.383(5) |
| C(5)-H(5)    | 0.9500   |
| C(6)-C(7)    | 1.363(5) |
| C(6)-H(6)    | 0.9500   |
| C(7)-C(8)    | 1.377(5) |
| C(7)-N(3)    | 1.473(5) |
| C(8)-C(9)    | 1.394(5) |
| C(8)-H(8)    | 0.9500   |
| C(9)-H(9)    | 0.9500   |
| C(10)-H(10A) | 0.9800   |
| C(10)-H(10B) | 0.9800   |
| C(10)-H(10C) | 0.9800   |
| C(11)-N(2)   | 1.459(4) |
| C(11)-H(11A) | 0.9800   |
| C(11)-H(11B) | 0.9800   |
| C(11)-H(11C) | 0.9800   |
| C(12)-C(13)  | 1.517(4) |
| C(12)-H(12A) | 0.9900   |
| C(12)-H(12B) | 0.9900   |
| C(13)-C(18)  | 1.372(4) |
| C(13)-C(14)  | 1.390(4) |
| C(14)-C(15)  | 1.381(5) |
| C(14)-H(14)  | 0.9500   |
| C(15)-C(16)  | 1.365(5) |
| C(15)-H(15)  | 0.9500   |
| C(16)-C(17)  | 1.373(4) |
| C(16)-H(16)  | 0.9500   |
| C(17)-C(18)  | 1.385(5) |
| C(17)-H(17)  | 0.9500   |
| C(18)-H(18)  | 0.9500   |
| O(2)-N(3)    | 1.197(5) |
| O(3)-N(3)    | 1.212(5) |

|                     |          |
|---------------------|----------|
| N(1)-H(1A)          | 0.9200   |
| N(1)-H(1B)          | 0.9200   |
| N(2)-C(1)-N(1)      | 99.6(2)  |
| N(2)-C(1)-C(10)     | 112.2(2) |
| N(1)-C(1)-C(10)     | 110.6(2) |
| N(2)-C(1)-C(4)      | 112.0(2) |
| N(1)-C(1)-C(4)      | 107.9(2) |
| C(10)-C(1)-C(4)     | 113.5(2) |
| N(1)-C(2)-C(12)     | 115.2(2) |
| N(1)-C(2)-C(3)      | 101.4(2) |
| C(12)-C(2)-C(3)     | 112.7(3) |
| N(1)-C(2)-H(2)      | 109.1    |
| C(12)-C(2)-H(2)     | 109.1    |
| C(3)-C(2)-H(2)      | 109.1    |
| O(1)-C(3)-N(2)      | 126.7(3) |
| O(1)-C(3)-C(2)      | 125.1(3) |
| N(2)-C(3)-C(2)      | 108.2(2) |
| C(9)-C(4)-C(5)      | 119.8(3) |
| C(9)-C(4)-C(1)      | 120.8(3) |
| C(5)-C(4)-C(1)      | 119.4(3) |
| C(6)-C(5)-C(4)      | 120.3(3) |
| C(6)-C(5)-H(5)      | 119.9    |
| C(4)-C(5)-H(5)      | 119.9    |
| C(7)-C(6)-C(5)      | 118.6(3) |
| C(7)-C(6)-H(6)      | 120.7    |
| C(5)-C(6)-H(6)      | 120.7    |
| C(6)-C(7)-C(8)      | 123.0(3) |
| C(6)-C(7)-N(3)      | 119.2(4) |
| C(8)-C(7)-N(3)      | 117.7(4) |
| C(7)-C(8)-C(9)      | 117.8(4) |
| C(7)-C(8)-H(8)      | 121.1    |
| C(9)-C(8)-H(8)      | 121.1    |
| C(4)-C(9)-C(8)      | 120.5(3) |
| C(4)-C(9)-H(9)      | 119.8    |
| C(8)-C(9)-H(9)      | 119.8    |
| C(1)-C(10)-H(10A)   | 109.5    |
| C(1)-C(10)-H(10B)   | 109.5    |
| H(10A)-C(10)-H(10B) | 109.5    |
| C(1)-C(10)-H(10C)   | 109.5    |
| H(10A)-C(10)-H(10C) | 109.5    |
| H(10B)-C(10)-H(10C) | 109.5    |
| N(2)-C(11)-H(11A)   | 109.5    |
| N(2)-C(11)-H(11B)   | 109.5    |
| H(11A)-C(11)-H(11B) | 109.5    |
| N(2)-C(11)-H(11C)   | 109.5    |

|                     |          |
|---------------------|----------|
| H(11A)-C(11)-H(11C) | 109.5    |
| H(11B)-C(11)-H(11C) | 109.5    |
| C(2)-C(12)-C(13)    | 116.9(3) |
| C(2)-C(12)-H(12A)   | 108.1    |
| C(13)-C(12)-H(12A)  | 108.1    |
| C(2)-C(12)-H(12B)   | 108.1    |
| C(13)-C(12)-H(12B)  | 108.1    |
| H(12A)-C(12)-H(12B) | 107.3    |
| C(18)-C(13)-C(14)   | 117.6(3) |
| C(18)-C(13)-C(12)   | 124.1(3) |
| C(14)-C(13)-C(12)   | 118.2(3) |
| C(15)-C(14)-C(13)   | 120.9(3) |
| C(15)-C(14)-H(14)   | 119.6    |
| C(13)-C(14)-H(14)   | 119.6    |
| C(16)-C(15)-C(14)   | 120.8(3) |
| C(16)-C(15)-H(15)   | 119.6    |
| C(14)-C(15)-H(15)   | 119.6    |
| C(15)-C(16)-C(17)   | 118.8(4) |
| C(15)-C(16)-H(16)   | 120.6    |
| C(17)-C(16)-H(16)   | 120.6    |
| C(16)-C(17)-C(18)   | 120.7(3) |
| C(16)-C(17)-H(17)   | 119.7    |
| C(18)-C(17)-H(17)   | 119.7    |
| C(13)-C(18)-C(17)   | 121.1(3) |
| C(13)-C(18)-H(18)   | 119.4    |
| C(17)-C(18)-H(18)   | 119.4    |
| C(2)-N(1)-C(1)      | 105.9(2) |
| C(2)-N(1)-H(1A)     | 110.5    |
| C(1)-N(1)-H(1A)     | 110.5    |
| C(2)-N(1)-H(1B)     | 110.5    |
| C(1)-N(1)-H(1B)     | 110.5    |
| H(1A)-N(1)-H(1B)    | 108.7    |
| C(3)-N(2)-C(11)     | 124.0(3) |
| C(3)-N(2)-C(1)      | 113.0(2) |
| C(11)-N(2)-C(1)     | 121.8(2) |
| O(2)-N(3)-O(3)      | 123.0(4) |
| O(2)-N(3)-C(7)      | 119.3(4) |
| O(3)-N(3)-C(7)      | 117.7(4) |

---

Symmetry transformations used to generate equivalent atoms:

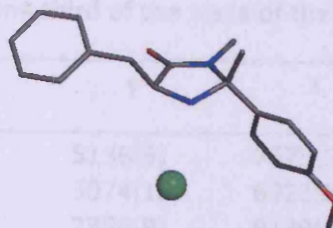
Table 4. Anisotropic displacement parameters ( $\text{\AA}^2 \times 10^3$ ) for nct0807. The anisotropic displacement factor exponent takes the form:  $-2\pi^2 [h^2 a^{*2} U^{11} + \dots + 2 h k a^* b^* U^{12}]$

|       | U <sup>11</sup> | U <sup>22</sup> | U <sup>33</sup> | U <sup>23</sup> | U <sup>13</sup> | U <sup>12</sup> |
|-------|-----------------|-----------------|-----------------|-----------------|-----------------|-----------------|
| C(1)  | 21(2)           | 23(2)           | 29(2)           | -2(1)           | -1(1)           | -1(1)           |
| C(2)  | 23(2)           | 19(2)           | 31(2)           | 1(1)            | 2(1)            | 1(1)            |
| C(3)  | 26(2)           | 20(2)           | 29(2)           | -3(1)           | 4(1)            | 0(1)            |
| C(4)  | 26(2)           | 26(2)           | 26(1)           | 1(1)            | -4(1)           | 1(1)            |
| C(5)  | 32(2)           | 33(2)           | 31(2)           | 1(1)            | 3(1)            | -8(2)           |
| C(6)  | 28(2)           | 54(2)           | 28(2)           | 4(2)            | 2(2)            | -7(2)           |
| C(7)  | 42(2)           | 51(2)           | 33(2)           | 4(2)            | 10(2)           | 17(2)           |
| C(8)  | 68(3)           | 33(2)           | 47(2)           | 3(2)            | 22(2)           | 12(2)           |
| C(9)  | 44(2)           | 30(2)           | 40(2)           | 3(1)            | 14(2)           | 2(2)            |
| C(10) | 30(2)           | 26(2)           | 44(2)           | 0(1)            | -2(2)           | 1(1)            |
| C(11) | 26(2)           | 41(2)           | 44(2)           | -5(2)           | -6(2)           | -7(2)           |
| C(12) | 27(2)           | 26(2)           | 33(2)           | 2(1)            | 2(2)            | 1(2)            |
| C(13) | 29(2)           | 26(2)           | 32(2)           | -1(1)           | 0(1)            | 0(1)            |
| C(14) | 36(2)           | 76(3)           | 32(2)           | -2(2)           | 1(2)            | -3(2)           |
| C(15) | 47(3)           | 85(3)           | 36(2)           | -1(2)           | -7(2)           | -6(2)           |
| C(16) | 34(2)           | 42(2)           | 52(2)           | -3(2)           | -14(2)          | 2(2)            |
| C(17) | 25(2)           | 37(2)           | 48(2)           | -1(2)           | 1(2)            | 5(2)            |
| C(18) | 27(2)           | 31(2)           | 37(2)           | -2(1)           | -1(2)           | 3(2)            |
| O(1)  | 34(1)           | 29(1)           | 40(1)           | 2(1)            | 3(1)            | -11(1)          |
| O(2)  | 74(2)           | 123(3)          | 93(2)           | 4(2)            | 54(2)           | 21(2)           |
| O(3)  | 225(6)          | 70(3)           | 184(5)          | -1(3)           | 153(4)          | 44(3)           |
| N(1)  | 17(1)           | 22(1)           | 30(1)           | -2(1)           | 2(1)            | -1(1)           |
| N(2)  | 20(1)           | 26(1)           | 33(1)           | -1(1)           | 1(1)            | -6(1)           |
| N(3)  | 84(3)           | 79(3)           | 60(2)           | 11(2)           | 37(2)           | 37(3)           |
| Cl(1) | 26(1)           | 30(1)           | 39(1)           | -5(1)           | 1(1)            | -7(1)           |

Table 5. Hydrogen coordinates (  $\times 10^4$ ) and isotropic displacement parameters ( $\text{\AA}^2 \times 10^3$ ) for nct0807.

|        | x     | y     | z     | U(eq) |
|--------|-------|-------|-------|-------|
| H(2)   | 6718  | 8911  | 8     | 29    |
| H(5)   | 6982  | 11327 | -1470 | 38    |
| H(6)   | 9071  | 10347 | -2067 | 44    |
| H(8)   | 7078  | 6888  | -1656 | 59    |
| H(9)   | 5038  | 7875  | -1033 | 46    |
| H(10A) | 3110  | 11310 | -1346 | 50    |
| H(10B) | 4593  | 12183 | -1054 | 50    |
| H(10C) | 2840  | 11834 | -704  | 50    |
| H(11A) | 1113  | 8416  | -576  | 55    |
| H(11B) | 2030  | 8738  | -1180 | 55    |
| H(11C) | 968   | 9822  | -841  | 55    |
| H(12A) | 5433  | 8879  | 982   | 34    |
| H(12B) | 5092  | 10368 | 897   | 34    |
| H(14)  | 6890  | 10075 | 1853  | 57    |
| H(15)  | 9612  | 10575 | 2248  | 67    |
| H(16)  | 12081 | 10774 | 1666  | 51    |
| H(17)  | 11818 | 10396 | 681   | 44    |
| H(18)  | 9108  | 9864  | 282   | 38    |
| H(1A)  | 6788  | 10908 | -311  | 27    |
| H(1B)  | 5137  | 11307 | -9    | 27    |

### 11.3 X-ray data for 119-HCl



|                                   |  |                  |
|-----------------------------------|--|------------------|
| Identification code               | nct1008  |                  |
| Empirical formula                 | C <sub>19</sub> H <sub>23</sub> Cl N <sub>2</sub> O <sub>2</sub> |                  |
| Formula weight                    | 346.84   |                  |
| Temperature                       | 150(2) K   |                  |
| Wavelength                        | 0.71073 Å  |                  |
| Crystal system                    | Monoclinic   |                  |
| Space group                       | P2 <sub>1</sub>  |                  |
| Unit cell dimensions              | a = 11.7339(14) Å  | α = 90°.         |
|                                   | b = 7.1391(6) Å  | β = 116.538(4)°. |
|                                   | c = 12.4541(14) Å  | γ = 90°.         |
| Volume                            | 933.35(17) Å <sup>3</sup>  |                  |
| Z                                 | 2  |                  |
| Density (calculated)              | 1.234 Mg/m <sup>3</sup>  |                  |
| Absorption coefficient            | 0.218 mm <sup>-1</sup>   |                  |
| F(000)                            | 368  |                  |
| Crystal size                      | 0.20 x 0.20 x 0.04 mm <sup>3</sup>                               |                  |
| Theta range for data collection   | 3.21 to 23.00°.  |                  |
| Index ranges                      | -12 ≤ h ≤ 12, -7 ≤ k ≤ 7, -13 ≤ l ≤ 13                           |                  |
| Reflections collected             | 2341   |                  |
| Independent reflections           | 2341 [R(int) = 0.0000]   |                  |
| Completeness to theta = 23.00°    | 99.4 %   |                  |
| Max. and min. transmission        | 0.9914 and 0.9578  |                  |
| Refinement method                 | Full-matrix least-squares on F <sup>2</sup>                      |                  |
| Data / restraints / parameters    | 2341 / 1 / 220   |                  |
| Goodness-of-fit on F <sup>2</sup> | 1.051  |                  |
| Final R indices [I > 2σ(I)]       | R <sub>1</sub> = 0.0659, wR <sub>2</sub> = 0.1401                |                  |
| R indices (all data)              | R <sub>1</sub> = 0.1003, wR <sub>2</sub> = 0.1603                |                  |
| Absolute structure parameter      | -0.22(15)  |                  |
| Largest diff. peak and hole       | 0.308 and -0.323 e.Å <sup>-3</sup>                               |                  |



Table 2. Atomic coordinates (  $\times 10^4$ ) and equivalent isotropic displacement parameters ( $\text{\AA}^2 \times 10^3$ )

for nct1008.  $U(\text{eq})$  is defined as one third of the trace of the orthogonalized  $U_{ij}$  tensor.

|       | x       | y        | z        | $U(\text{eq})$ |
|-------|---------|----------|----------|----------------|
| C(1)  | 3256(6) | 5136(9)  | 7679(5)  | 29(2)          |
| C(2)  | 1825(6) | 5074(10) | 6923(5)  | 34(2)          |
| C(3)  | 2280(6) | 2356(9)  | 8139(6)  | 34(2)          |
| C(4)  | 3999(6) | 4804(9)  | 6939(6)  | 33(2)          |
| C(5)  | 4033(5) | 6569(11) | 6286(5)  | 33(2)          |
| C(6)  | 4895(7) | 7999(10) | 6914(7)  | 43(2)          |
| C(7)  | 4926(8) | 9646(11) | 6342(7)  | 49(2)          |
| C(8)  | 4143(8) | 9884(13) | 5152(9)  | 60(2)          |
| C(9)  | 3296(7) | 8488(14) | 4508(7)  | 57(2)          |
| C(10) | 3244(6) | 6808(12) | 5082(6)  | 48(2)          |
| C(11) | 18(6)   | 3003(11) | 6555(6)  | 47(2)          |
| C(12) | 2504(6) | 555(9)   | 7601(6)  | 37(2)          |
| C(13) | 1932(6) | 2064(9)  | 9186(6)  | 30(2)          |
| C(14) | 1373(6) | 3472(9)  | 9526(6)  | 36(2)          |
| C(15) | 1137(6) | 3298(10) | 10516(6) | 38(2)          |
| C(16) | 1503(6) | 1679(10) | 11190(6) | 41(2)          |
| C(17) | 2084(6) | 250(10)  | 10873(6) | 38(2)          |
| C(18) | 2297(6) | 447(9)   | 9875(6)  | 34(2)          |
| C(19) | 814(9)  | 2884(12) | 12606(8) | 67(3)          |
| N(1)  | 1355(5) | 3568(8)  | 7221(5)  | 34(1)          |
| N(2)  | 3456(5) | 3590(7)  | 8572(4)  | 28(1)          |
| O(1)  | 1215(4) | 6259(8)  | 6161(4)  | 45(1)          |
| O(2)  | 1303(4) | 1367(9)  | 12188(4) | 47(1)          |
| Cl(1) | 4083(2) | 6328(2)  | 10627(1) | 38(1)          |

Table 3. Bond lengths [Å] and angles [°] for nct1008.

|                  |           |
|------------------|-----------|
| C(1)-N(2)        | 1.508(8)  |
| C(1)-C(2)        | 1.514(9)  |
| C(1)-C(4)        | 1.544(9)  |
| C(2)-O(1)        | 1.234(7)  |
| C(2)-N(1)        | 1.334(9)  |
| C(3)-N(1)        | 1.458(8)  |
| C(3)-N(2)        | 1.519(8)  |
| C(3)-C(12)       | 1.526(9)  |
| C(3)-C(13)       | 1.544(9)  |
| C(4)-C(5)        | 1.510(9)  |
| C(5)-C(10)       | 1.377(9)  |
| C(5)-C(6)        | 1.403(10) |
| C(6)-C(7)        | 1.384(10) |
| C(7)-C(8)        | 1.362(11) |
| C(8)-C(9)        | 1.382(12) |
| C(9)-C(10)       | 1.411(11) |
| C(11)-N(1)       | 1.466(8)  |
| C(13)-C(14)      | 1.367(9)  |
| C(13)-C(18)      | 1.387(8)  |
| C(14)-C(15)      | 1.384(9)  |
| C(15)-C(16)      | 1.380(9)  |
| C(16)-C(17)      | 1.379(9)  |
| C(16)-O(2)       | 1.382(7)  |
| C(17)-C(18)      | 1.381(9)  |
| C(19)-O(2)       | 1.428(9)  |
|                  |           |
| N(2)-C(1)-C(2)   | 101.6(5)  |
| N(2)-C(1)-C(4)   | 112.6(5)  |
| C(2)-C(1)-C(4)   | 112.9(5)  |
| O(1)-C(2)-N(1)   | 126.6(6)  |
| O(1)-C(2)-C(1)   | 124.0(6)  |
| N(1)-C(2)-C(1)   | 109.4(6)  |
| N(1)-C(3)-N(2)   | 100.0(5)  |
| N(1)-C(3)-C(12)  | 111.7(5)  |
| N(2)-C(3)-C(12)  | 109.7(5)  |
| N(1)-C(3)-C(13)  | 110.9(5)  |
| N(2)-C(3)-C(13)  | 108.6(5)  |
| C(12)-C(3)-C(13) | 114.8(5)  |
| C(5)-C(4)-C(1)   | 110.6(5)  |
| C(10)-C(5)-C(6)  | 118.9(7)  |
| C(10)-C(5)-C(4)  | 121.6(7)  |
| C(6)-C(5)-C(4)   | 119.5(5)  |
| C(7)-C(6)-C(5)   | 120.6(7)  |
| C(8)-C(7)-C(6)   | 120.4(8)  |

|                   |          |
|-------------------|----------|
| C(7)-C(8)-C(9)    | 120.1(7) |
| C(8)-C(9)-C(10)   | 120.1(7) |
| C(5)-C(10)-C(9)   | 119.8(8) |
| C(14)-C(13)-C(18) | 118.6(6) |
| C(14)-C(13)-C(3)  | 120.5(6) |
| C(18)-C(13)-C(3)  | 120.6(5) |
| C(13)-C(14)-C(15) | 121.7(6) |
| C(16)-C(15)-C(14) | 119.1(6) |
| C(17)-C(16)-C(15) | 120.3(6) |
| C(17)-C(16)-O(2)  | 116.3(6) |
| C(15)-C(16)-O(2)  | 123.4(6) |
| C(16)-C(17)-C(18) | 119.6(6) |
| C(17)-C(18)-C(13) | 120.8(6) |
| C(2)-N(1)-C(3)    | 116.2(5) |
| C(2)-N(1)-C(11)   | 122.4(6) |
| C(3)-N(1)-C(11)   | 120.9(5) |
| C(1)-N(2)-C(3)    | 110.2(4) |
| C(16)-O(2)-C(19)  | 117.6(6) |

---

Symmetry transformations used to generate equivalent atoms:

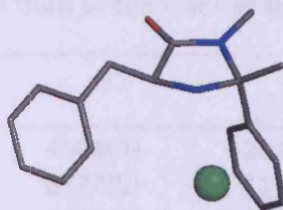
Table 4. Anisotropic displacement parameters ( $\text{\AA}^2 \times 10^3$ ) for nct1008. The anisotropic displacement factor exponent takes the form:  $-2\pi^2 [h^2 a^{*2} U_{11} + \dots + 2 h k a^* b^* U_{12}]$

|       | U <sub>11</sub> | U <sub>22</sub> | U <sub>33</sub> | U <sub>23</sub> | U <sub>13</sub> | U <sub>12</sub> |
|-------|-----------------|-----------------|-----------------|-----------------|-----------------|-----------------|
| C(1)  | 35(4)           | 23(4)           | 30(4)           | 0(3)            | 14(3)           | 4(3)            |
| C(2)  | 35(4)           | 46(5)           | 23(4)           | 4(3)            | 15(3)           | 8(4)            |
| C(3)  | 24(4)           | 35(4)           | 38(4)           | -2(3)           | 8(3)            | 0(3)            |
| C(4)  | 35(4)           | 31(4)           | 37(4)           | 0(3)            | 19(3)           | 4(3)            |
| C(5)  | 26(3)           | 49(5)           | 30(4)           | 3(4)            | 18(3)           | 8(4)            |
| C(6)  | 47(4)           | 48(5)           | 43(4)           | -2(4)           | 28(4)           | 10(4)           |
| C(7)  | 59(5)           | 41(5)           | 61(6)           | 12(4)           | 41(5)           | -1(4)           |
| C(8)  | 54(5)           | 66(6)           | 85(7)           | 38(5)           | 54(5)           | 25(5)           |
| C(9)  | 38(5)           | 94(7)           | 44(5)           | 35(5)           | 24(4)           | 15(5)           |
| C(10) | 33(4)           | 75(7)           | 41(5)           | 11(4)           | 20(4)           | 2(4)            |
| C(11) | 35(4)           | 59(5)           | 40(4)           | -3(4)           | 11(3)           | -11(4)          |
| C(12) | 36(4)           | 32(4)           | 45(4)           | -9(3)           | 21(3)           | -6(3)           |
| C(13) | 29(4)           | 29(4)           | 29(4)           | 3(3)            | 10(3)           | 4(3)            |
| C(14) | 40(4)           | 30(4)           | 38(4)           | 8(3)            | 19(4)           | 3(3)            |
| C(15) | 37(4)           | 42(4)           | 38(4)           | 8(4)            | 19(3)           | 11(4)           |
| C(16) | 37(4)           | 54(6)           | 31(4)           | 3(4)            | 14(3)           | -2(4)           |
| C(17) | 44(4)           | 32(4)           | 40(4)           | 7(3)            | 21(4)           | 3(4)            |
| C(18) | 29(4)           | 35(4)           | 42(4)           | -3(3)           | 18(3)           | 3(3)            |
| C(19) | 98(7)           | 65(6)           | 61(6)           | 2(4)            | 56(5)           | -1(5)           |
| N(1)  | 29(3)           | 37(3)           | 32(3)           | 2(3)            | 10(3)           | 0(3)            |
| N(2)  | 30(3)           | 28(3)           | 30(3)           | -1(2)           | 17(2)           | 2(3)            |
| O(1)  | 36(2)           | 60(3)           | 42(3)           | 16(3)           | 19(2)           | 13(3)           |
| O(2)  | 50(3)           | 58(3)           | 39(3)           | 3(3)            | 25(2)           | -3(3)           |
| Cl(1) | 36(1)           | 34(1)           | 42(1)           | -5(1)           | 16(1)           | -3(1)           |

Table 5. Hydrogen coordinates (  $\times 10^4$ ) and isotropic displacement parameters ( $\text{\AA}^2 \times 10^3$ ) for nct1008.

|        | x    | y     | z     | U(eq) |
|--------|------|-------|-------|-------|
| H(1)   | 3508 | 6365  | 8106  | 35    |
| H(4A)  | 4880 | 4407  | 7480  | 40    |
| H(4B)  | 3586 | 3788  | 6351  | 40    |
| H(6)   | 5463 | 7833  | 7739  | 51    |
| H(7)   | 5496 | 10617 | 6783  | 59    |
| H(8)   | 4179 | 11011 | 4762  | 72    |
| H(9)   | 2749 | 8659  | 3678  | 68    |
| H(10)  | 2666 | 5845  | 4638  | 58    |
| H(11A) | -434 | 3907  | 5911  | 71    |
| H(11B) | -378 | 2968  | 7101  | 71    |
| H(11C) | -27  | 1757  | 6208  | 71    |
| H(12A) | 1723 | -196  | 7269  | 55    |
| H(12B) | 3193 | -162  | 8227  | 55    |
| H(12C) | 2741 | 867   | 6960  | 55    |
| H(14)  | 1141 | 4598  | 9072  | 43    |
| H(15)  | 729  | 4280  | 10727 | 46    |
| H(17)  | 2336 | -864  | 11339 | 46    |
| H(18)  | 2698 | -537  | 9657  | 41    |
| H(19A) | 1397 | 3953  | 12803 | 100   |
| H(19B) | 735  | 2492  | 13324 | 100   |
| H(19C) | -25  | 3247  | 11977 | 100   |
| H(2A)  | 3619 | 4102  | 9304  | 34    |
| H(2B)  | 4148 | 2879  | 8666  | 34    |

## 11.4 X-ray data for 121·HCl



|                                   |   |                  |
|-----------------------------------|---|------------------|
| Identification code               | nct1007   |                  |
| Empirical formula                 | C <sub>18</sub> H <sub>21</sub> Cl N <sub>2</sub> O |                  |
| Formula weight                    | 316.82  |                  |
| Temperature                       | 150(2) K  |                  |
| Wavelength                        | 0.71073 Å   |                  |
| Crystal system                    | Monoclinic  |                  |
| Space group                       | P2 <sub>1</sub>                                     |                  |
| Unit cell dimensions              | a = 10.5272(4) Å                                    | α = 90°.         |
|                                   | b = 7.5333(3) Å                                     | β = 105.028(2)°. |
|                                   | c = 10.6980(5) Å                                    | γ = 90°.         |
| Volume                            | 819.38(6) Å <sup>3</sup>                            |                  |
| Z                                 | 2   |                  |
| Density (calculated)              | 1.284 Mg/m <sup>3</sup>                             |                  |
| Absorption coefficient            | 0.237 mm <sup>-1</sup>                              |                  |
| F(000)                            | 336   |                  |
| Crystal size                      | 0.25 x 0.15 x 0.02 mm <sup>3</sup>                  |                  |
| Theta range for data collection   | 3.15 to 27.46°.                                     |                  |
| Index ranges                      | -13 ≤ h ≤ 13, -9 ≤ k ≤ 8, -13 ≤ l ≤ 13              |                  |
| Reflections collected             | 3113  |                  |
| Independent reflections           | 3113 [R(int) = 0.0000]                              |                  |
| Completeness to theta = 27.46°    | 99.2 %  |                  |
| Max. and min. transmission        | 0.9953 and 0.9432                                   |                  |
| Refinement method                 | Full-matrix least-squares on F <sup>2</sup>         |                  |
| Data / restraints / parameters    | 3113 / 1 / 202                                      |                  |
| Goodness-of-fit on F <sup>2</sup> | 1.050   |                  |
| Final R indices [I > 2σ(I)]       | R1 = 0.0522, wR2 = 0.1082                           |                  |
| R indices (all data)              | R1 = 0.0696, wR2 = 0.1183                           |                  |
| Absolute structure parameter      | 0.04(9)   |                  |
| Extinction coefficient            | 0.077(7)  |                  |
| Largest diff. peak and hole       | 0.321 and -0.260 e.Å <sup>-3</sup>                  |                  |

Table 2. Atomic coordinates ( $\times 10^4$ ) and equivalent isotropic displacement parameters ( $\text{\AA}^2 \times 10^3$ )

for nct1007.  $U(\text{eq})$  is defined as one third of the trace of the orthogonalized  $U_{ij}$  tensor.

|       | x        | y       | z        | $U(\text{eq})$ |
|-------|----------|---------|----------|----------------|
| C(1)  | 7965(3)  | 4503(4) | -297(3)  | 20(1)          |
| C(2)  | 8697(3)  | 6234(5) | 111(3)   | 20(1)          |
| C(3)  | 7595(3)  | 5582(4) | 1701(3)  | 21(1)          |
| C(4)  | 7389(3)  | 4379(5) | -1756(3) | 23(1)          |
| C(5)  | 6964(3)  | 2553(5) | -2299(3) | 23(1)          |
| C(6)  | 7070(3)  | 1041(6) | -1546(3) | 27(1)          |
| C(7)  | 6638(3)  | -600(5) | -2118(4) | 32(1)          |
| C(8)  | 6116(4)  | -729(5) | -3433(4) | 35(1)          |
| C(9)  | 6025(4)  | 769(5)  | -4194(4) | 35(1)          |
| C(10) | 6439(4)  | 2395(6) | -3632(4) | 31(1)          |
| C(11) | 8929(4)  | 8444(5) | 1868(4)  | 28(1)          |
| C(12) | 6537(3)  | 6476(5) | 2195(3)  | 28(1)          |
| C(13) | 8470(3)  | 4311(5) | 2673(3)  | 21(1)          |
| C(14) | 9806(3)  | 4135(5) | 2742(3)  | 25(1)          |
| C(15) | 10577(4) | 2914(5) | 3583(3)  | 29(1)          |
| C(16) | 10031(4) | 1861(5) | 4370(3)  | 31(1)          |
| C(17) | 8709(3)  | 2049(5) | 4315(3)  | 30(1)          |
| C(18) | 7935(3)  | 3262(5) | 3478(3)  | 25(1)          |
| N(1)  | 8357(3)  | 6850(4) | 1161(3)  | 21(1)          |
| N(2)  | 6965(2)  | 4539(4) | 479(2)   | 19(1)          |
| O(1)  | 9457(2)  | 6915(3) | -438(2)  | 29(1)          |
| Cl(1) | 5615(1)  | 1152(1) | 1198(1)  | 28(1)          |

Table 3. Bond lengths [Å] and angles [°] for nct1007.

|                  |          |
|------------------|----------|
| C(1)-N(2)        | 1.501(4) |
| C(1)-C(2)        | 1.520(5) |
| C(1)-C(4)        | 1.524(5) |
| C(2)-O(1)        | 1.221(4) |
| C(2)-N(1)        | 1.347(4) |
| C(3)-N(1)        | 1.460(4) |
| C(3)-C(12)       | 1.509(4) |
| C(3)-N(2)        | 1.522(4) |
| C(3)-C(13)       | 1.533(4) |
| C(4)-C(5)        | 1.515(5) |
| C(5)-C(6)        | 1.382(5) |
| C(5)-C(10)       | 1.395(5) |
| C(6)-C(7)        | 1.402(6) |
| C(7)-C(8)        | 1.374(5) |
| C(8)-C(9)        | 1.380(6) |
| C(9)-C(10)       | 1.384(5) |
| C(11)-N(1)       | 1.463(4) |
| C(13)-C(18)      | 1.390(5) |
| C(13)-C(14)      | 1.396(5) |
| C(14)-C(15)      | 1.391(5) |
| C(15)-C(16)      | 1.385(5) |
| C(16)-C(17)      | 1.385(5) |
| C(17)-C(18)      | 1.386(5) |
|                  |          |
| N(2)-C(1)-C(2)   | 101.7(2) |
| N(2)-C(1)-C(4)   | 114.7(3) |
| C(2)-C(1)-C(4)   | 112.6(3) |
| O(1)-C(2)-N(1)   | 127.3(3) |
| O(1)-C(2)-C(1)   | 124.7(3) |
| N(1)-C(2)-C(1)   | 108.1(3) |
| N(1)-C(3)-C(12)  | 112.2(3) |
| N(1)-C(3)-N(2)   | 99.2(2)  |
| C(12)-C(3)-N(2)  | 109.6(3) |
| N(1)-C(3)-C(13)  | 112.5(3) |
| C(12)-C(3)-C(13) | 114.1(3) |
| N(2)-C(3)-C(13)  | 108.2(3) |
| C(5)-C(4)-C(1)   | 116.6(3) |
| C(6)-C(5)-C(10)  | 118.4(3) |
| C(6)-C(5)-C(4)   | 123.6(3) |
| C(10)-C(5)-C(4)  | 117.9(3) |
| C(5)-C(6)-C(7)   | 120.3(3) |
| C(8)-C(7)-C(6)   | 120.5(4) |
| C(7)-C(8)-C(9)   | 119.6(4) |
| C(8)-C(9)-C(10)  | 120.1(3) |



|                   |          |
|-------------------|----------|
| C(9)-C(10)-C(5)   | 121.1(4) |
| C(18)-C(13)-C(14) | 118.5(3) |
| C(18)-C(13)-C(3)  | 120.4(3) |
| C(14)-C(13)-C(3)  | 121.0(3) |
| C(15)-C(14)-C(13) | 120.5(3) |
| C(16)-C(15)-C(14) | 120.5(3) |
| C(15)-C(16)-C(17) | 119.1(3) |
| C(16)-C(17)-C(18) | 120.7(3) |
| C(17)-C(18)-C(13) | 120.7(3) |
| C(2)-N(1)-C(3)    | 113.4(3) |
| C(2)-N(1)-C(11)   | 123.4(3) |
| C(3)-N(1)-C(11)   | 121.8(3) |
| C(1)-N(2)-C(3)    | 105.8(2) |

---

Symmetry transformations used to generate equivalent atoms:

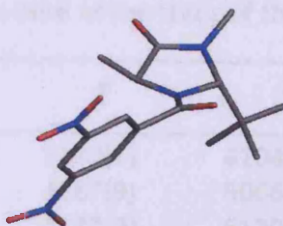
Table 4. Anisotropic displacement parameters ( $\text{\AA}^2 \times 10^3$ ) for nct1007. The anisotropic displacement factor exponent takes the form:  $-2\pi^2 [h^2 a^{*2} U_{11} + \dots + 2 h k a^* b^* U_{12}]$

|       | U <sub>11</sub> | U <sub>22</sub> | U <sub>33</sub> | U <sub>23</sub> | U <sub>13</sub> | U <sub>12</sub> |
|-------|-----------------|-----------------|-----------------|-----------------|-----------------|-----------------|
| C(1)  | 20(2)           | 16(2)           | 26(2)           | 0(1)            | 7(1)            | 1(1)            |
| C(2)  | 20(1)           | 16(2)           | 23(1)           | 3(2)            | 1(1)            | -1(2)           |
| C(3)  | 21(2)           | 20(2)           | 19(2)           | -1(1)           | 3(1)            | -4(1)           |
| C(4)  | 28(2)           | 19(2)           | 24(2)           | 3(2)            | 8(1)            | 0(1)            |
| C(5)  | 20(2)           | 21(2)           | 27(2)           | -4(2)           | 5(1)            | 3(1)            |
| C(6)  | 24(2)           | 26(2)           | 29(2)           | 0(2)            | 4(1)            | 4(2)            |
| C(7)  | 28(2)           | 22(2)           | 44(2)           | -2(2)           | 7(2)            | 2(2)            |
| C(8)  | 26(2)           | 27(2)           | 47(2)           | -15(2)          | 0(2)            | 4(2)            |
| C(9)  | 38(2)           | 36(3)           | 28(2)           | -13(2)          | 2(2)            | 3(2)            |
| C(10) | 32(2)           | 31(2)           | 29(2)           | 4(2)            | 5(2)            | 3(2)            |
| C(11) | 33(2)           | 18(2)           | 32(2)           | -5(2)           | 8(2)            | -8(2)           |
| C(12) | 26(2)           | 29(2)           | 30(2)           | -1(2)           | 10(1)           | 2(1)            |
| C(13) | 23(2)           | 19(2)           | 19(2)           | -3(1)           | 4(1)            | -3(1)           |
| C(14) | 25(2)           | 24(2)           | 24(2)           | 2(2)            | 6(1)            | 1(1)            |
| C(15) | 26(2)           | 32(2)           | 30(2)           | 1(2)            | 7(2)            | 5(2)            |
| C(16) | 37(2)           | 27(2)           | 24(2)           | 4(2)            | 1(2)            | 9(2)            |
| C(17) | 36(2)           | 29(2)           | 26(2)           | 5(2)            | 9(2)            | -5(2)           |
| C(18) | 22(2)           | 26(2)           | 25(2)           | -3(2)           | 6(1)            | -3(1)           |
| N(1)  | 24(1)           | 15(1)           | 25(1)           | -2(1)           | 6(1)            | -5(1)           |
| N(2)  | 18(1)           | 16(2)           | 23(1)           | 2(1)            | 3(1)            | 1(1)            |
| O(1)  | 28(1)           | 30(1)           | 31(1)           | 4(1)            | 9(1)            | -7(1)           |
| Cl(1) | 25(1)           | 22(1)           | 33(1)           | 2(1)            | 3(1)            | -5(1)           |

Table 5. Hydrogen coordinates ( $\times 10^4$ ) and isotropic displacement parameters ( $\text{\AA}^2 \times 10^3$ ) for nct1007.

|        | x     | y     | z     | U(eq) |
|--------|-------|-------|-------|-------|
| H(1)   | 8580  | 3485  | -2    | 24    |
| H(4A)  | 6617  | 5178  | -1997 | 28    |
| H(4B)  | 8051  | 4835  | -2184 | 28    |
| H(6)   | 7438  | 1114  | -638  | 32    |
| H(7)   | 6706  | -1630 | -1593 | 38    |
| H(8)   | 5819  | -1843 | -3816 | 42    |
| H(9)   | 5679  | 684   | -5105 | 42    |
| H(10)  | 6364  | 3421  | -4163 | 37    |
| H(11A) | 9569  | 8099  | 2671  | 42    |
| H(11B) | 8231  | 9156  | 2074  | 42    |
| H(11C) | 9370  | 9144  | 1332  | 42    |
| H(12A) | 6938  | 7074  | 3016  | 42    |
| H(12B) | 5908  | 5584  | 2330  | 42    |
| H(12C) | 6078  | 7352  | 1560  | 42    |
| H(14)  | 10193 | 4855  | 2210  | 30    |
| H(15)  | 11484 | 2801  | 3618  | 35    |
| H(16)  | 10557 | 1021  | 4939  | 37    |
| H(17)  | 8328  | 1340  | 4857  | 36    |
| H(18)  | 7031  | 3377  | 3453  | 30    |
| H(2A)  | 6765  | 3404  | 683   | 23    |
| H(2B)  | 6205  | 5085  | 21    | 23    |

## 11.5 X-ray data for 158



|                                   |   |                  |
|-----------------------------------|---|------------------|
| Identification code               | nct1004   |                  |
| Empirical formula                 | C <sub>16</sub> H <sub>20</sub> N <sub>4</sub> O <sub>6</sub> |                  |
| Formula weight                    | 364.36  |                  |
| Temperature                       | 150(2) K  |                  |
| Wavelength                        | 0.71073 Å   |                  |
| Crystal system                    | Monoclinic  |                  |
| Space group                       | P21   |                  |
| Unit cell dimensions              | a = 11.6652(16) Å   | α = 90°.         |
|                                   | b = 6.0708(7) Å   | β = 104.760(7)°. |
|                                   | c = 12.7801(15) Å   | γ = 90°.         |
| Volume                            | 875.18(19) Å <sup>3</sup>                                     |                  |
| Z                                 | 2   |                  |
| Density (calculated)              | 1.383 Mg/m <sup>3</sup>                                       |                  |
| Absorption coefficient            | 0.107 mm <sup>-1</sup>  |                  |
| F(000)                            | 384   |                  |
| Crystal size                      | 0.35 x 0.06 x 0.02 mm <sup>3</sup>                            |                  |
| Theta range for data collection   | 2.74 to 27.48°.   |                  |
| Index ranges                      | -14 ≤ h ≤ 14, -7 ≤ k ≤ 7, -16 ≤ l ≤ 16                        |                  |
| Reflections collected             | 3631  |                  |
| Independent reflections           | 3631 [R(int) = 0.0000]  |                  |
| Completeness to theta = 27.48°    | 97.3 %  |                  |
| Max. and min. transmission        | 0.9979 and 0.9634   |                  |
| Refinement method                 | Full-matrix least-squares on F <sup>2</sup>                   |                  |
| Data / restraints / parameters    | 3631 / 1 / 240  |                  |
| Goodness-of-fit on F <sup>2</sup> | 1.068   |                  |
| Final R indices [I > 2σ(I)]       | R1 = 0.0952, wR2 = 0.1635                                     |                  |
| R indices (all data)              | R1 = 0.1954, wR2 = 0.2009                                     |                  |
| Absolute structure parameter      | -1(3)   |                  |
| Largest diff. peak and hole       | 0.248 and -0.259 e.Å <sup>-3</sup>                            |                  |

Table 2. Atomic coordinates (  $\times 10^4$ ) and equivalent isotropic displacement parameters ( $\text{\AA}^2 \times 10^3$ )

for nct1004.  $U(\text{eq})$  is defined as one third of the trace of the orthogonalized  $U_{ij}$  tensor.

|       | x        | y        | z        | $U(\text{eq})$ |
|-------|----------|----------|----------|----------------|
| C(1)  | 2958(5)  | 8133(8)  | 6104(4)  | 36(2)          |
| C(2)  | 3072(5)  | 4987(9)  | 5066(4)  | 36(1)          |
| C(3)  | 4032(5)  | 4672(9)  | 6120(4)  | 33(1)          |
| C(4)  | 2032(6)  | 8227(9)  | 6770(5)  | 42(2)          |
| C(5)  | 1657(6)  | 5900(9)  | 7019(5)  | 49(2)          |
| C(6)  | 2553(6)  | 9430(9)  | 7833(5)  | 49(2)          |
| C(7)  | 932(6)   | 9495(11) | 6150(5)  | 56(2)          |
| C(8)  | 1832(5)  | 7961(9)  | 4076(4)  | 43(2)          |
| C(9)  | 5194(5)  | 3993(8)  | 5882(4)  | 38(2)          |
| C(10) | 4978(5)  | 7899(9)  | 7282(4)  | 34(1)          |
| C(11) | 5944(5)  | 6458(8)  | 7951(4)  | 32(1)          |
| C(12) | 5692(5)  | 4617(9)  | 8481(4)  | 32(1)          |
| C(13) | 6606(5)  | 3393(8)  | 9102(4)  | 33(1)          |
| C(14) | 7788(6)  | 3940(10) | 9227(4)  | 41(2)          |
| C(15) | 8000(6)  | 5810(10) | 8696(5)  | 41(2)          |
| C(16) | 7115(5)  | 7101(10) | 8069(4)  | 40(2)          |
| N(1)  | 4022(4)  | 6834(6)  | 6642(3)  | 31(1)          |
| N(2)  | 2566(4)  | 6959(7)  | 5071(3)  | 35(1)          |
| N(3)  | 6307(6)  | 1427(7)  | 9673(4)  | 43(1)          |
| N(4)  | 9256(5)  | 6483(12) | 8807(5)  | 60(2)          |
| O(1)  | 2865(4)  | 3652(7)  | 4322(3)  | 48(1)          |
| O(2)  | 5056(3)  | 9899(6)  | 7360(3)  | 41(1)          |
| O(3)  | 5274(5)  | 1186(7)  | 9695(3)  | 53(1)          |
| O(4)  | 7128(4)  | 192(7)   | 10095(4) | 62(1)          |
| O(5)  | 9443(4)  | 8188(10) | 8364(4)  | 75(2)          |
| O(6)  | 10041(4) | 5293(10) | 9320(5)  | 85(2)          |

Table 3. Bond lengths [Å] and angles [°] for nct1004.

|                 |          |
|-----------------|----------|
| C(1)-N(2)       | 1.467(6) |
| C(1)-N(1)       | 1.483(6) |
| C(1)-C(4)       | 1.538(9) |
| C(2)-O(1)       | 1.225(6) |
| C(2)-N(2)       | 1.335(7) |
| C(2)-C(3)       | 1.529(7) |
| C(3)-N(1)       | 1.474(7) |
| C(3)-C(9)       | 1.519(8) |
| C(4)-C(6)       | 1.525(8) |
| C(4)-C(7)       | 1.533(8) |
| C(4)-C(5)       | 1.536(8) |
| C(8)-N(2)       | 1.472(6) |
| C(10)-O(2)      | 1.219(6) |
| C(10)-N(1)      | 1.366(6) |
| C(10)-C(11)     | 1.508(8) |
| C(11)-C(12)     | 1.376(7) |
| C(11)-C(16)     | 1.391(8) |
| C(12)-C(13)     | 1.374(7) |
| C(13)-C(14)     | 1.387(8) |
| C(13)-N(3)      | 1.487(7) |
| C(14)-C(15)     | 1.377(8) |
| C(15)-C(16)     | 1.379(8) |
| C(15)-N(4)      | 1.493(8) |
| N(3)-O(3)       | 1.221(6) |
| N(3)-O(4)       | 1.228(6) |
| N(4)-O(6)       | 1.219(7) |
| N(4)-O(5)       | 1.225(7) |
|                 |          |
| N(2)-C(1)-N(1)  | 101.0(4) |
| N(2)-C(1)-C(4)  | 114.5(5) |
| N(1)-C(1)-C(4)  | 112.7(4) |
| O(1)-C(2)-N(2)  | 126.6(5) |
| O(1)-C(2)-C(3)  | 123.8(5) |
| N(2)-C(2)-C(3)  | 109.5(4) |
| N(1)-C(3)-C(9)  | 116.3(4) |
| N(1)-C(3)-C(2)  | 101.4(4) |
| C(9)-C(3)-C(2)  | 110.4(5) |
| C(6)-C(4)-C(7)  | 108.2(5) |
| C(6)-C(4)-C(5)  | 109.0(5) |
| C(7)-C(4)-C(5)  | 108.9(6) |
| C(6)-C(4)-C(1)  | 109.5(5) |
| C(7)-C(4)-C(1)  | 110.2(5) |
| C(5)-C(4)-C(1)  | 111.0(5) |
| O(2)-C(10)-N(1) | 123.5(5) |

|                   |          |
|-------------------|----------|
| O(2)-C(10)-C(11)  | 120.1(5) |
| N(1)-C(10)-C(11)  | 116.3(4) |
| C(12)-C(11)-C(16) | 120.1(5) |
| C(12)-C(11)-C(10) | 121.9(5) |
| C(16)-C(11)-C(10) | 118.0(5) |
| C(13)-C(12)-C(11) | 119.5(5) |
| C(12)-C(13)-C(14) | 122.6(5) |
| C(12)-C(13)-N(3)  | 118.3(5) |
| C(14)-C(13)-N(3)  | 119.1(5) |
| C(15)-C(14)-C(13) | 116.0(5) |
| C(14)-C(15)-C(16) | 123.6(6) |
| C(14)-C(15)-N(4)  | 118.3(6) |
| C(16)-C(15)-N(4)  | 118.1(6) |
| C(15)-C(16)-C(11) | 118.2(5) |
| C(10)-N(1)-C(3)   | 126.4(4) |
| C(10)-N(1)-C(1)   | 119.0(4) |
| C(3)-N(1)-C(1)    | 111.5(4) |
| C(2)-N(2)-C(1)    | 113.8(4) |
| C(2)-N(2)-C(8)    | 121.8(4) |
| C(1)-N(2)-C(8)    | 123.8(4) |
| O(3)-N(3)-O(4)    | 125.5(5) |
| O(3)-N(3)-C(13)   | 117.6(5) |
| O(4)-N(3)-C(13)   | 116.9(6) |
| O(6)-N(4)-O(5)    | 123.5(7) |
| O(6)-N(4)-C(15)   | 118.3(6) |
| O(5)-N(4)-C(15)   | 118.2(6) |

---

Symmetry transformations used to generate equivalent atoms:

Table 4. Anisotropic displacement parameters ( $\text{\AA}^2 \times 10^3$ ) for nct1004. The anisotropic displacement factor exponent takes the form:  $-2\pi^2 [h^2 a^{*2} U^{11} + \dots + 2 h k a^* b^* U^{12}]$

|       | U <sup>11</sup> | U <sup>22</sup> | U <sup>33</sup> | U <sup>23</sup> | U <sup>13</sup> | U <sup>12</sup> |
|-------|-----------------|-----------------|-----------------|-----------------|-----------------|-----------------|
| C(1)  | 42(4)           | 19(3)           | 43(3)           | 4(3)            | 1(3)            | 3(3)            |
| C(2)  | 46(4)           | 20(3)           | 42(3)           | 0(3)            | 15(3)           | -4(3)           |
| C(3)  | 39(4)           | 25(3)           | 37(3)           | -1(3)           | 16(3)           | -6(3)           |
| C(4)  | 43(4)           | 31(3)           | 51(4)           | -2(3)           | 10(3)           | 6(3)            |
| C(5)  | 56(4)           | 32(3)           | 63(4)           | 3(3)            | 22(4)           | 0(3)            |
| C(6)  | 61(4)           | 41(4)           | 46(3)           | 3(3)            | 17(3)           | 3(3)            |
| C(7)  | 49(4)           | 54(4)           | 62(4)           | 1(4)            | 11(3)           | 18(3)           |
| C(8)  | 40(4)           | 36(3)           | 49(4)           | 12(3)           | 7(3)            | 1(3)            |
| C(9)  | 50(4)           | 21(3)           | 41(3)           | -8(3)           | 11(3)           | -2(3)           |
| C(10) | 45(4)           | 26(3)           | 32(3)           | -2(3)           | 11(3)           | 2(3)            |
| C(11) | 42(4)           | 21(3)           | 32(3)           | -6(2)           | 7(3)            | 0(3)            |
| C(12) | 36(3)           | 22(3)           | 35(3)           | -7(2)           | 5(3)            | -3(3)           |
| C(13) | 44(4)           | 19(3)           | 36(3)           | 1(2)            | 8(3)            | 2(3)            |
| C(14) | 42(4)           | 37(3)           | 37(3)           | -4(3)           | -1(3)           | 10(3)           |
| C(15) | 38(4)           | 44(4)           | 37(3)           | -1(3)           | 2(3)            | -4(3)           |
| C(16) | 52(4)           | 34(3)           | 33(3)           | 2(3)            | 12(3)           | -8(3)           |
| N(1)  | 38(3)           | 16(2)           | 37(2)           | -1(2)           | 9(2)            | 0(2)            |
| N(2)  | 43(3)           | 23(2)           | 35(3)           | -3(2)           | 2(2)            | -3(2)           |
| N(3)  | 61(4)           | 24(3)           | 36(3)           | 0(2)            | 0(3)            | 3(3)            |
| N(4)  | 40(4)           | 88(5)           | 49(3)           | -3(4)           | 8(3)            | -3(4)           |
| O(1)  | 55(3)           | 36(2)           | 47(2)           | -12(2)          | 4(2)            | -2(2)           |
| O(2)  | 51(3)           | 20(2)           | 49(2)           | -5(2)           | 7(2)            | -7(2)           |
| O(3)  | 68(4)           | 38(2)           | 58(3)           | 12(2)           | 24(3)           | 2(2)            |
| O(4)  | 73(3)           | 39(2)           | 61(3)           | 11(2)           | -6(3)           | 2(3)            |
| O(5)  | 55(3)           | 93(4)           | 74(3)           | 12(3)           | 13(2)           | -23(3)          |
| O(6)  | 42(3)           | 98(4)           | 105(4)          | 25(4)           | 1(3)            | 3(3)            |

Table 5. Hydrogen coordinates ( $\times 10^4$ ) and isotropic displacement parameters ( $\text{\AA}^2 \times 10^3$ ) for nct1004.

|       | x    | y     | z    | U(eq) |
|-------|------|-------|------|-------|
| H(1)  | 3202 | 9664  | 5968 | 44    |
| H(3)  | 3777 | 3508  | 6567 | 39    |
| H(5A) | 1339 | 5104  | 6340 | 73    |
| H(5B) | 1046 | 6002  | 7421 | 73    |
| H(5C) | 2346 | 5108  | 7456 | 73    |
| H(6A) | 1948 | 9568  | 8237 | 73    |
| H(6B) | 2818 | 10900 | 7680 | 73    |
| H(6C) | 3230 | 8595  | 8263 | 73    |
| H(7A) | 1174 | 10907 | 5902 | 84    |
| H(7B) | 409  | 9762  | 6627 | 84    |
| H(7C) | 509  | 8627  | 5524 | 84    |
| H(8A) | 1996 | 7237  | 3444 | 64    |
| H(8B) | 2019 | 9533  | 4064 | 64    |
| H(8C) | 992  | 7782  | 4057 | 64    |
| H(9A) | 5684 | 3206  | 6508 | 56    |
| H(9B) | 5617 | 5308  | 5739 | 56    |
| H(9C) | 5031 | 3026  | 5247 | 56    |
| H(12) | 4893 | 4196  | 8417 | 38    |
| H(14) | 8413 | 3075  | 9653 | 49    |
| H(16) | 7299 | 8395  | 7726 | 48    |



## 12 References

- 1 D. Seebach, *Angew. Chem. Int. Ed.*, **1990**, 29, 1320.
- 2 K. A. Ahrendt, C. J. Borths, D. W. C. Macmillan, *J. Am. Chem. Soc.*, **2000**, 4243.
- 3 Scifinder search for journal articles using the concept “organocatalysis” for each year 2000–2010.
- 4 M. Aitken, IMS Health, **2010**.
- 5 J. C. A. N. Collins, G. N. Sheldrake, *Chirality In Industry II Developments in the Manufacture and Applications of Optically Active Compounds*, **1998**.
- 6 Scifinder search for journal articles using the concept “green chemistry” for each year 2000–2010.
- 7 J. H. Clark, *Green Chem.*, **1999**, 1, 1.
- 8 D. W. C. MacMillan, *Nature*, **2008**, 455, 304.
- 9 A. G. Doyle and E. N. Jacobsen, *Chem. Rev.*, **2007**, 107, 5713.
- 10 W. S. Jen, J. J. M. Wiener, and D. W. C. MacMillan, *J. Am. Chem. Soc.*, **2000**, 122, 9874.
- 11 R. K. Kunz and D. W. C. MacMillan, *J. Am. Chem. Soc.*, **2005**, 127, 3240.
- 12 N. A. Paras and D. W. MacMillan, *J. Am. Chem. Soc.*, **2001**, 123, 4370.
- 13 J. F. Austin and D. W. C. MacMillan, *J. Am. Chem. Soc.*, **2002**, 124, 1172.
- 14 Y. K. Chen, M. Yoshida, and D. W. C. MacMillan, *J. Am. Chem. Soc.*, **2006**, 128, 9328.
- 15 S. G. Ouellet, J. B. Tuttle, and D. W. C. MacMillan *J. Am. Chem. Soc.*, **2005**, 127, 32.
- 16 J. B. Tuttle, S. G. Ouellet, and D. W. C. MacMillan, *J. Am. Chem. Soc.*, **2006**, 128, 12662.
- 17 A. Erkkilä, I. Majander, and P. M. Pihko, *Chem. Rev.*, **2007**, 107, 5416.
- 18 M. P. Brochu, S. P. Brown, and D. W. C. MacMillan, *J. Am. Chem. Soc.*, **2004**, 126, 4108.
- 19 T. D. Beeson and D. W. C. Macmillan, *J. Am. Chem. Soc.*, **2005**, 127, 8826.
- 20 P. Kwiatkowski, T. D. Beeson, J. C. Conrad, and D. W. C. Macmillan, *J. Am. Chem. Soc.*, **2011**, 1738.
- 21 A. B. Northrup and D. W. C. MacMillan, *J. Am. Chem. Soc.*, **2002**, 124, 6798.
- 22 H.-Y. Jang, J.-B. Hong, and D. W. C. MacMillan, *J. Am. Chem. Soc.*, **2007**, 129, 7004.
- 23 H. Kim and D. W. C. MacMillan, *J. Am. Chem. Soc.*, **2008**, 130, 398.
- 24 T. H. Graham, C. M. Jones, N. T. Jui, and D. W. C. MacMillan, *J. Am. Chem. Soc.*, **2008**, 130, 16494.
- 25 M. Amatore, T. D. Beeson, S. P. Brown, and D. W. C. MacMillan, *Angew. Chem. Int. Ed.*, **2009**, 48, 5121.
- 26 J. C. Conrad, J. Kong, B. N. Laforteza, and D. W. C. MacMillan, *J. Am. Chem. Soc.*, **2009**, 131, 11640.

- 27 R. Gordillo and K. N. Houk, *J. Am. Chem. Soc.*, **2006**, 128, 3543.
- 28 J. B. Brazier, G. Evans, T. J. K. Gibbs, S. J. Coles, M. B. Hursthouse, J. A. Platts, and N. C. O. Tomkinson, *Org. Lett.*, **2009**, 11, 133.
- 29 J. B. Brazier, unpublished results.
- 30 Gibbs, T. J. K. *Ph.D. Thesis, Cardiff University*, **2008**.
- 31 J. B. Brazier, K. M. Jones, J. A. Platts, and N. C. O. Tomkinson, *Angew. Chem. Int. Ed.*, **2011**, 1613.
- 32 J. S. Birtill, personal communication to N. C. O. Tomkinson.
- 33 G. Evans, T. J. K. Gibbs, R. L. Jenkins, S. J. Coles, M. B. Hursthouse, J. A. Platts, and N. C. O. Tomkinson, *Angew. Chem. Int. Ed.*, **2008**, 47, 2820.
- 34 J. E. Baldwin, *J. Chem. Soc., Chem. Commun.*, 1976, 734.
- 35 N. Kuhnert and R. Walsh, *Org. Biomol. Chem.*, **2005**, 1694.
- 36 M. J. Bausch, B. David, P. Dobrowolski, V. Prasad, *J. Org. Chem.*, **1990**, 55, 5806.
- 37 W. J. Middleton and C. G. Krespan, *J. Org. Chem.*, **1965**, 30, 1398.
- 38 K. Burger, D. Hubl, and P. Gertitschke, *J. Fluorine Chem.*, **1984**, 27, 327.
- 39 W. Steglich, K. Burger, M. Durr, and E. Burgis, *Chem. Ber.*, **1974**, 107, 1488.
- 40 K.-W. Lee and L. A. Singer, *J. Org. Chem.*, **1974**, 39, 3780.
- 41 S. Fustero, A. Navarro, B. Pina, A. Asensio, P. Bravo, M. Crucianelli, A. Volonterio, and M. Zanda, *J. Org. Chem.*, **1998**, 63, 6210.
- 42 G. K. S. Prakash, T. Matthew, C. Panja, H. Vaghoo, K. Venkataraman, and G. A. Olah, *Org. Lett.*, **2007**, 9, 179.
- 43 G. A. Olah, O. Farooq, M. F. Farnia, and J. A. Olah, *J. Am. Chem. Soc.*, **1988**, 110, 2560.
- 44 J. Guilleme and E. Diez, with San Fabian J, *J. Magn. Reson.*, **1998**, 133, 255.
- 45 R. D. Roberts, H. E. J. Ferran, M. J. Gula, and T. A. Spencer, *J. Am. Chem. Soc.*, **1980**, 102, 7054.
- 46 D. M. Gale and C. G. Krespan, *J. Org. Chem.*, **1970**, 35, 1485.
- 47 H. Gotoh and Y. Hayashi, *Org. Lett.*, **2007**, 9, 2859.
- 48 Y. Hayashi, S. Samanta, H. Gotoh, and H. Ishikawa, *Angew. Chem. Int. Ed.*, **2008**, 47, 6634.
- 49 Y. Hayashi, H. Gotoh, T. Hayashi, and M. Shoji, *Angew. Chem. Int. Ed.*, **2005**, 44, 4212.
- 50 I. K. Mangion, A. B. Northrup, and D. W. C. MacMillan, *Angew. Chem. Int. Ed.*, **2004**, 43, 6722.
- 51 N. A. Paras and D. W. C. MacMillan, *J. Am. Chem. Soc.*, **2002**, 124, 7894.
- 52 S. P. Brown, N. C. Goodwin, and D. W. C. MacMillan, *J. Am. Chem. Soc.*, **2003**, 125, 1192.
- 53 Y. Huang, A. M. Walji, C. H. Larsen, and D. W. C. MacMillan, *J. Am. Chem. Soc.*, **2005**, 127, 15051-3.

- 54 S. Lee and D. W. C. MacMillan, *Tetrahedron*, **2006**, 62, 11413.
- 55 H.-Y. Jang, J.-B. Hong, and D. W. C. MacMillan, *J. Am. Chem. Soc.*, **2007**, 129, 7004.
- 56 S. G. Ouellet, A. M. Walji, and D. W. C. MacMillan, *Acc. Chem. Res.*, **2007**, 40, 1327.
- 57 D. A. Nagib, M. E. Scott, and D. W. C. MacMillan, *J. Am. Chem. Soc.*, **2009**, 131, 10875.
- 58 J. E. Wilson, A. D. Casarez, and D. W. C. MacMillan, *J. Am. Chem. Soc.*, **2009**, 131, 11332.
- 59 A. E. Allen and D. W. C. Macmillan, *J. Am. Chem. Soc.*, **2010**, 132, 4986.
- 60 S. Rendler and D. W. C. Macmillan, *J. Am. Chem. Soc.*, **2010**, 132, 5027.
- 61 N. T. Jui, E. C. Y. Lee, and D. W. C. MacMillan, *J. Am. Chem. Soc.*, **2010**, 132, 10015.
- 62 R. R. Knowles, J. Carpenter, S. B. Blakey, A. Kayano, I. K. Mangion, C. J. Sinz, and D. W. C. MacMillan, *Chem. Sci.*, **2011**, 2, 308.
- 63 A. B. Northrup and D. W. C. MacMillan, *J. Am. Chem. Soc.*, **2002**, 124, 2458.
- 64 S. Lee and D. W. C. MacMillan, *J. Am. Chem. Soc.*, **2007**, 129, 15438.
- 65 G. Lelais and D. W. C. Macmillan, *Aldrichimica Acta*, **2006**, 39, 79.
- 66 M. Reiter, S. Torssell, S. Lee, and D. W. C. MacMillan, *Chem. Sci.*, **2010**, 1, 37.
- 67 H.-W. Shih, M. N. Vander Wal, R. L. Grange, and D. W. C. Macmillan, *J. Am. Chem. Soc.*, **2010**, 3, 13600.
- 68 T. H. Graham, B. D. Horning, and D. W. C. MacMillan, *Org. Synth.*, **2011**, 88, 42.
- 69 A. Radzicka and R. Wolfenden, *J. Am. Chem. Soc.*, **1996**, 118, 6105.
- 70 P. Magnus, B. Mugrage, M. R. Deluca, and G. A. Cain, *J. Am. Chem. Soc.*, **1990**, 122, 5220.
- 71 A. D. Becke, *J. Chem. Phys.*, **1993**, 98, 1372.
- 72 M. P. Waller, A. Robertazzi, J. A. Platts, D. E. Hibbs, and P. A. Williams, *J. Comput. Chem.*, **2006**, 27, 491.
- 73 J. S. Rao and G. N. Sastry, *Int. J. Quantum Chem.*, **2006**, 106, 1217.
- 74 J. B. Brazier and N. C. O. Tomkinson, *Top. Curr. Chem.*, **2009**, 291, 281.
- 75 D. Seebach, R. Gilmour, *et. al.*, *Helv. Chim. Acta*, **2010**, 93, 603.
- 76 M. Makosza and R. Bujok, *J. Fluorine Chem.*, **2005**, 126, 209.
- 77 M. H. Abraham, P. L. Grellier, D. V. Prior, J. J. Morris, and P. J. Taylor, *J. Chem. Soc. Perkin Trans. 2*, **1990**, 521.
- 78 M. J. Kamlet and R. W. Taft, *J. Am. Chem. Soc.*, **1976**, 98, 377.
- 79 A Meyers, *Tet. Lett.*, **1995**, 36, 5877.
- 80 A. L. Smith *et. al.*, *J. Org. Chem.*, **1988**, 53, 5381.
- 81 W. M. Koppes, M. Chaykovsky, and H. G. Adolph, *J. Org. Chem.*, **1987**, 52, 1113.
- 82 W. J. Middleton and C. G. Krespan, *J. Org. Chem.*, **1970**, 35, 1480.
- 83 C. A. Panetta, T. G. Casanova, and C. C. Chu, *J. Org. Chem.*, **1973**, 38, 128.

